

**USING A HYBRID ADSORPTION-MEMBRANE FILTRATION
SYSTEM TO PRODUCE BIOLOGICALLY STABLE DRINKING
WATER**



LANDRY SENDANGO OMALANGA

A thesis submitted to the Faculty of Engineering and the Built Environment, University of the Witwatersrand, Johannesburg, in fulfilment of the requirements for the degree of Doctor of Philosophy.

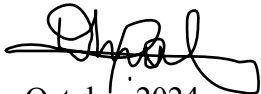
Johannesburg, 2024

DECLARATION

I declare that this thesis is my own work, which I hereby submit for the degree of Doctor of Philosophy to the University of the Witwatersrand, Johannesburg. It has not previously been submitted by me to any institution.

The thesis has been prepared maintaining the Rules of Good Scientific Practice.

Landry Sendango Omalanga



October 2024

Abstract

The purpose of water treatment is to produce clean and safe drinking water, for consumers. Water quality, both during treatment and distribution, is greatly affected by the presence of natural organic matter (NOM). The presence of NOM affects the effectiveness of water treatment processes and sometimes increases the cost of water treatment and leads to operational problems. Furthermore, the presence of biodegradable organic matter (BOM), which is a fraction of NOM, can degrade water quality during distribution resulting in the loss of biological stability. The excessive presence of BOM can be addressed using advanced water treatment processes or by relying on systems which combine multiple water treatment processes to increase treatment efficiency. The main aim of this study was to evaluate the effectiveness of a hybrid adsorption-membrane filtration system in lowering the bacterial regrowth potential in water.

Ready-made multi-walled carbon nanotubes (MWCNTs) were used as adsorbents in this study. MWCNTs were chosen because they exhibit high adsorption properties mainly because of their fibrous shape and external surface accessibility. MWCNTs have hydrophobic characteristics and a propensity to aggregate due to the presence of electrostatic interactions among them, therefore, functionalization of MWCNTs was required to improve their dispersion in the organic and inorganic solvents. A non-covalent functionalization process was employed using cetyltrimethylammonium bromide (CTAB) as a cationic surfactant to ameliorate the stability and dispersibility of MWCNTs in aqueous solution. The non-covalent functionalization was preferred to sustain the functionalities needed for BOM capture enhancement and environmental safety. Polysulfone (PSF) membranes were produced by phase inversion method using N, N-dimethylformamide as solvent for the removal of BOM from water. The phase inversion method was chosen in this study due to its simple processing, flexible production scales, and low cost. The MWCNTs and PSF membranes were characterized using microscopy techniques such as transmission electron microscopy (TEM), scanning electron microscopy (SEM), X ray diffraction (XRD), Raman spectroscopy, tensile strength test, and the hydrophilicity (contact angle) test. These techniques were selected because they enable the evaluation of the morphology, composition, physical characteristics, and dynamic behavior of nanostructured materials.

Batch adsorption experiments were employed to investigate the adsorption properties of functionalized MWCNTs for BOM removal. Four different concentrations of functionalized MWCNTs were tested to determine the ideal conditions for the adsorption of two forms of BOM; assimilable organic carbon (AOC) and biodegradable dissolved organic carbon (BDOC), from water. The concentrations of functionalized MWCNTs used were 4, 8, 12, and 16 mg in 100 mL of BOM solution. Furthermore, the cross-flow filtration mode, also known as tangential flow filtration, was used to separate the remaining BOM in water by passing water along the surface of the NF membrane using pressure difference. Cross-flow filtration was chosen because it removes the buildup from the surface of the membrane and provides the benefit of an improved membrane lifespan by helping to prevent irreversible fouling. A mathematical model of membrane filtration process in continuous system was also developed to better understand the correlations between the different variables of the membrane filtration process such as the inlet (feed) concentration (C_{in}) and flow rate (Q_{in}), and the outlet (retentate) concentration (C_{out}) and flow rate (Q_{out}), and the permeate concentration C_p .

Results obtained after the functionalization process of MWCNTs showed an improvement in their stability and dispersibility in aqueous solution. The characterization of both MWCNTs and PSF membranes showed some interesting features. For example, morphological and structural studies show that MWCNTs possess fibrous shapes with a high aspect ratio, and a hollow structure with an inner diameter. The finger-like structures found on the surfaces of PSF membranes play a crucial role in their adsorption capabilities. These structures, which vary in pore size, contribute to the overall capacity of the membranes to absorb BOM from water. During adsorption experiments, it was observed that the removal of BOM from water increased with an increase in the adsorbent (functionalized MWCNTs) concentration. This is likely due to high concentration gradient which acts as a driving force to overcome resistances to mass transfer of dye ions between the aqueous phase and the solid phase. However, the maximum removal of both AOC and BDOC was recorded at a concentration of functionalized MWCNTs of 12 mg, at a contact time of 4 hours and at an agitation speed of 180 rpm. The PSF membrane produced by phase inversion method demonstrated the highest flux of $0.0091 \text{ ml/cm}^2 \cdot \text{min}$ at room temperature (25°C) and after a filtration time of 90 minutes. The selectivity and permeate flux were increased with forward flushing and backwashing processes of the PSF membranes because it flushes out accumulated debris and particles on the surface and inside the pores of the membranes. After using the hybrid adsorption-membrane

filtration system, BDOC concentrations dropped to an average of 65% of the initial raw water BDOC and the AOC concentrations dropped to approximately 80% of the initial raw water AOC. Outputs from the mathematical model demonstrated that the change in initial conditions (C_{in} and Q_{in}) is responsible for the transient response (changes from one steady state to another) in these membranes.

The adsorption and membrane nanofiltration hybrid system adopted in this study, effectively removed both AOC and BDOC from water, and can therefore be used to produce biologically stable drinking water. The outcome of this study could be the application of the combination of BOM targeting strategies and residual disinfection to better control bacterial regrowth in drinking water distribution systems (DWDSs). This in turn could help water utilities with meeting distribution systems, water quality guidelines, and protect public health.

DEDICATION

Dedicated to the Holy Ghost: The spirit of wisdom and revelation; and to my parents, Pascal Daniel Pele Omalanga and Anne-Yvette Mulanga, to my relatives Armel Omalanga, Paola Omalanga, and Israel Omalanga, and to my wife Vanessa Omalanga, plus my sons David Pele Omalanga and Elijah Lombela Omalanga for love and indulgence.

ACKNOWLEDGEMENTS

“I always pray that the God of our Lord Jesus Christ, the Father of glory, may grant you a spirit of wisdom and revelation...” (Ephesians 1:17). Throughout my PhD studies, I felt the presence of a spirit of wisdom, and revelation. This spirit was always there for my rescue whenever I got stuck in my research progress.

It gives me great pleasure to sincerely thank and to be grateful to my supervisors Dr. Precious Biyela and Prof. Geoffrey S. Simate. I appreciate the excellent advice, contributions, and the efforts to make this research study a success. I would also like to express my gratitude toward the Head of School of Civil and Environmental Engineering, Prof. Mike Otieno for his kind advice, suggestions, and guidance toward the end of this work. I am extremely grateful to the NRF Thuthuka and postgraduate merit award (PMA), University of the Witwatersrand for financial assistance.

I am grateful to Prof. Pradeep Kumar from the Medical School at the University of the Witwatersrand for his help with the mechanical testing of the membranes. I am grateful to Mr. Stephan Wagenaar from the University of Johannesburg for his assistance with the contact angle (hydrophilicity) tests. It gives me great pleasure to thank Mr. Michael Tobin and Mrs. Lucretia Brink from the School of Molecular Biology at the University of the Witwatersrand for their help with microbiological laboratory procedures. To my entire family, I sincerely thank you for your support and wise counsel. Finally, I want to thank the All-Powerful God for his love, inspiration, revelation, and breath.

TABLE OF CONTENTS

Declaration.....	ii
Abstract.....	iii
Dedication.....	vi
Acknowledgement.....	vii
Table of contents.....	viii
List of figures.....	xiv
List of tables.....	xvi
List of abbreviation.....	xvii
Nomenclature.....	xx
CHAPTER ONE: INTRODUCTION.....	1
1.0 Introduction.....	1
1.1 Research objectives.....	4
1.2 Research questions.....	5
1.3 Expected contributions to knowledge.....	5
1.4 Scope of research.....	7
1.5 Organization of the thesis.....	7
1.6 Summary.....	8
1.7 References.....	8
CHAPTER TWO: LITERATURE REVIEW.....	11
2.1. Natural organic matter (NOM).....	11
2.2 Characterization and quantification of NOM.....	12

2.2.1 Sample collection and preparation.....	12
2.2.2 Assimilable Organic Carbon (AOC).....	13
2.2.3 Biodegradable Dissolved Organic Carbon (BDOC).....	13
2.2.4 Total Organic Carbon (TOC) and Dissolved Organic Carbon (DOC).....	14
2.2.5 Dissolved Organic Nitrogen (DON).....	16
2.2.6 XAD resin fractionation.....	17
2.2.7 Ultraviolet Absorbance.....	17
2.2.8 Differential Ultraviolet Absorbance	18
2.2.9 Size exclusion chromatography.....	18
2.2.10 Polarity evaluation technique.....	21
2.3 Presence of NOM in drinking water treatment.....	22
2.3.1 Impact of NOM on drinking water treatment.....	22
2.3.2 Application of water treatment techniques for the elimination of NOM.....	23
2.4 Physico-chemical parameters.....	29
2.5 Membranes.....	30
2.5.1 Symmetric membranes.....	31
2.5.2 Membranes with micropores.....	31
2.5.3 Dense membranes.....	31
2.5.4 Anisotropic filtration membranes.....	32
2.5.5 Liquid filtration membranes.....	32
2.5.6 Electrically active membranes.....	32
2.6 Membrane filtration processes.....	33
2.7 Synthesis of polymeric filtration membranes.....	34
2.7.1 Isotropic membranes.....	34
2.7.7 Membranes with asymmetric Structure.....	35

2.8	Generalities on membrane filtration processes.....	36
2.8.1	Introduction to membrane filtration of liquid solutions.....	36
	Microfiltration membranes.....	36
	Ultrafiltration membranes.....	36
	Nanofiltration membranes.....	38
	Reverse osmosis membranes.....	37
2.8.2	Applications of membrane filtration.....	38
	Hybrid membrane systems.....	38
2.8.3	Polymeric membrane fouling problems and its management.....	39
2.9	Discovery and definition of carbon nanotubes.....	39
2.9.1	Carbon nanotubes structure, composition, and properties.....	40
2.9.2	Production of carbon nanotubes.....	41
	Arc Discharge Method.....	41
	Chemical Vapor Deposition Technique.....	42
2.9.3	Electrical Properties of carbon nanotubes.....	43
2.9.4	Mechanical Properties of carbon nanotubes.....	44
2.9.5	Functionalization of carbon nanotubes.....	44
	Concept on covalent Functionalization.....	45
	Concept on non-covalent Functionalization.....	45
2.9.6	Cytotoxic properties of carbon nanotubes.....	46
2.9.7	Adsorption of biological contaminants using carbon nanotubes as sorbent media.....	47
	Adsorption of microorganisms from water by using carbon nanotubes.....	48
	Adsorption of natural organic matter from water by using carbon nanotubes.....	48
2.10	Summary.....	49
2.11	References.....	49

CHAPTER THREE: EXPERIMENTAL PROCEDURE AND MATERIALS.....82

3.1	Introduction.....	82
3.1.1	Chemicals and materials.....	82
3.2	Experimental procedure.....	84
3.2.1	Functionalization of MWCNTs.....	84
3.2.2	Fabrication of the polymeric (polysulfone) membrane.....	85
3.2.3	Batch Adsorption process for NOM removal from drinking water.....	85
3.2.4	Filtration tests.....	86
3.3	Analytical methods.....	87
3.3.1	Characterization of stain pseudomonas fluorescens P17.....	87
3.3.2	Characterization of carbon nanotubes and polysulfone (PSF) filtration membranes..	88
3.4	Water Quality Testing.....	94
3.4.1	Raw water and finished water quality.....	94
3.4.2	Water flux measurement.....	96
3.5	Summary.....	97
3.6	References.....	97

CHAPTER FOUR: MATHEMATICAL MODELING OF MEMBRANE FILTRATION PROCESS.....99

4.1	Introduction.....	99
4.2	Methodology.....	100
4.3	The Basic relationships in the complete mixing flow system (CMFS).....	100
4.4	Mathematical modelling of the CMFS.....	101
4.4.1	At steady state.....	102
4.4.2	The limiting concentration.....	102
4.4.3	The dynamic separation process.....	103
4.5	Validation of the mathematical model.....	104

4.5.1 Empirical parameters.....	104
4.5.2 Separation by the completely mixing flow system.....	106
4.6 Summary.....	108
4.7 References.....	108

CHAPTER FIVE: RESULTS AND DISCUSSION OF THE CHARACTERISATION OF MWCNTS, PSF MEMBRANES; AND AOC AND DOC DETERMINATION.....110

5.1 Introduction.....	110
5.2 Strain pseudomonas fluorescens P17 characterisation.....	106
5.3 MWCNTs characterisation.....	110
5.3.1 Scanning electron microscope.....	110
5.3.2 Transmission electron microscope.....	113
5.3.3 X-ray diffraction of raw MWCNTs.....	115
5.3.4 Raman spectroscopy of functionalised and unfunctionalized MWCNTs.....	116
5.4 Polymeric membrane characterisation.....	118
5.4.1 Scanning electron microscope observation of polymeric membrane.....	118
5.4.2 Contact angle (hydrophobicity) test of polymeric membrane.....	120
5.4.3 Mechanical test results of polymeric membranes.....	121
5.4.4 Porosity test of polymeric membranes.....	122
5.5 AOC determination.....	123
5.6 DOC and BDOC determination.....	126
5.7 Summary.....	128
5.8 References.....	129

CHAPTER SIX: ADSORPTION PROCESS AND MEMBRANES FILTRATION PROCESS FOR AOC AND BDOC REMOVAL.....133

6.1 Introduction.....	133
6.2 Adsorption of NOM by CTAB-functionalised MWCNTs.....	133
6.2.1 Impact of batch adsorption process using MWCNTs (as adsorbents) on AOC Concentration.....	134
6.2.2 Impact of batch adsorption process using MWCNTs (as adsorbents) on DOC and	

BDOC concentration.....	140
6.2.3 Adsorption isotherm models.....	144
6.2.4 Kinetics modelling.....	148
6.3 Membrane filtration process for NOM removal.....	148
6.3.1 Impact of membrane filtration process for the removal of AOC from water.....	149
6.3.2 Impact of membrane filtration process for the removal of DOC and BDOC from water.....	150
6.3.3 Impact of filtration time on membrane performance.....	151
6.3.4 Depletion of HPC abundance, DOC, and BDOC after using hybrid membrane Systems.....	152
6.3.5 Comparison between AOC and BDOC.....	154
6.3.6 Impact of forward flushing and backwashing on permeate flux.....	155
6.4 Summary.....	157
6.5 References.....	158
CHAPTER SEVEN: CONCLUSION AND RECOMMENDATIONS.....	163
7.1 Conclusions.....	163
7.1.1 Introduction.....	163
7.1.2 Mathematical model of membrane filtration process.....	164
7.1.3 Characterization of MWCNTs, PSF membranes and AOC/BDOC determination.....	164
7.1.4 Adsorption process and membranes filtration process for AOC and BDOC removal...166	
7.1.5 Industrial applications.....	168
7.2 Recommendations.....	169
APPENDICES.....	172
APPENDIX A: Characterisation of MWCNTs.....	172
APPENDIX B: PSF membrane characterisation.....	174
APPENDIX C: The solution of equation 4.15.....	176
APPENDIX D: DOC and BDOC determination results.....	178
APPENDIX E: AOC determination.....	180
APPENDIX F: Adsorption isotherm models.....	187
APPENDIX G: Analytical testing method.....	189

APPENDIX H: Error bars in graphs.....	189
--	------------

LIST OF FIGURES

Figure 2.1 Continuum of particulate and dissolved organic carbon in natural waters (Aiken and Leenheer, 1993).	15
Figure 2.2 SEC-DOC chromatogram illustrating different fractions of NOM.....	19
Figure 2.3 URI and SEC-UVA (at 210 nm and 254 nm) chromatograms of extracted foulant from a nanofiltration (NF) membrane (Adapted from Amy and Her, 2004).....	20
Figure 2.4 SEC-OCD chromatogram of surface water. A = Biopolymers; B = Humic substances; C = Building blocks; D = low molecular weight acids; E = low molecular weight neutrals; F, G = Ammonium Nitrate, (only OND). HOC (hydrophobic organic carbon) = calculated difference between bypass and sum of chromatographic fractions. Values in OCD chromatogram are concentrations in mg/L C. Values in OND chromatogram are concentrations in mg/L N.....	21
Figure 2.5 Schematic diagram representing the separation of two phases by non-porous and porous membranes.....	30
Figure 2.6: Theoretical illustration of a membrane process.....	34
Figure 2.7: Schematic of the solution diffusion mechanism.....	34
Figure 2.8: Cross-sectional surface of an asymmetric membrane (Integrally skinned Structure).....	35
Figure 2.9: The size range of water contaminants and the particle removal size range of different treatment processes (The size range shown for the membrane processes relates to their pore size).....	38
Figure 2.10: Illustration of the atomic structures of (12, 0) zigzag, (6, 6) armchair and (6, 4) chiral nanotubes.....	40
Figure 2.11: Graphene sheet with lattice vectors a_1 and a_2 , the chiral vector $C_h = 3a_1 + 5a_2$ represents a possible wrapping of the two-dimensional (2D) graphene sheet into a tube form. The resulting (5, 3) nanotube is shown on the right side having chiral character.....	41

Figure 2.12: Illustration of the diagrams of (a) Arc discharge method, (b) Laser ablation method and (c) CVD reactor, for carbon nanotube growth. (a) and (b) reproduced from [217] and (c).....	43
Figure 2.13: SEM images of (A) E. coli cells exposed to MWNT's, (B) E. coli cells exposed to SWNT's.....	47
Figure 3.1: Set up for functionalization of MWCNTs.....	86
Figure 3.2: The shaker (orbicult incubator Shaker IBS) and adsorption process experimental set up.....	86
Figure 3.3: Schematic Filtration system design.....	87
Figure 3.4: Olympus CX22 LED.....	88
Figure 3.5: FE-SEM in-lens equipment	89
Figure 3.6: FEI Tecnai T12	89
Figure 3.7: Horiba Lab RAM Raman spectrometer.....	90
Figure 3.8: Bruker D2 advance X-ray diffractometer.....	91
Figure 3.9: Bragg's diffraction illustration.....	91
Figure 3.10: SCA20 version 4.1.12 employed for contact angle measurements.....	92
Figure 3.11: TA.XT Plus Texture Analyzer used for mechanical tests.....	93
Figure 3.12: The Cross-flow filtration system	96
Figure 3.13: Proposed experimental setup.....	97
Figure 4.1: Complete mixing flow membrane system.....	101
Figure 5.1: SEM images of (a, b) raw MWCNTs and (c) functionalized MWCNTs.....	112
Figure 5.2 (a, b): Two different views of the TEM image of the raw MWCNTs.....	114
Figure 5.3: XRD pattern of MWCNTs.....	116
Figure 5.4: Raman spectroscopy for functionalized and unfunctionalized MWCNTs.....	117
Figure 5.5: SEM images of (a, b), the top surface and cross-sections of the polymeric (polysulfone) membrane.....	119
Figure 5.6: Illustration of the sessile drop measurement method.....	121

Figure 5.7: Mechanical test results of the polymeric filtration membranes.....	122
Figure 5.8: Colony count changes and growth curves of strain P17 over a number of days	124
Figure 5.9: ultrapure water inoculated with <i>P. fluorescens</i> P17, containing each 4, 8, 12 and 16 mg of CTAB – functionalized MWCNTs for adsorption process before membrane filtration process.....	124
Figure 6.1: Ultrapure water inoculated with strain P17, containing each 4, 8, 12, 16 mg of CTAB-functionalised MWCNTs for adsorption process before membrane filtration process.....	135
Figure 6.2: Impact of adsorbent concentration on percentage removal of AOC from P17-ultrapure water (Agitation speed= 180 rpm, contact time = 4 hours)	137
Figure 6.3: Effect of agitation speed on the percentage removal of AOC (initial concentration = 48.8 and 53.6 µg C/L, adsorbent concentration = 12 mg, contact time = 4 hours, and pH = 4).....	138
Figure 6.4: Impact of contact time on percentage removal of AOC (Initial concentration = 48.8 and 53.6 µg C/L, Agitation speed = 180 rpm, adsorbent concentration = 12 mg)	139
Figure 6.5: The variation of DOC concentration during adsorption process using CTAB-functionalized MWCNTs.....	142
Figure 6.6: The variation of BDOC concentration during adsorption process using CTAB-functionalized MWCNTs.....	143
Figure 6.7: Langmuir isotherm parameter for the adsorption onto CTAB-functionalized MWCNTs.....	146
Figure 6.8: Freundlich isotherm plot for AOC adsorption onto CTAB-functionalized MWCNT.....	147
Figure 6.9: The variation of the flux with filtration time at a constant pressure of 4.5 bar.....	151

LIST OF TABLES

Table 3.1: The Average water quality characteristics of ultrapure water (sample A) used in this study.....	95
Table 3.2: The average water quality characteristics of raw tap water (sample B) used in this study.....	95
Table 5.1: Contact angle test results.....	120

Table 5.2: Efficiency of BAS incubator 1.....	126
Table 5.3: Efficiency of BAS incubator 2.....	126
Table 5.4: Efficiency of BAS incubator 3.....	127
Table 6.1: Efficiency of adsorption process with 4 mg MWCNTs on DOC concentration in tap water.....	141
Table 6.2: Efficiency of adsorption process with 8 mg MWCNTS on DOC concentration in tap water.....	141
Table 6.3: Efficiency of adsorption process with 12 mg MWCNTS on DOC concentration in tap water.....	141
Table 6.4: Efficiency of adsorption process with 16 mg MWCNTS on DOC concentration in tap water.....	141
Table 6.5: Langmuir isotherm plot for AOC adsorption onto CTAB functionalised MWCNTs.....	146
Table 6.6: Freundlich isotherm parameters for the adsorption of AOC by functionalised MWCNTs.....	147
Table 6.7: Concentration of water sample A quality parameters obtained after hybrid membrane systems.....	155
Table 6.8: Concentration of water sample B quality parameters obtained after hybrid membrane systems.....	156

LIST OF ACRONYMS, ABBREVIATIONS AND SYMBOLS

AER	Anion exchange resin
AOC	Assimilable organic matter
ATRP	Transfer radical polymerization
BDOC	Biodegradable organic matter
BK	Bank filtration
BOM	Biodegradable organic matter
BAS	Biologically active sand
C	Carbon
CDFS	Complete displacement flow system
Cl⁻	Chloride ions

CNFs	Carbon nanofibres
CNTs	Carbon nanotubes
CMFs	Complete mixing flow system
CMLM	Couple mixing liquid media
CTAB	Cetyltrimethylammonium bromide
CVD	Chemical vapor deposition
¹³C NMR	Carbon-13 nuclear magnetic resonance
DBPs	Disinfection by-products
DMF	Dimethylformamide
DMSO	Dimethyl sulfoxide
DIN	Dissolved inorganic nitrogen
DO	Dissolved oxygen
DOC	Dissolved organic carbon
DON	Dissolved organic nitrogen
DWCNTS	Double-walled carbon nanotubes
DWDSs	Drinking water distribution systems
EEM	Excitation emission matrix
FTIR	Fourier-transformation infrared
GAC	Granular activated carbon
HPC	Heterotrophic plate count
HPLC	High performance liquid chromatographic
HTC	High temperature combustion
HTCO	High temperature catalytic oxidation
IC	Inorganic carbon
IEX	Ion exchange
LMW	Low molecular weight
MA	Maleic acid
MF	Microfiltration
MIEX	Magnetic ion exchange resin
MMA	Methyl methanolate
MS	Molecular size

MSP	Membrane separation process
MW	Molecular weight
MWCNTs	multi-walled carbon nanotubes
Na⁺	Sodium ions
N	Nitrate
NF	Nanofiltration
MOM	Natural organic matter
PAC	Powdered activated carbon
PEG	Poly-ethylene glycol
POC	Particulate organic carbon
PRAM	Polarity rapid assessment method
PSF	Polysulfone
PVA	Polyvinyl alcohol
RAFT	Reversible addition-fragment chain transfer
RO	Reverse osmosis
SAP	Sampling analysis plan
SEC	Size exclusion chromatography
SEM	Scanning electron microscope
SDS	Sodium dodecyl sulfate
SPPO	Sulfonated poly (phenylene oxide)
SUVA	Specific ultraviolet absorbance
SWCNTs	Single-walled carbon nanotubes
TDOC	Total dissolved organic carbon
TDN	Total dissolved nitrogen
TDS	Total dissolved solid
TEM	Transmission electron microscope
TFC	Thin film composite
TGA	Thermogravimetric analysis
THF	Tetrahydrofuran
TMPs	Transmembrane pressures
TNTC	Too numerous to count

UF.....Ultrafiltration
URI.....UVA ratio index
UV.....Ultraviolet
UVA.....UV light absorbance
XAD.....Resin adsorption
XRD.....X-ray diffraction

NOTATION

A, B.....Auxiliary parameters
b₀, b₁, b₂.....Coefficients
D, D₁..... Auxiliary parameters
C_{in}, C_P, C_{out}.....concentration of solute in the feed, permeate, and retentate (rejection)
f₀, f₁, f₂.....Coefficients
K₀, K.....Membrane permeability
Q_{in}, Q_P, Q_{out}.....Inlet, permeate, and outlet flow rate
T.....Time
V.....System volume
μ.....Auxiliary variable
α..... Auxiliary parameter

SUBSCRIPTS

0.....Initial values
Lim.....Limiting values
g.....Given values
*****.....Stationary values
b.....Boundary values

CHAPTER ONE: INTRODUCTION

1.0 Introduction

Bacterial growth has been identified as one of the foremost causes of water quality degradation within the drinking water distribution systems (DWDSs). Examples of undesired effects linked to bacterial growth include the proliferation of pathogens and coliforms, the reduction of hydraulic efficiency, unwanted colour, taste, odour, reduction of dissolved oxygen, the acceleration of pipe corrosion, and formation of biofilm [1,2,3].

The two major drivers of bacterial growth within DWDSs are the presence of nutrients and the lack of disinfectant residuals. Among other nutrients, organic carbon sustains heterotrophic bacteria (i.e. the group of microorganisms that use organic carbon as an electron donor to support growth and other functions). Humic and fulvic acids, carboxylic acids, proteins, carbohydrates, and other organic compounds contribute to the amount of organic carbon in DWDS. However, it is essential to indicate that the presence of natural organic matter (NOM) serves as a major nutritional factor limiting bacterial growth in many DWDSs [1, 2, 4]. Since the assimilable organic carbon (AOC) and biodegradable dissolved organic carbon (BDOC) being commonly used measures of biodegradable organic matter (BOM) concentration in DWDS, it becomes evident that the existence of natural organic matter (NOM) in water greatly affects its quality [1, 2, 3, 4, 5].

Previous studies have identified membrane separation process (MSP) as a reliable technology for enhancing the biological stability of contaminated water [6,7,8]. The Nanofiltration (NF) technology is the most preferred MSP ascribed to its ability to get rid of BOM from raw water and to subsequently reduce the possibility of bacterial regrowth within DWDS [6, 7, 8]. This is more likely due to the presence of small pore size on NF membranes [6, 7, 8]. However, there is only a few existing studies in the literature that discuss the removal of AOC and BDOC using MSP [6, 7, 8, 9, 10]. Previous studies have reported the success of utilizing NF membrane filtration in removing high molecular weight compounds (HMWC) commonly quantified as dissolved organic carbon (DOC) and BDOC. However, the rejection rate of low molecular weight compounds (LMWC), generally measured as AOC, depends on the membrane material and solution medium [6, 7, 8, 9, 10].

For example, a study on membrane filtration of water by Peter et al. [6] found that there was no statistically significant difference in AOC between raw water influent and membrane permeate. This means that biologically unstable drinking water was produced during the membrane filtration process. Whereas a study by Jurmu [7] investigated the effect of pretreatment on BOM elimination by nanofiltration. It was found that the removal of the lowest molecular weight fraction of BOM during the pretreatment process was significantly lower. In addition, the permeate contains organic compounds that can provide nutrients for microorganisms. Similarly, the results of the study conducted by Harma [10] in filtration experiments using dense NF membranes showed the total organic carbon (TOC) levels lower than 0.3 mg/L in all permeates. However, the eradication effectualness of AOC in water varies by about 25% depending on raw water quality. A study by Sari et al. [8] on the removal of BOM from water using MSP found that reducing the pore size of the ultrafiltration (UF) and NF membranes increased the removal potential of DOC. However, the removal of AOC in the study was incomplete. Another study by Hen and Efraim [9] on the removal of AOC and BDOC from water using 10 and 1 KDA membranes found that the removal efficiency was less than 30% and 48%, respectively.

These results highlight the varying levels of organic matter removal achieved through membrane technology, with differing impacts on AOC and BDOC removal. Overall, Zazouli and Kalenkesh [11] studied the applications of NF, UF, and microfiltration (MF) as different MSPs commonly used for the removal of DBPs precursors. It has been reported that NF is particularly efficacious in eliminating BOM compounds, even though it requires thorough pretreatment to prevent fouling. On the other hand, UF and MF membranes are not as efficient in retaining small BOM compounds. In conclusion, for the disinfection by-products (DBPs) precursors removal, NF appears to be the most suitable membrane separation process due to its effectiveness in removing BOM, provided that proper pretreatment measures are implemented to control fouling.

The goal of this study was to assess the effectualness of the hybrid adsorption-membrane filtration system in the removal of BOM from water and producing biologically stable water. Unfortunately, several studies have highlighted NF membrane fouling as a major challenge in NF technology [9, 10, 11, 12, 13, 14, 15, 16]. To date, powdered activated carbon (PAC) has been utilized in the adsorbent-NF membrane hybrid system. However, the bonding between BOM and PAC has led to

the formation of BOM-PAC particles that contribute to fouling of the membrane filtration [15]. Therefore, in this study, an ideal pretreatment process of drinking water was used before NF filtration tests to prevent membrane fouling. Multi-walled carbon nanotubes (MWCNTs) that have been functionalized with cetyltrimethylammonium bromide (CTAB) were used as the sorbent in the adsorption process to protect the membrane, enhance performance, and lessen fouling. The adsorption process offers several advantages for treating organic contaminants in drinking water. Firstly, it is a cost-efficient and practical method, making it suitable for large-scale implementation. The process uses adsorbent materials to remove contaminants effectively, resulting in improved water quality. Additionally, adsorption provides environmental benefits by minimizing the use of chemicals and producing less waste compared to other treatment methods [15, 16, 17].

Lijima [18] first identified carbon nanotubes, a form of carbon with a long, tubular structure and a graphitic lattice. Numerous studies aimed to assess the employment of carbon nanotubes (CNTs) for a variety of applications, including water treatment, to better understand their special physical, mechanical, electrical, magnetic, and thermal properties [19,20,21]. CNTs exhibit high adsorption ability for BOM, making them promising adsorbents for environmental remediation [19, 20, 21, 22]. The key challenge lies in enhancing the affinity of CNTs towards target compounds, and this can be achieved through functionalization techniques [23]. Their unique structural features, such as their mass, larger surface area, and thin, hollow, and layered structures, play a crucial role in adsorption [20, 22].

In this study, ready-made MWCNTs, purchased from Merck (South Africa) were used as adsorbents; however, unfunctionalized MWCNTs have hydrophobic characteristics and a propensity to aggregate. This is more likely due to electrostatic interactions between CNTs [24,25]. Therefore, the functionalization of MWCNTs was carried out using CTAB (a noncovalent functionalization process). The efficiency of CTAB as a reagent for functionalizing MWCNTs has been widely demonstrated [24]. Furthermore, it has been discovered that CTAB is a cationic surfactant with stable dispersion and hydrophilic properties that actively interacts with MWCNTs [25].

Fouling prevention is a critical aspect of nanofiltration (NF) membrane systems in water treatment. NF membranes, with their small pores ranging from 0.5 to 2 nm, effectively reject even tiny

uncharged solutes [26, 27, 28]. However, monovalent ions are still able to pass through, while multivalent ions are retained due to surface electrostatic properties. This ability to selectively fractionate and remove specific solutes makes NF membranes valuable in complex process streams. Nevertheless, because NF membranes are sensitive to fouling, extensive pretreatment is necessary to prevent scaling, colloidal, organic, and biological fouling during the water treatment process [27, 28, 29]. The hybrid adsorption-membrane filtration system, a key focus of this study, is a combine of the adsorption process and MSP. Its purpose is to effectively remove BOM from drinking water. By integrating these two processes, the system aims to address the issue of membrane fouling that typically occurs during membrane filtration, leading to increased operating costs. This innovative system offers a promising solution to improve the overall effectualness of water treatment processes, ensuring cleaner and safer drinking water for communities.

1.1 Research objective(S):

The key focus of this study was to assess the effectiveness of a hybrid adsorption-membrane filtration system in lowering the bacterial regrowth potential in water. Several filtration tests of raw water samples will be done after optimal pretreatment (with functionalized MWCNTs) to determine the improvement in operation (flux and rejection) of the NF membrane, contributing to the production of biologically stable drinking water.

The specific objectives of the research are as follows:

- To determine and validate the efficiencies of both AOC and BDOC protocols used in the measurement of bacterial growth in water collected from targeted water sources.
- To prepare flat sheet membranes using the phase inversion method.
- To functionalize MWCNTs through a noncovalent functionalization process.
- To characterize the nanostructured materials using microscopy techniques.
- To pretreat water by adsorption process of BOM in terms of AOC and BDOC.
- To test the effectualness of the MSP to remove BOM from the pre-treated raw water.

1.2 Research questions

In this research project, cogent scientific results will be provided to address the following questions:

- What are the methods to test the efficiencies of both AOC and BDOC protocols employed in the measurement of bacterial growth in water?
- What is the role of noncovalent functionalization of MWCNTs in the adsorption process of BOM from drinking water?
- What are the benefits of combining an adsorption process with an MSP?
- What are the performance characteristics of functionalized MWCNTs?
- What are the performance characteristics of NF polymeric membranes?

1.3 Expected contribution to knowledge

Strategies to mitigate the negative effects of BOM on water treatment methods are essential to make certain the production of safe and clean drinking water. However, the presence of BOM in drinking water influences significantly different water treatment processes, and it also affects water quality in the DWDSs. The presence of BOM in water increases water treatment costs and causes operational problems. Here are some ways NOM affects drinking water quality and water treatment processes:

- NOM significantly impacts taste, colour, and odour [1, 2].
- NOM results in increased requirements of disinfectants, coagulants, and oxidants in water treatment processes, making the treatment more challenging [1, 2].
- NOM can cause the corrosion of pipes and infrastructure within the water distribution system, leading to potential leaks and contamination of the water supply [1, 2].
- NOM contributes to the deterioration of the DWDSs, reducing its overall efficiency and reliability [1, 2].
- NOM promotes bacterial growth in the DWDS, posing a risk to public health [1, 2].
- NOM can interact with disinfectants, such as chlorine, resulting in the formation of hazardous DBPs. These DBPs can have adverse health effects when consumed [1, 2].

- NOM in the DWDS has significant implications for the overall water quality and the integrity of the infrastructure [1, 2].

The facts previously mentioned pose the greatest challenges to the production of biologically stable drinking water at lower cost. Therefore, it is essential to decide upon several problems associated with BOM in water during MSP. These problems include fouling, durability of the membrane, and cost among the doses of adsorbents, disinfectants, coagulants, and oxidants, needed for water treatment. As already stated, previous studies related to the BOM removal in water showed NF membrane filtration was effective in rejecting DOC and BDOC. However, AOC rejection varied according to the type of membrane and the environment in which the solution was being processed [6, 7, 8, 9, 10]. A review by Zazouli and Kalankesh [11] in their study on the removal of precursors of DBPs from drinking water demonstrated that NF membranes can effectively remove BOM, but a thorough pretreatment is needed to prevent fouling during membrane filtration. To date, PAC was employed to remove BOM fouling in adsorbent-membrane hybrid system by Elma et al. [15]; it has been found that the bonding of BOM with PAC particles produces additional foulants that block the pores of the membrane and leave a cake layer on the membrane surface. Therefore, in this study, an extensive adsorption process (with CTAB-functionalized MWCNTs) of drinking water was applied before NF filtration tests to avoid membrane fouling, protect the membrane, and improve the NF membrane performance for the optimal removal of both AOC and BDOC in drinking water. This will reduce the potential for bacterial regrowth within the DWDSs. It will consequently lower the cost of water treatment and operational problems during the production of biologically stable drinking water.

This study has developed an adsorption process coupled with NF membrane process based on the concept of multi-barrier approach which combines multiple drinking water treatment processes to enhance the reliability of the membrane.

- Hybrid adsorption-membrane filtration system, which is a combination of the adsorption process and membrane filtration process for the removal of BOM from drinking water was designed and introduced in this study to overcome membrane systems fouling that mainly occurs during the membrane filtration process and therefore will reduce the operation cost. This work contributed to the water quality engineering field and water treatment sector.

- The removal of AOC and BDOC from water was achieved using MWCNTs functionalized with CTAB. To preserve the functionalities needed for improved BOM capture and environmental safety, a non-covalent functionalization process was chosen in preference.
- This study offers sufficient details on the development and use of hybrid treatment technology to produce biologically stable drinking water. Future research on the removal of BOM from drinking water will be well-founded on the solid foundation created by this work.

1.4 Scope of research

The scope of this study includes the preparation and characterization of PSF membranes, the functionalization, and characterization of MWCNTs, the testing of both BDOC and AOC protocols for measuring bacterial growth in water collected from targeted water sources, and the evaluation of a hybrid adsorption-membrane filtration system to eradicate BOM from drinking water.

1.5 Organization of the thesis

In Chapter 1, a general introduction to the study, background information, problems, goals and objectives of the research, methods, and the anticipated contribution to knowledge are presented. The literature review of the basic ideas on earlier and more recent work related to this study are reviewed in Chapter 2. The materials and procedures used in the study are covered in Chapter 3 (Experimental Design). The mathematical modelling of the membrane filtration process is described in detail in Chapter 4 as a rational mathematical strategy created for the long-term viability of membrane filtration tests in this study. The findings following the characterization of CNTs and PSF membranes, as well as the identification of BOM are presented in chapter 5. The results of the processes for removing BOM (in terms of AOC and BDOC) from water through adsorption and membrane filtration are presented and discussed in Chapter 6. Chapter 7 presents a summary of the research, its findings, and suggestions for additional study. An extensive list of all references to this thesis appendices is provided at the end.

1.6 Summary

The background, problem statement, research questions, and research objectives were covered in this introductory chapter. The expected contribution to knowledge and the field of study were briefly described, and then the structure of the thesis.

1.7 References

- [1] Sillanpaa, M., (2014). Natural organic matter in water: Characterization and treatment methods. In proceedings. 57 Sillanp2014NaturalOM.
- [2] Miettinen, I., Vartiainen T., Martikainen T., (1999). Determination of assimilable organic carbon in humus-rich drinking waters, *Water Res.* 33, 2277–2282.
- [3] Yang, P., Huan, L., Xiangru, Z., Liang, A., (2016). Characterization of natural organic matter in drinking water: Sample preparation and analytical approaches, *Trends in Environ. Anal. Chem.* 12, 23–30.
- [4] Van der Kooij, (1992). Assimilable organic carbon as an indicator of bacterial regrowth, *J. Am. Water Works Assoc.*, 84, 57–65.
- [5] Moyo, G., Motsa, M., Chaukura, N., Msagato, T., Mamba, B., Heijman, S., Nkambule, T., (2022), Characterization of natural organic matter in South Africa drinking water treatment plants toward integrating ceramic membranes filtration, *Water Environ. Res.* 94, 10693.
- [6] Noble, P.A., Clark, D.L., Osborn, B.H., (2007). Biological stability of ground water treated for organic carbon removal by conventional and membrane filtration methods. *American water works association.* 88, 87-96.
- [7] Jurmu, J., (2016). Effect of prefiltration on natural organic matter removal by nanofiltration in drinking water treatment. In proceedings.
- [8] Sari, M., Mika, S., Amit, B., Mika, M., (2019). Natural organic matter removal from drinking water by membrane technology. *Academic journal.* 2, 13-22.

- [9] Hen, L.J., and Efrainsen, H., (2001). Assimilable organic carbon in molecular weight fractions of natural organic matter. *Water research*. 35, 1100-1410.
- [10] Harma, V., Tuloksia suomalaisilla pintavesiä ilia toksilla tehdyistä nanosuodatuskokeista *vestitalones*, 6 (1999) 5-10.
- [11] Mohammed, A.Z., Laleh, R.K., (2017). The removal of precursors and disinfection by-products (DBPs) by membrane filtration from water, a review. *Journal of Environmental health science and Engineering*, 15, DOI 10.1186.
- [12] Li, k., Liang, H., Qu, F.S., Shao, S.L., Yu, H.R., Han, Z.S., Du, X., Li, G.B., (2014). Control of natural organic matter fouling of ultrafiltration membrane by adsorption pretreatment. Comparison of mesoporous adsorbents resin and powdered activated carbon. *Journal of Membrane Science*, 471, 94-102.
- [13] Gong, H., Jin, Z.Y., Wang, Q.B., Zuo, J.N., Wu, J., Wang, K.J., (2017). Effects of adsorbent cake layer on membrane fouling during hybrid coagulation/ adsorption -microfiltration for sewage organic recovery. *Journal of Chemical Engineering*, 317, 751-757.
- [14] Kalaruban, M., Loganathan, P., Kandasamy, J., Vigneswaran, S., (2018). Submerged membrane adsorption hybrid system using four adsorbents to remove nitrate from water. *Journal of Environmental Science Pollution*, 25, 20328-20335.
- [15] Elma, M., Pratiwi, A.E., Rahma, A., Rampun, E.L.A., Mahmud, M., Abdi, C., Rosadi, R., Yanto, D.H.Y., Bilad, M.R., (2022). Combination of coagulation and ultrafiltration processes for Organic Matter removal from peat water. *Journal of Sustainability*, 13, 370.
- [16] Karwouska, B., Spierzynska, E., (2022). Organic Matter, and heavy metal removal from surface water in processes of oxidation with ozone, UV irradiation, coagulation, and adsorption. *Journal of Water*, 14, 3763.
- [17] Dabrowska, L., (2021). The effect of ozonation, coagulation, and adsorption on Natural Organic Matter removal. *Journal of Ecological Engineering*, 22, 216-223.
- [18] Lijima S., (1991). Helical microtubules of graphitic carbon, *nature*, 354 (7), 56-58.

- [19] Feifei, L., Jinlin, F., Guang, H.M., (2013). Adsorption of natural organic matter analogues by multi-walled carbon nanotubes. *Journal of Chemical Engineering* 219, 450-458.
- [20] Juta, S., Ateia, M., Yoshimura, C., (2018). Natural organic matter undergoes different molecular sieving by adsorption on activated carbon and carbon nanotubes. *Chemosphere* 203, 345-352.
- [21] Jeong, K., Kim, D.G., Ko, S., (2013). Adsorption characteristics of effluent organic matter and natural organic matter by carbon-based nanomaterials. *Journal of Civil Engineering* 339, 119-126.
- [22] De Volder, M.D., Tawfick, R., Baughman, R., Hart, A., (2013). Carbon nanotubes: Present and future commercial applications. *Journal of science* 339, 113-121.
- [23] Liu, X., Wang, M., Zhang, S., and Pam, B., (2013). Application potential of carbon nanotubes in water treatment. *Journal of Enviro. Sci.* 7, 1263-1280.
- [24] Thakur, V.K., and Thakur N.K., (2016). *Chemical functionalization of carbon nanomaterials: Chemistry and applications*. Boca Raton FL, CRC Press.
- [25] Jayant, F.G., Malappan, M., Sharanappa, T.N., (2017). CTAB functionalized multiwalled carbon nanotubes composite modified electrode for the determination of 6-mercaptopurine, sensing and bio-sensing research, 12, 1-7.
- [26] Shon, H.K., Phuntsho, S., Chandhay, D.S., Vigneswaran, S., Cho, J., (2013). Nanofiltration for water and wastewater treatment -a mini review. *Drink. Water Eng. Science* 6, 45-73.
- [27] Nystrom M., kaipi L., Luques S., (1995). Fouling and retention of nanofiltration membranes. *J. Membr. Sci.*, 98, 249 – 262.
- [28] Mohammed, A.Z., Susanto, H., Nasser, S., Ulbricht, M., (2010). Fouling effects of Humic and alginic acids in nanofiltration and influence of solution composition. *Journal of Desalination*, 2, 688-92.
- [29] Ersan, M.S., Ladner, D.A., Karanfil, T., (2016). The control of DBPs precursors by Nanofiltration. *Journal of Water Research*, 105, 274-81.

CHAPTER TWO: LITERATURE REVIEW

2.1. Natural organic matter

The NOM is a conglomerate of organic compounds with numerous molecular weights and structures. Animals, microbial organisms, and plants all degrade over time, which is where NOM comes from [1, 2, 3, 4, 5, and 13]. Depending on its place of origin, age, environment, and degree of transformation, NOM can vary greatly [6, 7, 8, 9, 10, 11, and 12]. The primary component of NOM is humic materials. Biopolymers like polysaccharides, proteins, lipids, and amino acids also contribute to the emergence of NOM. NOM causes aesthetic qualities like colour, odour, and taste in finished water, which poses serious problems. High NOM concentrations in raw water are also problematic as waters with high NOM concentrations require high coagulant doses when treated through coagulation, high ozone doses when treated through ozonation, shorter run times when treated by granular activated carbon filters and requires membrane regeneration, and when treated by chlorination waters with high NOM concentrations both had higher chlorine demands and a high potential for DBPs formation [13, 14, 15]. In addition to causing issues with the treatment of water, NOM acts as a source of nutrients for bacteria in the DWDSs [16], which result in bacterial growth [16]. Specifically, small organic acids can lead to the formation of biofilm in pipelines, and they can lead to bacterial activities in the DWDSs.

The structural characterization of NOM has drawn the attention of many studies; however, the exact nature of its structure is still unknown [17, 18, 19, 20, 21, 22, 23, 24, 26, 27, 28, 29, 30, and 31]. It is not practical to describe NOM because of an exhaustive compilation of the individual compounds because it may consist of a variety of chemical constituents [18]. As a result, scientists have discovered that classifying NOM into various chemical or fractional groups is more practical [20, 21, 22, 23, 24, and 25]. The concentration and fractionation of NOM into groups with similar properties is a step in several characterization techniques that have been used [32]. Some of these methods, however, have inherent flaws, such as those that may result from the overlapping of various fractions during fractionation [33, 34, 35, 36, 37, 38, and 39]. Additionally, the characterization process of NOM frequently requires deep pre-treatment of samples, which may change the NOM character [33, 34, 40, 41, and 42].

The DOC and total organic carbon (TOC), which also show how many unsaturated bonds are present in NOM, are the main techniques used to measure NOM concentration in water. While

NOM contains different compounds with different molecular weights and hydrophobicities, these methods use bulk parameters. The process must therefore be improved by using more NOM characterization techniques. SUVA in particular (UV254 absorbance) can be used to gauge the aromaticity of NOM [43]. Additionally, SUVA can be used to determine hydrophobicity [44, 45]. By using preparative DOC fractionation, the hydrophobicity of NOM fractions can be increased, and NOM is then split into hydrophilic and hydrophobic bases, neutrals, and acids [46, 47, 48, 49, 50]. BOM is organic material, plant, and animal matter with origin in living organisms, which can be converted by the action of microorganisms to water, carbon dioxide, and/or methane and biomass. The AOC method and BDOC method are the primary techniques employed for quantifying the LMW) and HMW of BOM influencing biological stability [48, 49, 50].

2.2 Characterization and quantification of natural organic matter

The efficiency of drinking water treatment processes to remove NOM can be influenced by the nature and character of the NOM present in the water prior treatment [51, 52, 53]. Therefore, the water treatment utilities must enhance the treatment processes for NOM removal to prevent the negative effects of NOM on water treatment and to guarantee that the treated water complies with standards. To achieve this, it is necessary to comprehend the properties of NOM and the effectiveness of its removal by different treatment processes. To better understand how the presence of NOM in water affects drinking water quality and water treatment processes, a variety of NOM characterization methods have been developed and discussed in this chapter [51, 52, 53, 54, 55, 56, and 57]. These characterization methods develop different analytical frameworks, NOM fractionations, the amount of time and expertise needed, the costs, and the outcomes [17, 58]. There is not a single method that can reveal all the characteristics of NOM required for the water treatment process, as demonstrated by a comparison of various NOM characterization techniques [18, 58, and 59]. To properly analyze the various fractions of NOM throughout the treatment process, a combination of various methods would be required.

2.2.1 Sample collection and preparation

Regardless of the procedure chosen for NOM analysis, strict adherence to the proper standard procedures (such as ASTM standards for water testing) should be ensured when collecting, handling, and analyzing samples. There should be as little external contamination during handling

as possible. Rapid analysis should be done on samples with an intense concentration in biodegradable organic matter to reduce the amount of NOM that is biodegraded and hydrolyzed. A sample should be stored at 4°C or lower if it cannot be analyzed right away.

2.2.2 Assimilable organic carbon

The concentration of AOC in water has a direct impact on microbial growth [110, 111]. Heterotrophic bacteria perform a negative role in water supplies, and their density is closely correlated to the AOC concentration. A study by Van der Kooij [110, 111] found that AOC concentrations below 10 g/l indicate that heterotrophic bacteria do not multiply significantly in unchlorinated water [110, 111]. This suggests that higher AOC concentrations promote microbial growth. As AOC represents the portion of TOC that can be easily assimilated by microbes for growth, measuring AOC concentration is an important factor in assessing water quality and determining its biostability [111]. Controlling AOC levels is therefore crucial in ensuring a safe water supply. The assessment of the AOC/BDOC ratio has important implications in understanding the biological stability of water [112]. A high AOC/BDOC ratio indicates a higher availability of organic carbon for microbial growth, suggesting a more biologically stable water system. This ratio can help in determining the potential for microbial activity and the overall health of the ecosystem [112]. Additionally, the AOC/BDOC ratio assessment is useful in water quality management, as it gives insights into the biodegradability of organic carbon and the potential for microbial contamination [102]. Additionally, the concentration of intracellular ATP [114], the heterotrophic plate count [113], or turbidity increase [115] are three ways to measure biomass in the methods for calculating AOC. These techniques evaluate the effectiveness of the treatment procedures, and there is ongoing discussion about which techniques the water treatment industry might find most beneficial.

2.2.3 Biodegradable dissolved organic carbon.

The BDOC can be measured using various biological methods [102, 103, 104, 105]. One commonly used method is the BDOC method, which involves measuring the amount of DOC mineralized by heterotrophic microorganisms [102, 103, 104, 105, 106, 107]. This method calculates the BDOC by determining the difference between the initial and final concentrations of DOC, utilizing an indigenous bacterial population [102, 103, 104, 105]. The key variation in

BDOC characterization techniques lies in the inoculation method. Some approaches employ suspended bacteria, while others use bacteria that are adhered to inert media or sand in a continuous reactor column. Standardizing BDOC measurement methods is important to ensure accurate and comparable results [106, 107]. The comparison study conducted on BDOC characterization procedures revealed that there is little variation among the different techniques used. This suggests that the procedure chosen may not have an important consequence on the results of BDOC experiments. Therefore, the choice of a characterization method is based on factors such as ease of use, time efficiency, and cost-effectiveness. These findings provide valuable insights for researchers and practitioners in the water treatment sector, allowing them to make informed decisions when conducting BDOC experiments. Additionally, the study highlights the potential for the proposed technique by Servais et al. [103, 104] as a viable option for BDOC characterization in both drinking water and surface water systems. Monitoring BDOC levels in water treatment is significant [103, 108]. BDOC contributes to a range of 10-30% of the TDOC in water [109]. It has been shown that the eradication of BOM from treated water constrains bacterial growth, as demonstrated by Block et al [110]. Furthermore, to make certain the production of biologically stable water, it is recommended that the BDOC concentration in water should not surpass 0.16 mg/L [104]. Therefore, monitoring BDOC levels in water treatment is essential for ensuring the quality and stability of drinking water [103, 104, 108, 109]. By understanding and managing BDOC, strategies can be implemented to reduce its presence in treated water, ultimately improving water treatment processes [103, 104]. However, potential challenges and future research in managing BDOC should also be considered to continually enhance water treatment techniques.

2.2.4 Total organic carbon and dissolved organic carbon.

The principle of TOC analysis is to measure the quantity of carbon in a sample that contains both organic and inorganic carbon. Sample preparation requires the elimination of inorganic carbon and the conversion of organic carbon to carbon dioxide [60, 61, 62]. Basically, TOC analysis utilizes high temperature combustion and non-dispersive infrared sensing [60]. Interpretation of TOC results provide information about the organic carbon content of the sample [60, 61]. DOC analysis aims to determine the amount of dissolved carbon in a sample. Sample collection and storage are critical to maintain the integrity of the concentration of DOC in water. Methods for

DOC analysis include filtration to separate dissolved carbon from particulate carbon and oxidation in order to make easy the conversion of organic carbon to carbon dioxide. Several factors can affect DOC concentrations, including microbial activity and land use [60, 61, 62]. Quantification of NOM using these methods is important for several applications. NOM can affect the environment and water quality, and its presence can help assess water quality. Understanding the proportions of POC and DOC in TOC is essential for comprehensively characterizing NOM. A key method for separating DOC and POC is filtration, using a 0.45 μm porosity membrane filter [62]. This filter effectively separates the larger particulate matter from the dissolved organic carbon. By analyzing the content that passes through the filter, the concentrations of DOC and POC can be determined [62]. This differentiation is significant as it provides insight into the distribution and composition of organic carbon in different environments. Additionally, it allows for an enhanced comprehension of the factors that influence TOC and DOC concentrations, such as the filtration process and the use of specific techniques like wet chemical oxidation and high-temperature combustion [62]. Figure 2.1 illustrates the dissociation between DOC and POC based on filtration through a membrane filter with a porosity of 0.45 μm .

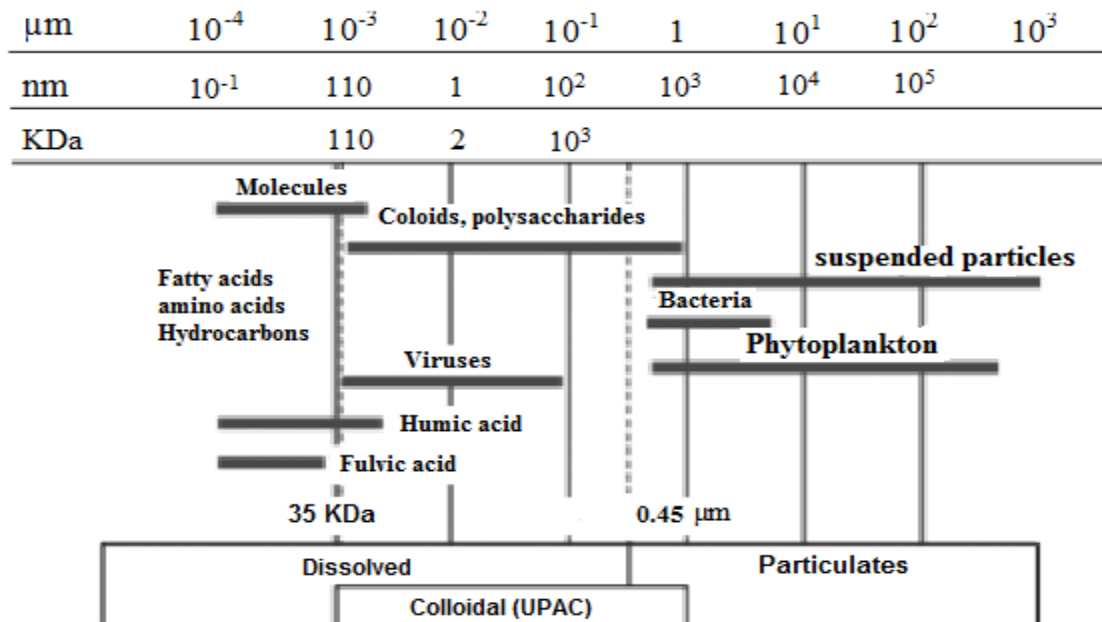


Figure 2.1 Continuum of dissolved and particulate organic carbon in natural waters (Aike and Leenheer, [62]).

2.2.5 Dissolved organic nitrogen.

The dissolved organic nitrogen (DON) is an important component of natural waters, consisting primarily of degraded peptides, porphyrins, and amino sugars [76, 77]. While DON makes up a smaller portion of total dissolved nitrogen (TDN) in waters impacted by human activity, it is the main type of TDN in unaffected waters [78]. DON takes a significant part in water quality, acting as a filtration membrane foulant and contributing to disinfectant demand and the production of DBPs [79, 80, 81]. Additionally, DON could react with free chlorine and inorganic chloramines to form organic chloramines, which have limited bacterial activity compared to their counterparts [82]. DON in water can be identified from several sources, such as runoff from agricultural areas that have been fertilized, forest litter, wastewater discharge, urban runoff, and naturally occurring biological processes like the excretion of algae products in eutrophic surface waters [83, 84, and 85].

Several methods can be used to quantitatively measure DON concentrations in water; however, subtraction methods are effective because they allow direct quantification of DON in water but can be challenging due to the presence of inorganic nitrogen species such as NH_4^+ , NO_2^- , and NO_3^- [85]. To overcome this challenge, the subtraction method involves measuring and quantifying the TDN concentration in the water sample, along with the dissolved inorganic nitrogen (DIN) concentration [86]. By subtracting the DIN concentration from the TDN concentration, the DON concentration can be calculated. This method allows for the accurate quantification of DON, providing valuable insights into nutrient cycling in aquatic ecosystems and assessing water quality and pollution levels [85, 86]. Additionally, it helps in monitoring the influence of human activities on the dynamics of DON in water.

Furthermore, large DIN/TDN ratios may cause the variance to exceed the estimated DON concentration. To convert all DON to DIN, oxidation or combustion is needed, which makes it impossible to measure the TDN concentration directly. While several techniques have been employed to quantify DIN species, ion chromatographic and colorimetric methods are the most widely used [76]. The various techniques for breaking down organic nitrogen were examined by Westerhoff and Mash [85]. There are now three different kinds of DON to DIN digestion techniques in use: wet oxidation, photolytic oxidation, and high-temperature oxidation. The measurement of inorganic nitrogen species in solution serves as the foundation for both wet and

photolytic oxidations. Through chemiluminescence and ozonation detection, the high-temperature oxidation method indirectly measures nitrogen oxide. Water samples with low DON concentrations cannot be analyzed using the digestion method, which is primarily used for wastewater analysis [87].

2.2.6 XAD resin fractionation

An alternative method for DOC fractionation is XAD resin fractionation. This method enables the classification of dissolved organics according to their properties (acidic, neutral, basic) polarity (hydrophobic/hydrophilic), compound-class properties, compound-specific properties, and compound-complex properties [73]. Polarity-based fractionation of NOM in water samples is a crucial step in analyzing NOM using non-ionic resin sorbents. This process involves the utilization of Amberlite XAD-4 and XAD-8 resins, which have different affinities for polar and non-polar compounds [74]. By applying sequential sorption chromatography, these resins can selectively capture, and separate NOM fractions in accordance with their polarity. This method is especially important for comprehending the role of NOM in water quality, as different polarity fractions may have varying impacts on water treatment processes and environmental behavior [74, 75].

Due to the chemical complexity and heterogeneous nature of NOM, introducing a fractionation step can help reduce the molecular heterogeneity of NOM and provide better insight into its chemical composition [73]. The characterization techniques based on fractionation isolate the group of compounds present in the NOM based on physical properties. These fractionation techniques may be used in combination with spectroscopic methods. Each fraction exhibits different characteristics in terms of molecular weight. For example, the hydrophobic fraction of NOM with high molecular weight is less soluble in water and can be effectively removed by coagulation, whereas the hydrophilic fraction with high molecular weight is more soluble in water and therefore they would be difficult to remove [74, 75].

2.2.7 Ultraviolet absorbance

Determining the optimal wavelength for NOM quantification is an important aspect of UV absorption [63, 64, 65]. By choosing the right wavelength, you can accurately ascertain the concentration of NOM in the sample. This is because the absorbance at certain wavelengths is

directly related to the NOM concentration [67, 68, 69]. The wavelength commonly used for this purpose is 254 nm, which has been shown to provide reliable and consistent results [67, 68, 69]. However, it is necessary to note that the optimal wavelength may vary based on the characteristics of the sample and the specific contaminants present. Therefore, careful analysis and experimentation are recommended and required to determine the most suitable wavelength for NOM quantification in different water sources. This information is essential for assessing water quality, NOM eradication from water treatment processes, and ensuring measurement accuracy and reliability [67, 68, 69, 70].

2.2.8 Differential ultraviolet absorbance

Exploring new forcing parameters for differential spectroscopy involves investigating additional factors that can cause a shift in the UV absorbance of NOM. These forcing parameters, such as different types of treatment like ozonation or halogenation could give valuable indications into the chemical characteristics of UV-absorbing species [70]. By using differential UV absorbance spectroscopy, it becomes possible to selectively analyze the chromophores that are influenced by these specific forcing functions [70]. The monitoring of the transformation of NOM species by procedures like ozonation or chlorination can also be done in water treatment facilities using UVA. For instance, UVA is measured in the ozonation process as the difference between a sample's UV absorbance before and after the process. The differential absorbance for chlorinated surface water at wavelengths around 272 nm (UV_{272}) depends on the concentrations of the various DBPs as well as total organic halogens [72].

2.2.9 Size exclusion chromatography

In the identification of various NOM components, size exclusion chromatography (SEC) is used to separate NOM components based on their size [93, 94]. This technique allows for the identification of different components, such as amphiphilic compounds, polysaccharides, humic substances, building blocks (hydrolysates of humic substances), LMW acids, and LMW neutrals [95]. By analyzing the peaks in SEC chromatograms, the molecular weights (MW) of these components can be determined. SEC chromatography is a valuable tool for studying the size differences and distributions of NOM components, providing important insights into their structure

and behavior [93, 94, 95]. Figure 2.2 shows a chromatogram (SEC-DOC) depicting of various fractions of NOM.

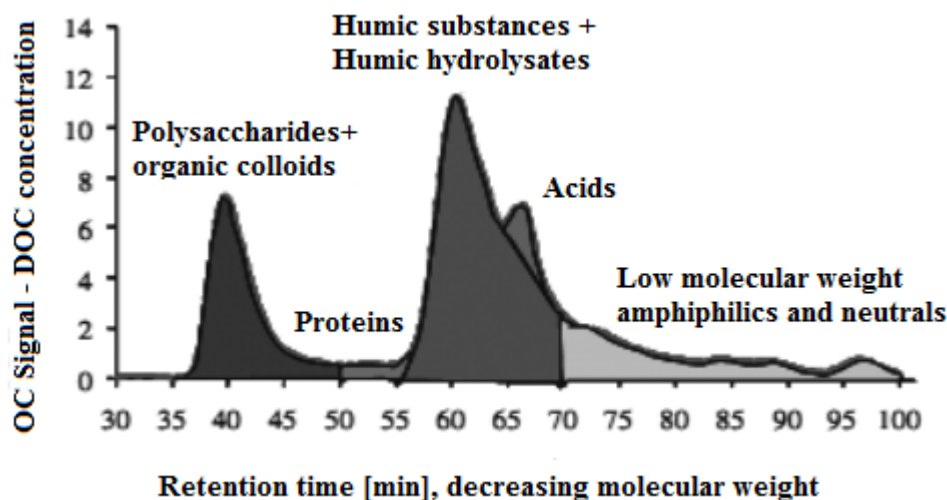


Figure 2.2 A chromatogram (SEC-DOC) depicting of various fractions of NOM.

UV detection takes a crucial part in the analysis of NOM in MW/MS calculations. It has been found that UV detection is particularly effective in detecting humic substances in NOM. However, UV detection is limited in its ability to accurately detect non-humic components such as proteins and polysaccharides. This ineffectiveness poses challenges in accurately analyzing and quantifying these components using UV detection methods [93, 94]. It has been found that non-humic components of NOM can cause problems with water treatment. For instance, it has been demonstrated that polysaccharides constitute a major membrane foulant [93, 94]. Certain other parameters such as hydrophobicity, hydrophilicity, steric effects charge, and molecular structure can also constitute the factors that may impact the result [95]. Figure 2.3 shows a chromatogram of the foulants that were extracted from a NF filtration membrane.

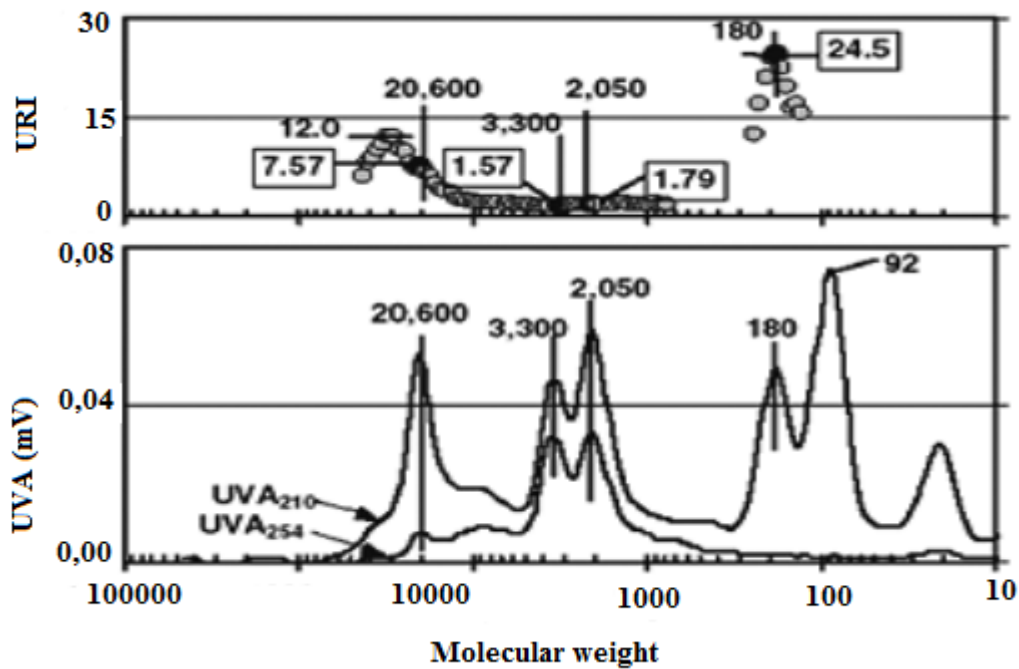


Figure 2.3 A chromatograms of the foulant that was extracted from a nanofiltration (NF) membrane at 210 nm and 254 nm (adapted from Amy and Her, 2004).

The variable wavelength UV detectors and fluorescence have been coupled with SEC by Her et al.[96] to study the differentiation between NOM substances that are more sensitively detected at 254 nm and NOM substances that are detected at other UV wavelengths. The UVA ratio index (URI) was established to differentiate between different substances. Proteins and amino acids have a wavelength of 210 nm (Figure 2.3), while humic components are located within a URI range of 1.5 to 2.0. Proteins and their amino acid building blocks exhibit higher URI values of 5 to 10 (Figure 2.4). The fluorescence intensity and spectral shape of NOM substances depend on their excitation under UV light, composition, and concentration [96]. Figure 2.4 shows a chromatogram of surface water.

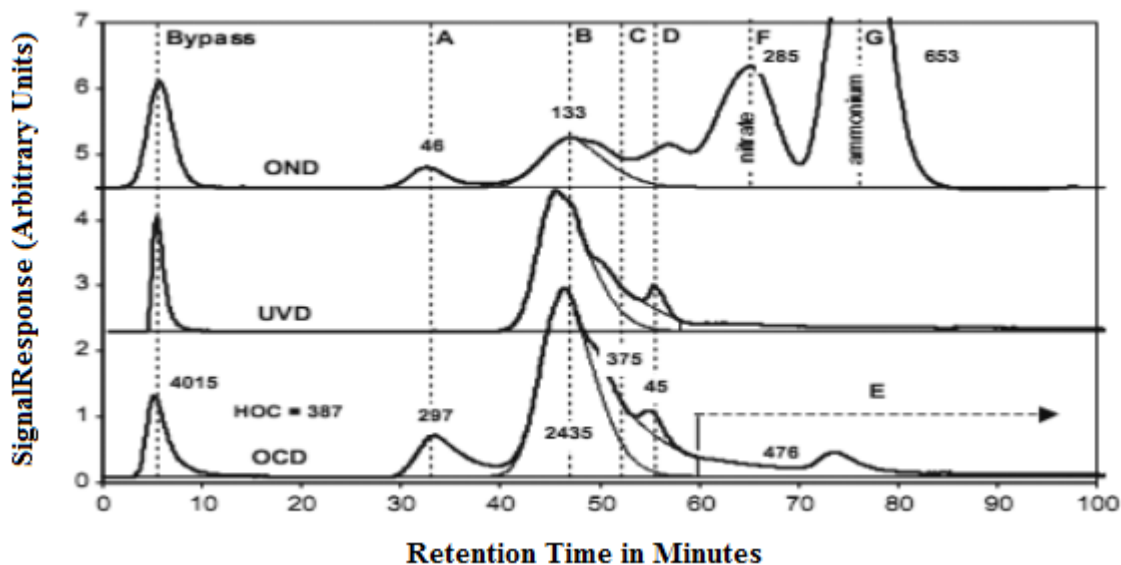


Figure 2.4 A chromatogram of surface water SEC-OCD data. (Heber et al.,2011).

2.2.10 The Polarity rapid evaluation technique

A brand-new method based on polarity that utilizes numerous solid-phase extraction cartridges in parallel is called the polarity rapid evaluation technique (PRET). The NOM characterization process has been used this method [116]. The absorption of NOM onto each other's SPE is analyzed and evaluated under ambient conditions to ascertain the total polarity of NOM. PRET was initially developed to specify the NOM polarity variation in the water treatment process. Later, its application was created to carry out the natural water analysis [117, 118]. PRAM offers distinct advantages over the XAD method, as it allows for the utilization of small sample volumes and ambient conditions. In PRAM, the characterization of organic matter is achieved using different sorbents placed in parallel in the cartridges. These sorbents include polar sorbents (Diol, CN, and Silica), non-polar sorbents (C_{18} and C_{12}), and anion exchange sorbents (NH_2 and SAX). Each sorbent serves a specific purpose in characterizing hydrophilic organic matter, hydrophobic organic matter, and the negative charge of bulk organic matter respectively [117, 118]. By utilizing these diverse sorbents, PRAM enables the comprehensive understanding and evaluation of organic matter composition in a rapid and efficacious manner. To quantify the specific fractions of NOM absorbed by the different SPE sorbents, PRAM uses DOC or UVA-254 concentration breakthrough curves normalized to the initial samples. Retention coefficient (RC) is a term used

to describe the ability of each SPE sorbent to absorb a particular NOM component [119]. Due to its simplicity, high sensitivity, and minimal interference, UVA-254 is the main detection method for samples of water.

In the United States of America, specifically in Las Vegas metropolitan area, PRAM was performed in four main tributaries of a lake reservoir to quantify and identify (characterize) DOM [118]. It has been proved through polarity analysis that there is a temporal variation of individual waters at a specific location. It has also been revealed that there are clear differences in hydrophobic and hydrophilic properties between various waters [118]. The effectiveness of ozonation compared to coagulation, flocculation, and biofiltration in treating NOM in water has been explored. Research conducted by Rozario et al. [116] demonstrated that the polarity of NOM changes throughout ozonation, with a reduction in hydrophobic character and a rise in polarity [116, 119]. Additionally, the study found that the coagulation, flocculation, and biofiltration processes also contribute to a decrease in the hydrophobic and hydrophilic characteristics of NOM [119, 120]. These findings highlight the contrasting impacts of ozonation and other treatment processes on the polarity and hydrophobicity of NOM, providing insights into the potential effectiveness of different treatment approaches for NOM removal. Since the variations of polarity occur during the pilot plant run, therefore an optimal evaluation and monitoring of NOM through unit operation must be performed.

2.3 The presence of natural organic matter in drinking water treatment

2.3.1 The impact of natural organic matter on water treatment

The existence of NOM in water has a significant effect on water treatment process and water quality. One significant impact is the development of issues with taste, colour, and odour [1, 2]. This requires additional measures to make certain that the water meets quality standards. Additionally, the existence of NOM in water increases the quantities of coagulants, oxidants, and disinfectants necessary for treatment, leading to higher costs and potential operational challenges [1,12]. Moreover, the reaction of NOM with chlorine or other oxidants and disinfectants can provoke the formation of hazardous DBPs [3]. Another consequence of NOM is membrane fouling, which blocks the clean water flux through the membrane permeates [3]. The NOM clashes with target organic micropollutants for adsorption sites in activated carbon filters, affecting their

adsorption capacity and kinetics [1, 2]. Additionally, NOM promotes the development of bacteria in distributed water systems, leading to potential health risks [3]. Lastly, NOM causes an increase in pipe corrosion and contributes to the deterioration of the overall distribution system integrity, further compromising water quality [1, 2]. These effects highlight the importance of effectively managing NOM to secure high-quality drinking water.

2.3.2 Application of water treatment techniques for the removal of natural organic matter.

Drinking water treatment methods are essential for the removal of NOM, which can pose health risks if not properly addressed [120]. This section provides an outline of various techniques applied in the removal of NOM from drinking water. The physical treatment methods include coagulation and flocculation, filtration, and sedimentation [120, 121]. Coagulation and flocculation imply the introduction of chemicals to assist the clumping together of particles, making them easier to remove. Sedimentation allows the particles to settle down by gravity, while filtration involves passing water through a porous medium to trap organic matter [120, 121]. Chemical treatment methods, including advanced oxidation, chlorination, and ozonation processes, utilize disinfectants and oxidants to destroy and remove organic compounds [120, 121]. Biological treatment methods, including activated carbon filtration, biological filtration, and membrane bioreactors, rely on living organisms or biological substances to degrade and remove organic matter [121]. These methods collectively contribute to make certain the quality and safety of drinking water by effectively removing organic contaminants [120, 121]. The efficiency of this removal process devolves on diverse aspects, such as the techniques used and the characteristics and concentration of the organic matter present in water. LMW organic matter, particularly the portion with a molecular weight around 500 Dalton, is more challenging to remove compared to HMW organic matter [120, 121]. Conventional treatment processes may have limitations in removing organic matter with high charge density (highest carboxylic functionality) due to their complex character. Advancements in water treatment techniques are being explored to overcome these challenges and improve the removal of organic matter [120, 121]. Following are water treatment technics that could be applied to eliminate NOM from water:

Enhanced coagulation

The process of enhanced coagulation involves neutralizing the charge and conditioning suspended colloidal and dissolved matter using chemical coagulants. Coagulation with iron salts and aluminium has shown to be more effective for the elimination of NOM, as measured by the TOC and eradication effectiveness ranging between 25% to 70%. Coagulation has a selective effect, with a preference for removing the HMW and hydrophobic fraction of NOM over the LMW compounds and hydrophilic fraction [124]. The HMW compounds consist primarily of nitrogenous organic carbon and aliphatic compounds, such as proteins, carbohydrates, and carboxylic acids, while the hydrophilic fraction is composed mainly of humic substances, including fulvic and humic acids. These humic substances are characterized by their significant presence of phenolic structures and aromatic carbon [122, 123, 124, 125, 126]. The coagulation process is more effective in reducing NOM when sufficient coagulant is added to address the charge demand of raw water [124]. Other factors that can affect the performance of coagulants are temperature, turbidity, several common anions which can form complexes with aluminium and iron this affecting the hydroxide precipitation and alkalinity pH [125, 126].

Adsorption process with activated carbon

Activated carbon (AC) serves as a highly effective method for water treatment, with various mechanisms at play [127]. The sorption process of organic compounds is a primary mechanism, whereby the activated carbon acts as a sorbent to eliminate undesirable organic compounds from drinking water. This includes the removal of pesticides, as well as substances responsible for colour, taste, and odour. Moreover, activated carbon has the capability to effectively clash with NOM for adsorption sites, further enhancing its water treatment capabilities [127]. Multiple aspects exert influence on the adsorption efficiency of AC, such as organic compounds and the nature of the water source [127]. Despite its effectiveness, considerations and limitations still exist, including cost and practicality, regeneration, and disposal of spent activated carbon, and the need for further research and development to improve its performance in different water sources. Additionally, AC can be applied in two forms: GAC and PAC [127]. PAC is particularly effective in eliminating NOM, which often results in unpleasant odours and tastes in water. Moreover, PAC can remove synthetic organic chemicals and reduce the levels of AOC. However, a previous study

has found that using PAC as adsorbent can lead to the bonding BOM with PAC particles and produce additional foulants that block the pores of the membrane and leave a cake layer on the membrane surface [127]. On the other hand, GAC filters assist as a biodegradation technique for the removal of organic carbon. These filters offer several advantages, although their efficiency can be influenced by various factors [127]. One disadvantage of GAC is that it is not feasible to regenerate activated carbon for high water purity applications without excessive operational costs because this process requires high temperatures (800-1000°C) and therefore excessive energy which in-turn implies higher costs [127].

Ion exchange

The most popular method for removing NOM from waters that contain LMW humic is ion exchange. The hydrophobic interactions take a significant part in the ion exchange process for the elimination of NOM from water [128, 129, 130]. However, the main mechanism for NOM removal is electrostatic interaction (IEX). Factors such as alkalinity, hardness, and pH of the water, as well as the characteristics of the anionic exchange resins (AER) used, can influence the effectiveness of NOM removal. Microporous AER is more effective because most NOM compounds are negatively charged. An innovative method in this field is the utilization of Magnetic Ion Exchange Resin (MIEX), which is smaller in size and offers 2 to 5 times better removal efficiency [130, 131, 132]. Enhancing NOM removal with MIEX resin involves utilizing its smaller size to allow for easier dispersion of NOM into or out of the resin. This not only improves NOM removal, but also increases regeneration efficiency [128, 129]. To address the challenges of high head loss and backwashing, MIEX resin is commonly employed in a continuously stirred reactor. MIEX resin could eliminate between 30% and 70% of DOC from water [128, 129, 130]. Research has shown that MIEX is more effective at removing organic acids and molecules of different weights compared to coagulation methods [128, 129, 130, 131, 132, 133].

Furthermore, MIEX is more effective in removing hydrophilic and low molecular weight (LMW) fractions of humic substances that are difficult to coagulate, especially when the water has low turbidity and colour [129, 130]. However, the effectualness of NOM removal by MIEX depends on the following conditions: the water quality, the properties of the resin, and the nature of the NOM [128, 129, 130].

Ozonation

The Ozonation process is typically performed in conjunction with other treatment techniques for the purpose of eliminating NOM from water. It is mainly used before the GAC filter to improve the biodegradation of ozonated organic carbon by degrading the recalcitrant organic matter. However, it is difficult to remove these fractions by adsorption on GAC or in biofilters due to their increased polarity. Generally, ozonation leads to a decrease of NOM absorbability because it provides more hydrophilic and polar compounds. Several parameters influence NOM removal by ozone-enhanced biofiltration, such as the water quality parameters (pH, temperature, alkalinity, and dissolved oxygen), the employed ozone dose, and the properties of NOM in the water [135]. It has been found that ozone interacts most strongly along with the aromatic portion of NOM before lowering the SUVA of the water. When using ozone-enhanced biofiltration to remove NOM from water, the ozone dose needs to be optimized [136]. Prior to the biofiltration process, specific ozone doses (0.15–1.0 mg/l) are frequently used. It has been found that the biodegradability of NOM does not actually increase with an increase in ozone dose [137]. However, when bromate, which is present in water, interacts with ozone during the ozonation process, bromate (DBPs) may be formed. The use of ozonation leads to a decrease in the formation of trihalomethanes (THMs) and halo acetic acids (HAAs) upon subsequent chlorination [135, 136]. When followed by biological treatment (biofiltration or activated carbon filtration), it is one of the promising processes for removing DOC by transforming it to a biodegradable form such as BDOC [136, 137].

Membrane separation process

Membrane separation processes are highly efficient and useful separation methods because they offer many advantages over conventional processes (liquid-liquid extraction, distillation, absorption) processes, such as simple and compact set-up [138], easy operation at room temperature and pressure [143], simple scaling and reduction [185], better energy efficiency [199], high purity products [1185] and much lower environmental impact [138]. The most common membrane separation processes include microfiltration, ultrafiltration, dialysis, nanofiltration, pervaporation, gas separation and reverse osmosis [143].

Advances in membrane separation technology have shown promising potential for improving the efficiency and effectiveness of water treatment processes [138, 143]. One notable advancement is the use of nanofiltration and ultrafiltration techniques in sequence, allowing for the targeted elimination of different portions of NOM from water sources [138]. Nanofiltration membranes are effective in removing BOM components with lower molecular weight, while ultrafiltration membranes are better suited for removing larger molecular weight fractions [185, 199]. This complementary approach ensures a more thorough removal of BOM, which can improve the overall water quality [138, 199, 200]. Additionally, ongoing research in membrane separation technology aims to improve the performance and durability of membranes filtration, leading to more sustainable and cost-effective water treatment solutions in the future.

Bank filtration

Bank filtration (BF) can be employed as a pre-treatment for lake or river water treatment to produce potable water. BF removes solid particles, nitrogen species, organic compounds, viruses, bacteria, and parasites [139]. It has been found that BF effectively removes organic micropollutants and bulk BOM [139]. Although BF has proven to be a good pretreatment technique for many organic compounds, it has been found that some compounds, such as certain pesticides, pharmaceuticals, and halogenated organic compounds are more resistant to removal [139, 140]. Furthermore, the removal of BOM through BF is most efficient when groundwater velocity is slow and when the aquifer consists of granular materials with high grain surface contact. Levels of many organic micropollutants can be reduced or even eliminated during both aerobic and anaerobic underground passages [139, 140]. Attenuation is extremely dependent on the underlying redox processes [139, 140].

Hybrid treatment systems

It has been investigated how various techniques can be combined to eradicate BOM from water. The aim of the hybrid processes is to maximize the complete removal of the various BOM portions from water [141]. These combined treatment methods may involve membrane separation processes, ozonation biofiltration, activated carbon filtration with reverse osmosis, ion exchange-activated carbon, coagulation-ultrafiltration, or other methods [142, 143].

Chloramination and nitrification

Initially, the combination of chlorine and ammonia to produce chloramines was performed to research on odour and taste control until it became globally adopted during the 1930s and 1950s [144]. DBPs regulations were the main drivers of the move to using chloramines as residual disinfectants, and eventually as a primary disinfectant in the USA [146, 147]. The combination of ammonia and chlorine lessens the formation of such DBPs formation as trihalomethanes [144, 145]. However, there is a lack of precise procedures and methods of chlorine addition [148].

Odell et al. [149] discovered that two-thirds of U.S.A DWDs experienced problems with chlorination due to the nitrification reaction. Appropriate monitoring techniques such as reducing the available ammonia, flushing (cleaning) the water distribution system, periodic breakpoint chlorination, increasing chloramine residual, and lowering system hydraulic retention times [149]. Storage time is a crucial factor in covered reservoirs and storage tanks because it has been seen that when nitrification associated with prolonged storage, the concentrations of ammonia fall, nitrite levels rise to 0.1 mg/L, and nitrate levels remain stable.

Generally, a dropping of chloramines residual in the dead ends of the treatment module can be used as one of the main indicators of nitrification. However, a significant lag occurs between the outset of ammonia to nitrate conversion and the depleting of chloramine residual [144, 149]. Researchers proved that increased HPCs and pH contribute to the acceleration of nitrification events. It has also been found that in scenarios where HPC remains stable while dissolved oxygen (DO) decreases the nitrification process can be accelerated [149]. Odell et al. [149] also discovered that nitrification is unlikely under low dissolved oxygen conditions but can occur in a system that contains low ammonia concentration if other conditions (e.g., availability of DO and temperatures above 25° C) are met. The removal of NOM leads to more biologically stable water [149]. Odell et al. [149] stated that treatment processes that lead to the NOM removal (for instance biologically active filters) decrease the Nitrification process efficiency in the DWDs [149,150 and 151]. Odell et al. [149] assessed the different Nitrification control methods for both short period and long-term; they found that once or twice a year for a duration of one week to four weeks, breakpoint chlorination is frequently used. The chloramine residuals (2, 3 mg/L) in the DWDs can be used as a factor of nitrification prevention [149].

2.4 Physico-chemical parameters

The assessment of physico-chemical parameters is generally considered to get guidelines and categorize the physico-chemical water quality. The parameters that are frequently sampled or monitored of water quality include the following:

pH

pH is crucial indicator in monitor the quality of water, which can be considered as a response and indicative through physical, chemical, and biological processes. Monitoring pH throughout the water distribution system can provide information necessary to understand and track stability [152, 153]. For instance, it has been found that the change in pH can indicate potential problems with corrosion control or can be the result of nitrification [153].

Temperature

Temperature is one of the parameters used to monitor the quality of water, which can be considered as an essential indicator in water systems since it can lead to every physical, chemical, and biological interaction. Therefore, it is particularly important for water quality monitoring programs to track temperature routinely [152].

Alkalinity

Alkalinity is simply defined as a gauge for how effectively water can neutralize acids [154,155]. Bicarbonate, carbonate, and hydroxide ions are primarily responsible for the alkalinity of water [155]. Furthermore, bicarbonate is ascertained as the primary source of water alkalinity, whereas carbonates and hydroxides are only more significant when algae activity is high and for specific kinds of industrial water and wastewater [155]. The presence of weak acids and salts like silicates, phosphates, and borates also helps to keep water alkaline [155,156]. Alkalinity is a key criterion in water treatment due to its capacity to control pH.

Conductivity

The conductivity of water is defined as the capacity of water to carry an electrical current. Generally, an ion can be described as an atom that has lost or gained an electron. A positive or negative state is produced by this activity [157]. For instance, when sodium chloride is dissolved

in water, it dissociates into chloride ions (Cl^-) and a solution of sodium ions (Na^+). These ions then enable the water to conduct electricity [158, 159]. Understanding the importance of conductivity in water is crucial, as it has various implications [158]. Water conductivity can affect drinking water quality, industrial applications, and even the behavior of aquatic ecosystems. By studying and monitoring water conductivity, we can gain valuable insights into its overall health and the potential presence of contaminants [159].

2.5 Polymeric filtration membranes

A filtration membrane is a porous barricade that selectively admits certain molecules to pass through while blocking others. It differs from a filter, which is typically used for larger particles. Membrane separation procedures involve the use of gradients in concentration, pressure, temperature, and other factors to facilitate the movement of molecules. These membranes can be either natural or artificial [160, 161]. Porous and non-porous membranes are both capable of separating two phases, as seen in Figure 2.5.

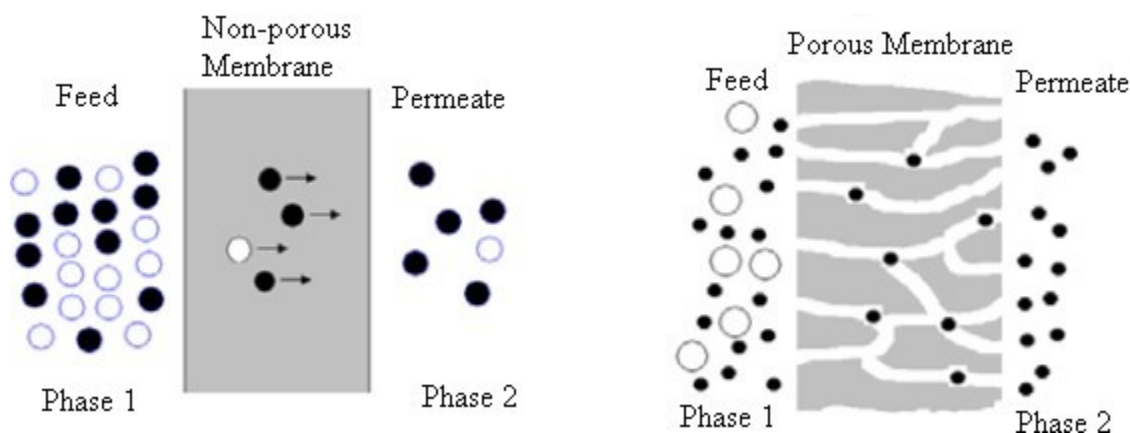


Figure 2.5 Schematic diagram of two-phase separation by non-porous and porous filter membranes.

Artificial made membranes could be subdivided into two main groups: inorganic membranes and organic membranes, depending on the materials that make them up. A polymer membrane is an organic membrane, while a ceramic, metal, or glass membrane is an inorganic membrane [161].

Its structure affects how membranes separate. Artificial filtration membranes can be categorized as symmetric or asymmetric depending on their morphology or structure [161].

2.5.1 Isotropic membranes

Isotropic filtration membranes mainly have a constant composition throughout, and it is designed with equal pore sizes throughout the membrane, allowing for consistent filtration performance [160]. It is characterized by its material composition, porosity, flow rate, and filtration effectualness [160]. The rate of permeation is accelerated by a reduction in membrane thickness. Symmetric membranes include dense, electrically charged, microporous, non-porous, and non-dense membranes [160].

2.5.2 Microporous membranes

Microporous membranes are like the conventional filter in their structure and function. They possess highly voided structures along with interconnected and randomly distributed pores [160]. The separation of the particles takes place by sieving effect mechanism where the particles larger than the membrane pores are rejected while the smaller particles pass through the membrane pores [160]. This type of membrane is used for microfiltration and ultrafiltration membrane processes which find application in breweries, the pharmaceutical industry and wastewater treatment from chemical industries. [161].

2.5.3 Non-porous membranes

In response to gradients in pressure, concentration, or electrical potential, permeation (liquid or gas) is transported through the non-porous membranes' non-porous films [160]. Separated species' solubility and diffusion in the membrane material control the rate at which they are transported through non-porous membranes [161]. Non-porous membranes are used in operations like reverse osmosis, pervaporation separation, and gas separation. Since mixtures typically permeate rigid films slowly, dense membranes often in the form of composite asymmetric membranes are frequently used in industrial settings to increase flux [162].

2.5.4 Anisotropic membranes

Anisotropic membranes, specifically composite membranes, offer advantages in water desalination due to their thin and dense selective layers [160, 162]. These membranes are designed with a noticeable difference in thickness between the two sides, providing different functional properties. This anisotropic enables the membranes to be employed in a diversity of applications, such as water filtration, gas separation, biomedical and pharmaceutical applications [160]. Loeb and Sourirajan [162] developed for the first time an asymmetric filtration membrane, which has been a breakthrough in desalination technology. These anisotropic membranes with thin and dense selective layers provide high permeability fluxes while using less energy. Composite membranes, which include a porous membrane support cast as a thin, dense selective layer, further contribute to the efficiency of water desalination processes [160, 161, 162].

2.5.5 Liquid filtration membranes

Liquid membranes have diverse applications in various fields. Pure liquid membranes, which are composed of a liquid without any immobilized components, are widely used due to their versatility [160]. These membranes are made from different kinds of liquids, including organic solvents, and could be utilized in numerous applications. Conversely, membranes with liquid immobilized within their pores offer distinct advantages and limitations [161]. The composition and structure of these membranes differ from pure liquid membranes, affecting their functionality. However, these membranes exhibit higher selectivity and efficiency compared to pure liquid membranes [160,161]. In the future, liquid membranes hold potential for further advancements and applications. A comparative analysis of different liquid membrane types reveals their selectivity and efficiency, providing insights for future research and development in this area. In conclusion, liquid membranes offer unique properties that make them suitable for specific applications, and further exploration and research are recommended to enhance their performance [160, 161].

2.5.6 Electrically active membranes.

Conductive membranes can be dense or microscopic. Electrically active membranes have a fine microporous structure with positive or negative charges in the pore walls [162]. These membranes can actively transport ions, electrons, or other charged species through their structure,

making them very versatile. A characteristic attribute of electroactive membranes is its capacity to generate a potential difference, which could be utilized in applications such as energy storage and conversion [160]. The electro dialysis process is used to process electrolyte solutions through these membranes [160].

2.6 Membrane filtration techniques

Membrane filtration techniques offer several advantages over traditional separation processes. These include flexibility in design, high selectivity, and low energy consumption. Nevertheless, there are also limitations to consider, such as concentration polarization and membrane fouling issues. [164,165, 166, 167, 168]. The most popular MSPs are microfiltration (MF), ultrafiltration (UF), nanofiltration (NF), and reverse osmosis (RO) [161]. The MF, for example, is commonly applied in the food industry for clarifying beer, wine, fruit juice, and wastewater treatment. It is also effective in separating oil and water emulsions [162]. These techniques take a significant part in various industries and provide efficient separation methods [162]. Pharmaceutical companies process enzymes, antibiotics, and pyrogens using UF techniques. Additionally, they were employed in wastewater treatment as well as the production of cheese and the processing of milk proteins [169]. Bivalent ions are separated using NF, and micropollutants like pesticides and herbicides are rejected using this method. Additionally, for the retention of dyes in the textile industry [168]. The reverse osmosis technique has relevance mainly in the food industry to concentrate fruit juices and sugars, in the desalination of sea and brackish water, and in the dairy industry to concentrate milk to dehydrate organic solvents. Hydrogen recovery, airborne organic vapours, nitrogen production, oxygen enrichment, and other important gas separation processes are just a few examples. [160; 162]. Figure 2.6 provides an illustration of the concept behind a membrane filtration process [170].

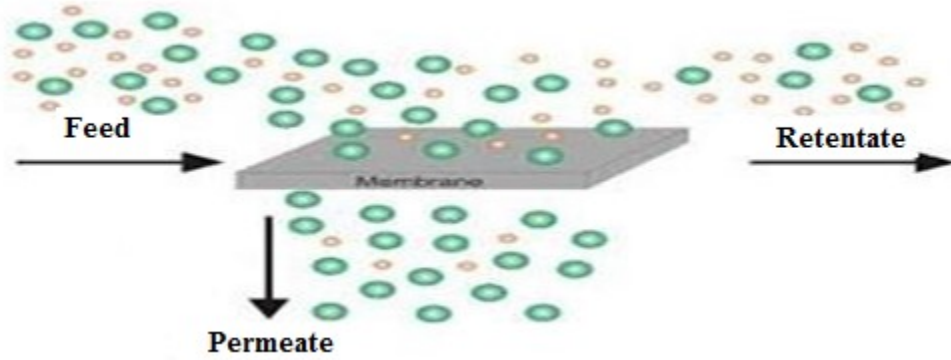


Figure 2.6: Illustration of the concept behind a membrane filtration process

Dissociation occurs due to an imbalance in the passive transport rates of effector molecules. The driving force is also called chemical potential difference across the membrane that causes passive transport [171]. Differences in temperature, concentration, pressure, or potential have been found to be the causes [172]. Figure 2.7. shows the mechanism of solution diffusion that takes place during membrane separation process.

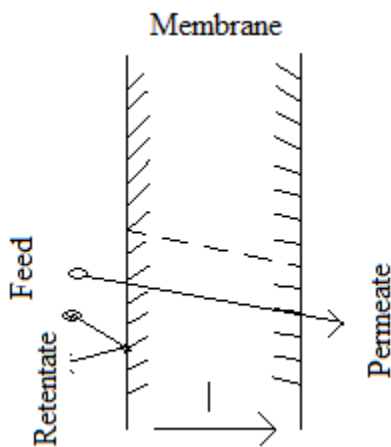


Figure 2.7: Diagram of the mechanism of solution diffusion during the membrane separation process.

2.7 Synthesis of filtration membranes

The two primary geometries for making membranes are:

1. Membranes made from flat sheets.

2. Hollow fiber membranes that are cylindrical.

Generally, ceramic and polymeric materials could both be employed to make filtration membranes [179]. More thermally and chemically stable than polymer materials are ceramic ones [179]. However, it has been found that 95% of a variety of real-world applications mainly employ polymers as their membrane material [178, 179]. Organic compounds are frequently employed as polymeric materials to create filtration membranes [179].

2.7.1 Membranes with symmetric structures

The most practical membranes in separation technology applications are typically isotropic membranes, which can be created by track etching or chemical vapor deposition (C.V.D) [180].

2.7.2 Membranes with asymmetric structures

Industrial membrane filtration processes basically employ membranes with asymmetrical structures [178, 179]. Anisotropic membranes take a significant part in filtration processes due to its unique properties and structures [180]. This membrane is designed with different pore sizes on both sides to increase filtration efficiency. The importance of anisotropic membranes is their ability to selectively retain particles and molecules relying on size and shape, allowing for more precise filtration [178, 179, 180]. Figure 2.8 illustrates a cross-sectional view of an anisotropic membrane with integral skin.

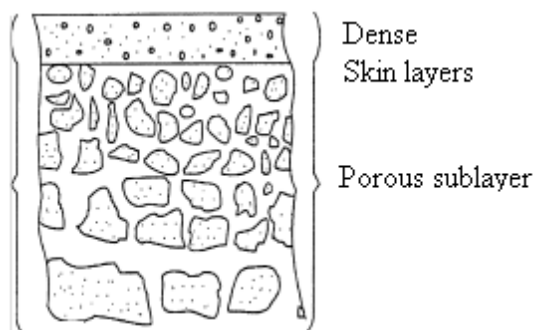


Figure 2.8: A cross-sectional view of an anisotropic membrane with integral skin, (Reprinted from [180]).

2.8 Generalities on membranes filtration processes

2.8.1 Introduction to membrane filtration of liquid solutions

Membranes used for solution separation are categorized according to their pore sizes:

Membrane separation technology is widely used in various industries [178, 179, 180]. Sorted by pore size, these membranes provide an efficient solution for separation processes. For example, MF membranes (0.1-10 μ m) have the specific ability to separate particles and microorganisms from liquids. Membrane separation techniques are often applied in industries such as food and beverage, pharmaceutical, and water treatment [178]. Conversely, UF membranes (100nm-2 μ m) have smaller pores and consequently they are more effective in removing macromolecules and colloidal substances [179]. Nanofiltration (between RO-UF) and reverse osmosis membranes have smaller pores to separate ions and organic molecules. MSP plays an important role in various industries because it provides efficient and reliable solutions for separating solutions [178, 179, 180].

Membranes for microfiltration

The MF membranes take a crucial part in various industries by offering a reliable and efficient method for separating and purifying different substances [188, 189]. The MF membranes are conventionally employed for water and wastewater treatment applications, food and beverage industry, and pharmaceutical and biotechnology applications. The significance of MF lies in its capacity to get rid of bacteria, suspended solids, and other contaminants from liquids, ensuring high-quality end products [188, 189].

Membranes for ultrafiltration

A pressure-driven membrane filtration method is called ultrafiltration (UF). According to [187], UF membranes typically have pores ranging between 2-100 nm and they can easily hold onto species with molecular weights between 3000 and 500000 Da. It has been found that in comparison to microfiltration membranes, ultrafiltration membranes have smaller pores [187]. They are primarily employed to remove colloids and macromolecules [187].

Membranes for nanofiltration

Nanofiltration (NF) membranes typically have pores between 0.1 and 10 nm in size. It is mainly used to remove organic molecules and polyvalent ions [185]. Membranes play a crucial role in NF, making them vital in various industries and applications. They are designed to have specific properties and characteristics that enable them to filter particles and molecules at the nanoscale level [185, 186]. One important aspect of membranes in NF is its pore size and molecular weight cut-off, which determines the size of particles that can be rejected. The selectivity and rejection efficiency of these membranes are also significant, as they determine how effectively certain substances can be filtered out [184, 185, 186].

Membranes for reverse osmosis.

The RO membrane is an essential component in MSPs, serving as a barricade that admits water molecules to pass through while blocking larger particles, contaminants, and salts [182]. The membrane's selectivity and permeability, preparation procedures, and membrane barrier layer structure all have an impact on retinol separation and permeate solution flux [182; 183]. By using a higher pressure, this technique overcomes the osmotic pressure.

2.8.2 Applications of membranes technology

Research advancements in membrane technology have led to an increased application of synthetic polymer membranes in engineering, biology, and medicine. For example, Faiz and Lee [188] published a report investigating the dissociation of light olefins and paraffins in the petrochemical industry using membranes technology. Choi et al. [189] investigated how to improve the membrane's physical and transport properties by adding graphene oxide to Nafion membrane. Furthermore, polymeric membranes could be used for gas separation, according to Budd and Mc Keown [190]. Initially, membranes have typically been used for desalination; however, various membrane structures have been created and alternative options have been depicted [191]. These involve the elimination of water contaminants that are microbial, inorganic, and organic. Polymeric filtration membranes are also employed for other purposes in the food and beverage industry [192,193], pharmaceutical industry [194], synthesis of electrodes [195], biomedicine [196] and beverages [197,198]. MFs require minimal operating pressures and provide superior water efficiency and turbidity removal while reducing energy consumption

and costs. However, it rarely appears in NOM [199, 200]. Figure 2.9 illustrates the size distribution of water contaminants sizes and particles removal sizes of various treatment methods.

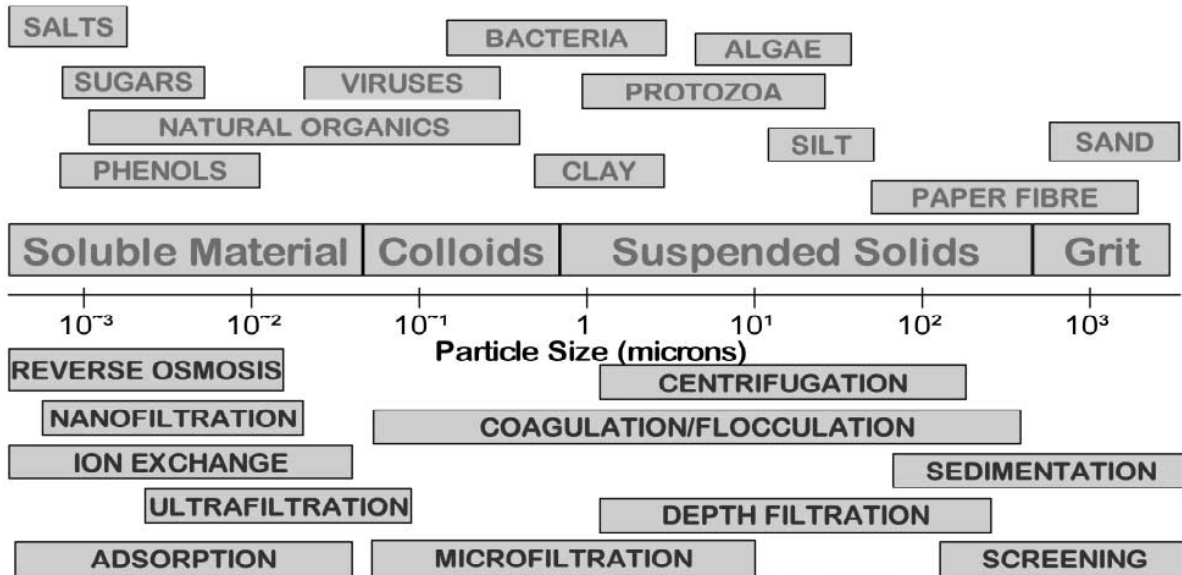


Figure 2.9: The size distribution of water contaminants sizes and particles removal sizes of various treatment methods, (Reproduced from [200]).

Hybrid membrane systems

Hybrid membrane systems are a promising field in membrane technology, combining the advantages of different materials to create membranes with enhanced properties [199]. These systems typically involve the integration of a polymeric material with an inorganic component, such as ceramics, metals, or graphene. The combination of these materials allows for improved separation performance for NOM removal, enhanced mechanical strength, and increased chemical stability [199]. However, the synthesis and scale-up of hybrid membranes pose challenges that need to be addressed for their practical application. The development of these systems is an interesting area of research that could provide solutions for various technological challenges in different industries [199, 201].

2.8.3 Polymeric filtration membrane fouling and its management.

Membrane filtration fouling refers to the accumulation of solid materials within the pores and on the surface of a polymeric membrane [202, 203, 204]. Membrane fouling can raise the cost and energy usage of the filtration membrane by reducing its selectivity and permeate flux during the MSP [202, 203, 204]. Understanding the mechanisms behind membrane fouling is crucial for effectively managing this issue. There are three main types of fouling: particulate fouling, adsorption fouling, and biofouling [205]. Each type has its own unique set of challenges and requires specific management strategies. Membrane filtration fouling can seriously cause the decrease of pure water flux, reduced membrane performance, and increased energy consumption. To combat membrane fouling, various strategies can be implemented, including pre-treatment methods, membrane cleaning techniques, and surface modification of the membrane. By implementing effective fouling management strategies, the performance and lifespan of polymeric membranes can be maximized [205, 206, 207]. Furthermore, According to Hong and Elimelech [208], NOM membrane fouling is accelerated by calcium ions when there is a higher ionic strength and lower pH. Chellam et al. [209], found that colloidal fouling in NF is more common than organic fouling. Baker et al. [207], found that the acceleration of membrane fouling during water treatment is attributable to inorganic ions like aluminum, calcium, and phosphorus.

2.9 Definition and discovery of carbon nanotubes

The CNTs are a unique form of carbon with a long, tubular structure and a graphitic lattice. They were first discovered by Iijima in 1991 [210]. CNTs have captivated prominent awareness due to its outstanding physical, mechanical, electrical, magnetic, and thermal properties [210, 211]. Ongoing research projects are exploring its eventual implementation in fields such as water purification, electronic devices, catalyst support, and as reinforcing materials for composites [210, 211]. CNTs can be produced through various methods, including C.V.D, arc discharge, and laser ablation processes. These production methods allow for the controlled production of CNTs for further exploration and potential commercial applications [210, 211, 212]. Furthermore, it has been demonstrated that CNTs can also be made from other hydrocarbon-based substances, including alcohol [213], paraffin wax candles [213], and polyethylene. The synthesis sample made

from methane contains nanorods, nanofibers, and multiwall CNTs, according to research by Camacho and Choudhuri [214]. Acetylene flame, on the other hand, produces only nanotubes, while propane flame produces both twisted and helical nanotubes [213, 214].

2.9.1 Carbon nanotubes structures, composition and properties

The CNTs are tubular structures composed of carbon atoms aligned in a graphitic lattice [214]. These structures give CNTs exceptional properties, such as high mechanical strength, electrical conductivity, and thermal stability [214, 215]. The tubular shape and lattice structure take a leading role in determining these properties. CNTs can have single-walled or multi-walled structures, depending on the number of concentric carbon tubes. The diameter and chirality of the tubes also influence the properties of CNTs [215]. Understanding the structure and composition of CNTs is crucial for their synthesis and application in various fields. Different production methods, such as C.V.D, arc discharge, laser ablation are used to synthesize CNTs with specific structures and properties. Ongoing research projects focus on further understanding the characteristics of CNTs and exploring their potential applications in various fields [213, 214, 215]. Figure 2.10 shows an instance of the atomic structures of nanotubes.

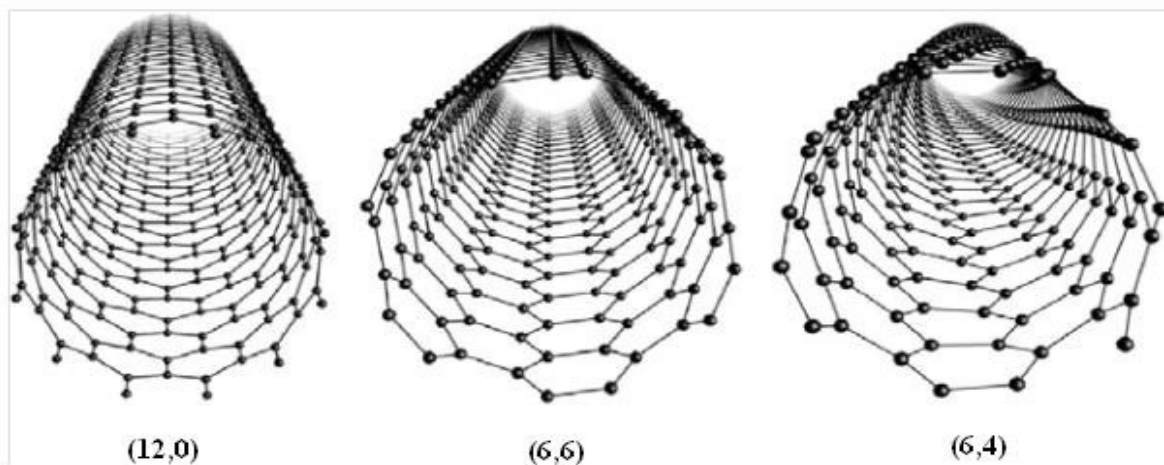


Figure 2.10: An instance of the atomic structures of the (6, 6) armchair, the (6, 4) chiral nanotubes, and the (12, 0) zigzag. (Reproduced from [215]).

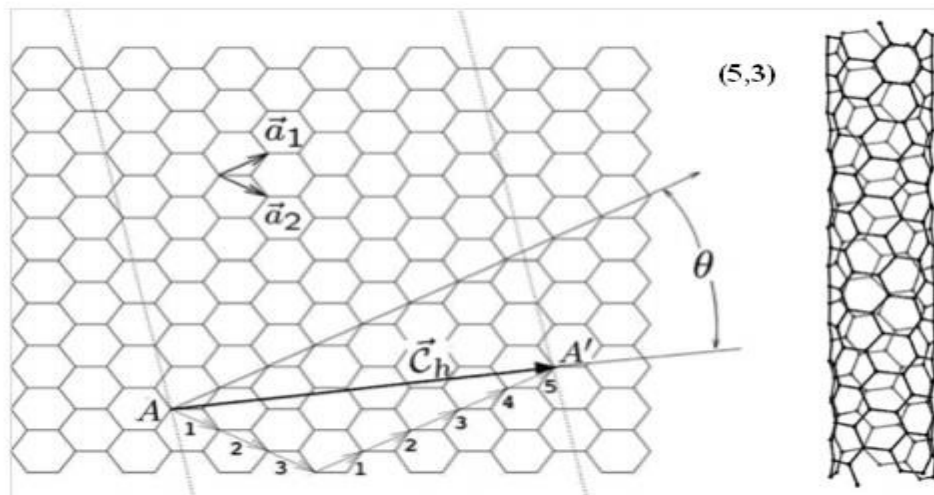


Figure 2.11: An illustration of a 2D graphene sheet (chiral vector $\vec{C}_h=3\vec{a}_1+5\vec{a}_2$ of the graphene sheet). (Reproduced from [215]).

CNTs possess unique properties that make them valuable in various applications [213, 214, 215]. These properties include thermal conductivity, electrical conductivity, and excellent mechanical strength [215]. CNTs also exhibit remarkable flexibility and can undergo significant elongation without breaking. Additionally, they exhibit excellent chemical stability and are highly resistant to corrosion [214, 215]. These characteristics, associated with their small size and high aspect ratio, make CNTs ideal for a large range of applications such as water purification, electronic devices, catalyst support, and reinforcing materials for composites. Due to ongoing research and advancements in production methods, the potential for future applications of CNTs is vast, despite the challenges and limitations that need to be overcome [213, 214, 215].

2.9.2 Methods of production of carbon nanotubes

The following methods are typically employed to synthesis CNTs: Arc discharge process, chemical vapor deposition process (C.V.D) and laser ablation process [209].

Arc discharge process

The CNTs were created by Lijima in 1991 [209] using the arc discharge method (ADM). The ADM is a method of making carbon nanotubes by vaporizing carbon electrodes using high voltage electricity [213]. This vaporized carbon condenses to form CNTs. The ADM is mostly based on

the capacity of high voltage current to generate extreme heat, causing the carbon to freeze and form nanotubes [214, 216]. In this method, the selection of electrode materials is very important because different materials can affect the quality and performance of the produced nanotubes [214, 215]. Furthermore, by carefully selecting the electrode materials and optimizing the ADM parameters, this technique can be an effective and efficient method to produce CNTs [216].

Chemical vapor deposition technique

The C.V.D of carbon was first described in 1959 [217]; however, it was not employed to synthesis CNTs until 1993 [218]. C.V.D is a commonly used technique to synthesis carbon nanotubes. The principle of the method involves the decomposition of hydrocarbon gases in the presence of a metal catalyst. The choice of catalyst and its preparation are pertinent aspects that determine the quality and performance of nanotubes [215]. In addition, growth parameters and conditions such as temperature, pressure, and gas flow must be carefully monitored to achieve the desired properties of nanotubes. The C.V.D method offers several advantages, including scalability, control of nanotube properties, and the potential for mass production [217, 219]. However, challenges remain, such as achieving uniform growth and controlling nanotube morphology. For the enhanced comprehension of the use of CNTs in multiple applications, further research, and optimization of the C.V.D process is required [215, 219]. Figure 2.12 (a, b, c) show the diagrams for the methods that are mainly employed to synthesize CNTs.

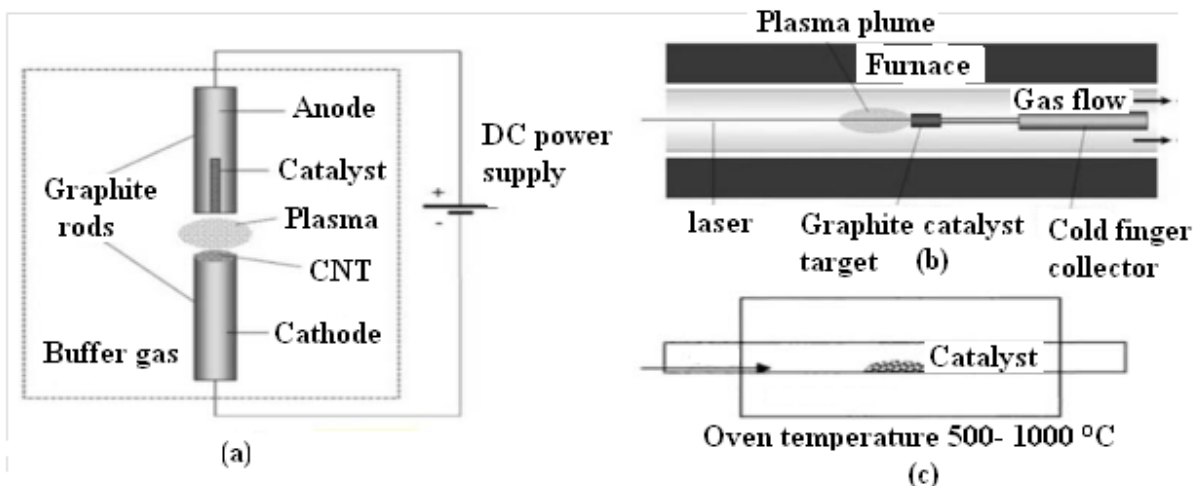


Figure 2.12 : Diagrams for the methods of growing of CNTs using: (a) C.V.D, (b) arc discharge, and (c) laser ablation (c) [215, 217].

Laser ablation technique

Laser ablation is a technique of synthesizing CNTs that utilizes a laser to vaporize a target material in the presence of a catalyst [216]. In this technique, CNTs are produced based on rapid heating and cooling of the target material. In this method, the laser source and wavelength are the important factors in optimizing the production process. This is because different laser characteristics can vary the quality and yield of the nanotubes. In addition to laser parameters, other factors such as catalyst selection and optimization of ablation parameters can facilitate the characterization of the properties of CNTs obtained by this method [219]. This technique cannot be used for mass production of CNTs, however; it can only be used to produce CNTs of high quality with controlled diameter and diameter distribution. SWCNT samples created using this technique have been heavily utilized for fundamental research [216, 219].

2.9.3 Electrical Properties of carbon nanotubes

Depending on its structure, CNTs exhibit either metallic or semiconducting behavior [220]. The electrical properties of CNTs are of keen interest because of its use in electronics [222]. The conductivity of CNTs is one of the most primordial electrical properties, and some types have excellent conductivity [220, 222]. The band structure of CNTs positively impact their electrical behavior by influencing their electrical and transmission properties [223].

2.9.4 Mechanical properties of carbon nanotubes

The CNTs exhibit remarkable mechanical properties, making them a subject of great interest in materials science [219]. With strengths and stiffnesses superior to traditional materials, carbon nanotubes have the potential to revolutionize various applications, including structural components and composite materials [223, 224, 225]. The elasticity and flexibility of CNTs also contribute to their unique mechanical behavior, allowing them to withstand strain without permanent deformation. These properties make CNTs highly desirable for applications requiring high mechanical performance, such as aerospace and automotive industries [226, 227]. However, there are challenges and future directions that need to be addressed to fully use the CNTs potentials in practical applications [228, 229, 230].

2.9.5 Carbon nanotubes functionalization

Functionalization process enhances the properties and applications of CNTs [231]. By modifying the surface of CNTs, desired chemical groups and functional moieties can be introduced via functionality, enabling tailored properties and improved performance in several applications. The importance of use is in the ability to enhance CNTs variation, dispersibility and compatibility in different matrices, such as polymers or solvents [231, 232]. Additionally, this feature addresses key CNTs issues such as reliability, scalability, and cost-effectiveness, enabling successful integration into real-world applications. To meet the changing needs, research continues to explore new functionalization methods and develop strategies for the stability and durability of functionalized CNTs [231, 232].

Two methods of functionalization are commonly used: covalent functionalization and non-covalent functionalization [234, 235]. Covalent functionalization implies the formation of strong chemical bonds between the CNTs and functional groups, which alters their physical and chemical properties. This method provides better control over the functionalization process, but it can also lead to structural damage [234]. Contrarily, the non-covalent functionalization relies on weak interactions such as the electrostatic interactions to attach functional groups to the CNTs [234, 235]. This method preserves the integrity of the nanotubes while providing reversible functionality. By exploring these methods of functionalization, researchers aim to overcome challenges related to stability, scalability, and cost-effectiveness, as well as to discover novel techniques for

functionalizing CNTs [235, 236]. Ultimately, the goal is to integrate functionalized CNTs into real-world applications in electronics, optoelectronics, energy storage, conversion, biomedical, and environmental fields [238, 239, 240].

Concept on covalent functionalization of carbon nanotubes

The concept on the covalent functionalization involves the direct attachment of functional groups to the surface of CNTs through chemical reactions [234, 235, 236]. This approach allows control of the type and density of functional groups, resulting in improved properties and enhanced compatibility with other materials [237]. Covalent functionalization also improves the stability and durability of CNTs, making them suitable for practical applications [238]. CNTs can also be integrated into electronics, optoelectronics, energy storage and conversion, as well as biomedical and environmental applications [237]. Despite these advantages, challenges remain, such as ensuring the stability and durability of functionalized CNTs, optimizing the scalability and cost-effectiveness of functionalization methods, and exploring new functionalization methods [239, 240, 241]. Solving these challenges will facilitate the widespread integration of functionalized CNTs in a variety of practical applications. Grafting onto or grafting from methods are used to covalently bond polymer functionalities to CNTs [241].

Concept on non-covalent functionalization of carbon nanotubes

The concept on the non-covalent functionalization refers to the process of modifying CNTs through non-covalent interactions (Van Waals forces, π - π stacking) [233, 234, 235]. This is a versatile and widely used method due to its simplicity and ability to preserve the properties of CNTs [234]. This is a method of improving solubility, dispersibility and stability by absorbing or encapsulating molecules on the surface of CNTs [235, 236, 237]. Noncovalent functionalization could be performed by diverse methods, such as physical adsorption, polymer encapsulation, supramolecular assembly, and chemical doping. This approach has important implications in a variety of fields, including electronics, optoelectronics, as well as biomedical and environmental applications [234, 235, 236]. Despite these advantages, the stability and durability of functionalized CNTs, the scalability, cost-effectiveness of new methods need to be carefully addressed to successfully integrate functionalized CNTs into practical applications [247, 248, 249, 250, 251, 261].

2.9.6 The cytotoxic properties of carbon nanotubes

According to some authors, CNTs already possess cytotoxic properties that inhibit and stop pathogen growth on their surface and may also improve the ability of CNT adsorption filters to self-clean [262, 263, 264, 265, 266, 267, 268 and 269]. Contrary to other granular activated carbon filters (GAC), it has been found that CNTs can inhibit the expansion of pathogens on their surface [262]. Compared to other microorganisms like bacteria (*Micrococcus lysodeikticus*) [264], *E. coli*, and other viruses, raw CNTs have antimicrobial properties. *Salmonella* [269], *E. coli* [265, 267, 268], *Tetrahymena pyriformis* [266], *Streptococcus mutans* [267, 269], bacteria endospores [270], and viruses like bacteriophages [271]. The images obtained after the SEM characterization of *E. coli* are presented in Figure 2.13(a, b). For 60 min, different *E. coli* species were incubated in SWCNTs and MWCNTs. Kang and al. [272] took the pictures., as well as Arias and Yang [273] after being incubated, SWCNTs and MWCNTs, the bacteria's physiology is depicted in Figure 2.13 (a, b). The fibrous shape of MWCNTs is also depicted in the same picture. This can constitute one of the main characteristics that MWCNTs can utilize in order to remove NOM and microorganisms from water systems. This situation increases the likelihood that pathogens do not build up inside CNT filters the way they do inside GAC filters. Backwashing is a method for removing the remaining contaminants from the filters. As a result of CNT filters' ability to both capture and deactivate pathogens, which other carbon-based filters cannot do, the cytotoxic properties of CNTs indirectly support the microbial sorption activities in this scenario. The antimicrobial properties of CNTs have been found to be correlated with their fibrous shape [274, 275]. After impact, oxidative stress causes the bacterial cell to rupture, releasing the contents inside [274]. CNTs fibers have the power to affect the surface of bacterial cells, disrupt intracellular metabolic pathways, and affect bacterial cell viability. Akasaka and Watari [276] found that *S. mutans* bacteria precipitate more readily on 30 nm partially hydrophobic MWCNTs than they do on 200 nm MWCNTs or SWCNTs that have been completely dispersed. Figure 2.13 (a, b) show the SEM pictures of *E. coli* cells captured by MWCNTs and SWCNTs respectively.

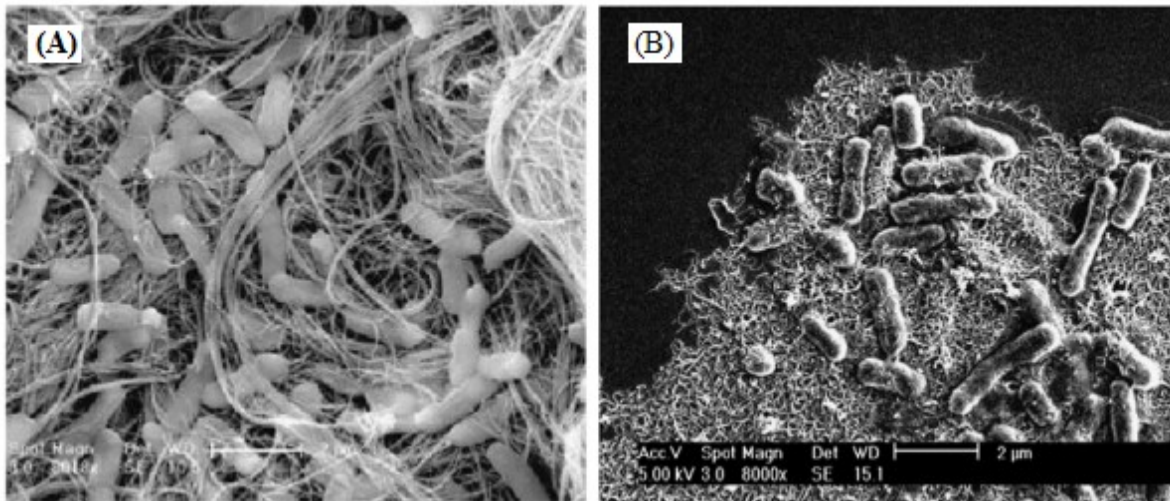


Figure 2.13: SEM pictures of (a) *E. coli* cells captured by MWCNTs, (b) *E. coli* cells captured by SWCNTs, (Kang et al. [274]).

2.9.7 Adsorption of biological contaminants from water using carbon nanotubes as sorbent media.

Biological contaminants in water pose a significant threat to human health [277]. Understanding the common types of biological contaminants and the associated health risks is crucial in developing effectiveness water purification methods [277]. Additionally, the challenges in removing these contaminants must be addressed to make certain safe drinking water for all. CNTs have emerged as a promising sorbent for eliminating biological contaminants from water due to their unique properties and structure [277].

Adsorption of microorganisms by using carbon nanotubes as adsorbents media.

There are three special benefits to using CNTs for bacterial adsorption [277, 278]. First, microbial adsorption capabilities of CNTs are said to be superior to those of any other commercially available adsorbents. In addition, CNTs exhibit selective bacterial adsorption, which is a benefit not typically observed during the applications of other adsorbents. Finally, CNTs enable immediate bacterial adsorption kinetics, recommending their use as pathogen sensors, where CNTs concentrate specifically on the target contaminant [278]. According to Upadhyayula et al. [278, 280], the raw CNTs' adsorption properties for *Bacillus subtilis* spores were superior to those

of two other adsorbent media. Which can be used to support the claim that CNTs have high microbial capacities. The adsorption of *Bacillus subtilis* spores by CNTS is significantly greater than that achieved with PAC and Nano Ceram™, an alumina-based adsorbent (AlOOH). The fibrous shape (size) and surface accessibility of CNTs, not present in other previously discussed adsorbents [278, 279], are the primary reasons for their high adsorption properties. CNTs could offer bacteria-specific adsorption, as previously mentioned. Studying pure and mixed cultures by Deng et al. provides evidence for this (2008) [280]. It was reported that bacteria that are adsorbed to CNTs do so with remarkably high and rapid kinetic rates [278, 279, 280]. Deng and al. [278] reported that *Staphylococcus aureus*, *E. coli*, and *Bacillus subtilis* all have different adsorption kinetics rates. Upadhyula et al. [280] had established that SWCNTs concentrated more than 95% of the bacteria in the solution between 5 and 30 minutes.

Adsorption of natural organic matter by using carbon nanotubes as adsorbents media.

The CNTs have demonstrated great promise as effectual adsorbents for the elimination of NOM from water [281, 282, 283, 284, 285, 286, 287, 288, 289]. Its distinctive adsorption properties, such as large surface area, strong affinity for organic compounds, the existence of mesopores, functional groups and positive charge on the surface area of CNTs enable them to efficiently eliminate NOM from water sources [281, 282, 288]. A further factor that aids in NOM adsorption is the chemical makeup of NOM and its average size, which ranges between 0-5 nm. Some microporous adsorbents only have pore openings of 1 nm [283, 284, 285]. Additionally, different fractions of NOM interact with the surface of the adsorbent media in different ways due to their polydisperse nature [281, 282, 288, 289]. Physical adsorption occurs when organic molecules are attracted to the surface of CNTs through electrostatic forces, while chemical adsorption implies the formation of covalent bonds between the organic molecules and the nanotube surface [290]. It has been reported that CNTs have superior NOM adsorption capacities than activated carbon (GAC and PAC) [285]. This is most likely due to the existence of larger mesopores and slighter negative surface charge on the CNTs surface [285]. Furthermore, it was reported that even in the presence of synthetic organics (SOC) [284], micropollutants [288], and non-foulant organic compounds [284], CNTs can still remove NOM, unwanted micropollutants, and other organic compounds due to its large surface area [284, 288]. Additionally, there is a need to explore and

comprehend the various factors that can affect the adsorption performance of CNTs [281, 290, 291]. Another challenge is finding ways to enhance the physical and chemical adsorption mechanisms of CNTs to improve their effectiveness as adsorbents [285].

2.10 Summary

This Chapter focuses on the quantification and measurement of NOM in water treatment, which negatively impacts the water treatment process and affects water quality in the DWDSs. It increases the cost of water treatment and leads to operational problems. Furthermore, this chapter reviews the literature on the fabrication and characterization of PSF membranes for an enhanced comprehension of the pertinent properties and characteristics of polymeric membranes necessary for the elimination of BOM during the MSP. It also reviews the structural and functional properties of CNTs before and after its functionalization process. A hybrid adsorption-membrane filtration system based on the multi-barrier approach for the elimination of BOM from water is discussed in this chapter. Subsequently, the application of CNTs were investigated as nanomaterials that may replace conventional adsorbents such as BAC, GAC, PAC because of its adsorption properties for BOM elimination from water. Further research is recommended to explore potential advancements in CNT pretreatment, as well as the implications for the future of NF membrane filtration. These recommendations aim to improve the overall effectiveness of CNTs as adsorbents for the eradication BOM in water and reduce membrane fouling, ultimately enhancing the quality and efficiency of the filtration process. The CNTs are evaluated for optimal pretreatment before the MSP to improve MSP performance, increase strength, and reduce membrane fouling in Chapters five and six

2.11 References

[1] Sillanpaa, M., (2014). Natural organic matter in water: Characterization and treatment methods. *In proceedings*. Sillanp Natural OM.

[2] Schanchez, M., Pilar, N., (2013). Fluorescence based approach to drinking water treatment plan natural organic matter (NOM) characterization, treatment, and management, *Journal of Enviro. Science*. In proceedings, Morcote Fluorescence BA.

- [3] Yang, P., Huan, L., Xiangru, Z., Liang, A., (2016). Characterization of natural organic matter in drinking water: Sample preparation and analytical approaches: *Trends in Enviro. Analyt. Chem.* 12, 23–30.
- [4] Van der Kooij D. (1992). Assimilable organic carbon as an indicator of bacterial regrowth, *J. Am. Water Works Assoc.*, 84, 57–65.
- [5] LeChevallier M.W., Babcock T., Lee R.G., (1987). Examination and characterization of distribution system biofilms, *Appl. Environ. Microbiol.* 53, 2714–2724.
- [6] Sibille I., Mathieu L., Paquin J., Gatel D., Block J., (1997). Microbial characteristics of a distribution system fed with nanofiltered drinking water, *Water Res.* 31, 2318–2326.
- [7] Noble P.A., Clark D.L., Olson B.H., (1996). Biological stability of groundwater, *J. Am. Water Works Assoc.* 88, 87–96.
- [8] Agbekodo K., Legube B., Cote P., (1996). Organic in NF permeate, *J. Am. Water Works Assoc.* 88, 67–74.
- [9] Hong S., Elimelech M., (1997). Chemical and physical aspects of natural organic matter (NOM) fouling of nanofiltration membranes, *J. Membr. Sci.*, 132, 159–181.
- [10] Lee E., Shon H., Sho J., (2010). Biofouling characteristics using flow field flow fractionation: Effect of bacteria and membrane properties, *Bioresource technology*, 101, 1487–1493.
- [11] Park, J.W., Joe, M., Maeng, S. (2020). Characterization of natural organic matter and assimilable organic carbon from an advanced full-scale drinking water treatment plant to tap. *Journal of desalination and water treatment*, 180 86-94.
- [12] Moyo, W., Motsa, M., Chaukura, N., Msagato, T., Mamba, B., Heijman, S., Nkambule, T., (2022). Characterization of natural organic matter in South Africa drinking water treatment plants toward integrating ceramic membranes filtration. *Water Enviro. Res.*, 94 10693.

- [13] Chow C.W.K., van Leeuwen, Drikas J.A., Fabris M., R., Spark, K.M. and Page, D.W. (1999). The impact of the character of natural organic matter in conventional treatment with alum. *Water Sci. Technol.* 40(9), 97-104.
- [14] Lankes, U., demann, H.D.L. and Frimmel, F.H. (2008). Search for basic relationships between “molecular size” and “chemical structure” of aquatic natural organic matter, Answers from ¹³C and ¹⁵N CPMAS NMR spectroscopy. *Water Res.* 42, 1051 – 1060.
- [15] Jacangelo, J.G.; DeMarco, J.; Owen, D.M.; Randtke, S.J. (1995). Selected processes for removing NOM: An overview. *J. Am. Water Works Assoc.* 87 64-77.
- [16] Srinivasan S., Harrington G. W., (2007). Biostability analysis for drinking water distribution systems. *Water Res.* 41 2127–2138. 10.1016/j.watres, 05.
- [17] Frimmel, F.H. (1998). Characterization of natural organic matter as major constituents in aquatic systems. *Journal of Contaminant Hydrology* 35, 201–216.
- [18] Frimmel, F.H. and Abbt-Braun, G. (1999). Basic Characterization of Reference NOM from Central Europe - Similarities and Differences. *Environment International* 25(2/3), 191-207.
- [19] Chen, J., Gu, B., LeBoef, E.J., Pan, H., Dai, S. (2002). Spectroscopic characterization of the structural and functional properties of natural organic matter fractions. *Chemosphere* 48, 59–68.
- [20] Sarathy, S., Mohseni, M., (2007). The impact of UV/H₂O₂ advanced oxidation on molecular size distribution of chromophoric natural organic matter. *Environ. Sci. Technol.* 41, 8315–8320.
- [21] Her, N., Amy, G., Chung, J., Yoon, J., Yoon, Y. (2008). Characterizing dissolved organic matter and evaluating associated nanofiltration membrane fouling. *Chemosphere* 70, 495–502.
- [22] Liu, R., Lead, J., Baker, A. (2007). Fluorescence characterization of cross flow ultrafiltration derived freshwater colloidal and dissolved organic matter. *Chemosphere* 68, 1304–1311.

- [23] Thurman, E., (1985). *Organic Geochemistry of Natural Waters*. Martinus Nijhoff / Dr W. Junk Publishers, Dordrecht, the Netherlands.
- [24] Swietlik, J., Dabrowska, A., Raczyk-Stanislawiak, U., Nawrocki, J. (2004). Reactivity of natural organic matter fractions with chlorine dioxide and ozone. *Water Res.* 38, 547–558.
- [25] Liu, S., Lim, M., Fabris, R., Chow, C., Drikas, M., Amal, R., (2010). Comparison of photocatalytic degradation of natural organic matter in two Australian surface waters using multiple analytical techniques. *Org. Geochem.* 41, 124–129.
- [26] Tercero Espinoza, L., ter Haseborg, E., Weber, M., Frimmel, F., (2009). Investigation of the photocatalytic degradation of brown water natural organic matter by size exclusion chromatography. *Appl. Catal. B Environ.* 87, 56–62.
- [27] Zhao, Z.-Y., Gu, D.-J., Li, H.-B., Li, X.-Y., Leung, K., (2009). Disinfection characteristics of the dissolved organic fractions at several stages of a conventional drinking water treatment plant in South China. *J. Hazard. Mater.* 172, 1093–1099.
- [28] Christy, A., Bruchet, A., Rybacki, D., (1999). Characterization of natural organic matter by pyrolysis/GC-MS. *Environ. Int.* 25, 181–189.
- [29] Matilainen, A., Gjessing, E.T., Lahtinen, T., Hed, L., Bhatnagar, A., Sillanpää, M., (2011). An overview of the methods used in the characterization of natural organic matter (NOM) in relation to drinking water treatment. *Chemosphere* 83, 1431–1442.
- [30] Croue, J.-P., Korshin, G.V., Benjamin, M.M., (2000). Characterization of Natural Organic Matter in Drinking Water. *American Water Works Association*. pp. 324.
- [31] Croue, J.-P., (2004). Isolation of humic and non-humic NOM fractions: structural characterization. *Environ. Monit. Assess.* 92, 193–207.

- [32] Assemi, S., Newcombe, G., Hepplewhite, C., Beckett, R., (2004). Characterization of natural organic matter fractions separated by ultrafiltration using flow field-flow fractionation. *Water Res.* 38, 1467–1476.
- [33] Leenher, J.A., (1985). Fractionation techniques for aquatic humic substances. In: Aiken, G., McKnight, D., Wershaw, R., MacCarthy, P. (Eds.), *Humic Substances in Soil, Sediment and Water*. John Wiley & Sons, pp. 409–429.
- [34] Leenher, J., (1981). Comprehensive approach to preparative isolation and fractionation of dissolved organic carbon from natural waters and wastewaters. *Environ. Sci. Technol.* 15, 578–587.
- [35] Chow, C., Fabris, R., Drikas, M., (2004). A rapid fractionation technique to characterize natural organic matter for the optimization of water treatment processes. *J. Water Supply Res. Technol. Aqua* 53, 85–92.
- [36] Fabris, R., Chow, C., Drikas, M., Eikebrokk, B., (2008). Comparison of NOM character in selected Australian and Norwegian drinking waters. *Water Res.* 42, 4188–4196.
- [37] Soh, Y., Roddick, F., van Leeuwen, J., (2008). The impact of alum coagulation on the character, biodegradability, and disinfection by-product formation potential of reservoir natural organic matter (NOM) fractions. *Water Sci. Technol.* 58, 1173–1179.
- [38] Li, A., Hu, J., Li, W., Zhang, W., Wang, X., (2009). Polarity based fractionation of fulvic acids. *Chemosphere* 77, 1419–1426.
- [39] Song, H., Orr, O., Hong, Y., Karanfil, T., (2009). Isolation and fractionation of natural organic matter: evaluation of reverse osmosis performance and impact of fractionation parameters. *Environ. Monit. Assess.* 153, 307–321.
- [40] Leenher, J., Croué, J.-P., (2003). Characterizing dissolved aquatic organic matter. *Environ. Sci. Technol.* 37, 18A–26A.
- [41] Chow, A.T., Dahlgren, R.A., Gao, S., (2005). Physical and chemical fractionation of dissolved organic matter and trihalomethane precursors: a review. *J. Water Supply Res. Technol.* 54, 475–507.

- [42] Moon, J., Kim, S., Cho, J., (2006). Characterizations of natural organic matter as nano particle using flow field-flow fractionation. *Colloids Surf. A Physicochem. Eng. Aspects* 287, 232–236.
- [43] Swietlik, J., Sikorska E., (2005). Characterization of NOM fractions by high pressure size – exclusion chromatography, specific UV absorbance and total luminescence spectroscopy. *Journal of Environmental studies* 15, 145-153.
- [44] Croue, J.P., (2004). Isolation of humic and non-humic NOM fractions: structural characterization. *Environmental Monitoring and Assessment*, 92:193–207.
- [45] Singer, P. C., (1999). Humic substances as precursors for potentially harmful disinfection by- products. *Water Science and Technology*, 40(9):25–30.
- [46] Leenheer, J. A., (1981). Comprehensive approach to preparative isolation and fractionation of dissolved organic carbon from natural waters and wastewater. *Environmental science and Technology*, 15(5):578–587.
- [47] Chen, W., Westerhoff, P., Leenheer, J. A., and Booksh, K., (2003). Fluorescence excitation emission matrix regional integration to quantify spectra for dissolved organic matter. *Environmental Science and Technology*, 37(24):5701–5710.
- [48] van der Kooij, D., Visser, A., and Hijnen, W. A. M. (1982)., Determining the concentration of easily assimilable organic carbon in drinking water. *Journal - American Water Works Association*, 74:540–545.
- [49] Joret, J. C. and Levi, Y., (1986). Methode rapide d’evaluation du carbone éliminable des eaux par voie biologique. *La Tribune du Cebedeau*, 39 :3–9.
- [50] van der Kooij, D., Veenendaal, H. R., Baars-Loristand, C., van der Klift, H. W., and Drost, Y. C., (1995). Biofilm formation on surfaces of glass and Teflon exposed to treated water. *Water Research*, 29(7):1655–1662.

- [51] Fabris R., Chow C.K.W., Drikas M., Eikebrokk B., (2008), Comparison of NOM character in selected Australian and Norwegian drinking waters. *Water Res.*, 42, pp. 4188-4196.
- [52] Culea, M., Cozar, O., Ristoiu, D., 2006. Methods validation for the determination of trihalomethanes in drinking water. *J. Mass Spectrom.* 41, 1594–1597.
- [53] Chen, C., Zhang, X., Zhu, L., Liu, J., He, W., Han, H., (2008). Disinfection by-products and their precursors in a water treatment plant in North China: seasonal changes and fraction analysis. *Sci. Total Environ.* 397, 140–147.
- [54] Cooper, W., Song, W., Gonsior, M., Kalnina, D., Peake, B., Mezyk, S., (2008). Recent advances in structure and reactivity of dissolved organic matter in natural waters. *Water Sci. Technol.* 8, 615–623.
- [55] Gjessing, E., Steiro, C., Becher, G., Christy, A., (2007). Reduced analytical availability of polychlorinated biphenyls (PCB's) in colored surface water. *Chemosphere* 66, 644–649.
- [56] Laborda, F., Ruiz-Beguería, S., Bolea, E., Castillo, J., (2009). Functional speciation of metal-dissolved organic matter complexes by size exclusion chromatography coupled to inductively coupled plasma mass spectrometry and deconvolution analysis. *Spectrochim. Acta B* 392, 392–398.
- [57] Park, J.-H., (2009). Spectroscopic characterization of dissolved organic matter and its interactions with metals in surface waters using size exclusion chromatography. *Chemosphere* 77, 485–494.
- [58] Leenheer, J.A., Croué, J.-P., Benjamin, M., Korshin, G.V., Hwang, C.J., Bruchet, A. and Aiken, G.R., (2000). Comprehensive Isolation of Natural Organic Matter from Water for Spectral Characterizations and Reactivity Testing In: *Natural Organic Matter and Disinfection By-Products*. American Chemical Society, pp. 68-83.
- [59] Peuravuori, J., Koivikko, R. and Pihlaja, K., (2002). Characterization, differentiation, and classification of aquatic humic matter separated with different sorbents: synchronous scanning fluorescence spectroscopy. *Water Res.* 36, 4552–4562.

- [60] Leenheer, J.A. and Croue, J.-P., (2003), Characterizing Dissolved Aquatic Organic matter: Understanding the unknown structures is key to better treatment of drinking water. *Environ. Sci. Technol.* 37(1), 19A-26A.
- [61] Thurman, E.M., (1985), *Organic geochemistry of natural waters*. Martinus Nijhoff/Dr. W. Junk Publishers, Dordrecht (Netherlands).
- [62] Sharp, J.H., (1993), The Dissolved Organic Carbon Controversy: An Update. *oceanography* 6(2).
- [63] Edzwald, J.K., Becker, W.C. and Wattier, K.L., (1985), Surrogate parameter for monitoring organic matter and THM precursors. *J. Am. Water Works Assoc.* 77, 122-132.
- [64] Amy, G.L., Chadik, P.A. and Chowdhury, Z.K., (1987), Developing models for predicting THM formation potential and kinetics. *J. Am. Water Works Assoc.* 79, 89-97.
- [65] Weishaar, J.L., (2003), Evaluation of Specific Ultraviolet Absorbance as an Indicator of the Chemical Composition and Reactivity of Dissolved Organic Carbon. *Environ. Sci. Technol.* 37, 4702-4708.
- [66] Traina, S.J., Novak, J. and Smeck, N.E., (1990), An Ultraviolet Absorbance Method of Estimating the Percent Aromatic Carbon Content of Humic Acids. *J. Environ. Qual.* 19(1), 151-153.
- [67] Korshin, G.V., Li, C.-W. and Benjamin, M.M., (1997), Monitoring the properties of natural organic matter through UV spectroscopy: A consistent theory. *Water Res.* 31(7), 1787-1795.
- [68] Reckhow, D.A., Singer, P.C. and Malcolm, R.L., (1990), Chlorination of Humic Materials by-Product Formation and Chemical Interpretations. *Environ. Sci. Technol.* 24(11), 1655-1664.
- [69] Li, C.W., Benjamin, M.M. and Korshin, G.V., (2000), Use of UV spectroscopy to characterize the reaction between NOM and free chlorine. *Environ. Sci. & Technol.* 34(12), 2570-2575.

- [70] Westerhoff, P., Aiken, G., Amy, G. and Debroux, J., (1999), Relationships between the structure of natural organic matter and its reactivity towards molecular ozone and hydroxyl radicals. *Water Res.* 33(10), 2265-2276.
- [71] Korshin, G.V., Benjamin, M.M., and Li, C.W., (1999), Use of differential spectroscopy to evaluate the structure and reactivity of humics. *Water Sci. Technol.* 40(9), 9-16.
- [72] Korshin, G.V., Li, C.-W. and Benjamin, M.M., (1997), Monitoring the properties of natural organic matter through UV spectroscopy: A consistent theory. *Water Res.* 31(7), 1787-1795.
- [73] Leenheer, J.A. and Huffman, E.W.D., (1976), Classification of organic solutes in water by using macroreticular resins. *J. Research U.S. Geol. Survey* 4, 737-751.
- [74] Thurman, E.M. and Malcolm, R.L., (1981), Preparative isolation of aquatic humic substances. *Environ. Sci. & Technol.* 15(4), 463-466.
- [75] Aiken, G.R., (1985), *Humic substances in soil, sediment, and water-Geochemistry, isolation, and characterization*. In: Isolation and concentration techniques for aquatic humic substances. Aiken, G.R., McKnight, D.M., Wershaw, R.L. and MacCarthy, P. (eds). John Wiley and Sons, New York, pp. 363-385.
- [76] Westerhoff, P. and Mash, H., (2002), Dissolved organic nitrogen in drinking water supplies: a review. *J. Water Supply Res. Technol. AQUA* 51(8).
- [77] Leenheer, J.A., (2004), Comprehensive assessment of precursors, diagenesis, and reactivity to water treatment of dissolved and colloidal organic matter. *Water Sci. Technol. Water Supply* 4(4), 1-9.
- [78] Perakis, S.S. and Hedin, L.O., (2002), Nitrogen loss from unpolluted South American forests mainly via dissolved organic compounds. *Nature* 415(6870), 416-419.

[79] Richardson, S.D., Thruston, A.D., Caughran, T.V., Chen, P.H., Collette, T.W. and Floyd, T.L., (1999), Identification of new drinking water disinfection byproducts formed in the presence of bromide. *Environ. Sci. Technol.* 33, 3378-3383.

[80] Najm, I. and Trussell, R.R., (2001), NDMA formation in water and wastewater. *J. Am. Water Works Ass.* 93, 92-99.

[81] Choi, J. and Valentine, R.L., (2002), Formation of N-nitrosodimethylamine (NDMA) from reaction of monochloramine: a new disinfection by-product. *Water Res.* 36, 817-824.

[82] Donnermair, M.M. and Blatchley Iii, E.R., (2003), Disinfection efficacy of organic chloramines. *Water Res.* 37(7), 1557-1570.

[83] Tuschall, J.R., and Brexonik, P.L., (1980), Characterization of organic nitrogen in natural waters: Its molecular size, protein content, and interactions with heavy metals *Limnol. Oceanogr.* 25(3), 495-504.

[84] Alberts, J.J. and Takács, M., (1999), Importance of humic substances for carbon and nitrogen transport into southeastern United States estuaries. *Organic Geochemistry* 30(6), 385-395.

[85] Westerhoff, P. and Mash, H. (2002), Dissolved organic nitrogen in drinking water supplies: a review. *J. Water Supply Res. Technol. AQUA* 51(8).

[86] Devore, J.L., (1995), *Probability and Statistics for Engineering and the Sciences*. Brooks/Cole Publishing, Pacific Grove, CA.

[87] Smart, M.M., Reid, F.A. and Jones, J.R., (1981), A comparison of a persulfate digestion and the Kjeldahl procedure for determination of total nitrogen in freshwater samples. *Water Res.* 15(7), 919-921.

[88] Sharp, J.H., Rinker, K.R., Savidge, K.B., Abell, J., Benaim, J.Y., Bronk, D., Burdige, D.J., Cauwet, G., Chen, W.H., Doval, M.D., Hansell, D., Hopkinson, C., Kattner, G., Kaumeyer, N.,

McGlathery, K.J., Merriam, J., Morley, N., Nagel, K., Ogawa, H., Pollard, C., Pujo-Pay, M., Raimbault, P., Sambrotto, R., Seitzinger, S., Spyres, G., Tirendi, F., Walsh, T.W. and Wong, C.S., (2002), A preliminary methods comparison for measurement of dissolved organic nitrogen in seawater. *Marine Chemistry* 78(4), 171-184.

[89] Walsh, T.H., (1989), Total dissolved nitrogen in seawater: a new high temperature combustion method and a comparison with photo – oxidation, *Marine chemistry* (26), 295-311.

[90] Ammann, A., Thomas, B., Felix, B., (2000), Simultaneous determination of TOC and TNB in surface and wastewater by optimized high temperature catalytic combustion. *Water research* 34 (14), 3573-3579.

[91] Vandenbruwane, J., Neve, S.D., Qualls, R.G., Salomez, J. and Hofman, G., (2007), Optimization of dissolved organic nitrogen (DON) measurements in aqueous samples with high inorganic nitrogen concentrations. *Sci. Total Environ.* 386, 103–113.

[92] Lee, W. and Westerhoff, P., (2005), Dissolved Organic Nitrogen Measurement Using Dialysis Pretreatment. *Environ. Sci. Technol.* 39(3), 879-884.

[93] Amy, G. and Her, N., (2004), Size exclusion chromatography (SEC) with multiple detectors: a powerful tool in treatment process selection and performance monitoring. *Water Sci. Technol. Water Supply* 4, 19-24.

[94] Leenheer, J.A., (2004), Comprehensive assessment of precursors, diagenesis, and reactivity to water treatment of dissolved and colloidal organic matter. *Water Sci. Technol. Water Supply* 4(4), 1-9.

[95] Aiken, G.R., (1985), *Humic substances in soil, sediment, and water-Geochemistry, isolation, and characterization*. In: Isolation and concentration techniques for aquatic humic substances. Aiken, G.R., McKnight, D.M., Wershaw, R.L. and MacCarthy, P. (eds). John Wiley and Sons, New York, pp. 363-385.

[96] Her, N., Amy, G., Park, H. and Von-Gunten, U., (2004), UV absorbance ratio index with size exclusion chromatography (URI-SEC) as a NOM property indicator. *J. Water Supply Res. Technol. AQUA* 57(1), 35-44.

[97] Fabris, R., Chow, C.W.K., Drikas, M. and Eikebrokk, B., (2008), Comparison of NOM character in selected Australian and Norwegian drinking waters. *Water Res.* 42(15), 4188– 4196.

[98] Vuorio, E., Vahala, R., Rintala, J. and Laukkanen, R., (1998), the evaluation of drinking water treatment performed with HPSEC. *Environment International* 24(5/6), 617-623.

[99] Buchanan, W., Roddick, F. and Porter, N., (2008), Removal of VUV pre-treated natural organic matter by biologically activated carbon columns. *Water Res.* (42), 3335 – 3342.

[100] Huber, S.A. and Frimmel, F.H., (1994), Direct Gel Chromatographic Characterization and Quantification of Marine Dissolved Organic Carbon Using High-Sensitivity DOC Detection. *Environ. Sci. Technol.* 28(6), 1194-1197.

[101] Huber, S.A., Balz, A., Abert, M. and Pronk, W., (2011), Characterisation of aquatic humic and non-humic matter with size-exclusion chromatography _organic carbon detection _ organic nitrogen detection (LC-OCD-OND). *Water Res.* 45, 879-885.

[102] Huck, P.M., (1990), Measurement of biodegradable organic matter and bacterial growth in drinking water. *J. Am. Water Works Ass.* 82, 78-86.

[103] Servais, P., Anzil, A. and Vantresque, C., (1989), Simple Method for Determination of Biodegradable Dissolved Organic Carbon in Water. *Appl. Environ. Microbiol.* 55(10), 2732-2734.

[104] Servais, P., Billen, G. and Hascoët, M.-C., (1987), Determination of the biodegradable fraction of dissolved organic matter in waters. *Wat. Res.* 21(4), 445-450.

- [105] Frias, J., Ribas, F. and Lucena, F., (1992), A method for the measurement of biodegradable organic carbon in waters. *Water Res.* 26(2), 255-258.
- [106] Ribas, F., Frias, J. and Lucena, F., (1991), A new dynamic method for the rapid determination of the biodegradable dissolved organic carbon in drinking water. *J. Appl. Bacteriol.* 71 371-378.
- [107] Lucena, F., Frias, J. and Ribas, F., (1991), A new dynamic approach to the determination of biodegradable dissolved organic carbon in water. *Environmental Technology* 12(4), 343-347.
- [108] Frias, J., Ribas, F. and Lucena, F., (1995), Comparison of methods for the measurement of biodegradable organic carbon and assimilable organic carbon in water. *Water Res.* 29(12), 2785-2788.
- [109] Joret J.C., Levi Y., Volk C., (1991), Biodegradable dissolved organic carbon (BDOC) content of drinking water and potential regrowth of bacteria. *Water Sci. Technol.*, 2, 95-101.
- [110] Block J.P., Haudidier K., Paquin J.L., Miazga J., Levi Y., (1993), Biofilm accumulation in drinking water distribution systems, *Biofouling*, 6, pp. 333-343.
- [111] Van der Kooij D., (1990), Assimilable organic carbon (AOC) in drinking water, in: G.A. McFeters (Ed.), *Drinking Water Microbiology*, New York.
- [112] LeChevallier M.W., Babcock T., Lee R.G., (1987), Examination and characterization of distribution system biofilms *Appl. Environ. Microbiol.*, 53, pp. 2714-2724.
- [113] Van der Kooij D., (1982), Assimilable organic carbon as an indicator of bacterial regrowth. *J. Am. Water Works Assoc.*, 84 (1982), pp. 57-65

- [114] Smith, B.G., Lye, D.J., Messer, J.W., (2001), Occurrence of heterotrophic bacteria with virulence characteristics in potable water, Poster Q-412. 100th Annual Conference American Society for Microbiology, Orlando, FL.
- [115] Kemmy, F.A., Fry, J.C., Breach, R. A., (1989), Development and operational implementation of a modified and simplified method for determination of assimilable organic carbon (AOC) in drinking water. *Water Science and Technology* 21, 155-161.
- [116] Rosario-Ortiz, F.L., Kozawa, K., Al-Samarrai, H.N., Geringer, F.W., Gabelich, C.J. and Suffet, I.H., (2004), Characterization of the changes in polarity of natural organic matter using solid-phase extraction: introducing the NOM polarity rapid assessment method (NOMPRAM). *Water Sci. Technol. Water Supply* 4(4), 11-18.
- [117] Rosario-Ortiz, F.L., Snyder, S. and Suffet, I.H., (2007), Characterization of the polarity of natural organic matter under ambient conditions by the polarity rapid assessment method (PRAM). *Environ. Sci. Technol.* 41(14), 4895-4900.
- [118] Rosario-Ortiz, F.L., Snyder, S.A. and Suffet, I.H.M., (2007), Characterization of dissolved organic matter in drinking water sources impacted by multiple tributaries. *Water Res.* 41, 4115 – 4128.
- [119] Rosario-Ortiz, F.L., Geringer, F.W. and Suffet, I.H.M., (2009), Application of a novel polarity for the characterization of natural organic matter during water treatment. *J. Water Supply Res. Technol. AQUA* 58(3), 159-169.
- [120] Collins, M.R., Amy, G.L. and King, P.H., (1985), Removal of Organic Matter in Water Treatment. *Journal of Environmental Engineering* 111(6), 850-864.
- [121] Collins, M.R., Amy, G.L. and Steelink, C., (1986), Molecular weight distribution, carboxylic acidity, and humic substances content of aquatic organic matter: implications for removal during water treatment. *Environ. Sci. Technol.* 20(10), 1028-1032.

- [122] Chow, C.W.K., van Leeuwen, J.A., Drikas, M., Fabris, R., Spark, K.M. and Page, D.W., (1999), The impact of the character of natural organic matter in conventional treatment with alum. *Water Sci. Technol.* 40(9), 97-104.
- [123] Edzwald, J.K. and Tobiason, J.E., (1999), Enhanced coagulation: US requirements and a broader view. *Water Sci. Technol.* 40(9), 63-70.
- [124] Owen, D.M., Amy, G.L. and Chowdhary, Z.K., (1993), Characterization of Natural Organic Matter and its Relationship to Treatability, American Water Works Association Research Foundation, Denver, CO.
- [125] Amy, G., (1994), Using NOM Characterisation for Evaluation of Treatment. In *Proceedings of Workshop on "Natural Organic Matter in Drinking Water, Origin, Characterization and Removal"*, September 19–22, 1993, Chamonix, France. American Water Works Association Research Foundation, Denver, USA, p. 243.
- [126] Humbert, H., Gallard, H., Suty, H. and Croue, J.P., (2005), Performance of selected anion exchange resins for the treatment of a high DOC content surface water. *Water Res.* 39(9), 1699-1708.
- [127] Walter J. Weber, J., (2004), Preloading of GAC by natural organic matter in potable water treatment systems: Mechanisms, effects, and design considerations. *J. Water Supply Res. Technol. AQUA* 53(7).
- [128] Humbert, H., Gallard, H., Suty, H. and Croue, J.P., (2005), Performance of selected anion exchange resins for the treatment of a high DOC content surface water. *Water Res.* 39(9), 1699-1708.
- [129] Mergen, M.R.D., Jefferson, B., Parsons, S.A. and Jarvis, P., (2008), Magnetic ion exchange resin treatment: Impact of water type and resin use. *Water Res.* 42(8–9), 1977-1988.

- [130] Boyer, T.H. and Singer, P.C., (2005), Bench-scale testing of a magnetic ion exchange resin for removal of disinfection by-product precursors. *Water Res.* 39(7), 1265-1276.
- [131] Johnson, C.J. and Singer, P.C., (2004), Impact of a magnetic ion exchange resin on ozone demand and bromate formation during drinking water treatment. *Water Res.* 38(17), 3738-3750.
- [132] Allpike, B.P., Heitz, A., Joll, C.A., Kagi, R.I., Abbt-Braun, G., Frimmel, F.H., Brinkmann, T., Her, N. and Amy, G., (2005), Size Exclusion Chromatography to Characterize DOC Removal in Drinking Water Treatment. *Environ. Sci. Technol.* 39(7), 2334-2342.
- [133] Boyer, T.H. and Singer, P.C., (2005), Bench-scale testing of a magnetic ion exchange resin for removal of disinfection by-product precursors. *Water Res.* 39(7), 1265-1276.
- [134] Morran, J.Y., Drikas, M., Cook, D. and Bursill, D.B., (2004), Comparison of MIEX® treatment and coagulation on NOM character. *Water Sci. Technol. Water Supply* 4(4), 129-137.
- [135] Odegaard, H., Eikebrokk, B. and Storhaug, R., (1999), Processes for the removal of humic substances from water - An overview based on Norwegian experiences. *Water Sci. Technol.* 40(9), 37-46.
- [136] Juhna, T. and Melin, E., (2006), Ozonation and biofiltration in water treatment – Operational status and optimization issues. *Techneau*.
- [137] Siddiqui, M.S., Amy, G.L. and Murphy, B.D., (1997), Ozone enhanced removal of natural organic matter from drinking water sources. *Water Res.* 31(12), 3098-3106.
- [138] Frimmel, F.H., Saravia, F. and Gorenflo, A., (2006), NOM removal from different raw waters by membrane filtration. *Water Sci. Technol. Water Supply* 4(4), 165-174.
- [139] Kuehn, W. and Mueller, U., (2000), Riverbank filtration: an overview. *J. Am. Water Works Assoc.* 92(12), 60-69.

- [140] Weiss, W.J., Bouwer, E.J., Ball, W.P., O'Melia, C.R., Aboytes, R. and Speth, T.F., (2004), Riverbank filtration: Effect of ground passage on NOMcharacter *J. Water Supply. Res. Technol.* - *AQUA* 53(2), 61 83.
- [141] Owen, D.M., Amy, G.L. and Chowdhary, Z.K., (1993) Characterization of Natural Organic Matter and its Relationship to Treatability, American *Water Works Association Research Foundation*, Denver, CO.
- [142] Matilainen, A., Lindqvist, N., Korhonen, S. and Tuhkanen, T., (2002), Removal of NOM in the different stages of the water treatment process. *Environment International* 28, 457– 465.
- [143] Osterhus, S., Azrague, K., Leiknes, T. and Odegaard, H., (2007), Membrane filtration for particles removal after ozonation-biofiltration. *Water Sci. Technol.* 56(10), 101-108.
- [144] White G.C. Handbook of Chlorination and Alternative Disinfectants, (1999), 4th Ed., *John Wiley & Sons, Inc.*, New York, New York.
- [145] U.S. Environmental Protection Agency. Disinfectant and Disinfection By-Products Rule. (1998).
- [146] Brodtmann N.V., Russo P.J., (1979), The use of chloramine for reduction of trihalomethanes and disinfection of drinking water. *J. AWWA*.71: 40–42.
- [147] Norman T.S., Harms L.L., Looyenga R.W., (1980), The use of chloramines to prevent trihalomethane formation. *J. AWWA*. 72(3):176
- [148] Haas C.N., (2000), Disinfection. In *Water Quality & Treatment, A Handbook of Community Water Supplies*, 5th Edition, Ed. R.D. Letterman, American Water Works Association, McGraw-Hill, Inc., New York, New York.
- [149] Odell L.H., Kirmeyer G.J., Wilczak A., Jacangelo J.G., Marcinko J.P., Wolfe R.L., (1996), Controlling Nitrification in Chloraminated Systems. *J. AWWA*. 88(7):86 98.

- [150] LeChevallier M.W., Cawthon C.D., Lee R.G., (1988), Factors promoting survival of bacteria in chlorinated water supplies. *Appl. Environ. Microbiol.* 54:649-654.
- [151] American Public Health Association. Standard methods for the examination of water and wastewater, 17th ed. Washington, DC, (1989).
- [152] The measurement of electrical conductivity and laboratory determination of the pH value of natural, treated and wastewaters. London, *Her Majesty's Stationery Office*, (1978).
- [153] Sawyer, C.N. and Mc Carty. P.L., (1978), Chemistry for Environmental Engineering (3rd Ed), *McGraw - Hill Book Company*, New York.
- [154] Snoeyink, V.L., and Jenkins, D., (1980), Water Chemistry, *John Wiley & Sons*, New York.
- [155] Standard Methods for the Examination of Water and Wastewater (18 th Ed.), American Water Works Association, (1992).
- [156] APHA., (1992). Standard methods for the examination of water and wastewater. 18th ed. *American Public Health Association*, Washington, DC.
- [157] Hach Company. (1992). Hach water analysis handbook. 2nd ed. *Loveland, CO*.
- [158] Mississippi Headwaters River Watch. (1991). Water quality procedures. *Mississippi Headwaters Board*.
- [159] Chang, C., Sommerfeldt, T. G., Carefoot, J. M. and Schaalje, G. B., (1983), 'Relationships of electrical conductivity with total dissolved salts and cation concentration of sulfate-dominant soil extracts', *Can. J. Soil Sci.* 63, 79–86.
- [160] Baker. R.W., (2014). Membrane Technology and Applications, 2nd edition, Wiley-VCH.
- [161] Mulder M., (1996). Basic Principles of Membrane Technology, 2nd edition, Kluwar Publishers

- [162] Alexandre, G., Andrea, M.B., (2022). Membrane separation process in wastewater and water purification 3, 259.
- [163] David, M.W., Sudop, C., Emily, W.T., Megan, H.P., (2018). A review of polymeric membranes and processes for potable water reuse. *Progress in polymer science* 81, 209-237.
- [164] Favre, E., (2020). Specialty grand challenges in separation process. *Front Chem. Eng.* 2, doi: 10.3389.
- [165] Nunes, S.P., Culfaz, E., Ranon, P.Z., Visser, G.Z., Koops, T., Jin, G.H., (2020). Thinking the future of membranes perspectives for advanced and new membrane materials and manufacturing processes. *Journal of membrane science* 598, 117761.
- [166] Castel, C. and Favre, E., (2018). Membrane separations and energy efficiency. *Journal of Membr. Science* 548, 345-357.
- [167] Favre, E., (2022). The future of membrane separation processes: A prospective analysis. *Separation Processes*, 4, doi: 10.3389.
- [168] Soni, V., Abildskov, J., Jonsson, G., Gani, R., (2009). A general model for membrane-based separation processes. *Computers and Chemical Engineering*, 33, 3. 644-659.
- [169] Koops, G.H., (1995). Nomenclature and symbols in membrane sand technology. University of Twente, Membrane Technology Group, Netherlands.
- [170] Strathmann, H., Giorno, L., Drioli, E., (2006), an introduction to membrane science and technology, Roma, Italia.
- [171] Ulbricht, M., (2006). Advanced functional polymer membranes. *Polymer*, 47, 7, 2217- 2262.
- [172] Mulder, M., (1996). Basic principles of membrane technology, Kluwer Academic Publishers, Dordrecht, the Netherlands.

- [173] Lashkari, S., Tran, A., Kruczek, B. (2008). Effect of back diffusion and back permeation of air on membrane characterization in constant pressure system. *Journal of Membrane Science*, 324, 1-2, 162-172, 03767388.
- [174] Baker, R.W. (2004). *Membrane technology and applications*, John Wiley & Sons, ISBN: 0-470-85445-6, Chichester, England.
- [175] Koros, W.J., Fleming, G.K. (1993). Membrane-based gas separation, *Journal of Membrane Science*, 83, 1, 1-80. 03767388.
- [176] Chakma, A. (1995). Separation of CO₂ and SO₂ from flue gas streams by liquid membranes. *Energy Conversion and Management*, 36, 6-9., 405-410.
- [177] Ravanchi, M.T., Kaghazchi, T., Kargari, A. (2010). Supported liquid membrane separation of propylene propane mixtures using a metal ion carrier. *Desalination*, 250, 1,130- 135.
- [178] Kocherginsky N.M., Yang Q., Seelam L. (2007). Recent advances in supported liquid membrane technology. *Separation and Purification Technology*, 53, 2, 171-177.,13835 866.
- [179] Peinemann, K. (2004). Next generation membrane materials. In: *Abstracts of the 15th annual meeting of the NAMS*, Honolulu, 26–30.
- [180] Matsuura T. (1994) *Synthetic membranes and membrane separation processes*. CRC, Boca Raton.15.
- [181] Loeb S., Sourirajan S. (1963). Sea water demineralization by means of an osmotic membrane. *Advances in Chemistry Series* 38, 117–132.
- [182] Sourirajan S., Matsuura T. (1985). *Reverse osmosis / ultrafiltration process principles*. National Research Council of Canada.

- [183] Lloyd D. (1985). Membrane materials science: an overview. In: Lloyd DR (ed) Materials science of synthetic membranes. ACS Symposium Series 269. American Chemical Society, Washington.
- [184] Matsuura T. (2001) Reverse osmosis and nanofiltration by composite polyphenylene oxide membranes. In: Chowdhury G, Kruczek B, Matsuura T (eds) Polyphenylene oxide and modified polyphenylene oxide membranes. Kluwer, Dordrecht.
- [185] Allegrezza A.E.Jr, Parekh B.S., Parise P.L., Swiniarski E.J., White J.L. (1987). Chlorine resistant polysulfone reverse osmosis modules. *Desalination* 64:285.
- [186] Guiver M.D, Tremblay AY, Tam CM (1985) Reverse osmosis membrane from novel hydrophilic polysulfone. In: Sourirajan S, Matsuura T (eds) Advances in reverse osmosis and ultrafiltration. National Research Council of Canada.
- [187] Kulkarni S.S., Funk E.W., Li N (1992). Ultrafiltration. In: Ho WSW, Sirkar K.K. (eds) Membrane handbook. Van Nostrand, New York, 393.
- [188] Faiz, R. and Li, K. (2012). Polymeric membranes for light olefin/paraffin separation. *Desalination*, 82-97.
- [189] Choi, B.G., Huh, Y.S., Park, Y.C., Jung, D.H., Hong, W.H., and Park, H., (2012). Enhanced transport properties in polymer electrolyte composite membranes with graphene oxid sheets. *Carbon*, 5395-5402.
- [190] Budd, P.M. and McKeown, N.B., (2010). Highly permeable polymers for gas separation membranes. *Polymer Chemistry*, 63-68.
- [191] Geise, G.M., Lee, H.S., Miller, D.J., Freeman, B.D., McGrath, J.E., and Paul, D.R., (2010), Water purification by membranes: The role of polymer science. *Journal of Polymer Science Part B: Polymer Physics*, 1685-1718.

- [192] Akin, O., Temelli, F., and Köseoğlu, S., (2012), Membrane Applications in Functional Foods and Nutraceuticals. *Critical Reviews in Food Science and Nutrition*, 2012. 52(4): 347-371.
- [193] Gyura, J., Šereš, Z., and Eszterle, M., (2005), Influence of operating parameters on separation of green syrup colored matter from sugar beet by ultra and nanofiltration. *Journal of Food Engineering*, 89-96.
- [194] López-Fernández, R., Martínez, L., and Villaverde, S., (2010), Membrane bioreactor for the treatment of pharmaceutical wastewater containing corticosteroids. *Desalination*.300: 19- 23.
- [195] Huang, M., Ding, Y., and Li, X., (2012), Improvement of lower detection limit of ion-selective electrodes based on PVC membrane. *Progress in Chemistry*, 24(8): 1560- 1571.
- [196] Ramakrishna, S., Ma, Z., and Matsuura, T., (2010), *Polymer membranes in biotechnology: Preparation, functionalization and application*, London: Imperial College Press.
- [197] Garcia-Castello, E.M. and Mc Cutcheon, J.R., (2011), Dewatering press liquor derived from orange production by forward osmosis. *Journal of Membrane Science*. 97-101.
- [198] Yazdanshenas, M., Nejad, S.A.R.T., Soltanieh, M., Tavakkoli, A., Babaluo, A.A., and Fillaudeau, L., (2010), Dead-end microfiltration of rough nonalcoholic beer by different polymeric membranes. *Journal of the American Society of Brewing Chemists*, 68(2): 83- 88.
- [199] Gray, S., (2003), NOM removal with membranes, CRC for water quality and treatment and CSIRO manufacturing and infrastructure technologies. *Natural Organic Matter in Drinking Water: Problems and Solutions*.
- [200] Booker, N., Bridger, J., Carrol, Gray, S., (2002), Final report hybrid membrane processes for water treatment. *Water quality and treatment project 3.1.3*.
- [201] Carrol, T., Booker, N.A., (2000). Improved performance of water microfiltration with hybrid

particle pretreatment. Proceedings of the International conference on membrane technology in water and wastewater treatment, Lancaster, UK.

[202] Mohanty, K. and Purkait, M.K., (2010), Membrane technologies and applications. Boca Raton FL: CRC Press. USA.

[203] Zhang, T.C., (2012), Environmental, Water Resources Institute. Membrane Technology Task, C., and American Society of Civil, E., Membrane technology and environmental applications, Reston, VA: American Society of Civil Engineers.

[204] DiGiano, F. A., Braghetta, A., Nilson, J., and Utne, B., (1994). Fouling of nanofiltration membranes by natural organic matter, National Conference on Environmental Engineering, American Society of Civil Engineers.

[205] Thorsen, T., (1999). Membrane filtration of humic substances – State of the art, Water Sci. Technol., 40, 105–112.

[206] Nystrom, M., Kaipia, L., and Luques, S., (1999). Fouling and retention of nanofiltration membranes, J. Membr. Sci., 98, 249–262.

[207] Baker, J., Stephenson, T., Dard, S., Cote, P., (1995). Characterisation of fouling of nanofiltration membranes used treat surface waters, Environ. Technol., 16, 977–985.

[208] Hong, S. and Elimelech, M., (1997). Chemical and physical aspects of natural organic matter (NOM) fouling of nanofiltration membranes, J. Membr. Sci., 132, 159–181.

[209] Chellam, S., Jacangelo, J. G., Bonacquisti, T. P., and Schauer, B. A., (1997). Effect of pretreatment for surface water nanofiltration, J. Am. Water Works Ass., 89, 77–88.

[210] Lijima, S., (1991). Helical microtubules of graphitic carbon, nature, 354(7) 56-58.

- [211] Brady A.S., Estevez, Kang S., Elimelech M., (2008). A single walled carbon nanotubes filter for removal of viral and bacterial pathogens. 4, 481- 484.
- [212] Singer J.M., Grumer J., (1958). Carbon formation in very rich hydrocarbon-air flames. Studies of chemical content, temperature, ionization and particulate matter, Symp. Int. Combust. Proc. 7(1), 559-569.
- [213] Hu W.C., Lin T.H., (2016). Ethanol flame synthesis of carbon nanotubes in deficient oxygen environments, Nanotech. 27(16), 165602.
- [214] Magrez A., Seo J.W., Smajda R., Mionic M., Forro L., (2010), Catalytic CVD synthesis of carbon nanotubes: towards high yield and low temperature growth. Materials 3, 4871-4891.
- [215] Dai H., (2001), Carbon Nanotubes: Synthesis, Structure, Properties and Applications. Springer. Account of Chemical Research. 1035-1044.
- [216] Thess A., Lee R., Nikolaev P., Dai H., Petit P., Robert J., Xu C., Lee Y. H., Kim S. G. Rinzler A.G., Colbert D. T., Scuseria G. E., Tomanek D., Fischer J. E., Smalley R. E., (1996). Crystalline ropes of metallic carbon nanotubes. Journal of Science, 273, 487.
- [217] Jose-Yacamán M., Miki-Yoshida M., Rendon L., Santiesteban J., (1993). Catalytic growth of carbon microtubes with fullerene structure. Applied Physics letters. 62, 202-204.
- [218] Walker P., Rakszawski J., Imperial G., (1959). Carbon formation from carbon monoxide hydrogen mixtures over iron catalysts. Journal of Physics and Chemistry, 63, 133-140.
- [219] Rummeli M.H., Ayala P., Pichler T., (2010), Carbon Nanotubes and Related Structures, 1-21.
- [220] Dai H., Javey A., Pop E., Mann D., Lu Y., (2006). Electrical transport properties and field effect transistors of carbon nanotubes. Nanotechnology, 1, 1-13.

- [221] Kataura H., Kumazawa Y. , Maniwa Y., Umezumi I. , Suzuki S. , Ohtsuka Y., Achiba, A., (1999). Optical properties of single-walled carbon nanotubes. *Synthetic Metals*, 103, 2555-2558.
- [222] Ebbesen T. , Lezec H., Hiura H. , Bennett J. , Ghaemi H. , Thio T., (1996). Electrical conductivity of individual carbon nanotubes. *Nature*, 382, 54-56.
- [223] Coleman J. N., Khan U., Gun'ko Y. K., (2006). Mechanical reinforcement of polymers using carbon nanotubes. *Advanced Materials*, 18, 689-706.
- [224] Overney G., Zhong W., Tomanek D., (1993). Structural rigidity and low frequency vibrational modes of long carbon tubules, *Molecules and Clusters*, 27, 93-96.
- [225] Treacy M., Ebbesen T., Gibson J., (1996). Exceptionally high young's modulus observed for individual carbon nanotubes. *Nature*, 381, 678-680.
- [226] Wong E. W., Sheehan P. E., Lieber C. M., (1997). nanobeam mechanics: elasticity, strength, and toughness of nanorods and nanotubes. *Science*, 277, 1971-1975.
- [227] Salvetat, J. P., Kulik A. J., Bonard J. M., Briggs G. D., Stöckli T., Méténier K., Bonnamy, S. , Béguin, F. , Burnham, N. A. , Forró, L., (1999). Elastic modulus of ordered and disordered multiwalled carbon nanotubes. *Advanced materials*, 11, 161-165.
- [228] Salvetat, J. P., Briggs, G. A. D., Bonard, J. M., Bacsá, R. R., Kulik, A. J., Stöckli, T., Burnham, N. A., Forró, L., (1999). Elastic and shear modulus of single-walled carbon nanotubes ropes. *Physics Review Letter*, 82, 944-947.
- [229] Salvetat, J. P., Bonard, J. M., Thomson N., Kulik A., Forro L., Benoit W., Zuppiroli, L., (1999). Elastic and shear modulus of single-walled carbon nanotubes ropes. *Applied physics. Material science processing*, 69, 255-260.
- [230] Xie, S., Li, W., Pan, Z., Chang, B., Sun, L., (2000). Mechanical and physical properties of

carbon nanotubes. *Journal of Physics and Chemistry of Solids*, 61, 1153-1158.

[231] Landry, O., Sunny, I., Bavon, K., Precious, B., (2019). Impact of carbon nanotubes on the polymeric membrane for oil – water separation. *Int. Journal of Nanosci. Nanotechnol.*, 15, 99 - 115.

[232] Al-Jammal, N., Abdullah, T.A., Juzsakova, T., Zsirka, B., Cretescu, I., Vagvolgyi, V., Sebestyen, V., Le Phuoc, C., Rasheed, R.T., Domokos E., (2020). Functionalized carbon nanotubes for hydrocarbon removal from water. *Journal of Environmental Chemical Engineering*, 8, 103570.

[233] Kim, S. W., Kim, T., Kim, Y. S., Choi, H. S., Lim, H. J., Yang, S. J., Park, C. R., (2012). Chemistry of carbon nanotubes, *Chemical review*, 50, 3-33.

[234] Qin, S., Qin, D., Ford, W. T., Resasco, D. E., Herrera, J. E., (2004). Polymer brushes on single-walled carbon nanotubes by atom transfer radical polymerization of n-butyl methacrylate. *Journal of the American chemical society*, 126, 170-176.

[235] Kong, H., Gao, C., Yan, D., (2004). Controlled functionalization of multi-walled carbon nanotubes by atom transfer radical polymerization. *Journal of the American chemical society*. 126, 412-413.

[236] Mickelson, E., Huffman, C., Rinzler, A., Smalley, R., Hauge, R., Margrave, J., (1998). Fluorination of single-walled carbon nanotubes. *Chemical Physics Letters*, 296, 188-194.

[237] Khabashesku, V. N., Billups, W. E., Margrave, J. L., (2002). Fluorination of single-walled carbon nanotubes and subsequent derivatization reactions. *Accounts Chemical research*. 35, 1087-1095.

[238] Liu, J., Zubiri, M. R. I., Dossot, M., Vigolo, B., Hauge, R. H., Fort, Y., Ehrhardt, J. J., Mcrae, E., (2006). Sidewall functionalization of single-walled carbon nanotubes through aryl free radical addition. *Chemical Physics Letters*, 430, 93-96.

- [239] Holzinger, M., Vostrowsky, O., Hirsch, A., Hennrich, F., Kappes, M., Weiss, R., Jellen, F., (2001). Sidewall functionalization of carbon nanotubes. *Angewandte Chemie.*, 40, 4002- 4005.
- [240] Tagmatarchis N., Georgakilas V., Prato M., Shinohara H., (2002). *Chemical Communications*, 2010-2011.
- [241] Liu, P., (2005). Modification of carbon nanotubes with polymers. *Euro Polymers Journal*. 41, 2693-2703.
- [242] Sano M., Kamino, A., Okamura, J., Shinkai, S., Langmuir, L., (2001). Self organisation of PEO-graft single-walled carbon nanotubes in solutions and Langmuir-blodgett films. *Langmuir*, 7, 5125- 5128.
- [243] Albuerne, J., Boschetti-de-Fierro, A., Abetz, V., (2010). Modification of multi-walled carbon nanotubes by grafting from controlled polymerization of styrene: Effect of characteristics of the nanotubes. *Journal of Polymer Science*, 48, 1035-1046.
- [244] Lin, Y., Zhou, B., Fernando, K. a. S., Liu, P., Allard, L. F., Sun, Y. P., (2003). Polymeric carbon nanocomposites from carbon nanotubes functionalized with matrix polymer. *Macromolecules*, 36, 7199 7204.
- [245] Lou X., Detrembleur, C., Sciannamea, V., Pagnouille, C., Jérôme R., (2004). Grafting of alkoxyamine end –capped (Co) polymers onto multi-walled carbon nanotubes, *Polymer*, 45, 6097- 6102.
- [246] Yao, Z., Braid, N., Botton, G. A., Adronov, A., (2003). Polymerization from the surface of single-walled carbon nanotubes- preparation and characterization of nanocomposite. *Journal of American Chemical Society*. 125, 16015-16024.
- [247] Islam, M., Rojas, E., Bergey, D., Johnson, A., Yodh, A., (2003). High weight fraction

surfactant solubilisation of single-walled carbon nanotubes in water. *Nano Letters*, 3, 269-273.

[248] Wenseleers, W., Vlasov, I. I., Goovaerts, E., Obraztsova, E. D., Lobach, A. S., Bouwen, A., (2004). Efficient isolation and solubilisation of pristine single-walled nanotubes in bile salt micelles. *Advanced Functional Materials*, 14, 1105-1112.

[249] Moore, V. C., Strano, M. S., Haroz, E. H, Hauge, R. H., Smalley, R. E., Schmidt, J., Talmon, Y., (2003). Individually suspended single-walled carbon nanotubes in various surfactants. *NanoLetters*, 3, 1379-1382.

[250] Fujigaya, T., Nakashima, N., (2008). Methodology for homogeneous dispersion of single-walled carbon nanotubes by physical modification. *Polymer Journal*, 40, 577-589.

[251] Tomonari, Y., Murakami, H., Nakashima, N., (2006). Solubilization of single-walled carbon nanotubes using polycyclic aromatic ammonium amphiphiles in water-strategy for the design of solubilizers with high performance. *Chemical European Journal*, 12, 4027-4034.

[252] Chen, R. J., Zhang, Y., Wang, D., Dai, H., (2001). Non-covalent sidewall functionalization of single-walled carbon nanotubes for protein immobilization. *Journal of the American Chemical Society*, 123, 3838-3839.

[253] Ji, Y. Y., Huang, Y., Tajbakhsh, A. R., Terentjev, E. M., (2009). Polysiloxane surfactants for the dispersion of carbon nanotubes in nonpolar organic solvents. *Langmuir*, 25, 12325-12331.

[254] Lui, A., Talbot, F.D. F, Sourirajan, S., Fouda, A.E., Matsuura, T., (1998). *Separation science technology* 23 :1839.

[255] Liu, J., Bibari, O., Mailley, P., Dijon, J., Rouvière, E., Sauter-Starace, F., Caillat, P., Vinet, F., Marchand, G., (2009). Stable non-covalent functionalization of multi-walled carbon nanotubes by pyrene-polyethylene glycol through π - π stacking. *New Journal of Chemistry*, 33, 1017-1024.

- [256] Meuer, S., Braun, L., Zentel, R., (2009). Pyrene containing polymers for the non-covalent functionalization of carbon nanotubes. *Macromolecular Chemistry and Physics*. 210, 1528-1535.
- [257] Star, A., Stoddart, J. F., Steuerman, D., Diehl, M., Boukai, A., Wong, E. W., Yang, X., Chung, S. W., Choi H., (2001). Preparation and properties of polymer-wrapped single-walled carbon nanotubes, *Angewandte Chemie*, 40, 1721-1725.
- [258] Giulianini, M., Waclawik, E.R., Bell, J.M., De Crescenzi, M., Castrucci, P., Scarselli, M., Motta, N., (2009). Regioregular poly (3-hexyl-thiophene) helical self-organization on carbon nanotubes. *Applied Physics Letters*, 95, 013304.
- [259] Zou, J., Liu, L., Chen, H., Khondaker, S. I., Mccullough, R. D., Huo, Q., Zhai, L., (2008). Dispersion of pristine carbon nanotubes using conjugated block copolymers. *Advanced materials*, 20, 2055-2060.
- [260] O'connell, M. J., Boul, P., Ericson, L. M., Huffman, C., Wang, Y., Haroz, E., Kuper, C., Tour, J., Ausman, K. D., Smalley, R. E., (2001). Reversible water – solubilisation of single-walled carbon nanotubes by polymer wrapping. *Chemical Physics Letters*, 342, 265-271.
- [261] Kang, Y., Taton, T. A., (2003). Micelle encapsulated carbon nanotubes: A route to nanotube composites. *Journal of the American Chemical Society*, 125, 5650-5651.
- [262] Camper, A.K., Lechevallier, M.W., Broadway, S.C., McFeters, G.A., (1985). Growth and persistence of pathogens on granular activated carbon filters. *Appl Environ Microbiol*, 50, 1378–82.
- [263] Shimp, R.J., Pfaender, F.K., (1982). Effects of surface area and flow rate on marine bacterial growth in activated carbon columns. *Appl Environ Microbiol*, 44, 471–7.
- [264] Nepal, D., Balasubramanian, S., Simonian, A.L., Davis, V.A., (2008). String antimicrobial coatings single walled carbon nanotubes armored with biopolymers. *Nano Lett* 2, 1896–902.

- [265] Kang, S., Pinault, M., Pfefferle, L.D., Elimelech, M., (2007). Single walled carbon nanotubes exhibit strong antimicrobial activity. *Langmuir*, 23, 8670–3.
- [266] Zhu, Y., Ran, T., Li, Y., Guo, J., Li, W., (2006). Dependence of cytotoxicity of multi walled carbon nanotubes on the culture medium. *Nanotechnology*, 17, 4668–74.
- [267] Akasaka, T., Watari, F., (2009). Capture of bacteria by flexible carbon nanotubes. *Acta Biomater*, 5, 607–12.
- [268] Arias, L.R., Yang, L., (2009). Inactivation of bacterial pathogens by carbon nanotubes in suspensions. *Langmuir*, 25, 3003–12.
- [269] Krishna, V., Pumprueg, S., Lee, S.H., Zhao, J., Sigmund, W., Koopman, B., (2005). Photocatalytic disinfection with titanium dioxide coated multi walled carbon nanotubes. *Trans IChemE, Part B Process Saf Environ Prot*, 83, 393–7.
- [270] Brady-Estevez, A.S., Kang, S., Elimelech, M., (2008). A single walled carbon nanotube filter for removal of viral and bacterial pathogens. *Small*, 4, 481–4.
- [271] Kang, S., Mauter, S.M., Elimelech, M., (2008). Physiochemical determinants of multiwalled carbon nanotube bacterial cytotoxicity. *Environ Sci Technol*, 42, 7528–34.
- [272] Arias, L.R., Yang, L., (2009). Inactivation of bacterial pathogens by carbon nanotubes in suspensions. *Langmuir*, 25, 3003–12.
- [273] Kang, S., Pinault, M., Pfefferle, L.D., Elimelech, M. (2007). Single walled carbon nanotubes exhibit strong antimicrobial activity. *Langmuir*, 23, 8670–3.

- [274] Kang, S., Herzberg, M., Rodrigues, D.F., Elimelech, M., (2008). Antibacterial effects of carbon nanotubes: size does matter. *Langmuir*, 24, 6409–13.
- [275] Ahmed, A.S., Surjith, A., Kateryna, B., Mohan, J., (2017). Review on the antimicrobial properties of carbon nanotubes nanostructures materials, 10, 1066.
- [276] Akasaka, T., Watari, F., (2009). Capture of bacteria by flexible carbon nanotubes. *Acta Biomater*, 5, 607–12.
- [277] Gerba, C.P., Sobsey, M.D., Wallis, C., Melnick, J.L., (1975). Adsorption of polio virus onto activated carbon in wastewater. *Environ Sci Technol*, 9, 727–31.
- [278] Upadhyayula, V.K.K., Deng, S., Smith, G.B., Mitchell, M.C., (2009). Adsorption of *Bacillus subtilis* on single walled carbon nanotube aggregates, activated carbon and nanoceram TM. *Water Res*, 43, 1–9.
- [279] Ounaies, Z., Park C., Wise, K.E., Siochi, E.J., Harrison J.S., (2003). Electrical properties of single walled carbon nanotube reinforced polyimide composites. *Compos Sci Technol*, 63, 1637–47.
- [280] Deng, S., Upadhyayula, V.K.K., Smith, G.B., Mitchell, M.C., (2008). Adsorption equilibrium and kinetics of microorganisms on single walled carbon nanotubes. *IEEE Sens*, 8, 954–62.
- [281] Feifei, L., Jinlin, F., Guang, H.M., (2013). Adsorption of natural organic matter analogues by multi-walled carbon nanotubes: Comparison with powdered activated carbon. *Journal of Chem. Eng.*, 219, 450-458.
- [282] Juta, S., Ateia, M., Yoshimura, C., (2018). Natural organic matter undergoes different molecular sieving by adsorption on activated carbon and carbon nanotubes. *Chemosphere*, 203, 345–352.

- [283] Jeong, K., Kim, D.G., Ko, S.O., (2017). Adsorption characteristic of effluent organic matter and natural organic matter by carbon-based nanomaterials. *Journal of Civil Engineering*, 21, 119–126.
- [284] Naghizadeh, A., Nasser, S., Rashidi, A., Kalantary, R.R., Nabizadeh, R., Mahvi, A., (2013). Adsorption kinetics and thermodynamics of hydrophobic natural organic matter removal from aqueous solution by multi-walled carbon nanotubes. *Journal of Water Science and Technology*, 13, 273–285.
- [285] Lu, C., Su, F., (2007). Adsorption of natural organic matter by carbon nanotubes. *Sep Purif Technol*, 58, 113 – 21.
- [286] Matilainen, A., Vieno, N., Tuhkanen, T., (2006). Efficiency of activated carbon filtration in the natural organic matter removal. *Environ Int*, 32, 324–31.
- [287] Matsui, Y., Fukuda, Y., Inoue, T., Matsuhita, T., (2003). Effect of natural organic matter on powdered activated carbon adsorption of trace contaminants: characteristics and mechanism of competitive adsorption. *Water Res*, 37, 4413–24.
- [288] Quinlivan, A.P., Li, L., Knappe, D.R.U., (2005). Effects of activated carbon characteristics on the simultaneous adsorption of aqueous organic micropollutants and natural organic matter. *Water Res*, 2, 39, 1663–73.
- [289] Schreiber, B., Brinkmann, T., Schmalz, V., Worch, E., (2005). Adsorption of dissolved organic matter onto activated carbon, the influence of temperature, adsorption, wavelength, and molecular size. *Water Res*, 39, 3449–56.
- [290] Newcombe, G., (1999). Charge vs porosity, some influences on the adsorption of natural organic matter (NOM) by activated carbon. *Wat Sci Technol*, 40, 191–8.

- [291] Hyung, H., Kim, J.H., (2008). Natural organic matter (NOM) adsorption to multi walled carbon nanotubes: effect on NOM characteristics and water quality parameters. *Environ Sci Technol*, 42, 4416–21.
- [292] Saleh, N.B., Pfefferle, L.D., Elimelech, M., (2008). Aggregation kinetics of multiwalled carbon nanotubes in aquatic systems: measurements and environmental implications. *Environ Sci Technol*, 42, 7963–9.
- [293] Yan X.M., Shi B.Y., Lu J.J., Feng C.H., Wang D.S., Tang H.X., (2008). Adsorption and desorption of atrazine on carbon nanotubes. *J Colloid Interface Sci*, 321, 30–8.
- [294] Hoffmann, J.R.H., (1976). Removal of microcystis toxins in water purification processes. *Water SA* 1976, 2, 58–60.
- [295] Momani, F.L., Smith, D.W., El-din M.G., (2008). Degradation of cyanobacteria toxin by advanced oxidation process. *J Hazard Mater*, 150, 238–49.
- [296] Yan, H., Pan, G., Hua, Z., Li, X., Chen, H., (2004). Effective removal of microcystins using carbon nanotubes embedded with bacteria. *Chin Sci Bull*, 49, 1694–8.
- [297] Yan, H., Gong, A., He, H., Zhou, J., Wei, Y., Lv, L., (2006). Adsorption of microcystins by carbon nanotubes. *Chemosphere*, 62, 142–8.
- [298] Albuquerque Junior, E.C., Mendez, M.O.A., Coutinho, A.D.R., Franco, T.T., (2008). Removal of cyanobacterial toxins from drinking water by adsorption on activated carbon fibers. *Material Research*, 11, 370–80.
- [299] Ye, C., Gong, Q., Lu, F., Liang, J., (2007). Adsorption of middle molecular weight toxins on carbon nanotubes. *Acta Phys-Chem. Sin*, 23, 1321.

CHAPTER THREE: EXPERIMENTAL PROCEDURE AND MATERIALS

3.1 Introduction

This chapter discusses and presents the experimental and analytical methods used to prepare and study the materials. Data analysis and interpretation are also encouraged. The actions that constitute the laboratory testing components of the study are presented as follows:

- Sample pick up and preparation (ultrapure water, tap water, and wastewater).
- Analysis for AOC and BDOC determination.
- Synthesis of PSF membrane.
- Functionalization of MWCNTs.
- Characterization of PSF membranes and MWCNTs.
- Experimental procedure.
- Data analysis and interpretation.

3.1.1. Chemicals, materials, and facilities required.

The MWCNTs, PSF, maleic acid, DMF, polyvinyl alcohol, CTAB, sulfuric acid, nitric acid, hydrochloric acid, water molecular biology reagent, nitrogen (total) cell test kit, nitrate cell test kit, ammonium cell test kit, chlorine cell test kit, and alkalinity (total) cell test kit were purchased from Merck (Johannesburg, South Africa). Bacterial strains (*Pseudomonas fluorescens* P17) for AOC measurement were purchased from Germany via Thermofisher Scientific (Johannesburg, South Africa). Ammonium sulphate, ethanol, nutrient broth, nitric acid, R2A agar, sodium acetate, sulfuric acid, sterilizer, agar plates, screw capped test tubes, glass spreaders were provided by the water quality laboratory (School of Environmental and Civil Engineering, Wits) for AOC measurement. Amber bottles, distilled water, measuring cylinder, pre-washed sand, syringe filter, sterile cotton wool, strings, aluminum foil, sodium acetate, 0.45 μm filter were provided by the water quality laboratory (School of Civil and Environmental Engineering, Wits) for BDOC measurement. Note: Nitric acid was used to clean every piece of glass that was utilized in this study, and it was then repeatedly rinsed with distilled water.

The biological microscope (Olympus Cx22 LED) was used to carry out the morphological and physiological tests of the strain *Pseudomonas fluorescens* P-17. Autoclave was used to

decontaminate and sterilize media, instruments and labware. SEM (Sigma series FE-SEM in-lens) was utilized to observe and analyze the morphology of both MWCNTs and membrane samples. TEM (TEI Technai T12) was utilized to depict the morphological pattern and the internal structure of both MWCNTs and membrane samples. XRD (Bruker D2 advance X-ray diffractometer) was utilized to investigate the structural properties (crystalline structure) of MWCNTs. Raman spectroscopy (Horiba Labram Raman spectroscopy) was utilized to provide the structural characteristics and indication of the degree of crystallinity on both raw and functionalized MWCNTs. TAX.XT plus texture analyzer was carried out the mechanical characterization of membranes. SCA.20 was utilized for contact angle (hydrophilicity) measurements of NF membranes. Spectroquant Pharo 300 M was used for water quality analysis (Alkalinity, free chlorine, turbidity, and Nitrogen species). An ultrasonic bath (Branson) was used for rapid preparation (sterilization) of samples and tools. Spectroquant Move (Merck) was utilized to measure free chlorine contained in water samples. Incubator shaker (Orbicult) was used to facilitate the growth and cultivation of cells. Lablime orbital shaker was used to facilitate cells culture. A Steamer (OT 40L Nuve) was used for the steam sterilization of liquid and culture media. An analytical balance was used to precisely measure the mass of nanostructured materials and chemicals. Drying ovens (Labotec) was used to remove water, moisture, and other solvents from instruments and labware. Bensen burner was used to provide a single, continuous flame to avoid any aerobic bacterial contamination in the laboratory. A TOC analyzer (Teledyne Tekmar) was used to accurately detect carbon content in water samples. A portable pH meter (Hi 9811-5) was used for temperature, pH, conductivity, and TDS. A DO meter (Orion Star A213) was used for dissolved oxygen measurement in water samples. Laboratory shaker was used for biologically activate Sand (BAS) reactors during the BDOC experiment, 100-1000 μL micropipettes was used to transfer volumes of liquid accurately and precisely in the microliter range.

Adsorbates

Ultrapure water (water sample A) and tap water (water sample B) were used as sources of adsorbates for the determination of AOC and BDOC in this study. Fresh wastewater sample used for BAS preparation, was collected from the Northern Wastewater Treatment Works (Joburg Water), situated in the city of Johannesburg, South Africa. Water sample A was pasteurized before the inoculation process for AOC analysis. Contrarily to water sample A, water sample B was

filtered through a membrane filter (0.45 μm) to remove any particulate organic carbon (POC) before analyzing DOC.

Adsorbents

As already stated, ready-made MWCNTs, purchased from Merck (South Africa), were used as adsorbents in this study. MWCNTs used had an average carbon > 98% carbon basis with amorphous carbon content < 5%, outer diameters (dp) < 10 nm and tube length in the range of 5-15 μm . These were selected due to high NOM adsorption capacities [7,9].

3.2 Experimental Methods

The depiction of the experimental procedures and the equipment used in this study are presented in detail in this study.

3.2.1 Functionalization of carbon nanotubes

The MWCNTs have hydrophobic characteristics and a propensity to aggregate due to the presence of electrostatic interactions among them, therefore, functionalization of MWCNTs was required to improve their dispersion in the organic and inorganic solvents [9]. The MWCNTs functionalization was carried out using CTAB (a noncovalent functionalization process) and the structure of MWCNTs is unharmed by noncovalent functionalization, which can be done under low operating conditions [10]. The effectiveness of CTAB as a reagent for functionalizing MWCNTs has been widely demonstrated [10]. Additionally, it has been discovered that CTAB is a cationic surfactant that actively interacts with MWCNTs to improve its dispersibility in water [10, 11]. As shown in figure 3.1, raw MWCNTs were dispersed in CTAB solution using the ratio (1:1) in order to obtain a stable suspension during the functionalization process [10, 11]. The MWCNTs-CTAB solution was then stirred under reflux for 24 hours at room temperature. Following filtration of the solution, the MWCNTs underwent a pH-neutralization wash with distilled water before being reduced in an oven to 100°C for 24 hours to complete the process of functionalization (Appendix A2). Raman spectroscopy was used to inquire into the degree of functionalization. Given its accuracy, this approach was chosen. Figure 3.1 presents the set up used for the functionalization process of MWCNTs in this study.

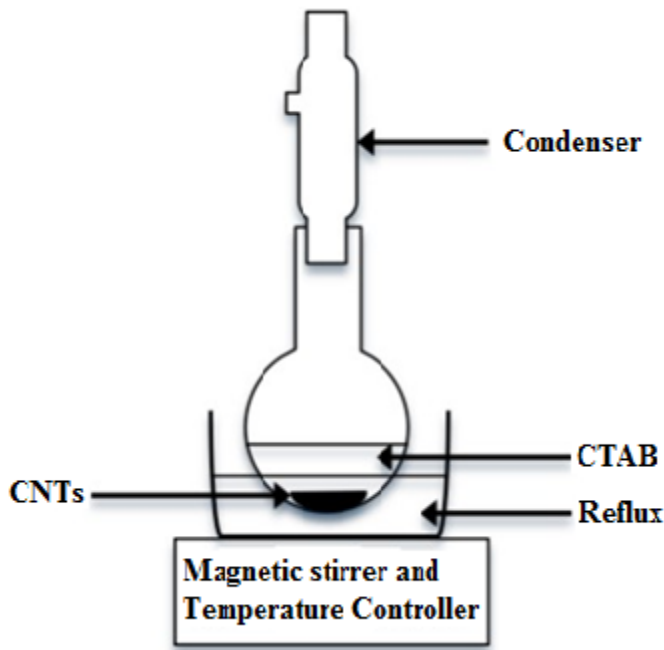


Figure 3.1: Set up for functionalization of MWCNTs.

3.2.2 Fabrication of the polymeric membranes

The phase inversion method was employed in this study to produce polymeric membranes with nanopores [1]. The phase inversion technique was chosen in this study because it is one of the conventional methods that could be utilized to produce polymeric membranes. This is due to its simple processing, flexible production scales, and low cost [1]. To create a homogeneous solution, the PSF was dissolved in DMF for 24 hours while being constantly stirred. In this study, an ultrasonicator set to a frequency of 60% was utilized to sonicate the solution for 10 minutes in order to produce a homogeneous solution. The solution was subsequently cast onto a glass substrate utilizing a casting blade. Another 24 hours were spent letting the membrane air-dry afterward. Finally, the membrane spent 30 minutes in a 125 °C oven to completely dry and detach from the glass substrate before its storage [1].

3.2.3 Batch adsorption process

The batch experiment was employed in this study to determine how well CTAB-functionalized MWCNTs adsorb BOM in terms of AOC and BDOC prior to membrane filtration. The amount of

organic carbon in water that is available for microbial growth was represented by AOC, as was previously mentioned. The indicator BDDOC was employed to measure the amount of BOM in water.

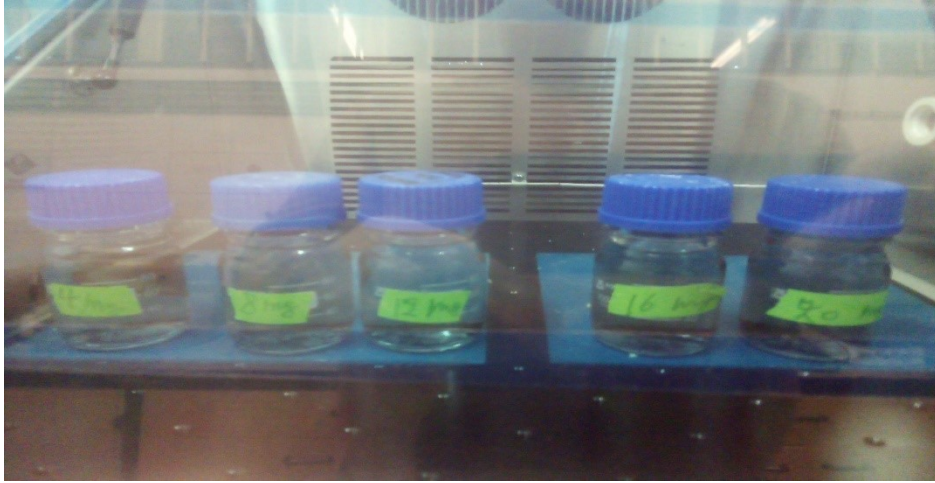


Figure 3.2: The shaker (Orbicult incubator benchtop shaker IBS) and adsorption process experimental set up.

Equations (3.1) and (3.2) were used, respectively, to calculate the NOM removal percentage and adsorption capacity:

$$\text{Removal efficiency (\%)} = \frac{C_0 - C_t}{C_0} \times 100 \quad (3.1)$$

$$\text{Adsorption capacity (q)} = \frac{(C_0 - C_t)V}{m} \quad (3.2)$$

Where C_0 is the initial concentration of NOM (mg/L) at the start of the experiment ($t = 0$), and C_t is the concentration at time t , V is the volume of the solution, m stands for the dosage amount (mg) of the adsorbent

3.2.4 Filtration tests

The filtration tests were conducted using the crossflow module depicted in Figure 3.3. At room temperature, a 45 cm² membrane was utilized. By running deionized water through the system, the PSF membranes were first compacted. The water emulsions were subsequently fed continuously using a pump. The amount of time needed to measure and analyse the collected

permeate was recorded. Equation (3.3) was employed to compute the flux (F) through the membrane:

$$F = \frac{V}{A \times t} \quad (3.3)$$

Where:

V is the liters equivalent of the volume of the collected permeate in Liters (L)

A stand for the membrane's surface area in square meters (m²) and

t is the amount of time needed to collect clean water flux (permeate) during MSP in hour (t).

Figure 3.3 shows the setup of the filtration module configuration used in this study.

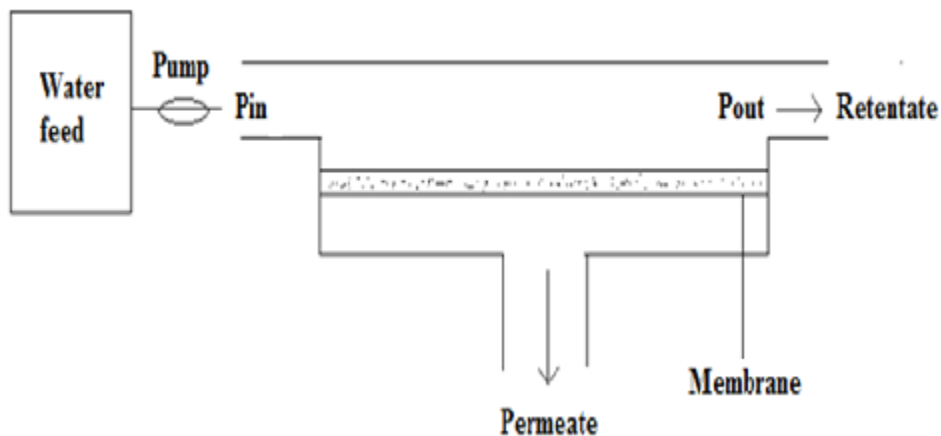


Figure 3.3: Exact setup of the filtration module configuration.

3.3 Analytical methods

The analytical methods that were used to characterize the materials in this study are depicted in this section as follows: (1) Characterization of strain *Pseudomonas fluorescens* P17, (2) Characterization of raw and functionalized MWCNTs, and (3) Characterization of polymeric filtration membranes.

3.3.1 Characterization of *Pseudomonas fluorescens* P17

A biological microscope Olympus Cx22 Led was used to carry out the morphological and physiological tests of the strain *Pseudomonas fluorescens* P17 used in this study by phase contrast

microscopy. Figure 3.4 shows the equipment employed for the tests to characterize strain P17 in this study.



Figure 3.4: Olympus Cx22 Led

3.3.2 Characterization of carbon nanotubes and polysulfone membranes filtration

In this study, the characterization of nanostructured materials was concentrated on three key methods: visual inspection of the results, qualitative analysis of the product composition, and application of analytical techniques to gauge the purity and quality of the produced materials. MWCNTs were characterized using SEM, TEM, Raman spectroscopy, XRD, and Raman spectroscopy. The physical structure of the MWCNTs was revealed by TEM imaging, while XRD analysis revealed the spectrum of typical MWCNTs. Raman has great potential to analyze the functionalization of CNTs. SEM, porosity measurement, contact angle (hydrophilicity), and mechanical tests were used to characterize PSF membranes. Microscopic techniques were chosen in this study to assess the morphology, composition, physical properties, and dynamic behavior of nanostructured materials.

Scanning electron microscopy technique

The SEM technique was utilized to detect and evaluate the morphologies of the PSF membrane and MWCNTs (operating at accelerating at 15kV and 17kV) for the MWCNTs and membranes respectively. The SEM provided morphological characterizations. To facilitate SEM imaging, the polymeric membranes were coated with palladium and gold [2]. The FE-SEM in lens apparatus depicted in Figure 3.5 shows the equipment that was used to analyse the morphological patterns

of the membranes and MWCNTs. Additionally, the SEM images was used to determine the dimensions of the MWCNT tubes.



Figure 3.5: FE-SEM in-lens equipment

Transmission electron microscopy technique

In the analysis of morphological patterns, the TEM (FEI Tecnai T12) was utilized to examine the internal structure of MWCNTs. With its magnification range of 1000 to 800000 and accelerating voltage range of 80 to 200 kV, the microscope provided precise imaging capabilities. Image capture was achieved using a Keen View Peltier-cooled CCD camera [2]. This equipment allowed for the visualization and interpretation of various morphological patterns observed in the MWCNT samples. The significance of using the FEI Tecnai T12 TEM in this study lies in its ability to provide high-resolution images and facilitate detailed analysis of morphological features. The TEI Tecnai T12 employed to view the internal structure of MWCNTs in this study is presented in Figure 3.6.



Figure 3.6: FEI Tecnai T12

Raman spectroscopy technique

Raman spectrometer was employed in this study to examine whether any defects were introduced into the MWCNT matrix because of the functionalization procedure. Defects in the functionalized MWCNT matrix were identified using Raman spectroscopy ($\lambda=785$ nm, 10 mw). The spectra of both unfunctionalized and functionalized MWCNTs were analyzed using a Raman spectrometer. By comparing the spectra, any differences or changes in the peak positions, intensities, or shapes were examined. These variations in the Raman spectra provided indications of defects present within the functionalized MWCNTs. The analysis allowed for the identification and characterization of the defects, providing valuable insight into the impact of the functionalization procedure on the MWCNT matrix. Further quantitative analysis of defect density was conducted to provide a comprehensive understanding of the defects introduced via functionalization [2]. The Horiba LabRAM Raman spectrometer employed in this study is presented in Figure 3.7.



Figure 3.7: Horiba Lab RAM Raman spectrometer

X-ray Diffraction

The structural characteristics of MWCNTs were analyzed using a Bruker D2 advance XRD (operating at 30KV of accelerating voltage). XRD is commonly employed in nanotechnology to accurately determine the composition, crystal structure, and crystalline grain size of nanoparticles. In this study, the chosen method of analysis was XRD due to its ability to provide precise data. The angle of incidence (Θ) and scattering of x-rays on a crystal surface were important factors in

determining constructive interference for n wavelengths [2]. This analysis was crucial in understanding the structural characteristics of MWCNTs and their application in nanotechnology research [2]. The equipment employed in this study for the XRD measurements of MWCNTs is depicted in Figure 3.8.

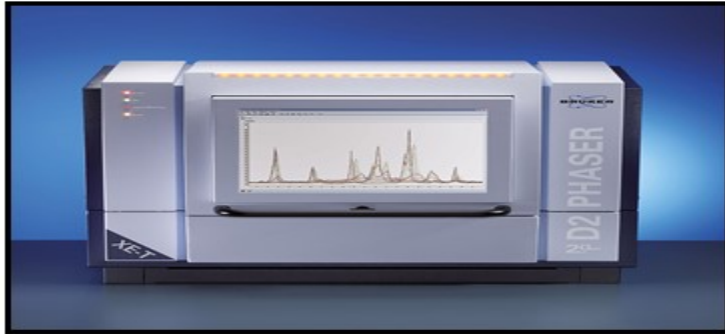


Figure 3.8: Bruker D2 advance X-ray diffractometer

Figure 3.9 describes Bragg's states the following:

The x-ray incidence angle when it strikes a crystal surface is θ , and the angle of scattering is θ . For n wavelengths, constructive interference will happen when the path difference, d , is a whole number.

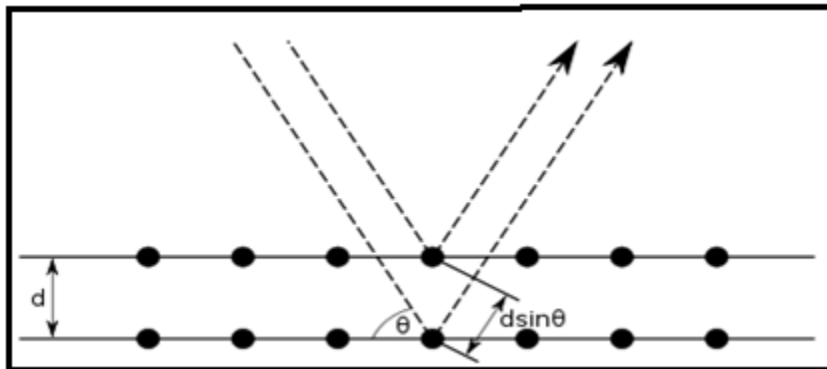


Figure 3.9: Bragg's diffraction illustration [9]

This finding is evidence for the atomic structure of crystals and serves as an illustration of the x-ray wave interface known as x-ray diffraction (XRD).

Porosity measurement technique

In terms of permeability and retention, a membrane's porosity is a key factor. Equation (3.5) was employed to calculate the membrane's porosity.

$$\text{Membrane porosity} = \frac{W_w - W_d}{\rho_w \times V} \quad (3.5)$$

Where V is the membrane's volume in a wet case (m^3) and ρ_w is the density of pure water at room temperature (kg/m^3). The masses of a membrane in its dry and wet states, respectively, are W_w and W_d .

Contact angle technique.

The contact angle technique was utilized to assess the wettability and surface hydrophilicity of the PSF membranes. Basically, a $2 \mu\text{L}$ drop of water was injected onto the PSF membrane surface using a Gilmont syringe. The advancing angle (Θ) of the water droplet was measured using the SCA 20 version 2 software. It was found that the hydrophilicity decreased as the contact angle increased [2]. The equipment employed for the contact angle tests in this study is shown in Figure 3.10.



Figure 3.10: SCA20 version 4.1.12 employed for contact angle measurements.

Mechanical characterization of PSF membranes

The PSF membranes' mechanical characterization was completed using an TA.XT Plus Texture Analyzer. On a tensile strength testing machine, sample membranes (1 cm x 5 cm) were set up and clamped while being pulled at a rate of 10 mm per minute. TA.XT plus was used to quantify strain and stress has already started. A value average was subsequently calculated. When the sample fractured, the test was complete, and data were computed for analysis. The equipment used to test membranes mechanically in this study is shown in Figure 3.11.



Figure 3.11: TA.XT Plus Texture Analyzer used for mechanical tests.

Both the elastic modulus of the test material and the geometry (area and length) of the specimen affect how much it deflects. It is beneficial to generalize the data in order to eliminate the influence of geometry because material behaviour is more important when geometry is considered. This is accomplished by converting the load values to stress values and the deflection values to strain values.

$$\text{Stress} = \frac{F}{A_0} \quad (3.6)$$

$$\text{Strain} = \frac{L-L_0}{L_0} = \frac{\Delta L}{L_0} \quad (3.7)$$

Where: F is the load in the equation for stress, and A_0 is the test specimen's initial cross-sectional area. L is the specimen's current length and L_0 is its initial length in the equation for strain. The ability of the material to stretch and deform is measured by the Young modulus (E).

E is determined using the ratio of the tensile stress to the tensile strain. The Young modulus was determined by using the equation (3.8):

$$E = \frac{\text{Tensile stress}}{\text{Tensile strain}} \quad (3.8)$$

A stress-strain curve can be drawn using the values of stress and strain gleaned from the tensile test.

3.4 Water Quality Testing

The analytical methods utilized in this study to analyse both the raw water and treated water quality flux measurement is covered in this section. The following methods were employed to preserve the sample's integrity following collection and to aid in obtaining an acceptable and representative sample for this experimental study [3]:

1. The creation of a sampling and analysis plan (SAP), which outlines the sampling sites, sample counts, sample types, and quality control specifications for the project.
2. Before taking samples, verify that the selected method for sampling is accurate and acceptable and that the preservatives, and equipment used are appropriate. Purchasing sampling supplies directly from the lab conducting the analyses is advised, and to assemble all the tools and materials required for the project.
3. Autoclave the glass bottles that need to be used for sample collection prior to chemical and microbiological analysis.
4. Use sodium thiosulfate ($\text{Na}_2\text{S}_2\text{O}_3 \cdot 5\text{H}_2\text{O}$) in order to neutralize any trace of chlorine prior to sample collection.
5. All samples that have been collected should be marked with the temperature, sampling location, time, and date of collection before sending them to the water quality laboratory.

3.4.1 Untreated water and finished water quality.

The quality of raw water is one of the fundamental elements in water treatment sector. Tap water and ultrapure water have different characteristics that can be analyzed to assess its quality. For

ultrapure water, Table 3.1 provides a summary of its sample characteristics. This includes parameters such as temperature, conductivity, pH, free chlorine, and DO. Chemical parameters like Alkalinity, TDS, organic matter, fluorides, hardness, metals, and nutrients are also important in evaluating tap water quality. Biological parameters, specifically the presence of algae, bacteria, and viruses, are also considered. Tap water, on the other hand, has its own set of characteristics summarized in Table 3.2. Analytical techniques for examining both tap water and wastewater adhere to accepted standards in water analysis. Overall, understanding the characteristics of these water sources is crucial in ensuring their suitability for various purposes.

Table 3.1: The average water quality characteristics of ultrapure water (sample A) used in this study.

Parameters	Unit	Concentration
pH	-	4
Temperature	°C	21.5
Conductivity	µs/cm	-
TDS	mg/L	0
Free chlorine	mg/L	0.01
DO	mg/L	4.54
Nitrates	mg/L	<4.4
Ammonium (NH ₄ ⁺)	mg/L	0.05
Alkalinity (total)	mg/L	0

Source: Merck (Pty).

Table 3.2: The average water quality characteristics of raw tap water (sample B) used in this study.

Parameters	Unit	Concentration
pH	-	7.3
Temperature	°C	19.5
Conductivity	µs/cm	160
TDS	mg/L	70
Turbidity	FAU	106
DO	mg/L	5.41

Alkalinity as CaCO ₃	mg/L	23
Chlorine (free)	mg/L	0.14

Source: Water quality lab (H2), School of Civil and Environmental Engineering, Wits.

3.4.2 Measurement of water flux during membrane filtration test

Water flux measurement during membrane filtration test was conducted using a crossflow module. The PSF membrane with an effective area of 45 cm² was used in this study. The water flux was computed by applying Equation (3.3). To analyze membrane compaction behavior, the flow rate was maintained at a constant value, and the resulting flux was determined using Equation 3.2. Furthermore, the difference in pressure from the feed was set at 4.5 bar for five different elapsed times (15, 30, 60, 90, and 120 minutes) while measuring the water flux. Figure 3.12. illustrates the crossflow filtration system used in this study.

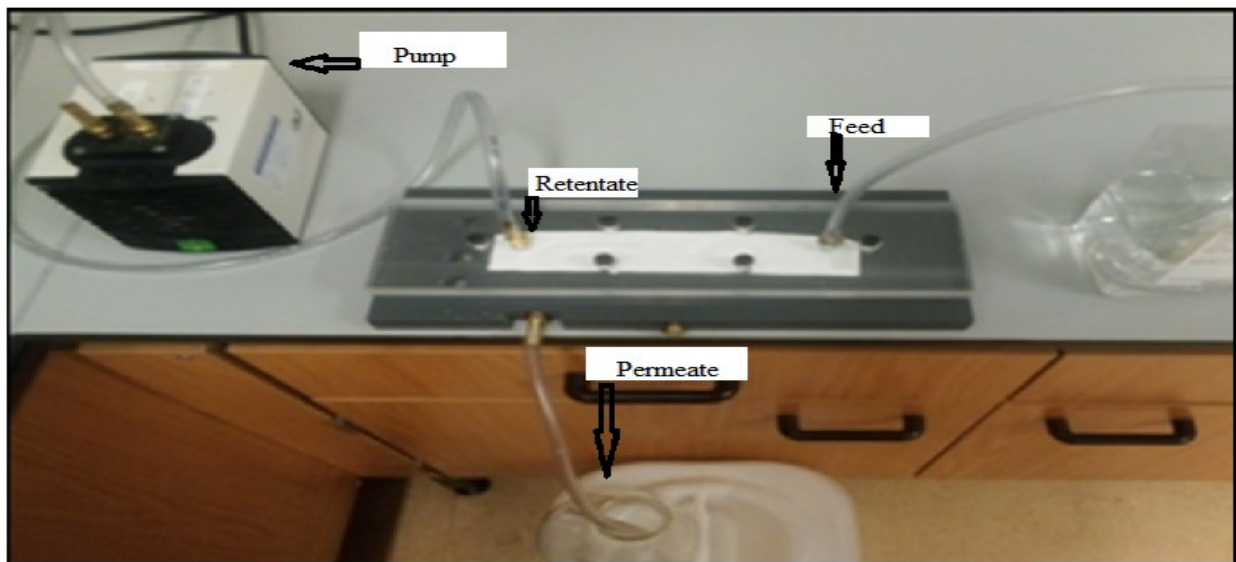


Figure 3.12: The crossflow filtration system employed in this study.

Figure 3.13 presents the proposed experimental setup based on the multi-barrier approach, as a better alternative to mitigate the issue of membrane fouling and to lead to higher operational efficiency and performance of the filtration membrane.

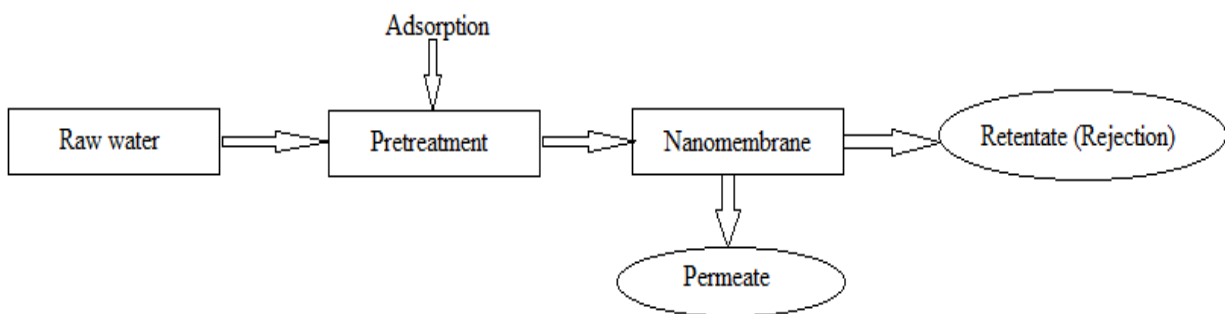


Figure 3.13: Proposed experimental setup.

3.5 Summary

The materials and procedures employed in the study are described in this chapter along with their use. The chapter presents and discusses the actions that constitute the laboratory testing component of the study. Microscopic techniques were applied to characterize nanostructured materials in this study. This is because it has the capacity to assess the morphology, composition, physical properties, and dynamic behavior of nanostructured materials in order to provide the necessary information. This makes a significant contribution to material science. They are necessary for both product quality control and the development of new materials.

3.6 References

- [1] Cristina, D.U., Nechifor, A., Albu, S.B., Ioana, A.D., Oprea, O., Nechifor, G., Eugenia, E.T., Isildak, P., (2020). Control of nanostructured polysulfone membrane preparation by phase inversion method. *Journal of nanomaterials*. 10.
- [2] Thakur, A., (2007). Nanomaterials and nanotechnology. *Material science*. In proceedings (Thakur 2007 Nanomaterials AN).
- [3] Clesceri, L. S., Greenberg, A. E., Eaton, A. D., (1998). Standard Methods for the examination of water and wastewater, 20th edition. *American Public Health Association*, Washington DC.
- [4] Van der Kooij, D. (1982). Assimilable organic carbon as an indicator of bacterial regrowth. *Journal of American Water Works Association* 84. 57-65.
- [5] Van der kooij, D., Visser, A., Hijnen W.A.M. (1982). Determining the concentration of easily assimilable organic carbon in drinking water, *American Water Work Association* 74. 540-545.

- [6] Van der Kooij, D., Visser, A, Orange J.P. (1982). Multiplication of fluorescens pseudomonas at low substrate concentrations in tap water. *Journal of Microbiology* 48, 229.
- [7] Joret, J.C., Levi, Y. (1986). Methode rapide d'evaluation du carbone eliminable des eaux par voie biologique. *Trib cebedeau* 39, 3-9.
- [8] Escobar, I., Randall, A. (1999). Influence of nanofiltration on distribution system. *Biostability Journal of American Water Works Associations* 6. 76-89.
- [9] Rolant, E.M. (2013). Characterization of carbon nanotubes, in book: *Physical and Chemical properties of carbon nanotubes, chapter 7*, DOI: 10.5772/51540.
- [10] Jayant, I.G., Malappan, M., Sharanappa, T.N. (2017). CTAB functionalized multiwalled carbon nanotubes composite modified electrode for the determination of 6–mercaptapurine. *Sensing and bio-sensing research* 12.
- [11] Primastari, S.D., Kusumastuti, Y., Handayani, M., Rochmadi, R. (2022). Functionalization of multiwalled carbon nanotubes (MWCNTs) with CTAB surfactant and polyethylene glycol as potential drug carrier. IOD Conf. series: *Earth and Environmental Science*. 963, 012033.

CHAPTER 4: MATHEMATICAL MODELING OF MEMBRANE FILTRATION PROCESS

4.1 Introduction

Mathematical modeling plays a crucial role in studying real-world systems, including the membrane filtration process [1,2,3,4]. By using logical principles and techniques, mathematical models provide a conceptual construct for understanding and analyzing complex phenomena. These models enable researchers to investigate the behavior of the membrane filtration process and make predictions based on the underlying mathematical equations. Various forms of mathematical models exist, each with its own advantages and disadvantages [1, 2, 3, 4, 8]. In the framework of MSP, mathematical models were implemented to evaluate the properties of various filter types, optimize operating conditions, and improve system design [3, 4]. The appropriate model form is implemented based on the specific characteristics of the membrane filtration module being studied. Overall, mathematical modeling is of great importance in comprehending and enhancing membrane filtration processes [1, 2, 3, 4, 5, 6, 7, 8]. This chapter presents and develops the mathematical modeling of the membrane filtration process in a complete mixing flow system (CMFS). Using logical principles and techniques, ideas about observed processes are presented in modeling, a general procedure in the mathematical sciences [1, 2, 3, 4, 8]. Mathematical modeling is the process of creating a conceptual representation of a real-world system or phenomenon using mathematical equations and logical principles.; and there are various forms a model can be presented in [3, 4]. Some steps that are particularly useful in the construction of a mathematical model include: (a) problem identification, (b) assumption specification, (c) variable classification, (d) solution and interpretation, (e) verification, (f) implementation, and (g) maintenance. Each of these steps exists for a specific reason. It is necessary to review a previous step at any stage of the sequence to make sure everything is correct. This is before continuing to the next stage. Furthermore, this chapter develops a theory about membrane filtration processes by applying equations of motion [1, 2, 3]. The CMFS was considered when developing the mathematical models in this study because the CMFS is considered an ideal system that can be used to describe a better membrane separation process (MSP). The chapter also discusses the relationships and correlation between the concentrations and flow rates of fresh feed, permeate, and retentate (rejection) and the membrane surface area.

Membrane filtration processes are determined by applying mass transfer phenomena and diffusion principles. Experimental relationships are used to depict the flux concentration and flow when passing through the membrane's pores. Some researchers have developed procedures (protocols) to calculate the CMFS [4,5,6]. However, despite the availability of procedures for determining membrane filtration processes, researchers are still struggling to develop proper mathematical models that describe membrane filtration properly. This is because some parameters are still unfixed (unresolved). For example, the maximum achievable concentration after a filtration process, the correlations between the main processing variables and the processing results, and the control of parameters for dynamic (non-steady state) processes [3,4].

4.2 Methodology

The mathematical models based on known and experimental conditions and relationships were developed in this study. For instance, the correlation between the solute concentrations in the filtration module (C_{out}) and in the permeate (C_p): $C_p = g(C_{out})$ (4.1); the membrane permeability $K = K_0 - f(C_{out}, Q_{out})$ (4.2) where Q_{out} is the flow rate of the retentate and K_0 is the membrane permeability for pure solvent, g and f are empirical functions.

4.3 The basic relationships in the complete mixing flow system

Due to thorough liquid mixing within the system, the perfect type of system is distinguished by the same concentration throughout the system. The separation process can be described using the following equation:

➤ Mass and flow balance equations

$$Q_{in} C_{in} = Q_p C_p + Q_{out} C_{out} \quad (4.1)$$

$$Q_{in} = Q_p + Q_{out} \quad (4.2)$$

➤ The differential equations for mass and flow change:

$$\frac{d(Q_p C_p)}{dQ_p} = g(C_{out}, Q_{out}) \quad (4.3)$$

$$\frac{dQ_p}{dA} = k = K_0 - f(C_{out} - Q_{out}) \quad (4.4)$$

If the concentration C_{out} is small, the functions g and f are assumed to be linear:

$$g(x) = C_p = \beta C_{out} ; f(x) = K = K_0 - \beta C_{out} \quad (4.5)$$

In the CMFS, it can be assumed that the solute concentration remains unchanged at any arbitrary point in the system of volume (V) and the permeate concentration $C_p = \beta C_{in}$ is the same all along the membrane surface (S). Figure 4.1 presents the configuration of the complete mixing flow membrane system.

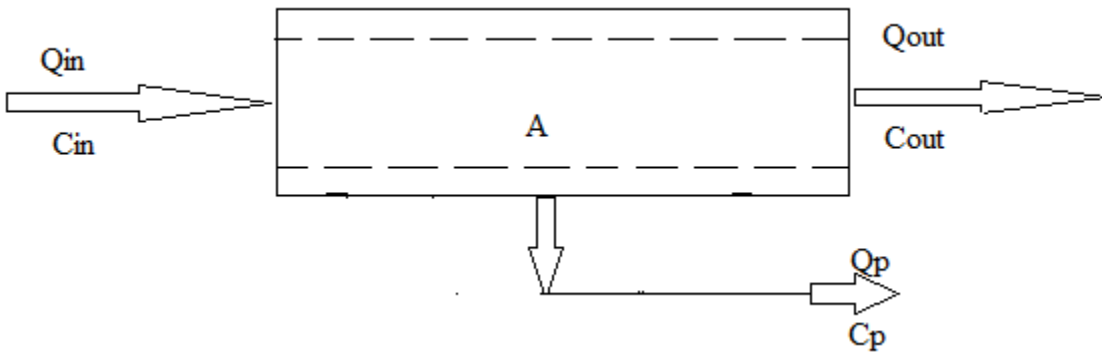


Figure 4.1: Complete mixing flow membrane system

4.4 Mathematical modeling of the complete mixing flow system

Because there has been extensive liquid mixing inside the system, this ideal membrane filtration system is characterized by identical concentrations throughout. The concentration of process in a CMFS is shown in Figure 4.1, where the solute concentration is the same at any point in the system volume V and the permeate concentration $C_p = \alpha C_{out}$ is the same all along the membrane surface A .

Therefore equation (4.1) can be transformed as follows:

$$Q_p = AK = A (K_0 - \beta C_{out}) \quad (4.6)$$

Contrary to equation (4.6), the differential equation for the solute quantity in the system can be expressed as follows:

$$V \frac{dC_{out}}{dt} = Q_{in} C_{in} - Q_{out} C_{out} - Q_p C_p \quad (4.7)$$

4.4.1 At steady state

When the initial process conditions (C_{in} , Q_{in}) are constants, then we observe a steady state separation process with stationary concentrations and flow rates. In this case $\frac{dC_{out}}{dt} = 0$. Equation (4.1) is identical to equation (4.7) and after substituting equation (4.6) and $C_p = \alpha C_{out}$ into equation (4.1) leads to a quadratic equation for C_{out} :

$$\beta (1-\alpha) C_{out}^2 + C_{out} [Q_{in} - (1-\alpha) A K_0] - C_{in} Q_{in} = 0 \quad (4.8)$$

The solution of equation (4.8) provides us with the stationary concentration as follows:

$$C^* = \frac{\sqrt{[Q_{in} - (1-\alpha) A K_0]^2 + 4\beta A (1-\alpha) C_{in} Q_{in}}}{2\beta(1-\alpha)} - \frac{Q_{in} - (1-\alpha) A K_0}{2\beta(1-\alpha)} \quad (4.9)$$

And the corresponding flow rates of the concentrate (Q_{out}^*) and permeate (Q_p^*) are:

$$Q_{out}^* = Q_{in} \frac{C_{in} - \alpha C^*}{(1-\alpha)C^*} \quad (4.10) \quad Q_p^* = Q_{in} \frac{C^* - C_{in}}{(1-\alpha)C^*} = A (K_0 - \beta C^*) \quad (4.11)$$

4.4.2. The Limiting concentration

It can be deduced from equation (4.14) that the function $C_{out}^* (Q_{in})$ has an inverse dependence. Under constant membrane system properties (α , β , K_0) and the initial concentration C_{in} , the stationary values C^* , Q^* , and Q_p^* are dependent on Q_{in} only. Equation (4.8) shows:

$$\text{If } Q_{in} \rightarrow 0: C_{out}^* \rightarrow C_{lim} = \frac{K_0}{\beta}$$

i.e., limiting concentration in CMFS under certain conditions.

Equation (4.9) describes the permeate flow rate as $Q_p^* \rightarrow 0$ because the membrane permeability $K = K_0 - \beta C^* \rightarrow 0$

However, it is not the only possibility. It can be shown from the first equation (4.11) that when $C^* = \frac{C_{in}}{\alpha}$, the concentrate flow rate $Q_{out}^* \rightarrow 0$. As the membrane system properties (α , β , K_0) and inlet

flow concentration C_{in} are independent, both variants: $C_{Lim.1} = (\frac{K_0}{\beta})$, and $C_{Lim.2} = (\frac{C_{in}}{\alpha})$ are possible. If the concentration C^* increases, then $C^* \rightarrow C_{Lim}$ but C_{Lim} is the minimum of two values:

$$C_{Lim} = \min \{ C_{Lim.1} = \frac{K_0}{\beta}; C_{Lim.2} = \frac{C_{in}}{\alpha} \} \quad (4.12)$$

The boundary of these cases is inlet concentration $C_{in}^b = \frac{\alpha K_0}{\beta}$: if $C_{in} < C_{in}^b$ then $C_{out-Lim} = \frac{C_{in}}{\alpha}$, i.e., does not depend on inlet flow.

4.4.3. The Dynamic separation processes

Two non-steady states exist: the transient response process, which is triggered by any change in the process conditions, and the process starting period $C_{out}(t)$, which changes from C_{in} to C^* . Following the substitution of the dependencies (4.2) into equation (4.6) and transformation into the Riccati equation, the function C_{out} for such non-steady states could be obtained.

$$\frac{dC_{out}}{dt} = -b_2 C_{out}^2 - b_1 C_{out} + b_0 \quad (4.13)$$

Where the coefficients:

$$b_0 = \frac{Q_{in} C_{in}}{V}; \quad b_1 = \frac{[Q_{in} - (1-\alpha) A K_0]}{V}; \quad b_2 = \frac{(1-\alpha) \beta A}{V} \quad (4.14)$$

Equation (4.11) can be solved as follows:

Substitute $z = x + (b_1/2b_2)$ and transform equation (4.13) to form:

$$\frac{dz}{dt} = -b_2 z^2 + \frac{b_1^2}{4b_2} + b$$

And after substitution $u = C^* + (b_1/2b_2)$:

$$\frac{dz}{dt} = b_2 (u^2 - z^2) dt$$

Where C^* is the stationary concentration according to Equation (4.9), after the separation of the variables, Equation (4.14) is transformed to:

$$\frac{dz}{u^2 - z^2} = b_2 dt \quad (4.15)$$

And integration with initial condition $u, t=0 = u(0)$ gives the solution:

$$Z(t) = u \frac{[u+z(0)]e^{2b_2ut} - u+z(0)}{[u+z(0)]e^{2b_2ut} + u-z(0)} \quad (C_2) \quad (4.16)$$

$$C_{out}(t) = (C^* + b_1/2b_2) \frac{[C^* + C_{out}(0) + \frac{b_1}{b_2}]e^{2ub_2t} - C^* + C_{out}(0)}{[C^* + C_{out}(0) + \frac{b_1}{b_2}]e^{2ub_2t} + C^* - C_{out}(0)} - \frac{b_1}{2b_2} \quad (4.17)$$

Where the auxiliary parameter $u = C^* + b_1/2b_2$ and the stationary concentration C^* are given in Equation (4.9).

If a startup period of separation is considered, $C_{out}(0) = C_{in}$, and the transient $C_{out}(t)$ from C_{in} to C^* is presented in solution (4.17). i.e., the change from startup to operating mode. The transient response is the solution in this case, and $C^*(0)$ becomes $C^* \neq C_{out}(0)$. This occurs if the CMFS was already in a steady state with $C^*(0)$, but one of the initial conditions (C_{in} , Q_{in}) was changed at any time after $t=0$. Under the following circumstances, $C_{out}(0) = C^*(0)$, the transient function $C_{out}(t)$ can be computed using Equation (4.17).

4.5 Validation of the mathematical model

In this section, the validation of the obtained mathematical model was achieved by comparing the predictions of our mathematical model with measurements taken by Duranceau [10]. The study aimed to evaluate the membrane permeate transient response for single-stage and three-stage nanofiltration membrane systems when each system's feed water experienced a perturbation in water quality with a sudden increase in chloride. The study also highlighted the impact of initial conditions on the system's transient response.

4.5.1 Empirical parameters

∂ , β , and K_0 were determined from the experimental data (C_p and K) as functions of medium concentration $C(t)$ during the filtration process. Statistical processing of the experimental data gives the parameters: $\partial = 0.23$, $\beta = 0.00968$, $K_0 = 1.08 \cdot 10^{-5}$ m/s and the operating characteristics for the three-stage NF plant are presented in Appendix C (table C.1). The functions $C_p(x)$ and $K(x)$ with these parameters are determined according to expression (4.5): $C_p = 0.23C_{out}$, $K = 1.08 \cdot 10^{-5} - 0.00968 C_{out}$, and are shown in Figures 4.2 and 4.3 plotted using experimental data. The

result confirms the adequacy of expression (4.5) for experimental data and allow calculations in the concentration range $C_{out} = 20\text{-}200$ mg/L. Figure 4.2 describes the variation of the permeate concentration versus outlet concentration according to Equation 4.5.

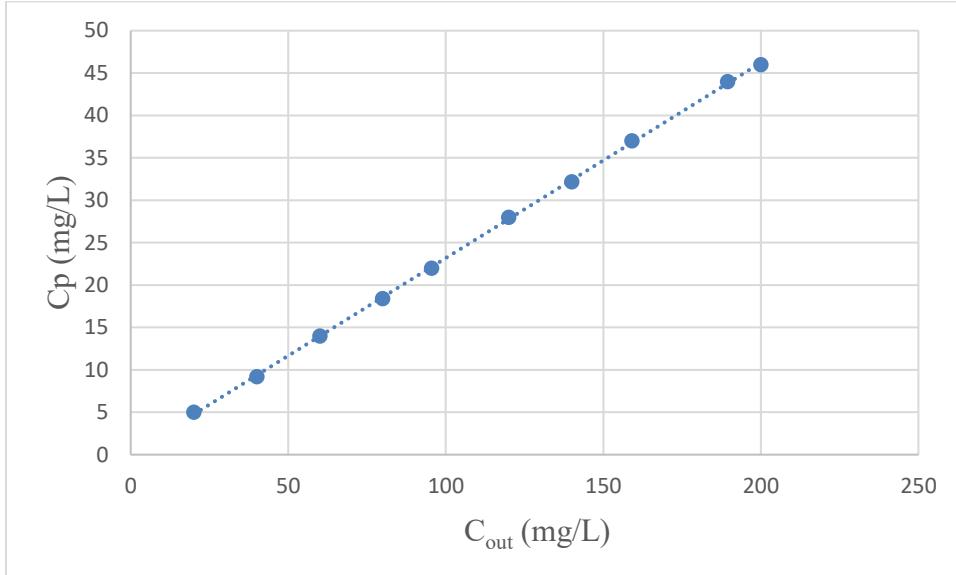


Figure 4.2: Membrane permeate concentration versus outlet concentration

Figure 4.3 describes the variation of membrane permeability with outlet concentration according to Equation 4.5.

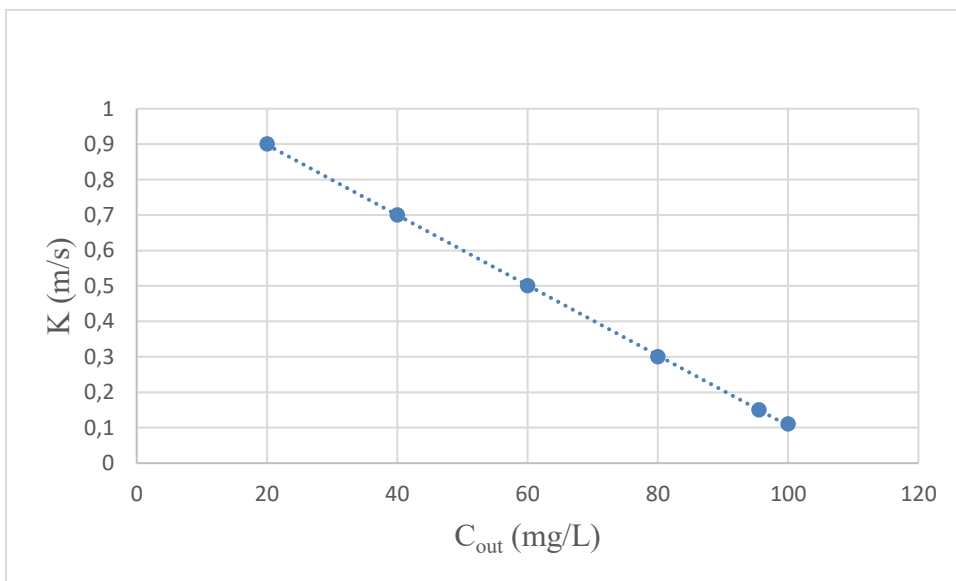


Figure 4.3: Membrane permeability versus outlet concentration

4.5.2 Separation by the completely mixing flow system

The initial concentration was $C_{in} = 182$ mg/L and the experimental parameters ∂ , β , k were used in this process as shown in Appendix C. The limiting concentration according to Equation 4.12, $C_{Lim} = \frac{K_0}{\beta} = C_{Lim.1} = 111.6$ mg/L $< C_{Lim.2} = \frac{C_{in}}{\partial} = 791.3$ mg/L. The initial value $C_{in} = 182$ mg/L and experimental parameters ∂ , β , K_0 give the stationary concentration according to Equation 4.9 as follows:

$$C^* = \frac{\sqrt{(Q_{in} - 0.77 \times 45 \times 1.08 \times 10^{-5})^2 + 4 \times 0.00968 \times 45 \times 0.77 \times 182 \times Q_{in}}}{0.014} - \frac{Q_{in} - 0.77 \times 45 \times 10^{-5}}{0.014}, \text{ mg/L} \quad (4.18)$$

Figure 4.4 presents the results on the stationary values for the CMFS with experimental data in according to equation (4.18) as described in Appendix C.

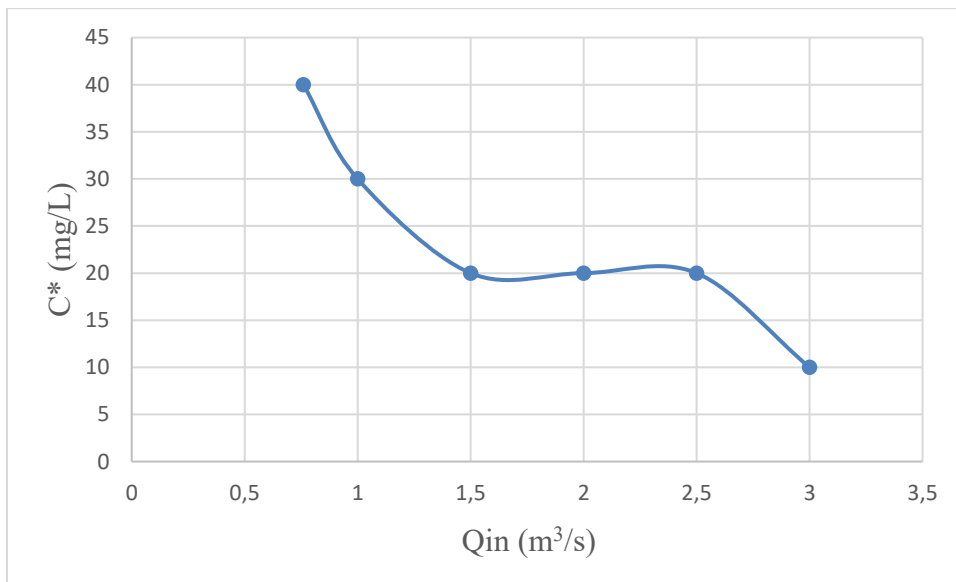


Figure 4.4: Stationary values for the CMFS with experimental data.

Furthermore, to achieve the dynamic response of a concentration process in CMFS, two different cases need to be considered as follows:

- (1) The start-up period from C_{in} and C_{out}^* (operating mode).
- (2) The transient response from one steady state to another when the flow rate Q_{in} undergoes a step of modification. For the first case there is a CMFS with parameters $C_{in} = 182$ mg/L,

and $Q_{in} = 1.35 \cdot 10^{-3} \text{ m}^3/\text{s}$. From these values, the calculation parameters are: $\frac{b_1}{b_2} = 2.9 \cdot 10^{-3}$; $u = 41.08$, $C^* = 41.0 \text{ mg/L}$ and expression 4.17 becomes:

$$C_{out}(t) = 41 \frac{223e^{0.027t} - 223}{223e^{0.027t} + 223} + 1.43 \cdot 10^{-3}, \text{ mg/L} \quad (4.19)$$

The process $C_{out}(t)$ decreases from $C_{in} = 182 \text{ mg/L}$ to a stationary value $C^* = 41 \text{ mg/L}$, calculated according to the previous equation. For the second case there is steady state in the same apparatus with the same $C_{in} = 182 \text{ mg/L}$ and the inlet flow rate undergoes a step modification from $Q_{in}(0) = 2.06 \cdot 10^{-3} \text{ m}^3/\text{s}$ to $Q_{in} = 0.81 \cdot 10^{-3} \text{ m}^3/\text{s}$ at time $t=0$. This gives the transient response for concentration from $C^* = 41.1 \text{ mg/L}$ to $C^* = 11.3 \text{ mg/L}$ according to Equation 4.9. After substituting these values into Equation (4.17), the following calculating formula is developed:

$$C_{out}(t) = 11.3 \frac{193.3e^{0.0076t} - 193.3}{193.3e^{0.0076t} + 193.3} - 1.43 \cdot 10^{-3}, \text{ mg/L} \quad (4.20)$$

The transient process according to (4.20) is shown in Figure 4.5 and requires practically one third of an hour from the start of the change.

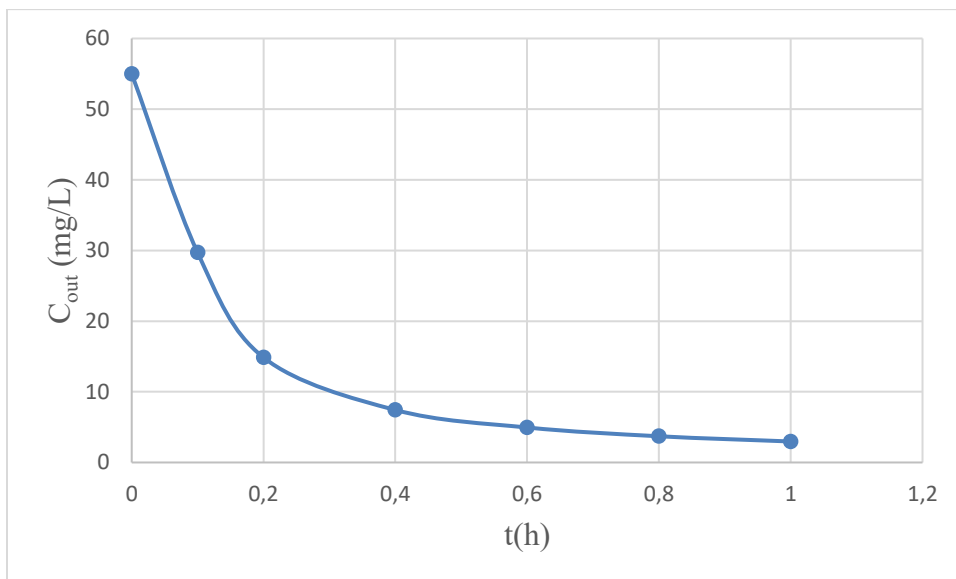


Figure 4.5: Non-steady states in the CMFS (transient process when Q_{in} undergoes a step modification).

After validating the model, it was found that transient response (changes from one steady state to another) is caused by a change in the initial conditions (C_{in} and Q_{in}), according to the mathematical modelling. Furthermore, the study also demonstrated that the membrane models that were produced could be used for the calculations of the primary system design parameters, as well as the selection of membrane properties and initial conditions for a successful separation process.

4.6 Summary

In Chapter 4, a mathematical model was developed to analyze the correlations between variables in membrane filtration within a CMFS. This model specifically focused on the relationships between inlet concentration and flow rate, outlet concentration and flow rate, and permeate concentration. The study also highlighted the impact of initial conditions on the system's transient response. Additionally, the mathematical model could be utilized to calculate important system design parameters and guide the selection of the membrane characteristics and initial conditions for optimal separation processes. This chapter dispenses a comprehensive understanding of membrane filtration and its application in system design. Future research directions in mathematical modelling of membrane filtration include further investigation into the correlations between inlet and outlet concentrations, flow rates, and permeate concentration. Additionally, there is a necessity to scrutinize the influence of different initial conditions on the transient response of the system. This will help in understanding and achieving the desired steady state conditions in membrane filtration. Furthermore, future research should focus on utilizing the mathematical model to optimize membrane filtration processes and predict membrane performance. Finally, there is a scope for potential improvements and advancements in the CMFS system through the application of mathematical modelling techniques. The next Chapter presents the outcome and analysis of the characterization of MWCNTs, PSF membranes; and AOC and BDOC determination.

4.7 References

[1] Fikar, M., (2018) Modelling, control, and optimization of membrane processes, *In proceedings, Per filov* 2018.

- [2] David, M.W., Sudip, C., Emily, W.T., Megan, H.P., (2018). A review of polymeric membranes and processes for potable water reuse. *Progress in polymer science* 81. 209-237.
- [3] Bogomolov, V., Lazarev, S., Abanosinov, O., (2019) Calculation of industrial membrane processes based on mathematical modelling. *1st international conference on control systems, mathematical modelling, automation, and energy efficiency (SUMMA)*, 94-98.
- [4] Castel, C. and Favre, E., (2018). Membranes Separations and Energy Efficiency. *Journal of Membrane Science*, 548, 345-357.
- [5] Favre, E., (2022). The future of membrane separation processes: A prospective analysis. *Separation processes*, 4, doi:10.3389.
- [6] Cheskih P. (2016). Pischevaya Promishlennost, Simulation and Optimization of Microbiology Processes. *Food Industry*, Moscow.
- [7] Niemi, H., Raimoaho, Y. & Palosaari, S., (2012). Statistical modelling of the interplay between solute shape and rejection in porous membranes. *Separation and Purification Technology*. 89 (2012) 261-269.
- [8] Carlson W.A., Shipton J., (2019) Mathematical modelling, applied physics, *Physics 1034, Course notes*, Wits University, Johannesburg.
- [9] Vinther, F., Pinelo, M., Brons, M., Jonsson, G., Meyer, A.S., (2013). Mathematical modelling of dextran filtration through hollow fibre membranes. *Separation and purification technology*, 15.
- [10] Steven, J.F., (2009). Modeling the permeate transient response to perturbations from steady state in a nanofiltration process. *Desalination and water treatment*, 1, 7-16.

CHAPTER FIVE: RESULTS AND DISCUSSION OF THE CHARACTERIZATION OF CARBON NANOTUBES, POLYMERIC MEMBRANES; AND DETERMINATION OF ASSIMILABLE ORGANIC CARBON AND BIODEGRADABLE DISSOLVED ORGANIC CARBON

5.1 Introduction

The results and discussion in this chapter focus on the characterization of MWCNTs, PSF membranes, and strain P-17. Additionally, the functionalization process of MWCNTs and the methods and techniques used for determining AOC, DOC, and BDOC are outlined. This chapter directly relates to the specific goals outlined in chapter one.

5.2 Characterization of strain *Pseudomonas fluorescens* P17

The Olympus Cx22 LED phase contrast microscope revealed that *Pseudomonas fluorescens* P-17 is a rod-shaped bacterium with long straight or curved axes. Strain P-17 has greenish yellow pigmentation and belongs to the *pseudomonas* genus. This study characterized the strain P17 in part, through morphology (size, shape, and arrangement of bacteria cells), and gram staining (a microbiology technique used to differentiate between bacterial species) based on their cell composition. The results obtained after the gram staining techniques revealed that the P17 strain used in this study has weak cell walls, therefore it is gram-negative.

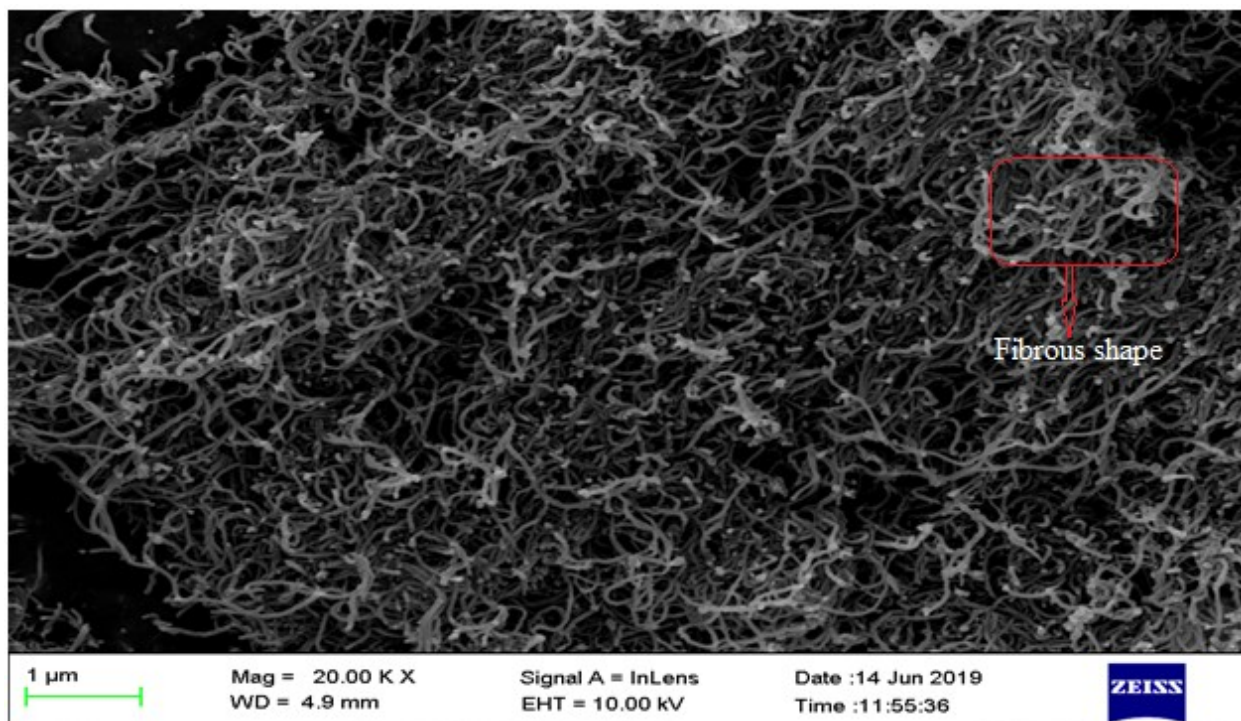
5.3 Characterization of carbon nanotubes

Ready-made MWCNTs, purchased from Merck (South Africa), were characterized using microscopy techniques to identify its functional and structural properties. The findings of the characterization of unfunctionalized and CTAB-functionalized MWCNTs are discussed in the subsequent subsections.

5.3.1 Observation of carbon nanotubes using scanning electron microscope

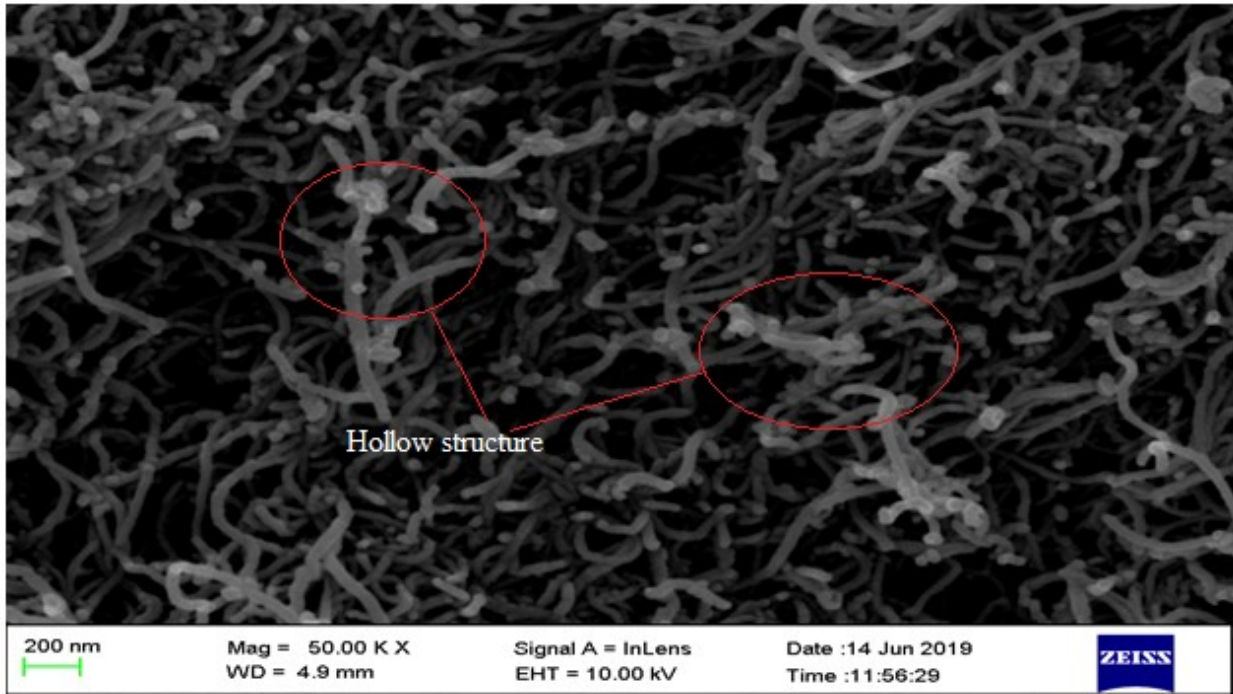
The surface morphology of MWCNTs was inspected using SEM with high resolution. The SEM images disclose the fine structures of the MWCNTs, providing valuable insights into their surface morphology [1]. The observation was conducted using the SEM, sigma series FE-SEM in-lens microscope (at 15kV and 17kV of accelerating voltage). The SEM images, acquired at both low

and high magnification, showcased different perspectives of unfunctionalized and functionalized MWCNTs [1]. The examination of the surface morphology using SEM imaging contributes to an enhanced comprehension of the properties and potential applications of CNTs in nanotechnology research. Figures 5.1 (a, b, and c) display three different perspectives of SEM images of unfunctionalized and functionalized MWCNTs that were acquired after observation using FE-SEM in-lens equipment at low and high magnification.

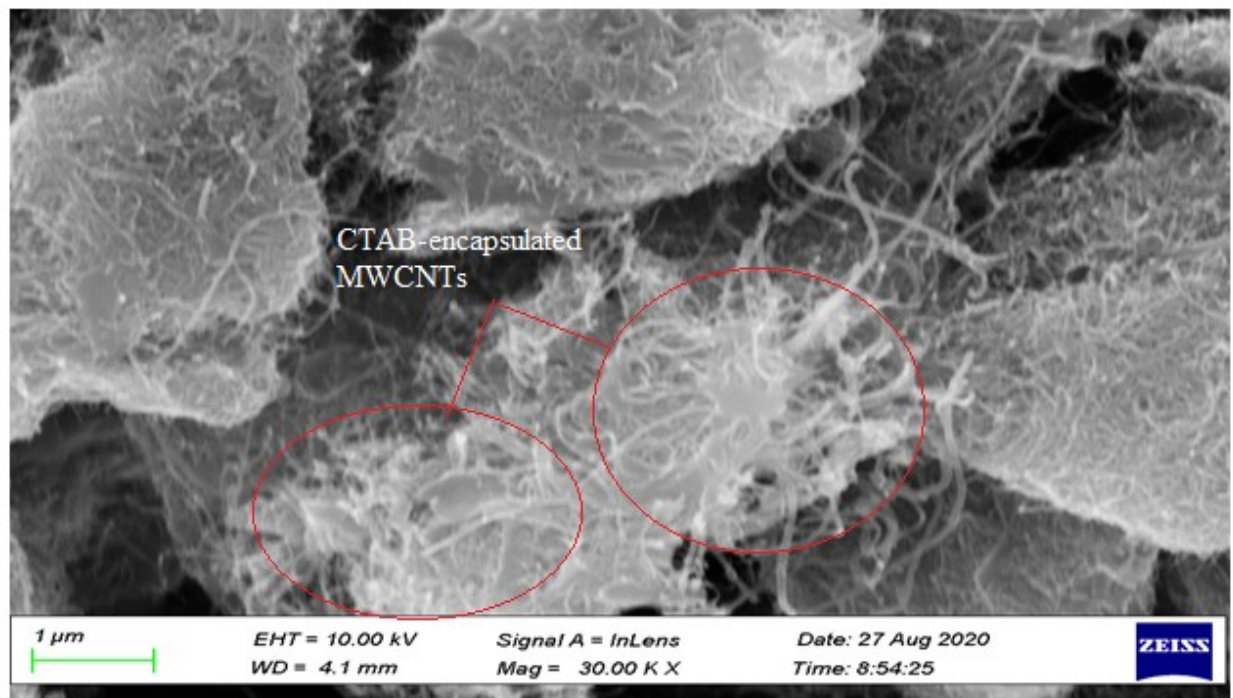


(a)

The characterization of MWCNTs was essential to establish the pertinent properties and features of MWCNTs that can be used during the adsorption process in this study. SEM characterization was used at low and high magnification to evaluate the surface morphology of unfunctionalized MWCNTs and functionalized MWCNTs. In this study, image quality is achieved by varying magnification. This procedure was repeated for all the other samples.



(b)



(c)

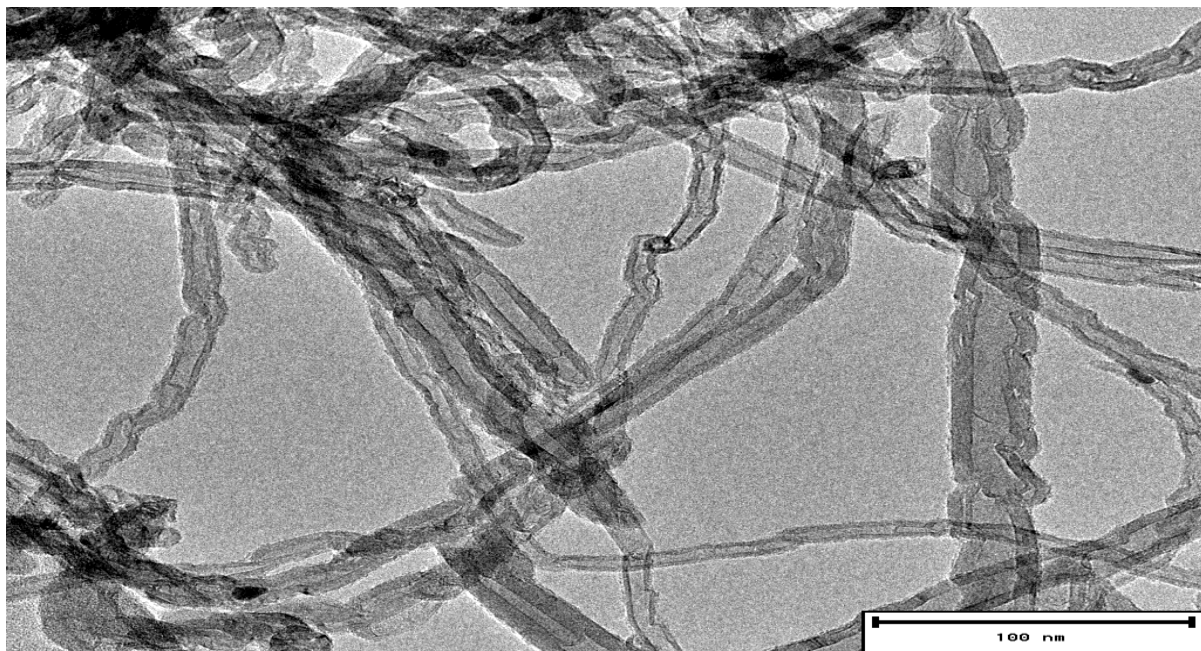
Figure 5.1: SEM pictures of (a, b) unfunctionalized and (c) functionalized MWCNTs

During the investigation the surface morphology of MWCNTs, Figure 5.1 (a, b) depicts MWCNTs with diameters less than 100 nm observed at low and high magnifications. The presence of MWCNTs was established by the existence of hollow structures in the SEM images, which have lengths of several nanometers. SEM images show that the outer diameter of raw MWCNT is estimated to be around 50 nm based on the image scale. This falls within the 2.4 to 100 nm range for MWCNTS described in the literature [2]. The fact that the tubes seem hollow in Figure 5.1 (c) indicates that MWCNTs were functionalized. The CTAB-encapsulated MWCNTs are depicted in Figure 5.1 (c). The surfactant CTAB seems to have created a bilayer on the MWCNTs' surface and gradually encircled the entire MWCNTs floss. MWCNTs were bundled together rather than individually coated when they were encapsulated by CTAB. These bundles might serve as the adsorption sites that can be used during the adsorption process.

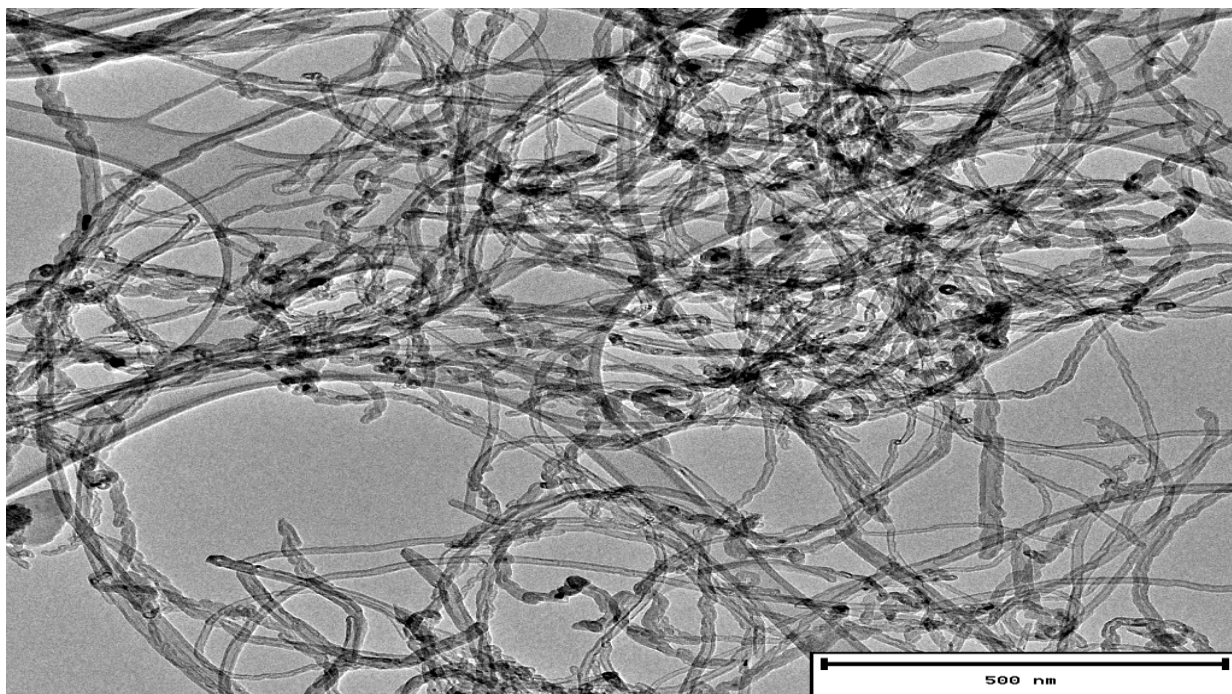
TEM spectroscopy is covered in subsection 5.3.2 MWCNTs were also employed to characterize MWCNTs. SEM mainly offers details on the morphology of MWCNTs, which are insufficient to determine the true nature of the CNTs [3]. Based on SEM observations, CNTs and nanofibers are easily confused [3]. As a result, TEM analysis of the samples was required to gather more details about the produced MWCNTs [2].

5.3.2 Observation of carbon nanotubes using transmission electron microscope

The internal structure of the sample was examined using a TEM using an FEI Tecnai T12 (with accelerating voltage range of 80 to 200 KV) [4]. The Peltier-cooled Keen View CCD camera was utilized to perceive the images. In this study, a magnification of 100000–400000 times and an accelerating voltage of about 120 kV were employed. The TEM images of untreated MWCNTs captured using the FEI Tecnai T12 are shown in Figures 5.2 (a and b).



(a)



(b)

Figure 5.2 (a, b): Two different views of the TEM image of the raw MWCNTs

Tube diameters in the bundle were measured using the TEM [4]. The TEM image in figure 5.2 (a) shows nanotubes with inner diameters, hollow structures, and lengths of multiple nanometers, confirming the existence of CNTs. It was found to be feasible to measure the diameter of a single nanotube and the bundle diameter directly from the obtained TEM images (Figures 5.2 (a) and 5.2 (b)) [4]. This knowledge can assist in determining the total number of nanotubes in a bundle. Most of the time, the samples of nanotubes are found alone (Figure 5.2 b). The TEM images show that the obtained nanotubes exhibit vastly different morphologies in response to certain variable parameters. The SEM study demonstrated that morphology could be controlled while maintaining a moderate plasma power level. However, these samples show various mutually varying orientations towards one to another. Under idealized circumstances, highly oriented films are produced, while medium- and poorly films are also produced, exhibiting many flaws.

Despite the high resolution of TEM images that allow for even atomic-level observation, the TEM images were unable to count the exact number of walls in each MWCNT sample (Figures 5.2 (a, b)). This shortcoming could be brought on by fabrication and material manipulation flaws (pentagons, heptagons, vacancies, or dopants) [4]. The average diameter of MWCNTs as seen in TEM images is about 25 nm. MWCNTs could be seen to be extremely thin in the TEM image, but the precise number of walls cannot be determined.

5.3.3 X-ray diffraction of raw carbon nanotubes

The XRD of raw MWCNTs was employed to study the crystal structure of untreated MWCNTs [5]. The XRD pattern of raw MWCNTs shows two representative peaks, one at 26.14 (002 levels) and the other at 44.22 (100 levels). In this study, the Bruker D2 advanced diffractometer was employed to obtain the XRD patterns of raw MWCNTs at different intensities. Figure 5.3 presents the XRD pattern of the raw MWCNTs employed in this study.

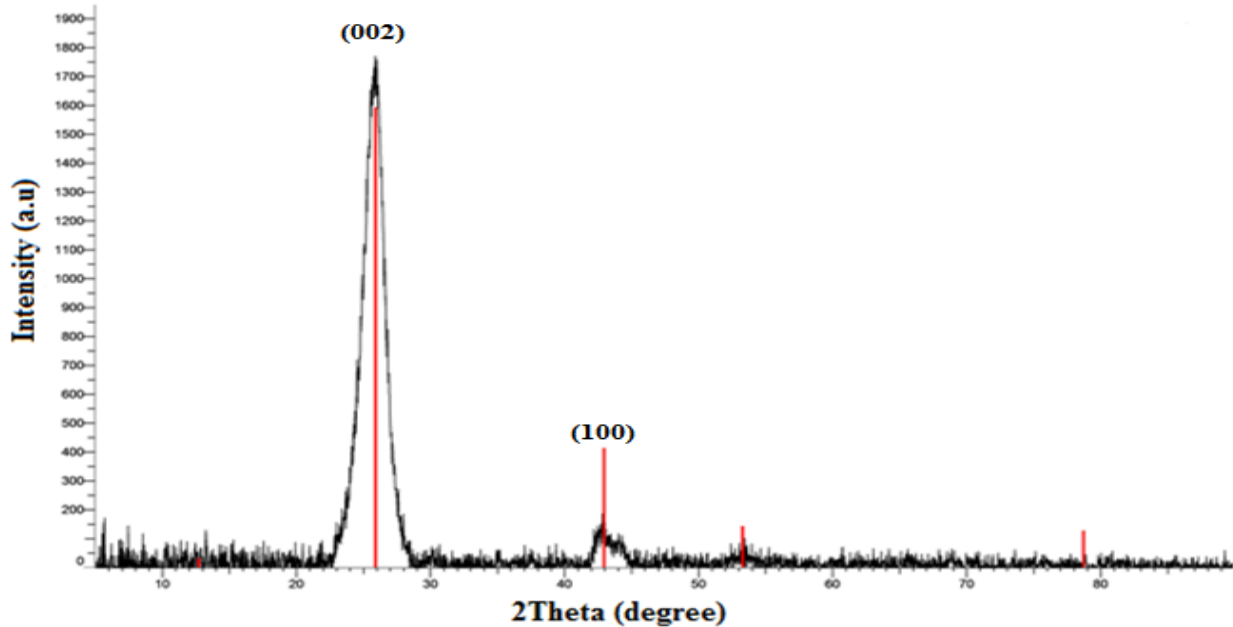


Figure 5.3: XRD pattern of raw MWCNTs

The MWCNTs interlayer distance d , the interplane distance corresponding to each plane, was determined by XRD. For MWCNTs, this is approximately 3.388 angstroms. The primary XRD pattern characteristics of MWCNTs are almost identical to those of graphite [6], as presented in Figure 5.3, due to the intrinsic nature of MWCNTs. Equation (3.4) can be used to measure the spacing d and the crystallite size of MWCNTs.

5.3.4 Raman spectroscopy of functionalized and unfunctionalized carbon nanotubes

In the interpretation of Raman spectra of the MWCNTs, with samples directly measured using a argon ion laser (with 514.5 nm line of a Lexel Model 95 SHG). A Horiba LabRAM Raman spectrometer was utilized to analyze the incident beam onto the sample. Additionally, this procedure can be utilized to identify the sort of CNTs produced, including SWCNTs and MWCNTs [7]. From the Raman spectroscopy analysis, it is observed that both functionalized and unfunctionalized MWCNTs exhibit two distinct peaks: the G-band (graphitic) and the D-band (disorder) [7]. Deviations in the plot indicate an increase in wall matrix defects in functionalized MWCNTs. However, the overall shape of the graph obtained after the functionalization process remained unchanged, indicating that the functionalization process did not alterate the composition

of the raw material. The Raman spectra of unfunctionalized and functionalized MWCNTs are presented in Figure 5.4. These results dispense valuable insights into the structural features of MWCNTs and their behaviour under the functionalization process.

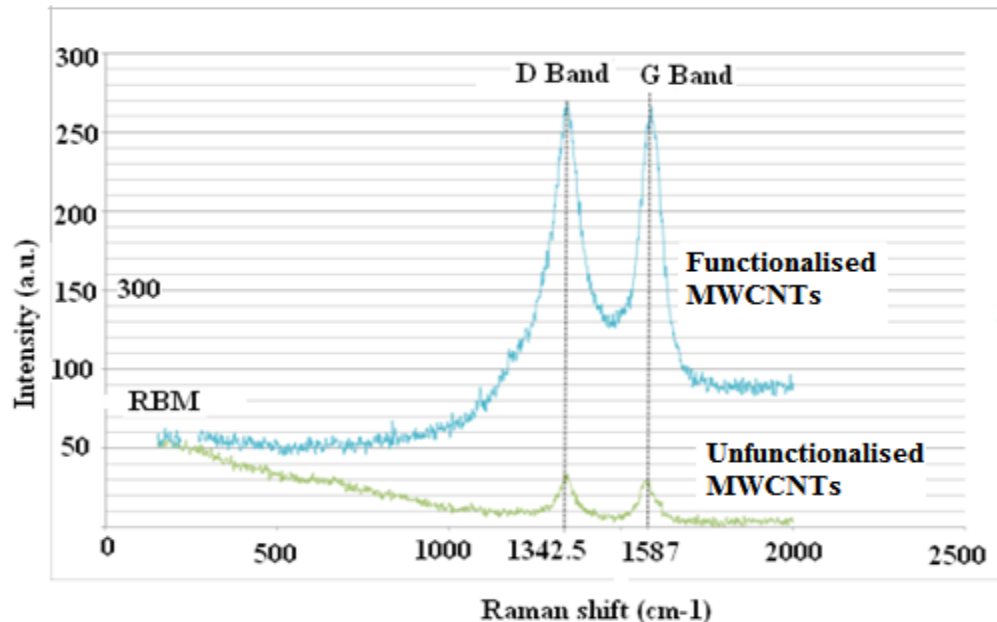


Figure 5.4: Raman spectroscopy spectra of unfunctionalized and functionalized MWCNTs

The relative intensities of the D-band and G-band in the Raman spectra are compared in this section. The D-band and G-band are two distinct peaks of MWCNTs, with the D-band located at 1342.5 cm^{-1} and the G-band at 1587 cm^{-1} . By analyzing the relative intensities of these peaks, valuable information about the sample can be obtained. Furthermore, the ID/IG ratio, which represents the intensity ratio between the D-band and G-band, is explained and its significance in Raman spectroscopy is discussed. The interpretation of the ID/IG ratio in relation to MWCNTs is also explored, providing insights into the properties and characteristics of these materials [7, 8, 9]. This deviates by 0.90 and 0.44% from the literature that states values of 1330 cm^{-1} and 1580 cm^{-1} , respectively [10]. These numbers demonstrate the formation of graphene sheets and show that the MWCNT walls had fewer flaws. These distinctive peaks can be seen even after nanotubes have undergone CTAB functionalization, demonstrating that the surfactant did not wreak havoc on the MWCNTs' structural integrity. It has been observed that MWCNTs that have undergone CTAB functionalization exhibit greater Raman intensity than raw MWCNTs. The ratio

ID/IG, a measure of defects in the MWCNTs wall matrix, increases slightly after functionalization compared to raw and CTAB functionalized samples. The increasing intensity of the D-band implies the presence of surfactant coverage on the MWCNTs' surface. This increase is important for detecting the sp³ C-C stretching mode. Additionally, the ratio ID/IG could serve as a rough indicator of the degree of functionalization in the absence of quantitative methods [12, 13, 14].

The findings in this section highlight the existence of imperfections in the wall matrix of MWCNTs, as indicated by the increased ID/IG ratio. The functionalization process led to only 5.5% increase in the ID/IG ratio, confirming that the introduction of defects in the MWCNTs was negligible. Additionally, the lack of the radial breathing mode (RBM) in the Raman spectra suggests that the MWCNTs sample had multiple walls, as RBM is specific to single-walled nanotubes [13, 14]. These characterizations provide valuable insights into the structural properties of the MWCNTs and give an improved comprehension of their nature and potential applications [13, 14]. Additional research is required to explore the implications of these defects and to identify future research directions in this field.

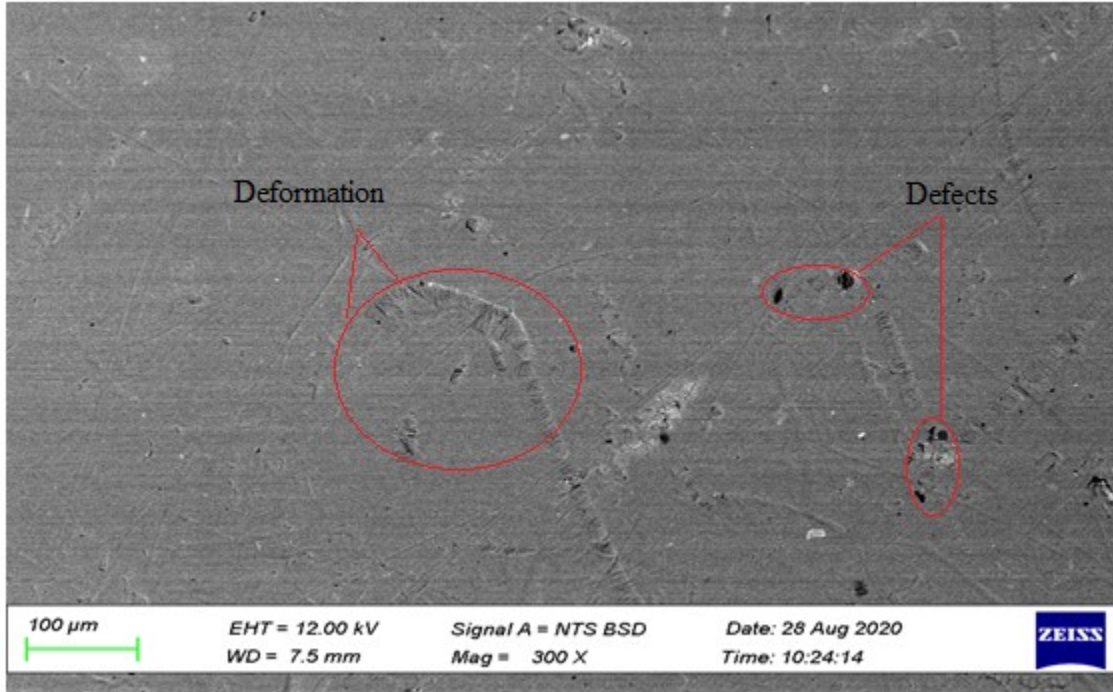
5.4 Polysulfone membrane characterization

SEM, porosity measurement, contact angle (hydrophilicity), and mechanical tests were used to characterize PSF filtration membranes. Microscopic techniques were chosen in this study to assess the morphology, composition, physical properties, and dynamic behavior of PSF membranes.

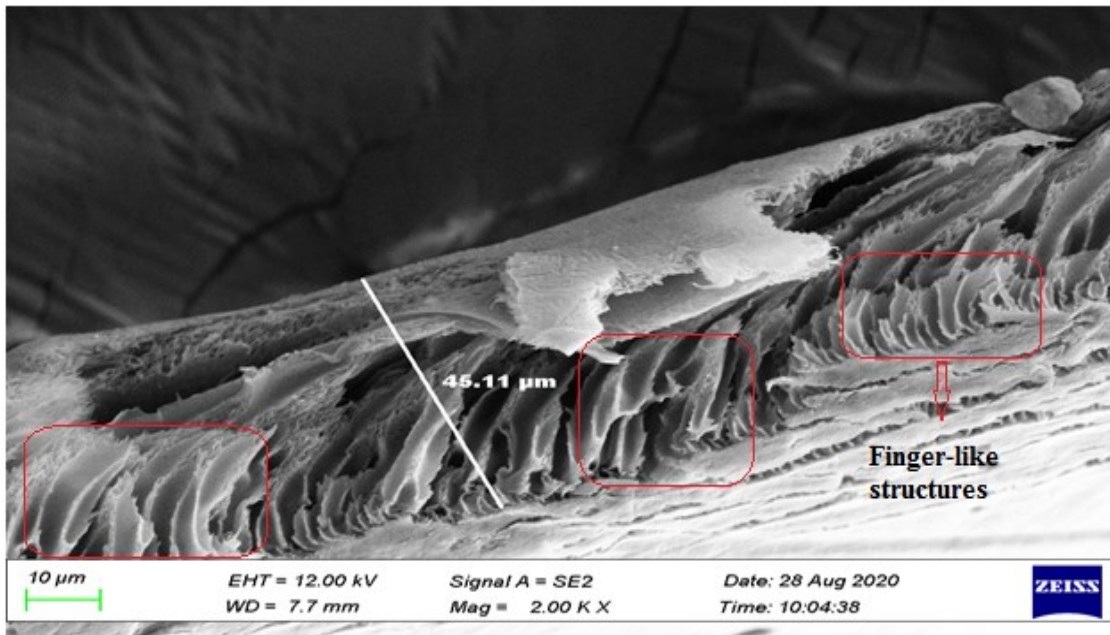
5.4.1 Observation of the scanning electron microscope images of polysulfone membrane

The SEM allowed for the examination of the morphology of the polysulfone membrane surfaces. In Figure 5.5 (a), the SEM picture of the top surface of the PSF filtration membrane is displayed, showing the characteristic plane image of an anisotropic membrane. Figure 5.5 (a) also shows the surface morphology of the membrane PSF associated with defects and deformation caused by the impacts during the casting process of the phase inversion method. However, a closer analysis of Figure 5.5 (b) reveals the presence of tiny, asymmetrical pores that traverse the membrane. Furthermore, the cross-sectional view of the membrane exhibited finger-like structures, which displayed a range of pore sizes. These observed features hold potential for application in membrane separation processes [15]. Specifically, the asymmetrical pores and finger-like structures could be

utilized to enhance separation efficiency, while the range of pore sizes offers important flexibility in selecting the optimal membrane for specific separation requirements [15]. Figure 5.5 (a, b) shows the SEM images of the top surface and cross-sections of a PSF membrane.



(a) PSF membrane surface view from the top.



(b) PSF membrane in cross-section.

Figure 5.5 (a, b): SEM images of the top surface and cross-sections of a PSF membrane respectively.

5.4.2 Contact angle (hydrophobicity) test of polymeric membrane

A common method for assessing the wettability of a solid surface is contact angle (CA) [16]. The solid is referred to as hydrophobic if the measured contact angle is above 90°, and hydrophilic if the CA is below 90° [16]. The CA (hydrophilicity) test was conducted on the polymeric membrane to assess its hydrophobicity using a goniometer. It was discovered that all the components of the membrane had contact angles below 90°, indicating their hydrophilic nature. After performing 10 runs and calculating the mean value, the CA of the PSF membrane was determined to be 73.28°, further confirming its hydrophilic properties. These findings are summarized in Table 5.1 highlighting the membrane's favorable hydrophilicity [16].

Table 5.1: Contact angle test results.

Run- Number	Contact angle (°)
1	74.89
2	72.31
3	71.81
4	69.96
5	74.52
6	71.57
7	58.21
8	70.81
9	85.69
10	83.65
Mean	73.28

Figure 5.6 illustrates the sessile drop measurement method employed in this study.



Figure 5.6: Illustration of the sessile drop measurement method [16]

5.4.3 Mechanical test results for polymeric membranes

The sample membranes of 1 cm width and 5 cm initial gauge length were arranged and clamped on a tensile strength testing machine with 10 mm/min or less tensile rate. The strain and stress were measured using TA. *XT plus*, Texture Analyzer, as mentioned in chapter three. The average value was computed thereafter. The test was ended when the specimen was fractured, and data were computed for analysis. High toughness, a crucial component of the membranes' exceptional compressive resistance properties, which are required during the filtration process, was demonstrated by the developed PSF membranes [17]. Figure 5.7 shows the strain-stress graph obtained after the mechanical test of the PSF membranes.

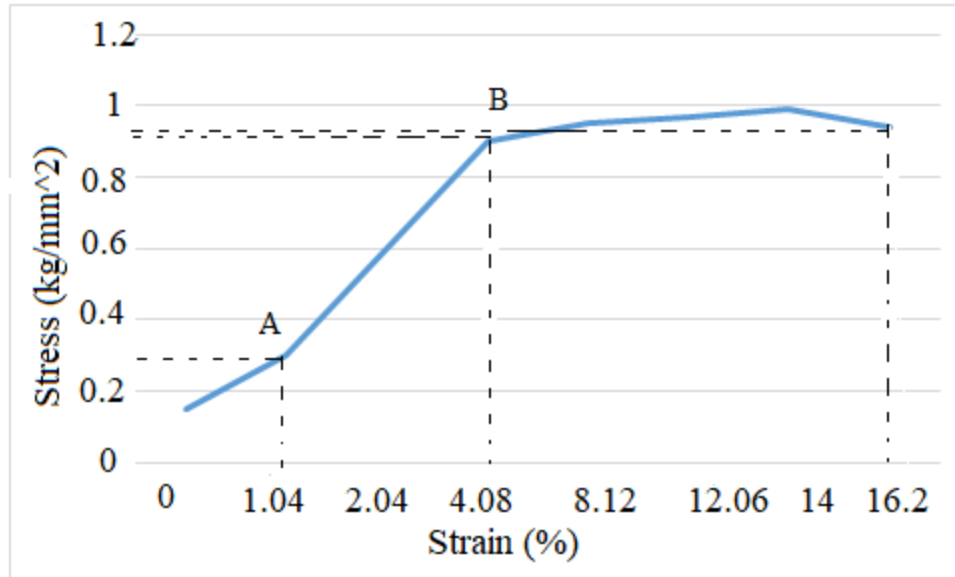


Figure 5.7: Mechanical test results of the polymeric filtration membranes

To analyze Young's modulus of PSF membranes, the study performed the phase inversion method to create flat sheet PSF membranes. The Young's modulus was then calculated using Equation (3.8). The obtained values for the Young's modulus at points A and B were 2.8 and 2.4 KN/mm², respectively. These results give quantitative information into the mechanical properties of the PSF membranes. Further interpretation and comparison of these values will be discussed in the subsequent sections, offering a comprehensive understanding of Young's modulus of PSF membranes. The results obtained from Figure 5.7 strongly support that PSF membranes produced with DMF as the solvent can be considered as nanocomposites that contain a good toughness that can support sufficient transmembrane pressures during the membrane filtration process [1, 18]. Materials' toughness, which is associated with their capacity to absorb energy, is determined in the region located under the stress-strain curve. For mechanical testing of polymeric membranes, the uniaxial tensile test is the most popular technique [18, 19]. The original cross-sectional area of flat sheet membranes could be used to calculate the nominal stress [17, 18, 19].

5.4.4 Porosity test of polymeric membranes

The porosity measurements for the PSF membranes were performed using the formula (3.5) mentioned in Chapter 3. The highest porosity value obtained was 61.4 % and the mean porosity value found after 7 different porosity tests was 58.3 %. The significance of the porosity test in

polymeric membrane research lies in its ability to come up with enhanced insights into the morphology and pore size of the membranes. Through the analysis of SEM images, the mean porosity value obtained from the test can be correlated to the membrane's structure and composition [15]. In this study, the porosity test revealed that the produced PSF filtration membranes have a pore size about 0.01 micrometer. Furthermore, the results indicated that these membranes can be classified as NF membranes. This finding is important as it suggests that these membranes could be potentially applied in the water treatment field, particularly in the removal of BOM from drinking water [15, 19]. Overall, the porosity test serves as a crucial tool in membrane research and offers valuable information for future studies in this field.

5.5 Determination of assimilable organic carbon

The AOC analysis was performed using the Van der Kooij method, which is widely recognized as the original and most popular technique for this purpose [20, 21, 22, 23]. The method involved inoculating the P17 strain of *Pseudomonas fluorescens* into 600 ml of pasteurized water and incubating it at 15 °C. Microbial density was measured every 2 days over a period of 21 days, and the maximum number of strains and conversion factors were used to determine the AOC concentration [23]. The heterotrophic plate counts method was employed to count the number of colonies that developed in the water [22, 23]. The results obtained from this study were correlated with previous studies, providing a basis for analysis and discussion of the findings.

Moreover, duplicate isolate cells of strain P17, which were used to inoculate the water samples, were grown in ultrapure water (Samples A₁ and A₂) and into autoclaved tap water (Samples B₁ and B₂) in the presence of sodium acetate (NaCH₃COO) and nutrient broth. The nutrient broth was made up of simple peptone and a beef extract. In the study, the growth of strain P17 in water samples A and B was tracked over a period of 48 hours at 25°C using periodic heterotrophic plate counts (HPC). The maximum population of strain P17 (i.e., the maximum number of colonies, N_{max}) was reached between days 19-21, (N_{max} = 200 × 10⁴ CFU/mL) and on day 15, (N_{max} = 220 × 10⁴ CFU/ mL) for water samples A and B respectively. The maximum concentration of strain P17 and its growth yield on sodium acetate were used in this study to calculate the AOC concentration, which was expressed as "acetate-carbon equivalents" [22, 23, and 24]. Figure 5.8 exhibits the colony count changes and growth curves of strain P17 over several days.

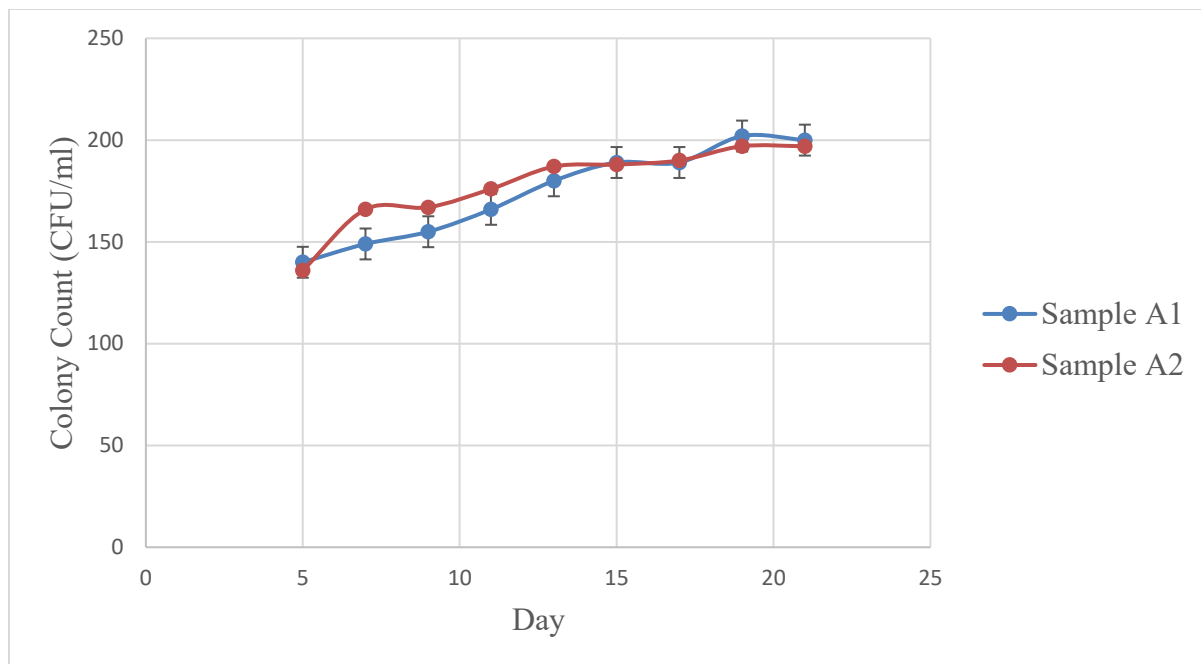


Figure 5.8: Colony count changes and growth curves of strain P17 over several days

It has been discovered that the presence of sodium acetate and nutrient broth significantly improved strain P17's ability to grow in ultrapure water. These ingredients were added to the inoculum. Figure 5.8 presents the HPC of 21 days. An average HPC estimation of 200×10^4 CFU/mL was obtained after 19 days. In the presence of sodium acetate and nutrient broth, in the initial experiments, a 13-day period of rapid linear growth in colony counts was noted. Thereafter, the growth rate tended to be flattening (between days 17-21) before it started declining for the low levels. This is likely due to the depletion of the amount of nutrients required for their growth. Figure 5.9 shows the growth of strain P17 in tap water (water sample B).

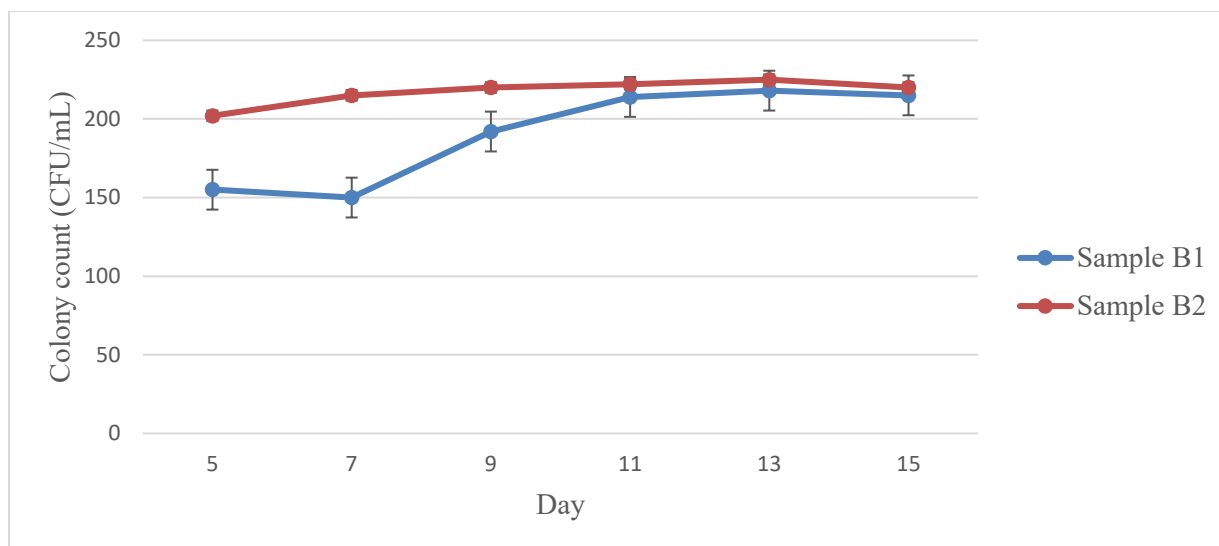


Figure 5.9: The number of colonies and growth curve of the P17 strain change over several days

It has been discovered that when organic matter and sodium acetate are added to the inoculum, strain P17's grows significantly in tap water. Figure 5.9 presents the HPC of 15 days, an average HPC estimation of 220×10^4 CFU/mL was obtained after 15 days. In the presence of sodium acetate and nutrient broth in the initial experiments, a 7-day period of rapid proliferation in colony counts was noted. Thereafter, the growth rate tended to be flattening between days 11-13 for sample B₁ and days 9-15 for sample B₂ before it started declining to a low level. This is likely due to the depletion of the amount of nutrients required for their growth.

The mean strain P17 counts for each sample were used to calculate the AOC concentrations. The sample's CFU/mL was calculated by dividing these counts by the dilution factor. The calculation of AOC concentration in strain P17 was performed using the average counts obtained from duplicate spread plates. This concentration was worked out in micrograms of acetate-C equivalents per liter [23]. Over the course of 21 days, a constant release of AOC was seen in ultrapure water (water sample A) (Figure 5.8), and the AOC concentration was found to be 48.8.4 $\mu\text{g C/L}$ (as acetate carbon). While in tap water (water sample B), the average concentration of AOC determined was 53.6 $\mu\text{g C/L}$ (as acetate carbon) after a period of 15 days. These variations in AOC levels could be the result of various water treatment methods, as strain P17 grows depending on the type of water [20]. It has been found that the increase in colony counts in the first run of the experiment was comparable to the increase in colony counts seen in the second run because we

conducted this experiment in duplicate. The findings indicate that the rate of AOC release in tap water was marginally higher than the rate of release in ultrapure water. This is most likely due to the presence of natural substrates in tap water [20, 23].

5.6 Measurement of the dissolved organic carbon and biodegradable dissolved organic carbon in water samples.

The high-density BDOC test is a method used to ascertain the DOC and BDOC in water samples [26, 27]. This test is chosen for its rapidity and ease of measurement [26, 27]. It involves the use of biologically active sand (BAS) as a substrate for the growth of the inoculum, enabling efficient measurement of organic matter in water [27]. To perform the test, a batch reactor is utilized, and the water sample is filtered before analysis. The test also involves the introduction of an indigenous bacterial population and monitoring the drop in DOC concentration resulting from bacterial carbon oxidation [26, 27]. Overall, the high-density BDOC test offers several advantages in terms of measurement speed and simplicity. Using BAS in the determination of DOC and BDOC in water samples offers several advantages [26, 27]. Firstly, BAS provides a rapid test procedure for BDOC determination, allowing for efficient and time-saving measurements of organic matter in water [26]. The BAS also simplifies the process, making it easier to measure the organic matter content. Furthermore, a batch reactor setup is employed for the incubation procedure, ensuring accurate and controlled conditions for the analysis. To carry out the BDOC procedure, the water sample must be filtered to remove any impurities. Finally, BAS enables the introduction of autochthonous bacterial populations, which achieve a major role in monitoring the drop in DOC concentration due to bacterial carbon oxidation. Overall, the use of BAS offers advantages regarding the speed, simplicity, and accuracy in determining the levels of DOC and BDOC in water samples. As a result, BDOC was calculated by measuring the water sample's DOC, incubating it in a batch reactor for 5 days in duplicate (reactors A and B), and then measuring its DOC once more. To calculate BDOC, the following formula was used:

$$\text{BDOC} = \text{DOC}_0 - \text{DOC}_5$$

Tables 5.2, 5.3, and 5.4 describe the variation in DOC and BDOC values obtained from the BAS after 5 days of incubation.

Table 5.2: Efficiency of BAS incubator 1

BATCH	DOC ₀ (mg/L)	DOC ₅ (mg/L)	BDOC (mg/L)	reactor efficiency (%)
REACTOR A ₁	5.65	5.09	0.47	9.9
REACTOR B ₁	5.54	5.00	0.54	9.7

Table 5.3: Efficiency of BAS incubator 2

BATCH	DOC ₀ (mg/L)	DOC ₅ (mg/L)	BDOC (mg/L)	reactor efficiency (%)
REACTOR A ₂	5.65	4.26	1.39	24.6
REACTOR B ₂	5.54	4.46	1.08	19.5

Table 5.4: Efficiency of BAS incubator 3

BATCH	DOC ₀ (mg/L)	DOC ₅ (mg/L)	BDOC (mg/L)	reactor efficiency (%)
REACTOR A ₃	5.65	4.26	1.39	24.6
REACTOR B ₃	5.54	4.46	1.08	19.5

Regular monitoring and maintenance of DOC levels in tap water is of utmost importance. This is because high concentrations of DOC can lead to the growth of bacteria and microorganisms, posing a risk to water systems and public health. The results from Tables 5.2–5.4 show a range of DOC concentrations from 4.26 mg/L to 5.65 mg/L, indicating the presence of organic compounds in tap water. Furthermore, the average DOC values collected between May and June 2021, ranging from 5.54 to 5.65 mg/L, suggest an elevated potential for bacterial growth during that period. The DOC concentration for samples B₁ and B₂ dropped to 4.26 and 4.46 mg/L, respectively, after 5 days of incubation. Since it has a relatively short incubation period and a high degree of precision, the high-density sand bioassay is superior to other methods for determining BDOC [26, 27]. This approach was selected because it measures DOC directly. This is regarded as an all-purpose sign of organic matter in water [24, 26, 27].

The BDOC changes varied slightly across the three distinct incubation periods, as shown in Tables 5.2, 5.3, and 5.4. The incubation procedure, on the other hand, demonstrated a BDOC range between 1.08 and 1.39 mg/L with 2 data points, which was much more consistent. Following the incubation period, the BDOC concentrations may have varied with changes in DOC concentration in the source water, which may indicate heterotrophic activity. [26, 27]. When the bioavailable DOC (BDOC) exceeds 0.5 mg/L, it signifies a significant risk of biofilm formation and bacterial proliferation. Taking this into consideration, regular tracking and maintenance protocols should be implemented to mitigate the growth of bacteria and ensure the safety and quality of tap water [26, 27]. It has been observed that there are variations in the BDOC from the data presented in Tables 5.2–5.4.

5.7 Summary

The nanostructures in this chapter were characterized using microscopy methods. These techniques were selected because it enables the evaluation of the morphology, composition, physical characteristics, and dynamic behavior of nanostructured materials. This contributes to material science. During a hybrid treatment system, characterization of both MWCNTs and PSF membranes was necessary to determine the relevant properties for removing BOM, in terms of AOC and BDOC, from water. Subsequently, the surface morphology of PSF membranes and MWCNTs was investigated using low and high magnifications for both SEM and TEM images. (Image quality was achieved by varying the magnification). This procedure was conducted on all other samples. Furthermore, it was found that MWCNTs and NF membranes exhibit interesting features and properties. These features could be utilized to eradicate BOM compounds from drinking water. The high adsorption and selectivity capacities of functionalized CNTs and NF membranes respectively should be mostly attributed to their structural and functional properties. This study also characterized the strain P17 in part, through morphology (size, shape, and arrangement of bacterial cells), and gram staining (a microbiology technique used to differentiate between bacterial species) based on their cell composition. The results obtained after gram staining techniques revealed that the P17 strain used in this study has weak cell walls, therefore it is gram-negative.

The biological stability of water samples, both raw and finished, was evaluated in this chapter using both the AOC and BDOC methods. More specifically, the findings demonstrate that the

rate of AOC release in tap water was marginally higher than the rate of release in ultrapure water. This is most likely caused by the naturally occurring organic substrates in tap water. However, data that was collected after the BDOC was determined showed variations in the BDOC. When BDOC exceeds 0.5 mg/L, it is a cause for concern because it shows that there is a high likelihood that bacteria and other microorganisms will grow into biofilms and multiply in the water systems. Additionally, future research could focus on the dynamic behavior of nanostructured materials in water treatment processes, to better understand their performance and optimize their use. By characterizing the morphology, composition, and physical characteristics of nanostructures, researchers can continue to advance material science and improve the elimination of BOM from water. These characterization techniques are essential for developing a comprehensive understanding of nanostructures and their potential applications in water treatment. The goal of the following chapter is to assess the viability of using an adsorption process (with functionalized CNTs) in combination with a membrane filtration process (with NF membranes) to remove BOM from drinking water. This is done by comparing the performance of the hybrid adsorption-membrane filtration system for BOM removal to those of conventional standalone such as NF, UF, or MF membranes, as well as the hybrid treatment system with conventional adsorbents such as PAC.

5.8 References

- [1] Natsuko, A., Jinfenf, L., Shunsuke, A., Seichi, T., (2021). Direct observation techniques using scanning electron microscope for hydrothermally synthesized nanocrystals and nanoparticlusters. *Nanomaterials (basel)*, 11, 908.
- [2] Stadtländer, C. T. K. H, (2007). Scanning electron microscopy and transmission electron microscopy of mollicutes: challenges and opportunities. In: Mendez-Vilas, A., Diaz, J. (Editors), *Modern Research and Educational Topics in Microscopy, Series 2*. Formatex, Badajoz, pp.122-131.
- [3] Alaa, M., (2019). Synthesis, characterisation and applications of carbon nanofibers. *Carbon nano-objects*, 243-257.
- [4] Martinez, M.T., Callejas, M. A., Benito, A. M., Cochet, M., Seeger, T., Ansón, A., Schreiber, J., Gordon, C., Marhic, C., Chauvet, O., Fierro, J. L. G., Maser, W. K., (2003). Sensitivity of single

wall carbon nanotubes to oxidative processing: structural modification, intercalation and functionalisation. *Carbon* 41, 2247-2256.

[5] Soleimani, H., Yahya, N., Bawg, M.K., Khodapanah, L., Sabet, M., Burda, M., Oechsner, A., Awang, M. (2015). Synthesis of carbon nanotubes for oil-water interfacial tension reduction. *Oil gaz res*, 104, 2472-0518.

[6] Anjalin, F.M. (2014). Synthesis and characterisation of MWCNTs nanocomposite and its electrical studies. *Der pharmachemics* 6, 354-359.

[7] Costa, S., Borowiak-Palen, E., Kruszyńska, M., Bachmatiuk, A., Kaleńczuk, R.J. (2008). Characterisation of carbon nanotubes by Raman spectroscopy. *Materials Science – Poland* 26 (2), 433-441.

[8] Susana, L.H.R., Alexandra, G., Monika, E.S., Andre, M.P., Joao, P., Cristina, F. (2016). Progress in the Raman spectra analysis of covalently functionalised multiwalled carbon nanotubes: unraveling disorder in graphitic materials. *Royal society of chemistry*, 18. 12784.

[9] Potgieter-Vermaak, S., Maledi, N., Wagner, N., van Heerden, J. H. P., van Grieken, R., Potgieter, J. H., (2011). Raman spectroscopy for the analysis of coal: a review. *Journal of Raman Spectroscopy* 42, 123-129.

[10] Osswald, S., Havel, M., Gogotsi, Y., (2007). Monitoring oxidation of multiwalled carbon nanotubes by Raman spectroscopy. *Journal of Raman Spectroscopy* 38, 728-736.

[11] Osorio, A. G., Silveira, I. C. L., Bueno, V. L., Bergmann, C. P., (2008). H₂SO₄/HNO₃/HCl - functionalization and its effect on dispersion of carbon nanotubes in aqueous media. *Applied Surface Science* 255, 2485-2489.

[12] Jorio, A., Pimenta, M. A., Filho, A.G.S., Saito, R., Dresselhaus, G., Dresselhaus, M.S., (2003). Characterizing carbon nanotube samples with resonance Raman scattering. *New Journal of Physics* 5, 139.1-139.17.

[13] Graupner, R., (2007). Raman spectroscopy of covalently functionalized single-wall carbon nanotubes. *Journal of Raman Spectroscopy* 38 (6), 673-683.

- [14] Singh, P., Campidelli, S., Giordani, S., Bonifazi, D., Bianco, A., Prato, M., (2009). Organic functionalisation and characterisation of single-walled carbon nanotubes. *Chemical Society Reviews* 38, 2214-2230.
- [15] Hoan, T.V., Thn, H. A., Khai, D.D., Minh, N.N., NUT, T., Than, T.H., Vo, V., Tuan, A.V. (2019). Preparation and characterization of a hydrophilic polysulfone membrane using graphene. *Journal of Chemistry* 10, 3164373.
- [16] Wen, Y.W., Jing, Y.S., Jin, L.W., Yan, L.L., Ning, N.G., Zheng, X.L., Wei, T.L. (2015). Preparation and characterization of PEG-g-MWCNTs / PSF nano-hybrid membranes with hydrophilicity and antifouling properties. *Royal Society of Chemistry* 5, 84746.
- [17] Mehdi, M., Mahmoud, G.K., Hossein, M., Henri, V., Mojtaba, E. (2018). Investigation of structure-performance properties of a special type of polysulfone blended membranes. *Polymeric Advanced Technologies*, 10, 1-18.
- [18] Zhaoyue, S., Rujing, L., Xiu, Y.L., Renxin, X., Wei, C. (2016). Influence of membrane materials and operational modes on the performance of ultrafiltration modules for drinking water treatment. *International Journal of polymeric science*, 6895235.
- [19] Scott, K. (1998). Introduction to membrane separations. *Handbook of industrial membranes* 2, 3-185.
- [20] Van der Kooij, D. (1987). The effect of treatment on assimilable organic carbon in drinking water, treatment of drinking water for organic contaminant. *Pergamon press*, New York. 317-328.
- [21] Van der Kooij, D. (1982). Assimilable organic carbon as an indicator of bacterial regrowth. *Journal of American Water Works Association* 84. 57-65.
- [22] Van der kooij, D., Visser, A., Hijnen W.A.M. (1982). Determining the concentration of easily assimilable organic carbon in drinking water, *American Water Work Association* 74. 540-545.
- [23] Van der Kooij, D., Visser, A., Orange J.P. (1982). Multiplication of fluorescens pseudomonas at low substrate concentrations in tap water. *Journal of Microbiology* 48, 229.

- [24] Fleck, J.A., Bossoio, D.A., Fuji, R. (2004). Dissolved organic carbon and disinfection by-product precursor release from managed peat soils. *Journal of Environmental Quality*, 33, 465-475.
- [25] Dumitru, R., Urs, V.G., Sodoniu, V. (2009). Trihalomethane formation during water disinfection in four water supplies in some river basin in Romania. *Environmental Science and Pollution Research* 16. 55-65.
- [26] Joret, J.C., Levi, Y. (1986). Methode rapide d'évaluation du carbone éliminable des eaux par voie biologique. *Trib cebedeau* 39, 3-9.
- [27] Joret, J.C., Levi Y., Volk, C. (1991). Biodegradable dissolved organic carbon (BDOC) content in drinking water and potential regrowth of bacteria. *Water Science Technology* 2, 95-101.
- [28] Escobar, I., Randall, A. (1999). Influence of nanofiltration on distribution systems. *Biostability Journal of American Water Works Associations* 6. 76-89.

CHAPTER SIX: HYBRID ADSORPTION-MEMBRANE FILTRATION SYSTEM FOR THE REMOVAL OF BOM IN DRINKING WATER

6.1 Introduction

This chapter presents and discusses the outcomes of a hybrid adsorption-membrane filtration system used to eradicate BOM from drinking water. For the purpose of evaluating the biological stability of the water samples used in this work, additional water quality parameters counting pH, temperature, conductivity, TDSs, ammonium ions, dissolved oxygen, alkalinity, free chlorine, and nitrate were measured. Results related to plate counts for colonies enumeration (AOC) and water filtrations permeate (flux) for AOC and BDOC determination are also discussed.

6.2 Adsorption process of natural organic matter by CTAB-functionalized carbon nanotubes

Bacterial growth has been identified to be part of the foremost causes of water quality degradation within DWDSs. Example of undesired effects that can be linked to bacterial growth include the proliferation of pathogens and coliforms, the reduction of hydraulic efficiency, unwanted colour, taste, odour, reduction of dissolved oxygen, the acceleration of pipe corrosion, and formations of biofilm [1, 2, 3, 4]. The adsorption procedure was selected for this study since it is the most effective way to treat a variety organic contaminant in water. This is most likely due to its adaptability, broad applicability, cost-efficiency, and practicability [5, 6].

The CNTs are exceptional and have exceptional chemical and thermal stability. It has been demonstrated that CNTs have excellent potential as superior sorbents that could absorb diverse types of organic and inorganic pollutants, including lead [15], 1, 2-dichlorobenzene [7], cadmium [8], fluoride [9], nickel [10], THMs [11], and zinc [12] from aqueous solutions, and volatile organic compounds and dioxin [13,14] from the air stream. Researchers compared MWCNTs with different other types of adsorbents and found that CNTs are a promising sorbent for applications involving environmental protection [10, 11, 16]. In addition, MWCNTs ought to be effective at removing BOM from aqueous solutions. As a viable alternative nanomaterial to conventional membrane filtration, CTAB-functionalized MWCNTs were investigated in this study for their ability to adsorb BOM in terms of AOC and DOC.

6.2.1 Impact of batch adsorption process using carbon nanotubes (as sorbents) on assimilable organic carbon concentration

It is expected that MWCNTs' batch adsorption will reduce AOC concentrations in aqueous solutions [17, 18, and 19]. The batch adsorption process was performed by dispersing functionalized MWCNTs in ultrapure water (water sample A) and tap water (water sample B) inoculated with strain P17.

A constant volume of water (100 mL) was inoculated with strain P17 and sodium acetate (the only source of carbon for some microorganisms) was added in 5 different sample tubes. Nutrient broth, a pre-enrichment medium made of peptone and beef extract, was also added. Each tube received different dosages of CTAB-functionalized MWCNTs (0, 4, 8, 12, and 16 mg). Subsequently, the tubes were then placed on a shaker that was placed in a temperature-controlled box (Orbicult Incubator Benchtop Shaker, running at 25°C and 180 rpm for 4 hours) after which the shaker was turned on. Then, to separate MWCNTs from aqueous solutions, the 0.45 µm syringe filter was used. For the AOC analysis, duplicate runs of each batch adsorption experiment were completed. For the batch adsorption procedure, the pH and initial solution temperature were maintained at 4 and 25°C, respectively. The following equation was used to determine how much NOM adsorbs onto MWCNTs:

$$q = (C_0 - C_t) \frac{V}{m} \quad (6.1)$$

Where q is the amount of BOM adsorbed on MWCNTs (mg/g), C_0 and C_t are the BOM concentrations at the beginning and after a specific period, V is the initial solution volume (L), and m is the CNT mass (g).

The ability of CTAB-functionalized MWCNTs to remove BOM prior to membrane filtration was tested in an experiment. Adsorption process was identified as an attractive approach for AOC removal from water [17, 18]. Furthermore, due to its large mesopores, fibrous shape, and accessible external surface area, MWCNTs are well known to have high adsorption properties [17, 18, and 19]. This is most likely because CNTs possess highly assessable adsorption sites that enable charge neutralization; as a result, by adding positively charged CNTs to BOM in

water, BOM can be absorbed. Before the membrane filtration process, P17 inoculated-water samples were prepared for the adsorption process with CTAB-functionalized MWCNTs. Figure 6.1. illustrates water sample A inoculated with strain P17, containing each 4, 8, 12 and 16 mg of CTAB – functionalised MWCNTs for adsorption process.

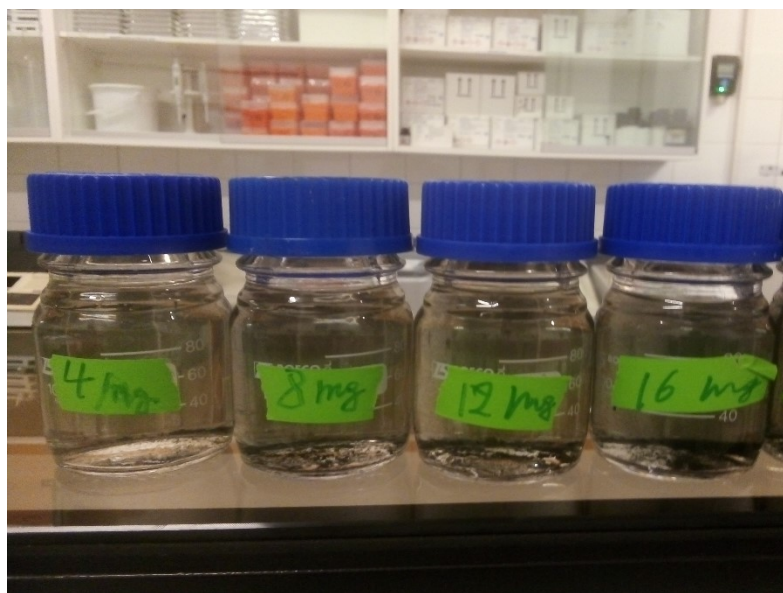


Figure 6.1: Water sample A inoculated with strain P17, containing each 4, 8, 12 and 16 mg of CTAB – functionalised MWCNTs for adsorption process.

Figure 6.1 illustrates the ultrapure (water sample A) containing 4, 8, 12, and 16 mg of CTAB-functionalized MWCNTs, respectively (To assess adsorption capacity of different concentrations of CTAB-functionalized MWCNTs before membrane filtration test). Some preceding studies have shown that MWCNTs are more effective adsorbents for the removal AOC in water [17, 18, 19]. After the adsorption process, the HPC results decreased from 200×10^4 CFU/mL to 95×10^4 , 86×10^4 , 85×10^4 , and 102×10^4 CFU/mL for P17-inoculated ultrapure water (water sample A) treated with 4,8,12, and 16 mg of functionalized MWCNTs, respectively. Furthermore, the AOC concentration decreased from $48.8 \mu\text{g C/L}$ to $20.7 \mu\text{g C/L}$ (as acetate carbon) after the adsorption process with 12 mg MWCNTs, which show the best result compared to other concentrations of MWCNTs. This is likely due to superior adsorption capacities of CNTs that could be elucidated

by the presence of large mesopores and positive surface charge that facilitate charge neutralization mechanism during adsorption process.

The HPC results of strain P17-tap water (water sample B) after the adsorption process with a constant concentration of 12 mg of functionalized MWCNTs, it has been found a drop from 220×10^4 CFU/mL to 105×10^4 CFU/mL and the AOC concentration drop from 53.6 to 25.6 $\mu\text{g C/L}$ (as acetate carbon). The heterotrophic plate count results show that despite the high concentration of strain, P17 inoculated in both ultrapure water and tap water, the adsorption process with CTAB-functionalized MWCNTs has succeeded to significantly reduce the AOC concentration in water. The comparison of the HPC of the 2 different water samples A and B recorded after the adsorption process easily detected that AOC dropped significantly with the use of CTAB-functionalized MWCNTs.

Before the adsorption process, AOC concentrations averaged 48.8 and 53.6 $\mu\text{g/L}$ (as acetate-C), thereafter adsorption as the treatment process they averaged 20.7 and 25.6 $\mu\text{g/L}$ (as acetate-C). It has been found that the average AOC concentrations after the adsorption process with 12 mg functionalized MWCNTs decreased by 57.5 and 52.2 % for samples A and B respectively. This decrease was statistically discernible. This is likely due to the adsorption removal efficiency of AOC on CTAB-functionalized MWCNTs, and it is also well known that the adsorption ability of NOM on MWCNTs devolves on the concentration of adsorbent [17, 18]. It has also been found that AOC has been removed at high percentages from both the P17-ultrapure water sample and the P17-tap water after the adsorption process performed with a CTAB-functionalized MWCNTs concentration of 12 mg. This is because the amount of 12 mg of functionalized MWCNTs gives the most effective and most appreciable adsorption results compared to other functionalized MWCNTs concentrations. The HPC results reveal an optimal eradication of AOC from water at the same concentration of MWCNTs. Figure 6.2 demonstrates the influence of adsorbent concentration on the percentage removal of AOC from P17-ultrapure water.

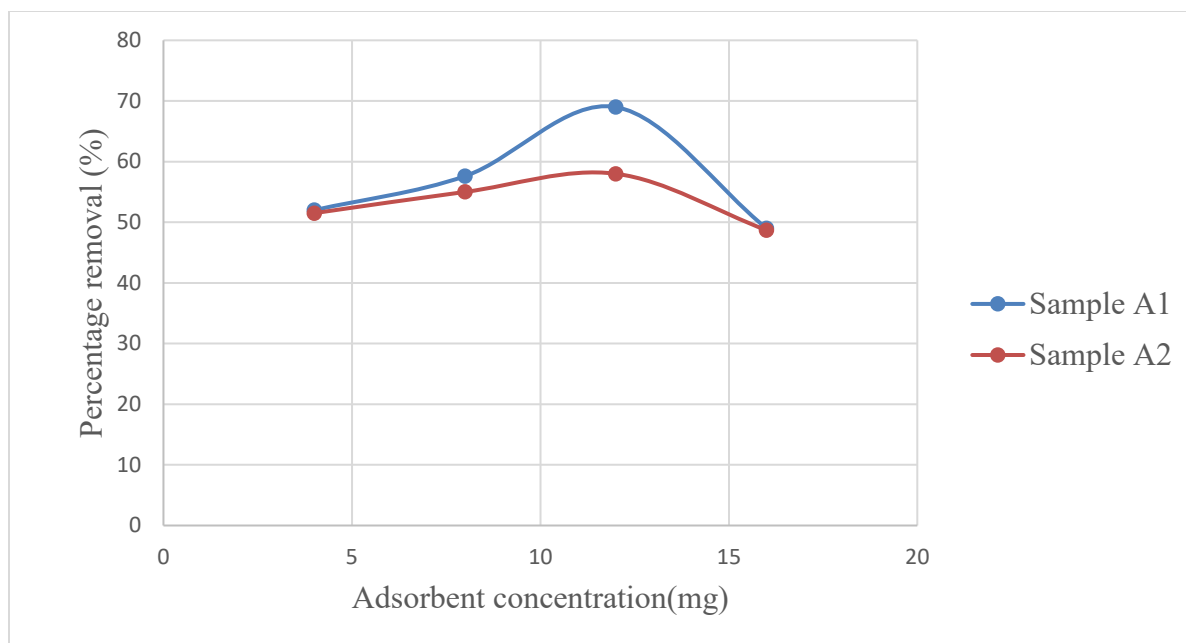


Figure 6.2: Impact of adsorbent concentration on percentage removal of AOC from P17-ultrapure water (With agitation speed = 180 rpm and contact time = 4 hours)

The impact of CTAB-functionalized MWCNTs (adsorbent) on the removal of AOC from sample A is depicted in Figure 6.2. The complete adsorption process for AOC removal was performed only on ultrapure water (sample A), because of a low amount of functionalized MWCNTs needed to be saved for the rest of the experiment. Therefore, only 12 mg of functionalized was used in the adsorption process for AOC removal from tap water (water sample B), while the pH, initial concentration of AOC, agitation speed, and contact time were maintained constant at 4, 48.8 $\mu\text{g C/L}$ (as acetate C), 180 rpm, and 4 hours respectively, retained as optimum conditions from the adsorption process on sample A. For all adsorbents, a direct correlation between adsorbent concentration and AOC removal was seen. With increasing adsorbent concentration, it was discovered that the AOC removal from water sample A increased. At a functionalized MWCNT concentration of 12 mg, maximum removal was noted. More AOC can be adsorbed onto the adsorbent surface as the available active sites rises with an increase in adsorbent concentration. The density of functionalized MWCNTs (adsorbent), which increases with higher CTAB concentrations and leads to the steric hindrance between the MWCNTs to aggregate attributable to the presence of electrostatic forces, which has an adverse effect on the adsorption process [18, 20]. As a result, a lower percentage of AOC was removed from the mixture [18, 20]. On the other

hand, at 12 mg dosage, CTAB-functionalized MWCNTs removed 57.5 percent of the initial concentration of AOC from water sample A and 52.5 percent from tap water sample B. These findings demonstrated that CTAB-functionalization significantly affects the effectiveness of AOC removal from water. The influence of agitation speed on the percentage removal of AOC is presented in Figure 6.3.

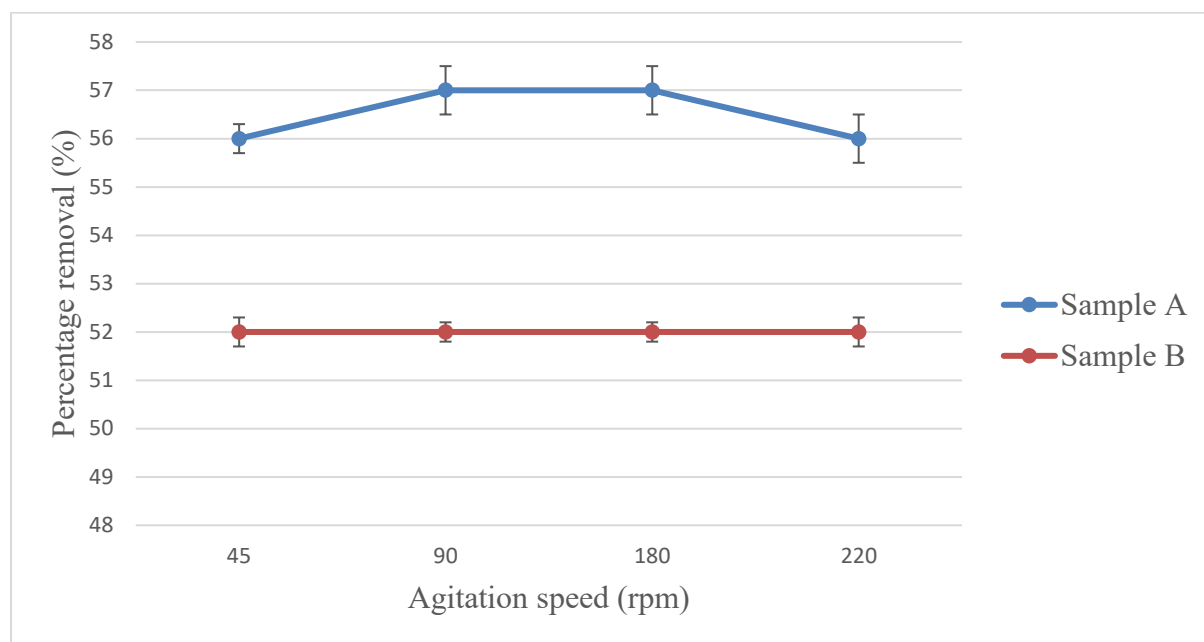


Figure 6.3: Impact of agitation speed on the percentage removal of AOC (initial concentrations of 48.8 and 53.6 g C/L, 12 mg of adsorbent, 4 hours of contact time, pH of 4).

Adsorbent dispersion in the solution is greatly aided by the effect of adsorption speed, which is a crucial factor. Throughout the adsorption procedure, it lessens its agglomeration. Functionalized MWCNTs were discovered to evenly disperse in both inoculated water solutions for strain P17 (water samples A and B) used in the current study. Due to the electrostatic forces among CNTs, a slight MWCNTS agglomeration was only noticed at the adsorbent dosage of 16 mg. [18, 20]. The removal of AOC from strain P17 inoculated in both water samples (A and B) is shown as a function of agitation speed in Figure 6.3. The agitation speed was adjusted from 45 to 220 rpm for both water samples A and B. Acetate-C was used as the adsorbent, and the pH, contact time, and initial concentrations were all held constant at 4, 4 hours, 48.8 μg and 53.06 μg C/L (for A and B, respectively). It was found that as the agitation speed was increased, more AOC was

removed from water sample A (strain P17-ultrapure water). This is because agitation makes ion diffusion towards the adsorbent surface more efficient. Van der Waals forces, however, resulted in a slight agglomeration at the adsorbent concentration of 16 mg. On the other hand, for water sample B, the variation in agitation speed did not clearly affect the percentage of removal of the AOC from the tap water. Since water sample A (strain P17-ultrapure water) produced notable results at 180 rpm, it was decided to maintain this speed as the ideal agitation speed for the rest of the experiments. This is most likely because at higher agitation rates, a desorption process could occur at the equilibrium time. It was established that the equilibrium adsorption capacity, and the adsorption kinetics change because of the difference in agitation speed during the adsorption process. Figure 6.4. shows the impact of contact time on the percentage removal of AOC from water.

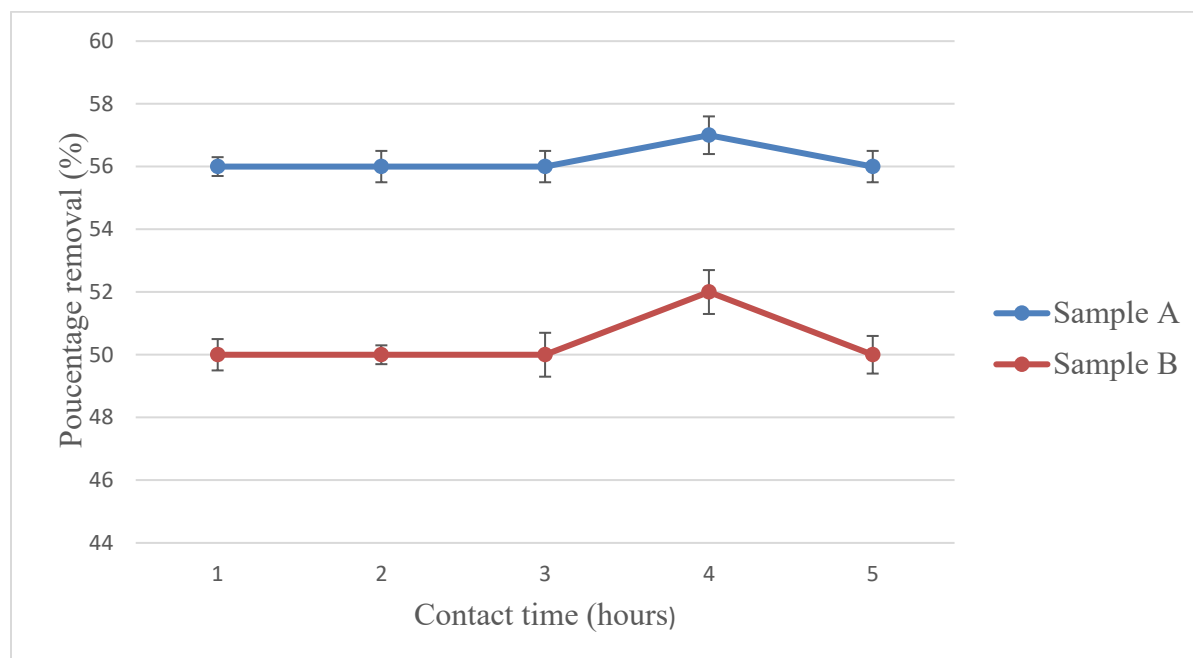


Figure 6.4: Impact of contact time on the removal of AOC (initial concentration = 48.8 and 53.6 $\mu\text{g C/L}$ (for A1 and B1 respectively), Agitation speed = 180 rpm, adsorbent concentration = 12 mg)

Figure 6.4 shows the experimental findings that illustrate how contact time affects the removal of AOC by CTAB-functionalized CNTs. The contact time was adjusted from one to five hours while the pH, the initial AOC concentration, the adsorbent concentration, and the agitation speed

were maintained at 48.8 and 53.0 $\mu\text{g C/L}$ (for samples A and B, respectively), 12 mg, and 180 rpm, respectively. The removal of AOC from both water samples (A and B) slightly enhanced with the increase of the contact time from one to four hours. Furthermore, after 4 hours of contact time, however, there was no discernible increase in removal. Because no adsorption occurs and the surface coverage of the adsorbent increases over time, this shows that equilibrium has been reached. Previous studies have shown that conventional adsorbents like PAC, GAC, and BAC have been used extensively during the adsorption of BOM; however, a low rejection of NOM compounds due to the use of PAC; this is likely because the contact of BOM with PAC particles led to the BOM-PAC particles that create a supplementary barrier due to its negatively charged surface [16, 17, 18]. Previous studies have demonstrated that CNTs are superior sorbents for a variety of contaminants in water [16, 17, 18]. After 4 hours of contact time, it was found in this study that CTAB-functionalized MWCNTs (positively charged MWCNTs) could only remove a maximum of 57% of AOC from water sample A and 52% from water sample B. The interaction of MWCNTs and BOM compounds results in charge neutralization.

6.2.2 Impact of batch adsorption process using carbon nanotubes (as sorbents) on dissolved organic carbon and biodegradable organic carbon concentrations

In batch adsorption, MWCNTs are expected to reduce DOC and BDOC concentrations from aqueous solutions [17, 21, and 22]. A batch adsorption process was performed by dispersing functionalized MWCNTs in tap water (sample B) collected after 5 days of incubation. After each stage of the incubation procedure, a fixed volume of raw water sample (1L) was added to 4 different sample tubes. Each tube received four different doses of CTAB-functionalized MWCNTs: 4, 8, 12, and 16 mg respectively. The tubes were then placed on an incubator-shaker (the Orbicult Incubator Benchtop Shaker) operating at 25°C and 180 rpm for 4 hours. This shaker was housed in a temperature-controlled box. Then, to separate MWCNTs from aqueous solutions, the 0.45 μm syringe filter was used. All batch adsorption experiments were performed in duplicate (samples B₁ and B₂) for the DOC and BDOC analysis. The initial solution temperature, pH, contact time, initial DOC concentrations, and agitation speed were 18.9°C, 7.3, 4 hours, 4,26 and 4,46 mg/L, and 180 rpm respectively. They were kept constant for an enhanced comprehension of the adsorption process [16, 17, 19]. The amount of DOC adsorption onto MWCNTs was calculated using equation (6.1) as previously discussed. Tables 6.1-6.4 present the

results obtained after adsorption process with 4, 8, 12, and 16 mg of CTAB-functionalized MWCNTs on the variation of DOC, and BDOC in tap water in duplicate (B₁ and B₂) collected after 5 days incubation.

Table 6.1: Efficiency of adsorption process with 4 mg MWCNTs on the DOC concentration in tap water collected after 5 days incubation.

Batch reactor	DOC before adsorption (mg/L)	DOC after adsorption (mg/L)	BDOC (mg/L)	Batch reactor efficiency (%)
REACTOR B ₁	4.26	4.06	0.20	4.7
REACTOR B ₂	4.46	4.26	0.20	4.4

Table 6.2: Efficiency of adsorption process with 8 mg MWCNTs on the DOC concentration in tap water collected after 5 days incubation.

Batch reactor	DOC before adsorption (mg/L)	DOC after adsorption (mg/L)	BDOC (mg/L)	Batch reactor efficiency (%)
REACTOR B ₁	4.26	3.85	0.41	9.6
REACTOR B ₂	4.46	4.04	0.42	9.4

Table 6.3: Efficiency of adsorption process with 12 mg MWCNTs on the variation of DOC concentration in tap water collected after 5 days incubation.

Batch reactor	DOC before adsorption (mg/L)	DOC after adsorption (mg/L)	BDOC (mg/L)	Batch reactor efficiency (%)
REACTOR B ₁	4.26	4.09	0.17	4
REACTOR B ₂	4.46	4.25	0.21	4.7

Table 6.4: Efficiency of adsorption process with 16mg MWCNTs on the variation of DOC in tap water collected after 5 days incubation.

Batch reactor	DOC before adsorption (mg/L)	DOC after adsorption (mg/L)	BDOC (mg/L)	Batch reactor efficiency (%)
REACTOR B ₁	4.26	4.26	0	0

REACTOR B ₂	4.46	4.80	0.34	7.6
------------------------	------	------	------	-----

Figure 6.5 presents the variation of DOC concentration during adsorption process using CTAB-functionalized MWCNTs as adsorbent.

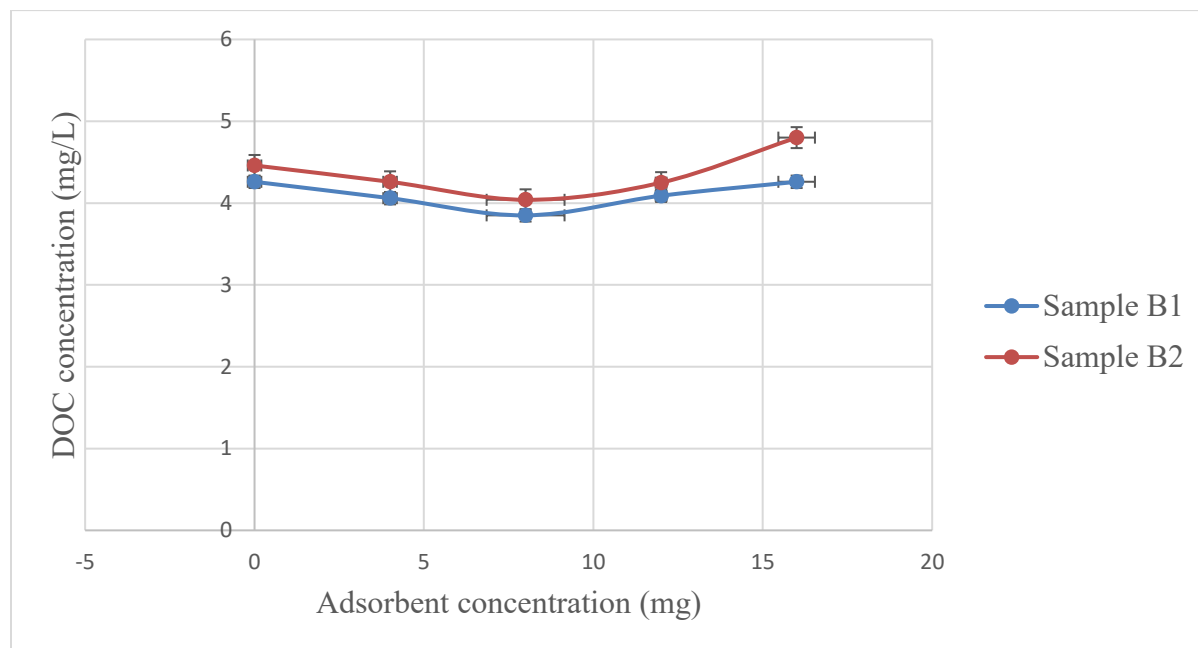


Figure 6.5: Variation of DOC concentrations during adsorption process using functionalised MWCNTs as adsorbent (Initial DOC concentrations = 4, 26 and 4, 46 mg/L for B1 and B2 respectively, agitation speed = 180 rpm, and adsorbent concentrations = 4, 8, 12, and 16 mg)

Figure 6.5 and tables 6.1, 6.2, 6.3, and 6.4 show the variation in DOC concentrations obtained after the adsorption process with CTAB-functionalized MWCNTs. It has been found that in water sample B, DOC concentration decreases with increasing functionalized MWCNTs. However, the DOC concentration in water sample B tended to flatten after the adsorption process performed with concentrations of 8 and 12 mg of CTAB-functionalized MWCNTs, before increasing to a significant level. This behavior may be a result of MWCNT aggregation brought on by strong electrostatic Van der Waals forces. Whenever the solution's MWCNT density is high [18, 20]. The highest drop in DOC concentration was obtained after the adsorption process with 8 mg of CTAB-functionalized MWCNTs. After using the TOC analyzer for DOC analysis, it has been found that DOC has dropped from 4.26 to 3.85 mg/L and from 4.46 to 4.04 mg/L for samples B₁ and B₂ respectively, with the addition of 8 mg of CTAB-functionalized MWCNTs that acted as adsorbent

during the adsorption process. Observations could also show a change in tap water colour after the adsorption process, especially for 12 mg of CTAB-functionalized MWCNTs. Figure 6.6 presents the variation in BDOC concentration during the adsorption process using different concentration of CTBA-functionalized MWCNTs as adsorbent.

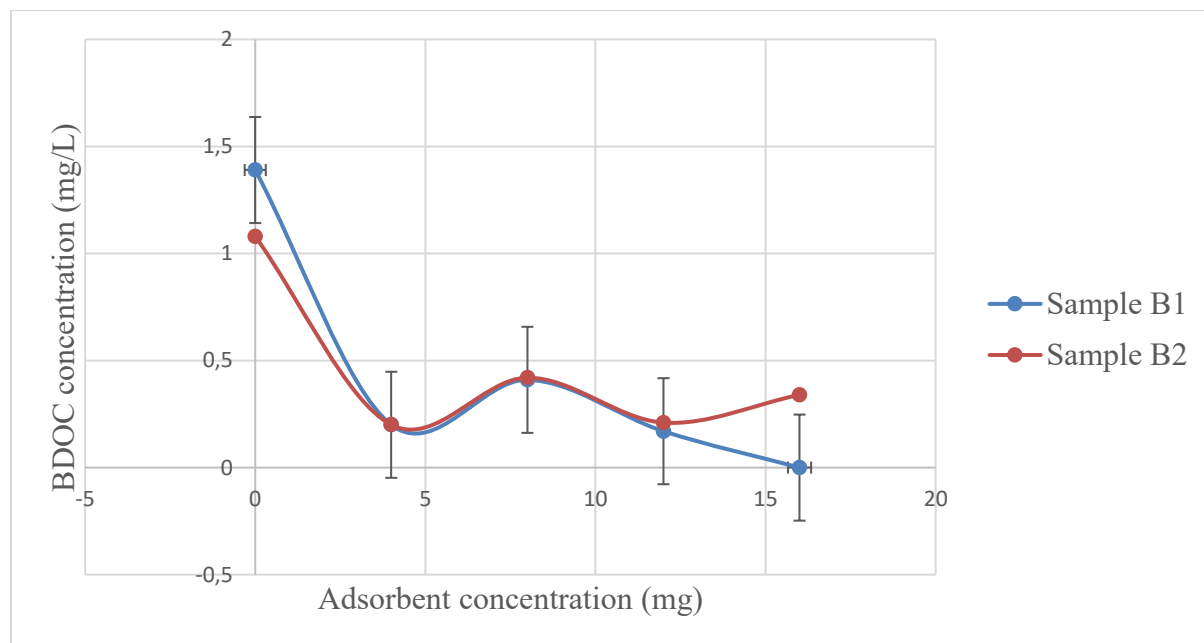


Figure 6.6: Variation of BDOC concentration during adsorption process using CTBA-functionalized MWCNTs as adsorbent (Initial BDOC concentrations = 1.08 and 1.39 mg/L for B₁ and B₂ respectively, agitation speed = 180 rpm, and adsorbent concentration = 4, 8, 12, and 16 mg)

Figure 6.6 illustrates the variation in BDOC concentration obtained after an adsorption process using different concentrations of CTAB-functionalized MWCNTs (4, 8, 12, and 16 mg). According to the BDOC data, batch adsorption removed approximately 30% of the initial BDOC. The variation of BDOC concentrations shown in Figure 6.6 also showed that after the adsorption process with 4 mg of CTAB-functionalized MWCNTs, the BDOC concentrations decreased significantly from 1.39 to 0.20 mg/L and from 1.08 to 0.20 mg/L for samples B₁ and B₂ respectively. It has also been observed that after the adsorption process with 8 mg functionalized MWCNTs, the BDOC concentrations of both water samples B₁ and B₂ increased to 0.41 and 0.42 mg/L respectively before they started decreasing to a lower level for the 16 mg functionalized MWCNTs adsorption process. However, this was a statistical decrease.

CNTs are superior sorbents for a variety of contaminants, according to earlier research [40, 43, 48]. The findings of this study have also shown a great deal of variability in BDOC changes via CTAB-functionalized MWCNT adsorption, as was already mentioned. With three data points, the adsorption process was more effective in demonstrating a reduction in BDOC. Furthermore, based on just one data point, it also indicated a decrease. Given that the initial BDOC concentration of water sample B in duplicate (B_1 and B_2) varied between 1.08 and 39 mg/L. These minor fluctuations could also be ascribed to the discrepancy in the quality of the untreated tap water and the effectiveness of the adsorption of DOC onto the CTAB-functionalized MWCNTs.

6.2.3 Adsorption isotherm models

The study focuses on the adsorption of the BOM onto the CTAB-functionalized MWCNTs using the Freundlich and Langmuir isotherm models. The Freundlich model provides an overview of the adsorption process, while the Langmuir model offers a different perspective. Understanding these models allows for a comprehensive analysis of the adsorption behavior [23, 24, 25]. AOC (as acetate C) is selected as the study parameter due to its easy conversion from g/L to $\mu\text{g/L}$ and the availability of experimental data. The relationships between the concentrations of the adsorbed AOC, referred to as adsorption isotherms in this study, also represent the AOC initial concentration in solution at the specified temperature [23, 24, 25].

As discussed earlier in this chapter, four different concentrations of CTAB-functionalized MWCNTs (4, 8, 12, and 16 mg) were added to 100 mL of strain P17 inoculated- ultrapure water (sample A) and tap water (sample B). Different solutions of ultrapure water and tap water samples both inoculated with strain P17 with initial concentration range of 48.8-53.6 $\mu\text{g/L}$ (as acetate C) for the AOC were prepared before the adsorption process. Factors influencing adsorption efficiency were investigated for an enhanced comprehension of the adsorption of AOC and DOC onto MWCNTs. The experiment involved stirring the solutions at 180 rpm for approximately 4 hours to achieve equilibrium. The amount of AOC and DOC adsorbed onto the MWCNTs at a given time (t) was computed using the mass balance relationship equation as follows:

$$A_t = C_0 - C_t \times \frac{V}{m} \quad (6.2)$$

Where A_t denotes the amount of BOM adsorbed onto MWCNTs (mg/g); C_0 denotes the initial concentration of NOM (mg/L) in the liquid phase; C_t denotes the concentration of BOM at time t (mg/L) in the liquid phase; V denotes the initial volume of the solution (L) and m denotes the mass of the MWCNTs (g) added to the solution. This equation considered the initial volume of the solution, the initial concentration of BOM in the liquid phase, the concentration of BOM at time t , and the mass of MWCNTs added to the solution. By analyzing these factors, the researchers aimed to gain insights into the efficiency of adsorption onto MWCNTs.

The characteristics of the adsorption mechanism were ascertained using Freundlich and Langmuir models, as was previously discussed. The Langmuir adsorption model, which assumes that the adsorbate forms a monolayer on the adsorbent surface, can be expressed using two equations. The non-linear expression (Equation 6.3) calculates the amount of BOM adsorbed per unit mass of MWCNTs at equilibrium, taking into account the maximum adsorption capacity and the Langmuir constant associated with the energy of adsorption. On the other hand, the linearized expression (Equation 6.4) relates the reciprocal of the adsorption quantity to the reciprocal of the concentration. These equations provide a quantitative understanding of the adsorption mechanism and allow for comparisons with other adsorption models.

$$A_e = \frac{A_m K_L C_e}{1 + K_L C_e} \quad (6.3) \quad \text{and} \quad \frac{1}{A_e} = \frac{1}{A_m} + \left(\frac{1}{K_L A_m} \right) \frac{1}{C_e} \quad (6.4)$$

Where A_e denotes the amount of BOM adsorbed per unit mass of MWCNTs at equilibrium (mg/g); A_m denotes the maximum amount of BOM adsorbed per unit mass of MWCNTs for the formation of a complete monolayer on the surface of MWCNTs (mg/g); and K_L denotes the Langmuir constant associated with the energy of adsorption (L/mg). The linear plot of $1/q_e$ versus $1/C_e$ could be applied to estimate the q_m and the Langmuir constant [26, 27]. The formation of multilayers can be considered as a component of the Freundlich isotherm, which is pertinent to reactions involving heterogeneous adsorption [26, 27]. Equation (6.5) or Equation (6.6) that has been linearized can be used to represent the Freundlich isotherm.

$$A_e = K_F C_e^{1/n} \quad (6.5)$$

$$\ln A_e = \ln K_F + 1/n \ln C_e \quad (6.6)$$

The Langmuir isotherm plot in Figure 6.7 allows for the application of Langmuir constants in the adsorption of AOC. The plot shows the relationship between $1/q_e$ and $1/C_e$, with the intercept and slope representing the Langmuir constants A_m and K_L , respectively. Comparing the Langmuir constants with Freundlich constants provides further insight into the adsorption process. Additionally, the coefficients of determination (R^2) for the Langmuir isotherms are listed in Table 6.6. When discussing Figure 6.7 and Figure 6.8, referencing the experimental data in Appendix F (Table F1) is important for a comprehensive analysis.

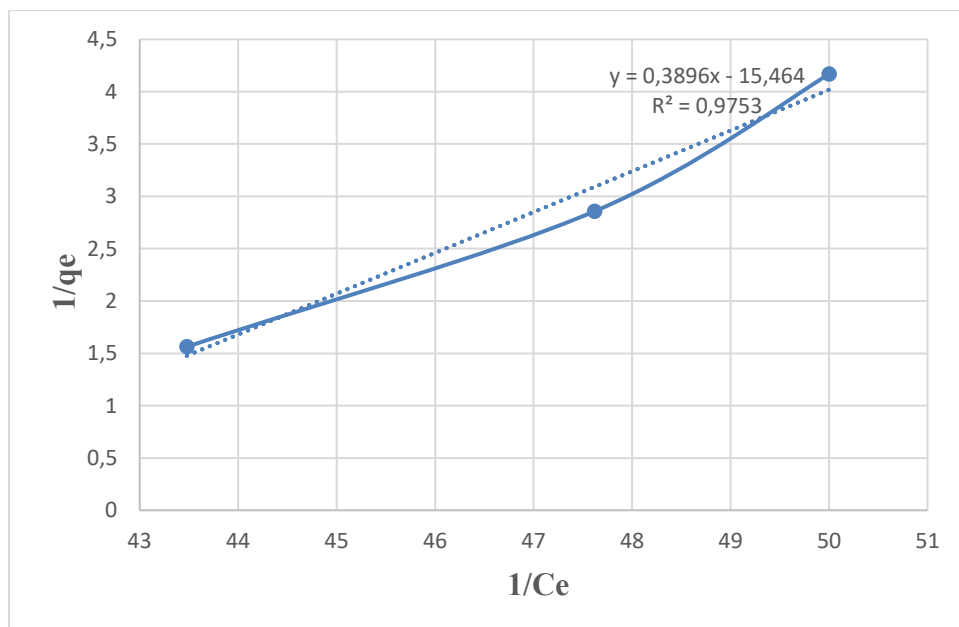


Figure 6.7: Illustration the adsorption of AOC onto CTAB-functionalized MWCNTs using the Langmuir isotherm plot.

Table 6.5: Langmuir isotherm parameters for the adsorption of AOC by CTAB-functionalised MWCNTs.

Slope	Intercept	q_m (mg/g)	K_L (L/mg)	R^2
0.3896	15.464	0.0646	39.7327	0.9753

Figure 6.8 shows the Freundlich isotherm plot for AOC adsorption onto CTAB-functionalised MWCNTs.

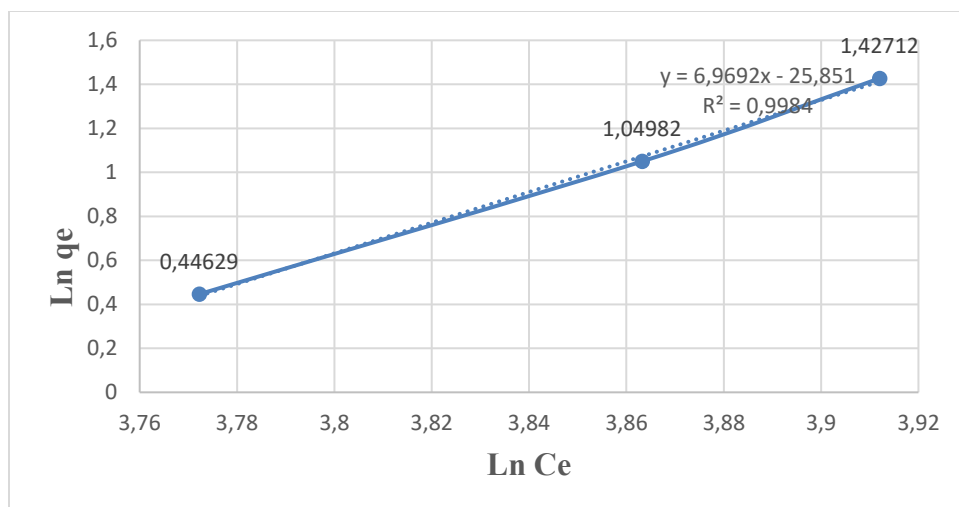


Figure 6.8: Illustration of AOC adsorption onto CTAB-functionalised MWCNTs using the Freundlich isotherm plot.

Table 6.6: Freundlich isotherm parameters for the adsorption of AOC by CTAB-functionalised MWCNTs.

Slope	Intercept	n	K_F (mg/L)	R^2
6.9692	28.851	0.1434	7.0958	0.9984

The importance of the R_2 value in assessing the goodness-of-fit to isotherm models cannot be overstated. In our study, the R_2 value served as a crucial measure of how well the experimental data aligned with the Freundlich and Langmuir models. The findings from Tables 6.5 and 6.6, as well as Figures 6.7 and 6.8, clearly demonstrated the superiority of the Freundlich model, as it exhibited a high R_2 value of 0.9984. This R_2 value demonstrates a strong connection between the model and the experimental data, suggesting a reliable fit. In contrast, the Langmuir model yielded a lower R_2 value of 0.9753, highlighting its lesser accuracy. This underscores the significance of the R_2 value in evaluating the performance and suitability of isotherm models for data analysis [28].

The application of BOM compounds and CTAB-functionalized MWCNTs in organic compounds is explored in this section. These compounds exhibit adsorption activity, which is determined applying the Langmuir and Freundlich isotherms in the heterogeneous adsorption process. Interactions between organic compounds and MWCNTs commonly involve heterogeneous

adsorption and adsorption on the surface. In heterogeneous systems, the Freundlich isotherm is frequently utilized, especially in the context of organic compounds and highly interactive species. This is particularly relevant in applications involving activated carbon and molecular sieves [31].

6.2.4 Kinetics Modelling

It has been found that the solute adsorbate removal rate is largely influenced by adsorption kinetics. It displays the adsorbent's adsorption effectiveness. Kinetics modelling performs an important part in water treatment field by providing valuable insights within the adsorption process. One of the conventional models is the pseudo-second-order model, which could be delineated by the Equation (6.7) as follows:

$$\frac{t}{qt} = \frac{1}{K_2 q_e^2} + \frac{t}{q_e} \quad (6.7)$$

In this equation, K_2 represents the equilibrium rate constant of the model, while q_e and q_t denote the amounts of adsorbent at equilibrium and at a specific time point, respectively. However, due to the limited supply of functionalized MWCNTs, the contact time had to be kept constant in all batch adsorption experiments. As a result, it was not possible to plot the graph depicting the experimental data with the pseudo-second-order model. Nonetheless, the insights gained from kinetics modelling contribute to the development of effective water treatment strategies [31, 32].

6.3 Membrane filtration process for the removal of biodegradable organic carbon

The immersion precipitation phase inversion method [32] was performed to synthesis the porous flat sheet PSF NF membranes that were used in this project. PSF filtration membrane is a thin film composite NF membrane with a 200 Da MWCO. The ideal operating pressure ranged from 2 to 10 bars. However, the PSF filtration membrane employed in this study was a flat sheet membrane operating at a constant pressure of 4.5 bars. This study made use of a crossflow filtration module that had a cell with a 45 cm² rectangular flat sheet active membrane area. The top inlet was used to supply the cell with feed water in this cell configuration. From the right side and bottom of the cell, respectively, the retentate and permeate were collected. As a result, it was impossible to determine the tangential flow velocity or define the flow pattern inside the cell. An individual pressure pump provided the feed flow. The membranes were stabilized for the first 30

minutes with distilled water before adjusting the flow rate. For this study, six distinct filtration tests were created. Flat sheet PSF membranes, a pressure force of 4.5 bars, a pH of 7.3, and a TDS concentration of 70 mg/L were the independent parameters used. After the batch adsorption, the water solutions A and B were collected to assess the PSF NF membranes' performance in removing the potential for bacterial growth (quantified as AOC and BDOC). MSP was chosen for this study since it is the most frequently used process to treat water, this is primarily ascribable to its high selectivity and efficiency, tiny pore sizes, minimal chemical use, simple scale-up, and minimal sludge production. Due to its small pore sizes, the NF membrane was chosen for this study among the MSP.

6.3.1 Impact of membrane filtration process on the removal of assimilable organic carbon from water

PSF filtration was used in this study to reduce the AOC concentration after the adsorption process. The adsorption process performed with CTAB-functionalized MWCNTs during the previous stage has removed a good fraction of AOC for both water samples A and B. However, a couple of colonies were still observed during the HPC of some dilutions of samples A and B after the batch adsorption process. Thus, membrane filtration was essential for the optimal removal of AOC in water, as NF membrane could be used to remove BOM fractions that could not be removed by adsorption. The relative AOC removal percentage was assessed for PSF membranes at a pH value of 7.3. Following the batch adsorption procedure, water solutions A and B had AOC concentrations of 20 µg/L as acetate-C and 25 µg/L as acetate-C, respectively.

Additionally, after the application of the NF membrane filtration procedure, it was discovered that AOC concentrations for water samples A and B at pH=7.3 dropped to 10 and 11 µg/L (as acetate C), respectively. It was determined that the rejection of AOC barely acceptable for both water solutions after the membrane filtration process. However, this was a removal rate of about 80% based on the quality of the influent into the nanofiltration process. Which makes it about double what is the removal efficiency of the NF membrane based on previous research by Sari et al. [49], Hen and Efraim [50], and Harma [51]. Since the size of AOC compounds, primarily acetate, was too large to pass through NF membranes, it is most likely that size exclusion is to blame for the rejection of AOC from water. Additionally, it has been found that charge repulsion between

the AOC components and the NF membranes may be one of the primary mechanisms by which AOC is removed by NF membranes. A polymeric filtration membrane could be employed for the treatment of drinking water after the adsorption process for the removal of AOC in water, according to the heterotrophic plate count results and AOC concentrations obtained after filtration tests of both water solutions A and B with the NF membrane filtration system. The heterotrophic plate count results show that despite the persistence of some colonies of strain P17 in both ultrapure and tap water after the adsorption process, the membrane filtration process has significantly reduced AOC concentrations in water. However, we recommend that future research assess the impact of solution hardness, ionic strength, and pH on the charge repulsion between the PSF filtration membranes and the AOC compounds.

6.3.2 Impact of membrane filtration process on dissolved organic carbon and biodegradable dissolved organic carbon concentrations

The PSF-NF filtration membrane was used in this study to reduce BDOC concentration to an acceptable range [33]. The adsorption processes performed with CTAB-functionalized MWCNTs during the previous stage removed a substantial fraction of BDOC from water sample B in duplicate (B₁ and B₂). However, BDOC concentrations were still high after adsorption process; therefore, it was necessary to use the MSP for optimal removal of BDOC from water, as the NF filtration membrane has the capacity to remove BOM fractions that cannot be removed by the adsorption process.

The measurement of water fluxes through polymeric membranes took 45 minutes at ambient temperature (25°C). as the optimal filtration time retained from the previous membrane filtration test, with the membrane filtration module set up at constant pressure (4.5 bars). After using the TOC analyzer for DOC analysis, it has been found that the DOC concentrations obtained after the NF membrane filtration process slightly decreased from 4.09 to 3.80 mg/L and from 4.25 to 4.06 mg/L for samples B₁ and B₂ as well, respectively. Therefore, the BDOC concentrations determined after membrane filtration were 0.29 and 0.17 mg/L for water solutions B₁ and B₂ respectively. This shows a removal percentage of BDOC in the range of 54% and 65 % for B₁ and B₂ respectively. On the other hand, Small, highly charged organic carbon compounds like acetate make up most AOC compounds. BDOC compounds are made up of larger, more heterogeneous organic

substances with a variety of sizes and charge characteristics, especially in natural water. Therefore, it was anticipated that the removal of BDOC compounds would be more difficult than the one for AOC compounds. However, in terms of AOC removal, we recommend that future studies also assess the influence of hardness, ionic strength, and pH on the size exclusion and charge repulsion between the NF membranes and the BDOC compounds for the BDOC removal.

6.3.3 Impact of filtration time on the effectiveness of the PSF filtration membrane

The influence of filtration time on the effectiveness of the membrane was assessed using water samples A and B. The membrane filtration module was set up at a constant pressure of 4.5 bars and the water fluxes were measured at ambient temperature (25°C) for various filtration times (15, 30, 60, 90, and 120 minutes). The flux variation over 4.5 bars of constant pressure is shown in Figure 6.9.

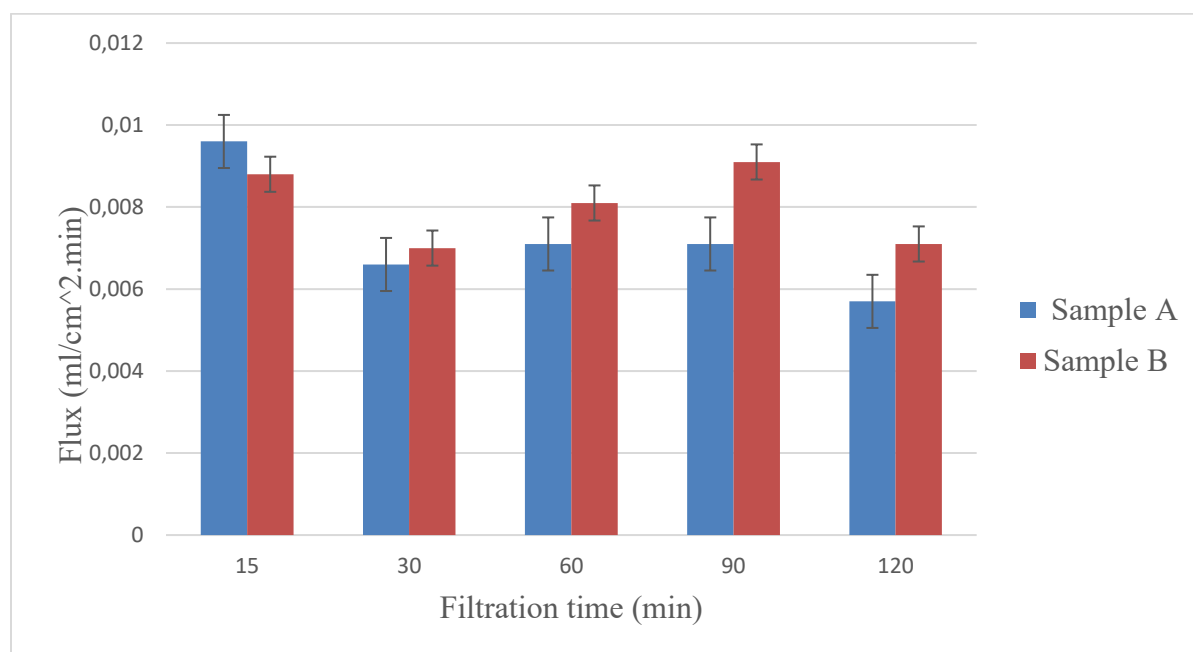


Figure 6.9: The change in flux over the course of filtration at 4.5 bar of constant pressure. The water flux collected after adsorption with 12 mg CTAB-functionalized MWCNTs was utilized for membrane permeation test.

The results showed that the permeate flux decreased over time during pure polymeric membrane fouling. Both water samples A and B exhibited appreciable flux for 90 minutes. However, the largest decrease in flux occurred after the first 120 minutes of filtration for both water samples A and B. This outcome highlights the significance of understanding the effect of filtration time on membrane effectiveness for the purpose of optimizing the filtration process. The spread of organic species on the surface of the membrane following the initial introduction of the solution can be blamed for this flux reduction [34]. Membrane fouling, specifically organic fouling, is a major concern in filtration processes as it causes a reduction in permeate flux [34]. This occurs due to the spread of organic materials on the surface of the membrane and within its pores, along with the formation of various organic species and surfactant monomers [35]. The permeate flux experiences a rapid decrease during the initial feed concentration, which could be attributed to the concentration polarization. This phenomenon involves the rapid deposition of organic species on the surface of the membrane, effectively blocking the pores. [35] Over time, the permeate flux gradually decreases, indicating the long-term negative impact of membrane fouling. Implications of concentration polarization and organic species deposition in membrane fouling can have significant effects on permeate flux in filtration processes. Concentration polarization refers to the rapid deposition of organic species on the surface of the membrane, leading to the blockage of membrane pores and a rapid decrease in permeate flux [34, 35]. This phenomenon occurs within the first 45 minutes of filtration with initial feed concentration. Additionally, the existence of surfactant monomers and other unknown factors contribute to the formation of pre-micelles and organic species, further exacerbating the fouling process. As a result, permeate flux remains constant and gradually decreases over time. These findings highlight the importance of determining the ideal filtration time, with 90 minutes being selected as the optimal duration for this research.

6.3.4 Depletion of heterotrophic plate count abundance dissolved organic carbon, and biodegradable dissolved organic carbon after using the hybrid adsorption-membrane filtration system.

The variations of HPC concern, DOC, and BDOC concentrations after using the hybrid adsorption-membrane filtration system is related firstly to the structure of MWCNTs that contain large

external surface area, fibrous shape, and large mesopores, which lead to a higher adsorption efficiency of BOM (AOC and BDOC). And secondly, the polymeric membrane contains mesopores which can capture BOM (AOC and BDOC) by charge repulsion, size exclusion, and hydrophobic interactions during the MSP. For the purpose of investigating on the effectualness of the hybrid adsorption-membrane filtration system to lower the bacterial growth potential of different water samples in this research, we have compared the concentrations of AOC, DOC, and BDOC before and after the hybrid adsorption-membrane filtration system. It appeared that the water samples collected from the sampling point had high BDOC concentrations. In addition, the initial ultrapure water and tap water inoculated with strain P17 had high AOC concentrations compared to the corresponding samples collected after the hybrid adsorption-membrane filtration processes. The discrepancy in the concentrations of AOC, DOC, and BDOC throughout the treatment process with the hybrid adsorption-membrane filtration system were clearly defined after the membrane filtration process. It has been found that DOC concentration dropped from 4.26-4.46 mg/L to 4.09-3.80 mg/L. BDOC concentrations dropped from 0.41 mg/L to 0.17 mg/L (for water sample A) and from 0.42 mg/L to 0.19 mg/L (for water sample B), and the AOC concentrations dropped from a range of 48.8-53.6 $\mu\text{g C/L}$ as acetate-C to a range of 11.7-10.7 $\mu\text{g C/L}$ as acetate-C. This variation in concentrations after hybrid adsorption-membrane filtration system technology may have been due to BOM removal.

Overall, A few studies have demonstrated that BOM in terms of BDOC in drinking water can be successfully removed using pre-treatment NF, UF, or MF membrane hybrid systems. The AOC values for the influent and permeate were said to not significantly differ from one another, though. In order to reduce the amount NOM from drinking water, this investigation showed the benefits of combining the adsorption process with CTAB-functionalized CNTs and the membrane filtration process with NF membranes. As a pre-treatment for NF filtration, the adsorption process had a favourable outcome. A reduced tendency for membrane fouling was evident in the pre-treated feed. The ideal adsorption condition was 12 mg doses of CTAB-functionalized CNTs, and the NF membrane module's optimum pressure was 4.5 bar, and its permeability value was 0.0091 mL/min. In terms of BDOC and AOC, the BOM removal rate was 65% and 80%, respectively. According to the results, a hybrid system can treat BOM compounds that are otherwise challenging to handle.

6.3.5 Comparative study between assimilable organic carbon and biodegradable dissolved organic carbon

The Range of AOC to BDOC ratios in treated water is an important aspect of assessing the biological stability of finished water [40]. In this study, it was found that the AOC values in finished water are quite low, ranging from 0.1% to 1% of the DOC concentration in river water. Conversely, the BDOC values in water treatment can significantly influence the DOC concentration, with values ranging from 19% to 54% [40, 41]. Furthermore, the concentrations of AOC and BDOC showed a clear relationship, indicating their interdependence. However, the extensive range of AOC to BDOC ratios resulted in relatively low correlation coefficients. In treated water, the AOC concentration was found to range between 5% and 10% of the BDOC concentration. This information suggests that the biostability of biodegradable organic compounds in water can vary greatly, highlighting the complexity of assessing and maintaining biological stability in finished water.

Prevention of multiplication in treated water is a crucial aspect of ensuring the safety and stability of water systems. The usage of an adjusted microbial community in the AOC test and the utilization of biomass in the BDOC test contribute to the differences between AOC and BDOC concentrations in microbial communities [40, 41]. Biomass production is a significant factor in the AOC test, as it provides valuable insight into the microbial community. On the other hand, BDOC concentrations between 0.1 and 0.2 mg/L serve as a benchmark for biostability in various studies [40, 41, 42]. To prevent multiplication in treated water, it is recommended to maintain the concentration of easily biodegradable compounds below 1 µg of C/L of acetate-C [41, 42]. Understanding these differences and adhering to prevention measures is critical for maintaining the quality of treated water systems. Conversely, it is not requisite to achieve total cytotoxicity, and it cannot be done. The objective is to restrict microbial growth to the point where water quality does not deteriorate. It can be difficult to define a suitable growth rate because it may vary depending on the system and season [40, 41, 42].

6.3.6 Impacts of forward flushing and backwashing on permeate flux .

A key parameter is the amount of time that must pass between two successive filtration cycles [43]. Figure 6.9 demonstrates that after 45 minutes of filtration, permeate flux initially decreased rapidly before tending to stabilize. The filtration period should therefore be set at 45 minutes, and the cleaning cycle should be 10 minutes, to reduce operating costs. The importance of sufficient forward flushing time for complete flushing is highlighted in this section. Figure 6.9 demonstrates that the flushing effect of polymeric membranes improves with longer flushing time. As the experiment progressed, the permeate flux gradually decreased until it stabilized. This reduction in flux could be likely due to the foulant deposition and concentration polarization on the membrane surface [44, 45]. It was found that if the time allotted for forward flushing is insufficient, complete flushing and removal of foulant deposition cannot be achieved. Therefore, it is suggested that a minimum forward flushing time of 60 seconds is preferred to ensure optimal energy and water savings [45]. These case studies provide valuable insights into the practical application and outcomes of various cleaning methods. Through these case studies, we will explore the effectiveness of forward flushing and backwashing in removing fouling from membranes [46]. Additionally, we examined the impact of convective transport prevention on fouling and the mechanism of lifting off and suspending foulants during backwashing. These case studies offer valuable evidence-based information that can help in the choice and implementation of the most suitable cleaning technique for specific membrane fouling situations [46].

Table 6.7: Concentration of water sample A, quality parameters obtained after hybrid treatment system.

Parameter	Unit	Average concentration
pH	-	3.3
Temperature	°C	19.9
Conductivity	µs/cm	0
Total dissolved solids (TDS)	mg/L	0
Ammonium ions (NH ₄ ⁺)	FAU	0.04
Dissolved oxygen (DO)	mg/L	6.09
Alkalinity as CaCO ₃	mg/L	144

Free chlorine	mg/L	0.01
Nitrate (NO ₃)	mg/L	4.8

Table 6.8: Concentration of water sample B quality parameters obtained after hybrid system.

Parameters	Unit	Concentration
pH	-	7.4
Temperature	°C	19.5
Conductivity	µs/cm	170
TDS	mg/L	80
Turbidity	FAU	< 1
DO	mg/L	5.1
Alkalinity	mg/L	-
Free chlorine	mg/L	0.075

Tables 6.7 and 6.8 present the concentrations of different water quality parameters obtained after a hybrid adsorption-membrane filtration system. Some small variations in water quality parameter concentrations were observed after the use of a hybrid adsorption-membrane filtration system. However, significant changes were observed in conductivity and nitrate concentration after the hybrid adsorption-membrane filtration system. The initial ultrapure water solution (sample A) used for AOC determination had concentrations of 4, 21.5 °C, 454 mg/l, 144 mg/l, 0.05 mg/l, < 4.4 mg/l, 0.01 mg/l of pH, temperature, DO, alkalinity, Ammonium ions (NH₄⁺), Nitrate and free chlorine, respectively. After the use of the hybrid adsorption-membrane filtration system, it has been found that the pH increased from 4 to 3.3, the DO increased from 4.54 mg/l to 6.09 mg/l, the alkalinity increased from 144 mg/l to 165 mg/l, the ammonium increased from 0.05 mg/l to 0.04 mg/l, nitrate increased from < 4.44 mg/l to 5.1 mg/l, and free chlorine remained intact. The initial tap water solution (sample B) used for BDOC determination had concentrations of 7.3, 19.5 °C, 160 µs/cm, 70 TDS, 106 FAU, 5.41 mg/l, 23 mg/l and 0.14 mg/l of pH, temperature, conductivity, TDS, turbidity, DO, alkalinity, and free chlorine, respectively.

Overall, after the use of the hybrid adsorption-membrane filtration system, it was found that the dissolved oxygen dropped from 5.41 mg/l to 5.1 mg/l, the conductivity increased from 160 $\mu\text{s}/\text{cm}$ to 170 $\mu\text{s}/\text{cm}$, the pH increased from 7.3 to 7.4, the turbidity dropped from 106 FAU to 0 FAU, the total dissolved solids increased from 70 mg/l to 80 mg/l, the free chlorine dropped from 0.14 to 0.075 mg/l and the temperature remained intact. The small variations observed after the use of hybrid adsorption-membrane filtration system technology may have been an outcome of the removal of organic matter.

6.4 Summary

Research on CNTs and NF membranes has enabled new approaches and applications in the fields of materials science, water quality engineering, and water treatment. According to the findings, AOC and BDOC can be removed from drinking water using both MWCNTs and NF membranes. Previous studies related to the removal of BOM from water showed that the standalone NF membrane filtration rejected BDOC. The type of membrane filtration used, however, affected how much (insignificantly) AOC were rejected [39, 40, 43, 47, 48]. Nevertheless, this study was able to show that adsorption in conjunction with NF membranes can successfully remove both AOC and BDOC from drinking water. Therefore, by applying CTAB-functionalized MWCNTs to drinking water treatment, BOM can be absorbed. This is mostly likely due to CNTs' large external surface area, fibrous shape, large mesopores, and a less negative charge surface. This leads to a higher adsorption and removal efficiency of BOM (AOC and BDOC). The remaining BOM can be removed through the NF membrane. This results from mesopores that capture NOM (AOC and BDOC) by size exclusion, charge repulsion, and hydrophobic interactions during membrane filtration. This will reduce bacterial regrowth within the DWDSs. It will reduce the cost of water treatment and operational problems during the production of biologically stable water.

In this chapter, we summarize the findings regarding the absorption of BOM onto functionalized MWCNTs. The process of functionalizing MWCNTs with CTAB is described, highlighting the importance of achieving stable dispersion and hydrophilic properties. The efficiency of adsorption of BOM from drinking water is examined, showcasing the potential for using functionalized MWCNTs in water treatment. These findings highlight the significance of non-covalent functionalization of MWCNTs and the application of the Freundlich isotherm in understanding

this adsorption process. Further research on MWCNTs for enhanced water treatment processes focuses on exploring the potential applications and future directions in the field. One potential application is the expansion of MWCNTs and NF membranes in materials science, where they can be utilized for various purposes. Additionally, advancements in water quality engineering can be achieved through the continued investigation of MWCNTs and NF membranes. These materials have shown promise in the successful eradication of AOC and BDOC from drinking water, indicating potential for further research and development. By understanding the components that assist the effectiveness of MWCNTs in the water treatment sector, researchers can optimize their application and improve water treatment processes. Overall, further research on MWCNTs holds the prospects to transform the field of water treatment and provide more efficient and effective methods for ensuring water quality.

6.5 References

- [1] Tom, B., Enea, H.G., Simon, A.P., (2019). A critical review of trihalomethane and haloacetic acid formation from natural organic matter surrogates. *Environmental technology reviews* 1, 93-113.
- [2] Surbhi, T., Bham, P.V., (2018). Natural organic matter as precursor to disinfection byproducts and its removal using conventional and advanced processes, state of the art review. *Journal of water health* 16, 681-703.
- [3] Don, D.R., Malcolm, J.B., Michael, K.J., (2009). Chapter 2-Disinfection of water. *Water supply* 6, 425-461.
- [4] Nomba, M.N.B., Kfir, R., Venter, S.N., Cloete, T.E., (2000). An overview of biofilm formation in distribution systems and its impact on the deterioration of water quality. *Water SA* 26 (1), 0378-4738.
- [5] Amit, B., Mika, S., (2017). A review-Removal of natural organic matter (NOM) and its constituents from water by adsorption. *Journal of chemosphere* 66, 497-510.
- [6] Lesley, J., Joseph, R.V.F., Yong, G.P., Mohammed, B., Hazem, S., Yeomin, Y., (2012). Removal of natural organic matter from potential drinking water sources by combined coagulation and adsorption using carbon nanomaterials. *Separation and purification technology* 95, 64-72.

- [7] Peng, X., Li, Y., Luan, Z. Di, Z., Wang, H., Tian B., Jia, Z., (2003). Adsorption of 1, 2-dichlorobenzene from water to carbon nanotubes, *Chem. Phys. Lett.* 376, 154–158.
- [8] Li, Y.H., Wang, S., Luan, Z., Ding, J., Xu, C., Wu, D., (2003). Adsorption of cadmium (II) from aqueous solution by surface oxidized carbon nanotubes, *Carbon* 41, 1057–1062.
- [9] Li, Y.H., Wang, S., Zhang, X. Wei, J., Xu, C., Luan, Z., Wu, D., (2003). Adsorption of fluoride from water by aligned carbon nanotubes, *Mater. Res. Bull.* 38, 469–476.
- [10] Lu, C., Liu, C., (2006). Removal of nickel (II) from aqueous solution by carbon nanotubes, *J. Chem. Technol. Biotechnol.* 81, 1932–1940.
- [11] Lu, C., Chung Y.L., Chang, K.F., (2005). Adsorption of trihalomethanes from water with carbon nanotubes, *Water Res.* 39, 1183–1189.
- [12] Lu, C., Chiu, H., (2006). Adsorption of zinc (II) from water with purified carbon nanotubes, *Chem. Eng. Sci.* 61, 1138–1145.
- [13] Long R.Q., Yang, R.T., (2001). Carbon nanotubes as superior sorbent for dioxin removal, *J. Am. Chem. Soc.* 123, 2058–2059.
- [14] Agnihotri, S., Rood M.J., Rostam-Abadi, M., (2005). Adsorption equilibrium of organic vapors on single-walled carbon nanotubes, *Carbon* 43, 2379–2388.
- [15] Li, Y.H., Wang, S., Wei, J., Zhang, X., Xu, C., Luan, D. Wu, B. Wei, B., (2002). Lead adsorption on carbon nanotubes, *Chem. Phys. Lett.* 357, 263–266.
- [16] Rao, G.P., Lu, C., Su, F., (2007). Adsorption of divalent heavy metal ions from aqueous solutions by carbon nanotubes: a review, *Sep. Purif. Technol.* 58, 224–231.
- [17] Lu, C., Su, F., (2007). Adsorption of natural organic matter by carbon nanotubes. *Separation purification technology* 58, 113-121.
- [18] Saleh, N.B., Pfefferle, L.D., Elimelech, M., (2008). Aggregation kinetics of multiwalled carbon nanotubes in aquatic systems: Measurements and environmental implications. *Environmental science technology* 42, 7963-9.

- [19] Niu, J.J., Wang, J.N., Jiang, Y., Su, L.F., Ma, J., (2007). An approach to carbon nanotubes with high surface area and large pore volume. *Microporous mesoporous matter* 100, 1-5.
- [20] Zhbanov, A.I., Pogorilov, E.G., Chang, Y.C., (2010). Van der waals interaction between two crossed carbon nanotubes. *ACS Nano* 4(10), 5937-45.
- [21] Schreiber, B., Brinkmann, T., Schmalz, V., Worch, E., (2005). Adsorption of dissolved organic matter onto activated carbon-the influence of temperature, adsorption, wavelength, and molecular size. *Water research* 39, 3449-56.
- [22] Wei, L.S., Jing, X., Si, L., Fang, S., (2012). Effect of natural organic matter (NOM) on Cu (II) adsorption by multi-walled carbon nanotubes: Relationship with NOM properties. *Journal of Chemical Engineering* 200-202, 627-636.
- [23] Wachsstock, D.H., Pollard, T.D., (1994). Biophysical principles-Van der Waals interactions. *Cell biology* 3, 1260-1273.
- [24] Noble, R., Terry, P., (2004). Adsorption: In principles of chemical separation with environmental applications, *Journal of Cambridge series in Chemical Engineering*, 182-213.
- [25] Auguste, R., (1911). Chapter 7: Adsorption, Principles of Chemical Separation with Environmental Applications. Handbook.
- [26] Toor, M., Jin, B., (2012). Adsorption characteristics, isotherm, kinetics, and diffusion of modified natural bentonite for removing diazo dye. *Chemical Engineering Journal* 187, 79-88.
- [27] Annadurai, G., Ling, L. Y., Lee, J. F., (2008). Adsorption of reactive dye from an aqueous solution by chitosan: isotherm, kinetic and thermodynamic analysis. *Journal of Hazardous Materials* 152, 337-346.
- [28] El-Ashtoukhy, E. S. Z., Amin, N. K., Abdelwahab, O., (2008). Removal of lead (II) and copper (II) from aqueous solution using pomegranate peel as a new adsorbent. *Desalination* 223 (1-3), 162-173.
- [29] Pan, B., Xing, B., (2008). Adsorption mechanisms of organic chemicals on carbon nanotubes. *Environmental Science and Technology* 42 (24), 9005-9013.

- [30] Ren, X., Chen, C., Nagatsu, M., Wang, X., (2011). Carbon nanotubes as adsorbents in environmental pollution management: A review. *Chemical Engineering Journal* 170, 395-410.
- [31] Ng, J.C.Y., Cheung, W.H., McKay, G., (2003). Equilibrium studies for the sorption of lead from effluents using chitosan. *Chemosphere* 52, 1021-1030.
- [32] Anjalin, F.M., (2014) Synthesis and characterization of MWCNTs/PVDF nanocomposite and its electrical studies. *Der PharmaChemica* 6: 354-359.
- [33] Jianying, S., Markus, Flury, James, B., Richard, L., (2008). Comparison of different methods to measure contact angles of soil colloids. *Journal of colloid and interface science*, 328,299-307.
- [34] Zhao, Y., Wu, K., Wang, Z., Zhao, L., Li S., (2000). Fouling and cleaning of membrane. *Journal of Environmental Sciences*.12, 241-251.
- [35] Vinder, A., Simonic, M., Novak Z., (2014). Influence of surfactants on the removal of AOX using micellar-enhanced ultrafiltration. *Journal of Membrane Research*. 1, 205-212.
- [36] Persson, K., Milson, J., (1991). Fouling resistance models in MF and UF. *Desalination*, 80, 123.
- [37] Sibille, I., Mathieu, L., Paquin, J., Gatel, D., Block, J., (1997). Microbial characteristics of a distribution system fed with nanofiltered drinking water, *Journal of Water Research* 31, 2318–2326.
- [38] Noble, P.A., Clark, D.L., Olson, B.H., (1996). Biological stability of groundwater, *Journal of American Water Works Associations* 88, 87–96.
- [39] Isabel, C.E., Seungkwan, H., Andrew, A.R., (2000). Removal of assimilable organic carbon and biodegradable dissolved organic carbon by reverse osmosis and nanofiltration membranes. *Journal of Membrane Science* 175, 1-17.
- [40] Volk, C.J., Lechevallier, M.W., (2000). Assessing biodegradable organic matter. *Journal of American Water Works Associations* 92(5), 64-76.
- [41] Servais, P., Laurent, P., Random, G., (1993). Impact of biodegradable dissolved organic carbon (BDOC) on bacterial dynamics in distribution systems. *Proceedings American Water*

Works Association Water Quality Technology Conference, American Water Works Association, 963-980.

[42] Servais, P., Laurent, P., Billen, G., Gatel, D., (1995). Development of a model of BDOC and bacterial biomass fluctuations in distribution systems. *Revue des sciences de l'Eau* 8, 427-462.

[43] Ning, M., jing, X., Dequiag, C., Xi, S., (2015). Comparison of filtration performances between membrane and non-membrane filters. *International symposium on computers and informatics (ISCI 2015)*.

[44] Zhao, Y., Wu, K., Wang, Z., Zhao, L., Li, S., (2000). Fouling and cleaning of membrane. *Journal of Environmental Sciences* 12, 241-251.

[45] Vinder, A., Simonic, M., Novak, Z., (2014). Influence of surfactants on the removal of AOX using micellar – enhanced ultrafiltration. *Journal of Membrane Research* 1, 205-212.

[46] Jinhui, H., Liuxia, L., Guangming, Z., (2014). Influence feed concentration and transmembrane pressure on membrane fouling and effect of hydraulic flushing on the performance of ultrafiltration. *Desalination* 335, 1-8.

[47] Mohammed, A.Z., Laleh, R.K., (2017). Removal of precursors and disinfection by products (DBPs) by membrane filtration from water; a review, *Journal of Environmental Health science and Engineering* DOI 10.1186.

[48] Elma, E., Pratiwi, A.E., Rahma, A., Rampun, E.L.A., Mahmud, M., Bilad, M.R., (2021). Combination of coagulation, adsorption, and ultrafiltration processes for organic matter removal from peat water, *Journal of sustainability*, 14, 370.

[49] Sari, M., Mika, S., Amit, B., Mika, M., (2019). Natural organic matter removal from drinking water by membrane technology. *Academic journal*. 2, 13-22.

[50] Hen, L.J., and Efrainsen, H., (2001). Assimilable organic carbon in molecular weight fractions of natural organic matter. *Water research*. 35, 1100-1410.

[51] Harma, V., Tuloksia suomalaisilla pintaves ilia toksilla tehdyista nanosuodatuskokeista vestitalones, 6 (1999) 5-10.

CHAPTER SEVEN: CONCLUSIONS AND RECOMMENDATIONS

7.1 Conclusions

The research was designed to develop a hybrid adsorption-membrane filtration system to produce biologically stable drinking water. The purpose was to combine the adsorption process with membrane filtration based on the multi-barrier approach, as a better alternative to mitigate the issue of membrane fouling and to lead to higher operational efficiency and performance of the filtration membrane.

7.1.1 Introduction

Effectively managing BOM in drinking water treatment is of utmost importance due to the significant impact it has on water quality. As already stated, the presence of BOM can lead to fouling issues, which can decrease the performance and longevity of membranes used in treatment processes. Additionally, the cost implications of using adsorbents, coagulants, oxidants, and disinfectants to remove BOM can be substantial. These challenges make it necessary to optimize the selection of treatment chemicals and enhance membrane performance. Innovative techniques must also be developed to mitigate fouling issues. By addressing these challenges, the production of biologically stable drinking water can be achieved at a lower cost, ensuring the provision of safe and high-quality water to consumers. The capacity of the membrane filtration system was tested to evaluate its effectiveness in removing BOM from drinking water. The study utilized the BDOC and AOC protocols to measure bacterial growth in water collected from targeted sources. These protocols were validated to ensure accurate results. Flat sheet membranes were prepared using the phase inversion method, and the nanostructured materials were characterized using microscopy techniques. The water was then pretreated through an adsorption process of BOM, focusing on both AOC and BDOC. Finally, the membrane filtration system was tested to determine its ability to effectively remove BOM from the pre-treated raw water. This research aimed to explore the potential of a hybrid treatment system in removing NOM from drinking water systems.

7.1.2 Mathematical modeling of the membrane filtration process

A mathematical model was developed for membrane filtration in continuous systems of complete mixing liquid media (CMLMs) in this study. The idea consisted of constructing a theory on the

membrane filtration process by applying the equations of motion. The complete mixing flow system (CMFS) was also considered to develop mathematical models in this study. It has been found that despite the availability of the above-mentioned procedures of determination of the membrane filtration processes, researchers are still struggling to construct the proper mathematical models that can describe properly the membrane filtration scenario. This is due to the fact that some parameters are still unfixed (unresolved), for example, the maximum achievable concentration after a filtration process, the correlations between the main processing variables and the processing results and the control of parameters for dynamic (non-steady state) processes [3,4]. Therefore, in this study, a mathematical model of the membrane filtration process in a continuous system was also developed to better understand the correlations between the different variables of the membrane filtration process such as the inlet concentration and flow rate, outlet concentration and flow rate, and permeate concentration, we can optimize the separation process. The mathematical model developed in this study reveals that changes in initial conditions have a significant impact on the transient response of the system. Moreover, the membrane models derived from the mathematical model can be utilized to calculate crucial system design parameters. Ultimately, this knowledge can guide the selection of membrane properties and initial conditions for achieving the most effective separation process. This study provided adequate information on the design and application of membrane system technology to produce biologically stable water.

7.1.3 Characterization of carbon nanotubes, polymeric membranes; and assimilable organic carbon and biodegradable dissolved organic carbon determination

Adsorption and MSP technologies, especially with the use of MWCNTs and polymeric NF membrane have gained the attention of many researchers in the drinking water treatment sector; however, its implementation is still at the pilot scale stage due to certain inconveniences, which include adsorbent degradation, cost, high energy requirement for regeneration, etc.

In this study, the characterization of both MWCNTs and PSF membranes showed some interesting features that can be utilized to remove BOM compounds from water. For example, morphological and structural studies show that MWCNTs possess fibrous shapes with a high aspect ratio, and a hollow structure with an inner diameter. The finger-like structures found on the surfaces of PSF

membranes play a crucial role in their adsorption capabilities. These structures, which vary in pore size, contribute to the overall capacity of the membranes to absorb BOM from water. The introduction of functional groups on the surface of MWCNTs further enhances the adsorption process by providing multiple chemical sites for charge neutralization. To fully understand the adsorption mechanism, it is important to characterize both the surface and cross-section of the PSF membranes. This characterization reveals the presence of finger-like structures and highlights the variation in pore sizes within the membranes. By studying these features, we can gain valuable insights into the relationship between capacity and the structural and functional properties of membranes. The contact angle and mechanical analyses demonstrated that the pure PSF membranes have an acceptable degree of hydrophilicity and tensile strength. This can be exploited during the membrane filtration process.

Nanostructured materials have shown promising effectiveness in removing BOM from drinking water systems. The results obtained from the characterization of MWCNTs and PSF membranes highlight the structural and functional properties that make these materials suitable for BOM removal. Specifically, the use of CTAB as a cationic surfactant has been found to enhance the dispersibility of MWCNTs during the batch adsorption process. This interaction between CTAB and MWCNTs contributes to the overall effectiveness of the nanostructured materials in removing NOM. However, the application of these materials in drinking water systems still presents some challenges that need to be addressed to fully exploit their potential. Prospects include finding innovative solutions to overcome these challenges and further improving the utilization of nanostructured materials for BOM removal. Based on a comparison of a few existing studies that addressed the covalent functionalization of MWCNTs. As a result of the CTAB-functionalization of MWCNTs in this study, the required capabilities of MWCNFs for BOM capture enhancement and environmental safety were preserved. Furthermore, the analysis of the results reveals that both AOC and BDOC protocols were successfully established and validated in measuring bacterial growth in water from the targeted sources. This provides valuable information for assessing the biological stability of water samples and ensuring the safety of drinking water sources.

7.1.4 Adsorption and membrane filtration processes for assimilable organic carbon and biodegradable dissolved organic carbon removal

The implications for water treatment in relation to the removal of BOM are significant. The presence of BOM in the DWDs can lead to the formation of DBPs, loss of biological stability, and biofilm formation. These issues not only increase the cost of water treatment but also result in operational problems. The adsorption process, which involves charge neutralization, is a well-known and widely used technique in the water industry for the removal of BOM. In chapter 6, the efficacy of CTAB-functionalized MWCNTs in the batch adsorption process was evaluated through a series of experiments. These findings have important implications for the improvement of water treatment processes and can guide future research directions.

Several studies have highlighted the application of PAC in the adsorbent-NF membrane hybrid system. However, the bonding between BOM and PAC has led to the formation of BOM-PAC particles that contribute to fouling of the membrane filtration. To address these challenges, it is crucial to apply appropriate water treatment methodologies. Therefore, in this study, an extensive adsorption process (with CTAB-functionalized MWCNTs) of drinking water was applied before membrane filtration tests to avoid membrane fouling, protect the membrane, and improve the membrane performances for the optimal removal of both AOC and BDOC in drinking water. Unlike activated carbon, which relies on its strength for adsorption properties, MWCNTs' adsorption process is influenced by the accessibility of surface area. This means that high molecular weight compounds of BOM can be absorbed effectively. Additionally, the chemical composition of BOM and the physical properties of CTAB-functionalized MWCNTs play a crucial role in adsorption efficiency. These potential advantages highlight the promising implications of using CTAB-functionalized MWCNTs in water treatment for BOM removal. However, challenges and limitations of this adsorption process must be addressed, and future research directions should focus on improving BOM removal technology. However, the adsorption removal efficiencies of LMW compounds of BOM, AOC are higher on MWCNTs than on activated carbon adsorbents. The superior adsorption capacities of CTAB-functionalized MWCNTs may also be explained by the presence of large mesopores, and the less negative surface charge of these MWCNTs that facilitates the charge neutralization mechanism, further contributing to their superior adsorption capacities. These findings have important practical applications in water treatment and purification

processes. Further investigations are required to optimize the use of CTAB-functionalized MWCNTs, which could have significant implications for improving water purification technologies in the future.

The findings have shown that CTAB-functionalized MWCNTs have high adsorption capacities during the batch adsorption process, thus confirming that CTAB-functionalized MWCNTs possess basic functional groups on the surface. These basic sites play a significant role in adsorbing NOM from drinking water. Moreover, the interaction between CTAB as a cationic surfactant and MWCNTs enhances the dispersibility and hydrophilic properties of the adsorbents. It has been found that charge neutralization is the primary mechanism responsible for BOM adsorption by CTAB-functionalized MWCNTs. This mechanism is enabled by the introduction of the necessary functional properties during CTAB-functionalization, which enhances the capture of BOM and ensures environmental safety.

The performance testing of the NF PSF membrane included an examination of its overall impact on membrane permeability. After 90 minutes, a significant increase in water flux was observed, indicating improved permeability. This increase can be attributed to the presence of pores on the membrane surface and the lack of fouling inside these pores. The extensive pre-treatment process, which involved CTAB-functionalization, as well as the forward flushing and backwashing processes, played a vital role in preventing fouling and maintaining high permeability. These findings highlight the effectiveness of the NF PSF membrane in enhancing water flux and maintaining optimal membrane permeability. The rejection mechanisms involved size exclusion, charge repulsion, and hydrophobic interactions. These findings highlight the potential application of the hybrid adsorption-membrane filtration system in drinking water treatment.

Previous studies have reported the success of utilizing membrane filtration in removing BOM in water. However, the rejection rate of AOC depends on the membrane material and solution medium. The hybrid adsorption-membrane filtration system discussed in this study has a significant impact on water quality engineering. By combining the adsorption process with membrane filtration, this system effectively removes BOM from drinking water. The system addresses the issue of fouling that commonly occurs during membrane filtration, leading to reduced operation costs. The study evaluates the performance of the system through experimental setup, measuring the removal efficiency of BOM and analyzing fouling reduction. The findings

provide important insights for further research and improvement in this area. By addressing these areas, the research can contribute to the advancement of water quality engineering and the development of innovative and efficient water treatment technologies.

7.1.5 Potential applications

The research findings highlight the success of a hybrid adsorption-membrane filtration system in removing BOM from drinking water. The use of MWCNTs in the adsorption process proves advantageous, this is most likely due to its large mesoporous structure and the presence of a less negative surface charge for effective charge neutralization. However, the regeneration capacity and cost considerations of MWCNTs pose significant challenges, especially in large-scale plants. The hybrid system offers a novel application that combines the benefits of adsorption and membrane filtration, resulting in efficient removal of BOM. Experimental results demonstrate high efficiency in BOM removal, making this system a promising solution.

The development of the adsorption process before the NF membrane was rendered possible through the noncovalent functionalization of MWCNTs using CTAB at low operating conditions. The BOM adsorption capacity of CTAB-functionalized MWCNTs was characterized by remarkably high rapid kinetic rates at the time between 15 and 45 minutes; however, the removal of both AOC and BDOC was not complete after the pre-treatment. Therefore, NF membrane filtration was coupled to remove the remaining fractions of BOM that cannot be removed by the adsorption process with CTAB-functionalized MWCNTs.

Blending techniques have been explored to reduce membrane fouling in NF membrane filtration. Researchers have focused on modifying the membrane surface using chemical materials, such as grafting hydrophilic monomers and incorporating CNTs. However, these blending techniques have not proven to be completely effective in reducing membrane fouling. Despite efforts to mitigate this drawback, membrane fouling remains a major challenge in the NF membrane filtration process. The findings of this study highlight the benefits of combining the adsorption process and NF membrane filtration for the removal of BOM in drinking water. By using the pre-treated feed, the membrane fouling propensity was significantly reduced. The optimal adsorption capacity was achieved with a dosage of 120 mg/L of CTAB-functionalized MWCNTs for a duration of 4 hours. Furthermore, the study showed that higher filtration pressure enhanced water permeability. The

optimum pressure for the NF membrane filtration process was found to be 4.5 bar, resulting in a permeability value of 0.0091 ml/cm².m. This pressure also led to the removal of 80% of AOC and 65% of BDOC. These findings suggest that combining adsorption and NF membrane filtration can effectively remove BOM from drinking water, providing a promising approach for water treatment.

Finally, the findings highlight the importance of an adsorption process with CTAB-functionalized MWCNTs coupled to the NF membrane filtration process for optimal removal of both AOC and BDOC in drinking water, which otherwise proved difficult when applying a standalone treatment process; or when using inappropriate adsorbents during the pre-treatment process prior to membrane filtration process. From this trend, the adsorption process with CTAB-functionalized MWCNTs coupled to NF membrane filtration process should be preferentially considered for industrial applications. This will reduce the potential for bacterial regrowth within DWDS. It will consequently reduce the cost of water treatment and operational problems during the production of biologically stable drinking water.

7.2 Recommendation for future research

As a result of this study, CTAB-functionalized MWCNTs were found to be suitable as adsorbents for removing BOM (AOC and BDOC) from the water before the MSP. Further research is needed to optimize the adsorption process by testing different concentrations of MWCNTs. It is important to thoroughly investigate the impact of MWCNTs on humans and the environment, as they have been found to have toxicity due to metal catalysts. Health effects associated with MWCNTs include cancer, fibrosis, granulomas, and inflammation. To ensure safe and efficient use of MWCNTs in water treatment, it is necessary to limit their use and implement strict measures for their removal during treatment operations. By comprehending the toxicity, researchers can identify any risks associated with the use of MWCNTs and develop appropriate safety measures. This understanding will also aid in determining the optimal conditions for the application of MWCNTs in water treatment processes, ensuring that they can effectively remove pollutants without causing harm to the environment or human health. Further research is essential to fully understand the toxicity of CNTs and CNTs-related nanomaterials, and to unlock their potential in water treatment applications. Furthermore, after the membrane filtration process, it was suspected that charge repulsion, size exclusion, and hydrophobicity interaction could be the main mechanisms leading

to BOM removal by NF membranes; therefore, it can be suggested that it will be more explicit for future studies to investigate the impact of solution properties, such as hardness, ionic strength, and pH, on the interaction between BOM compounds and NF membranes. By examining this aspect, we contribute to understanding the factors affecting charge repulsion and size exclusion in NF membrane filtration. Our results provide insights into the effectiveness of the membranes in removing AOC and BDOC and highlight the potential for future studies to optimize pump pressure for improved efficiency. With the use of a larger pump range. The comparison of the BDOC and AOC protocols for water quality assessment in this study revealed that the BDOC protocol is more reliable in quantifying water biological stability and biodegradable organic matter. The AOC determination method faced challenges due to the limitations of plate counts, as the density of bacterial colonies was often too numerous to count. This made the AOC determination method complex and fastidious. To enhance accuracy in the HPC method, alternative methods such as flow cytometry (FCM) should be considered for future studies. FCM offers benefits in AOC determination and can maximize accuracy in water quality assessment. Overall, the findings suggest that the BDOC protocol and FCM method show promise for improving water quality assessment measures.

The implications of this study for the South African water treatment sector are significant. The research focuses on the use of hybrid adsorption-membrane filtration system to address the problem of high bacterial growth potentials in potable water. By utilizing this technology, it is possible to reduce or remove AOC and BDOC concentrations in water, thus producing biologically stable drinking water. This is crucial for the South African water treatment sector, as the production costs of drinking water depend on chemical inputs, the model specifications, and it ranges between R4.69 and R6.25/m³. Using the hybrid adsorption-membrane filtration system can help minimize the costs associated with adsorbents, coagulants, oxidants, and disinfectants. Additionally, the hybrid treatment system offers a promising solution to improve the overall effectualness of water treatment processes, ensuring cleaner and safe drinking water for communities. However, the energy and plant cost are the main components that can affect the hybrid adsorption-membrane filtration system. The cost estimation of the hybrid adsorption-membrane filtration system for drinking water treatment ranges between R4,18 and R5,25/m³. Overall, water treatment system using hybrid adsorption-membrane filtration system constitute a viable option for producing drinking water for human consumption in South Africa.

Future research could focus on the dynamic behavior of nanostructured materials in water treatment processes, to better understand their performance and optimize their use. By characterizing the morphology, composition, and physical characteristics of nanostructures, researchers can continue to advance material science and improve the removal of BOM from water. These characterization techniques are essential for developing a comprehensive understanding of nanostructures and their potential applications in water treatment.

Future research directions in mathematical modelling of membrane filtration include further investigation into the correlations between inlet and outlet concentrations, flow rates, and permeate concentration. Additionally, there is a need to analyze the impact of different initial conditions on the transient response of the system. This will help in understanding and achieving the desired steady state conditions in membrane filtration. Furthermore, future research should focus on utilizing the mathematical model to optimize membrane filtration processes and predict membrane performance. Finally, there is a scope for potential improvements and advancements in the CMFS system through the application of mathematical modelling techniques.

Future research directions in the field of hybrid adsorption-membrane filtration system for biologically stable drinking water could include the investigation of novel adsorbents and membranes. Researchers can explore the use of advanced materials with higher adsorption capacities and selectivity for target contaminants. Additionally, the development of improved membrane technologies that enhance filtration efficiency and reduce fouling potential can be a promising avenue for future studies. Another potential research direction could involve optimizing the hybrid treatment system's operating conditions, such as flow rate, contact time, and adsorbent or membrane regeneration methods. Moreover, investigating the long-term performance and stability of the hybrid treatment system under various water quality conditions would provide valuable insights for its practical application. Finally, further research can focus on assessing the economic feasibility and sustainability of implementing hybrid adsorption-membrane filtration system in large-scale water treatment plants. These research directions are essential for advancing the field and ensuring the continued production of biologically stable drinking water.

APPENDICES

APPENDIX A: Characterisation of MWCNTs

A.1 Diameter measurement of MWCNT

The measurement of MWCNTs is an important aspect of their characterization. One method for a rough calculation of the MWCNT diameter is by using a ruler. By analyzing a SEM image and utilizing the scale bar, the diameter of the MWCNTs can be estimated. In Figure A.1, the image shows an average diameter of the MWCNTs of 5 nm. Using this information, the diameter could be calculated by dividing the wall diameter (5 nm) by the scale bar length (15 nm) and multiplying it by the scale bar value (200 nm). Therefore, the estimated wall diameter of the MWCNTs was 66.67 nm. This measurement is valuable in understanding the impact of diameter on properties of MWCNTs, such as mechanical properties, electrical conductivity, chemical reactivity, and optical and thermal properties.

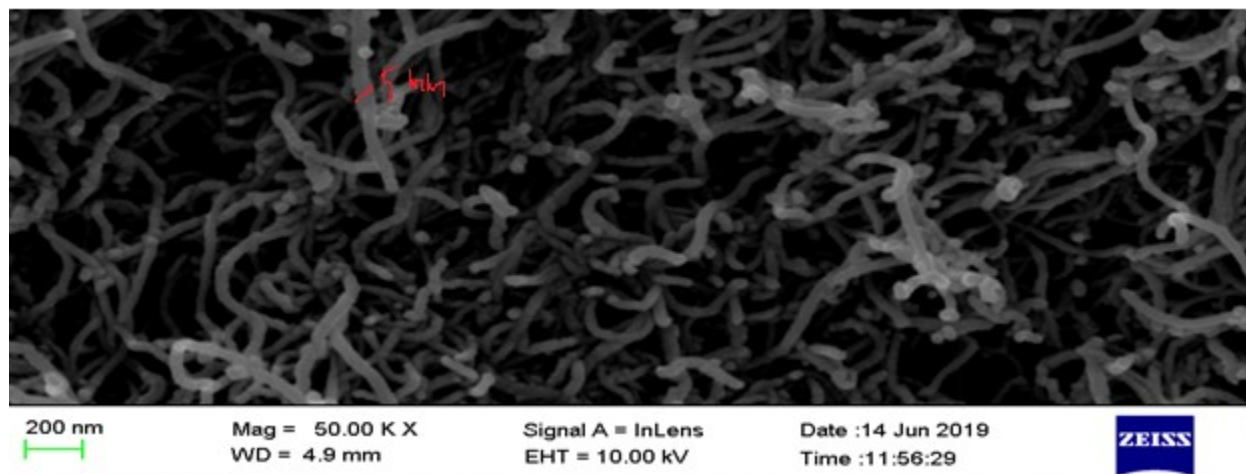


Figure A.1: SEM picture of raw MWCTs

A.2 Functionalization process of MWCNTs

Raw MWCNTs were dispersed in CTAB solution using an ultrasonic bath for 1 hour (the ratio was 1:1 to obtain a stable suspension during the functionalization process. Then the MWCNTs-CTAB solution was centrifuged at a speed of 4500 rpm for 1 hour. After that, samples were filtered and rinsed with distilled water. Result solid were dried using vacuum oven temperature of 80°C for 3 hours.

A.3 Determination of the ID/G ratio

The ID/G ratio is calculated by dividing the intensity of the D band (30) by the intensity of the G band (31). In this case, the ID/G ratio was equal to 0.97. The D band is observed at a wavelength of 1342.5cm^{-1} , while the G band is perceived at a wavelength of 1587cm^{-1} . This ratio is important as it provides insights into the disorder and defects in the carbon structure of the MWCNTs. By analyzing this ratio, valuable information can be obtained regarding the quality and purity of the MWCNTs and their potential applications.

Table A.1: Calculation of the intensity ratio for the functionalized and raw MWCNTs.

Unfunctionalized MWCNTs		Functionalised MWCNTs	
D Band	G Band	D Band	G Band
1342	1587	1340.5	1572.5
30	31	270	264
0.97		1.02	

From the table above: % increase = $\frac{1.02-0.97}{0.97} \times 100 = 5.51 \%$

A.4 X.R.D Pattern: Determination of the average crystallite size of MWCNTs (D)

The (002) peak in the XRD pattern, along with the Scherrer equation, provides a means to compute the average crystallite size of MWCNTs. The Scherrer equation, represented by equation (1), is a conventional method employed to determine the average crystallite size of MWCNTs using XRD pattern.

$$D = \frac{K\lambda}{\beta \cos\theta} \quad (1)$$

It involves the measurement of the full width at half maximum (FWHM) denoted as β , the diffraction angle θ , and the X-ray wavelength λ . The Scherrer constant, K , is a value of 0.91. The Scherrer equation specifically applies to nanoscale particles. In carbon materials, as the order of crystallinity decreases, the XRD peaks will widen. Therefore, the Scherrer equation is a valuable tool in quantifying the average crystallite size of MWCNTs based on their XRD patterns.

Table A.2: Crystallite size and d-spacing

Run no.	POS. [°2Th.]	d-spacing [Å°]	(hkl)	FWHM Left [°2TH.]	Crystalline size (nm)
1	26.2989	3.38885	(002)	0.551	16.80

APPENDIX B: PSF membrane characterisation

B.1 Measurement of the membrane's permeate flux.

To calculate the pure water flux (permeate) of a membrane, the following equation is used:

$$F = \frac{V}{A \times t} \quad (B1)$$

In this equation, V refers to the amount of collected permeate in milliliters, A represents the membrane's specific area in square centimeters, and t is the time in minutes indispensable for the permeate to pass through the membrane. By plugging in the corresponding values for V, A, and t, the permeate flux can be determined. This calculation is essential in understanding the rate at which the filtration membrane allows the permeate to flow through and is a crucial parameter in membrane filtration processes.

Table B.1: Table displaying the calculations for membrane flux (water sample A).

Membrane specific area (cm ²)	45	45	45	45	45
Filtration time (min)	15	30	60	90	120
Volume of permeate (cm ³)	6.5	9	14.5	29	31
Flux (ml/cm ² .min)	0.0096 0.0086	0.0066 0.0056	0.0054 0.0056	0.0071 0.0007	0.0057 0.005
Error	0.001	0.001	0.003	0.006	0.0007

Table B.2: Table displaying the calculations for membrane flux (water sample B).

Membrane specific area (cm ²)	45	45	45	45	45
Filtration time (min)	15	30	60	90	120

Volume of permeate (cm ³)	6	9.5	22	37	38.5
Flux (ml/cm ² .min)	0.0088 0.0086	0.0070 0.0067	0.0081 0.008	0.0091 0.0088	0.0071 0.006
Error	0.0002	0.0003	0.0001	0.0003	0.0011

B.2 Mechanical test results of the polymeric filtration membranes

Strain and stress:

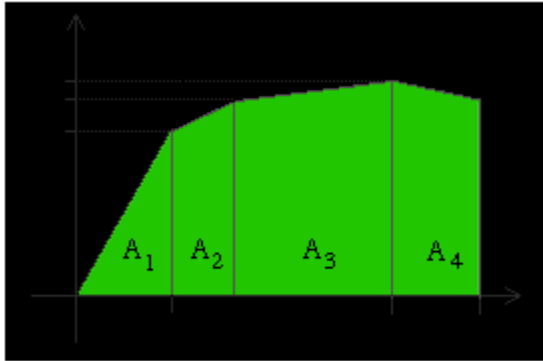
The relationship between stress and strain in material testing is determined through compression or tension tests. These tests involve applying an axial force to a test specimen and recording the resulting deflection as the load increases. By plotting these values on a load-deflection curve, we can analyze the material's behavior. The deflection of the test specimen is influenced by the elastic modulus of the material and the shape of the specimen, specifically its area and length. To eliminate the effect of geometry and focus solely on the material's behavior, it is essential to convert the load values to stress values and the deflection values to strain values. This can be done using the equations $\text{Stress} = \frac{P}{A_0}$ and $\text{Strain} = \frac{L-L_0}{L_0} = \frac{\Delta L}{L_0}$, where P represents the load, A₀ is the initial cross-sectional area of the specimen, L is the current length of the specimen, and L₀ is the starting length. The material's ability to stretch and deform is determined by a property known as the young's modulus (Y). Y can be calculated as follows:

$$Y = \frac{\text{Tensile stress}}{\text{Tensile strain}}$$

B.3 Toughness of a material:

The calculation method for toughness involves determining the area under the stress-strain curve, which constitutes the material's ability to absorb energy before failing. The toughness modulus was calculated by excluding the small area under the elastic portion of the curve. In order to simplify the calculations, the nonlinear portion of the curve is estimated using straight lines. This approach allows for a more concise and practical analysis of the material's toughness. By understanding the calculation method for toughness, engineers can acquire valuable insights into the performance and durability of different materials. The ability to accurately determine

toughness is crucial in various engineering applications as it directly impacts the structural integrity and overall performance of materials.



By adding the areas A_1 through A_4 in the figure presented above, the modulus of toughness can be calculated.

APPENDIX C: Mathematical modelling of membrane filtration process

C.1 The solution to equation 4.15 developed in chapter 4.

Substitute $z = x + (b_1/2b_2)$ and transform equation (4.15) to get:

$$\frac{dz}{dt} = -b_2 z^2 + \frac{b_1^2}{4b_2} + b$$

And after substitution $u = C^* + (b_1/2b_2)$:

$$\frac{dz}{dt} = b_2 (u^2 - z^2) \quad (C_1)$$

After separating the variables, equation (C₁) is changed to where x^* is the stationary concentration.

$$\frac{dz}{u^2 - z^2} = b_2 dt$$

The answer is given by integrating the initial condition u with time $t=0$, $u(0)$.

$$Z(t) = u \frac{[u+z(0)]e^{2b_2 z t} - u+z(0)}{[u+z(0)]e^{2b_2 z t} + u-z(0)} \quad (C_2)$$

Considering the above substitutions lead to the solution (4.16)

C.2 The stationary concentrations

Table C.1: Operating characteristics for a chloride tracer evaluation of the three-stage NF plan

Stage	$Q_{in}(m^3/s)$	$Q_p(m^3/s)$	$Q_{out}(m^3/s)$	$C_{in}(mg/L)$	$C_p(mg/L)$	$C_{out}(mg/L)$	Flux ($L/m^2 \cdot h$)
1	2.08 . 10^{-3}	0.88 . 10^{-3}	1.12 . 10^{-3}	110	14.1	95.9	15.3
2	1.17 . 10^{-3}	0.36 . 10^{-3}	0.81 . 10^{-3}	182	22.9	159.1	12.5
3	8.1 . 10^{-3}	2.08 . 10^{-3}	6.02 . 10^{-3}	254	64.6	189.4	13
Mean	1.35. 10^{-3}	0.48. 10^{-3}	0.87 $\cdot 10^{-3}$	182	33.9	148.1	13.6

The stationary values were calculated using the following Equation:

$$C^* = \frac{\sqrt{[Q_{in} - (1-\alpha)AK_0]^2 + 4\beta A(1-\alpha)C_{in}Q_{in}}}{2\beta(1-\alpha)} - \frac{Q_{in} - (1+\alpha)AK_0}{2\beta(1-\alpha)} \quad (C3),$$

The auxiliary parameters ∂ , β , K_0 were determined as follows:

$$C_p = \partial C_{out},$$

$$\diamond \partial = \frac{C_p}{C_{out}} = 33.9/148.1 = 0.23$$

$$\diamond \beta = 0.00968$$

$$\diamond K_0 = 1.08 \cdot 10^{-5} \text{ m/s}$$

$$\diamond A = 0.450 \text{ m}^2$$

C.3 The Dynamic separation processes

The dynamic separation process was evaluated using the following equation:

$$C_{out}(t) = (C^* + b_1/2b_2) \frac{[C^* + C_{out}(0) + \frac{b_1}{b_2}]e^{2ub_2t} - C^* + C_{out}(0)}{[C^* + C_{out}(0) + \frac{b_1}{b_2}]e^{2ub_2t} + C^* - C_{out}(0)} - \frac{b_1}{2b_2} \quad (C4)$$

Where the auxiliary parameter $u = C^* + b_1/2b_2$ and the boundary parameters were calculated using as follows:

$$b_0 = \frac{Q_{in} C_{in}}{V}; \quad b_1 = \frac{[Q_{in} - (1-\alpha) A K_0]}{V}; \quad b_2 = \frac{(1-\alpha) \beta A}{V} \quad (C5)$$

$$\diamond \frac{b_1}{b_2} = \frac{[Q_{in} - (1-\alpha) A K_0]}{[(1-\alpha) \beta A]} = 2.9 \cdot 10^{-3}$$

$$\diamond \frac{b_1}{2b_2} = 1.43 \cdot 10^{-3}$$

Appendix D: DOC and BDOC determination results

D.1 DOC and BDOC determination after 5 days of incubations

Table D.1: Triplicate results of DOC after BAS incubator 1 on reactor A

Reactor A1				
Date	Replicate	Day 0 Results (ppm)	Day 5 Results (ppm)	BDOC (ppm)
04/08/2020	1	5.59	4.80	0.79
	2	5.60	4.70	0.9
	3	5.76	5.78	0.02
Mean		5.65	5.09	0.56

Table D.2: Triplicate results of DOC after BAS incubator 1 on reactor B

Reactor B1				
Date	Replicate	Day 0 Results (ppm)	Day 5 Results (ppm)	BDOC (ppm)
04/08/2020	1	5.32	5.0	0.32
	2	5.57	5.0	0.57
	3	5.74	5.0	0.74
Mean		5.54	5.0	0.54

Table D.3: Triplicate results of DOC after BAS incubator 2 on reactor A

Reactor A2				
Date	Replicate	Day 0 Results (ppm)	Day 5 Results (ppm)	BDOC (ppm)
11/08/2020	1	5.59	4.36	1.23
	2	5.60	4.13	1.47
	3	5.76	4.27	1.49
Mean		5.65	4.26	1.39

Table D.4: Triplicate results of DOC after BAS incubator 2 on reactor B

Reactor B2				
Date	Replicate	Day 0 Results (ppm)	Day 5 Results (ppm)	BDOC (ppm)
10/08/2020	1	5.32	4.32	1.00
	2	5.57	4.44	1.13
	3	5.74	4.62	1.12
Mean		5.54	4.46	1.08

Table D.5: Triplicate results of DOC after BAS incubator 3 on reactor A

Reactor A3				
Date	Replicate	Day 0 Results (ppm)	Day 5 Results (ppm)	BDOC (ppm)
19/08/2020	1	5.59	4.36	1.23
	2	5.60	4.13	1.47
	3	5.76	4.27	1.49

Mean		5.65	4.26	1.39

Table D.6: Triplicate results of DOC after BAS incubator 3 on reactor B

Reactor B3				
Date	Replicate	Day 0 Results (ppm)	Day 5 Results (ppm)	BDOC (ppm)
19/08/2020	1	5.32	4.32	1
	2	5.57	4.44	1.13
	3	5.74	4.62	1.12
Mean		5.54	4.46	1.08

APPENDIX E:

E.1 AOC determination

In the summary of the AOC determination method, the study outlines the steps involved in calculating the number of heterotrophic bacteria in water using the heterotrophic plate count method. Firstly, several diluted bacterial cultures are prepared in broth. These cultures are then spread on nutrient agar plates, and based on the resulting colonies, the number of bacteria in the original culture tube is determined. The CFU/ml could be determined using the equation E₁ as follows:

$$\text{CFU/ml} = (\text{colonies}) \times (\text{dilution factor}) / \text{volume of culture plate}$$

Finally, the maximum colony count is converted to AOC concentration using the formula $\text{AOC} (\mu\text{g/L as acetate C}) = N_{\text{max}}/Y \times 100$, where Y is the yield factor for acetate.



Figure E.1: Illustration of heterotrophic plate count technics (spread plate method)

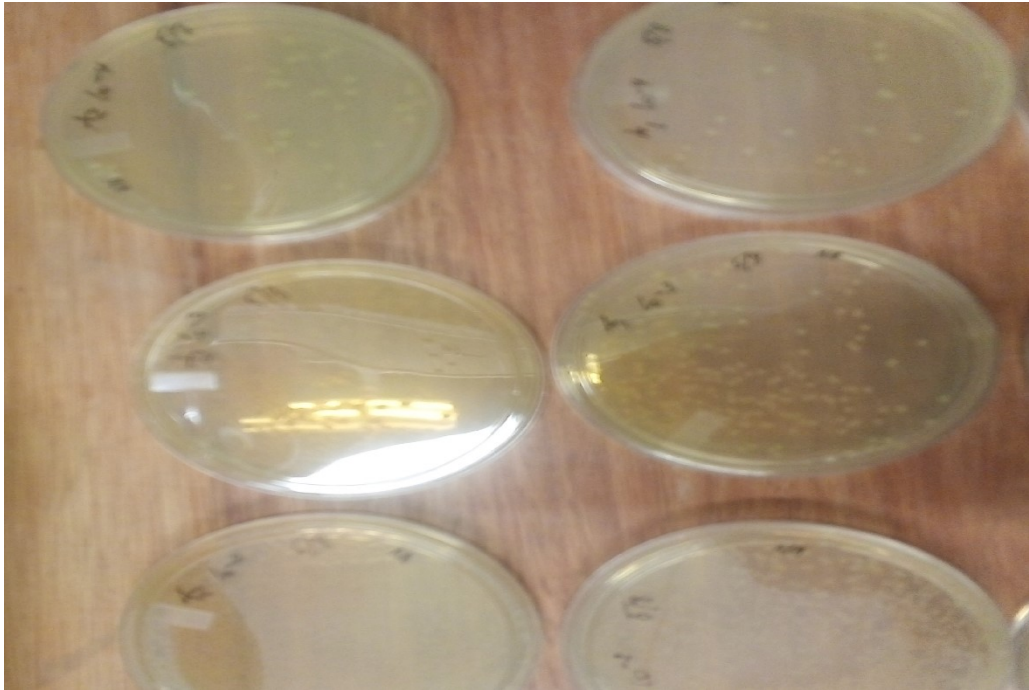


Figure E.2: Illustration of heterotrophic plate count technics (spread plate method)

Table E.1: Colony counts of Day 5 plates (Samples A₁ and A₂)

Plates A ₁	Colony Counts (Cfu/ml)
10 ⁻¹	TNTC
10 ⁻²	TNTC
10 ⁻³	140.10 ³
10 ⁻⁴	20.10 ⁴
10 ⁻⁵	5.10 ⁵
10 ⁻⁶	0
Plates A ₂	Colony Counts (Cfu/ml)
10 ⁻¹	TNTC

10^{-2}	TNTC
10^{-3}	136.10^3
10^{-4}	32.10^4
10^{-5}	4.10^5
10^{-6}	1.10^6

Table E.2: Colony counts of Day 7 plates (Samples A₁ and A₂)

Plates A₁	Colony Counts (Cfu/ml)
10^{-1}	TNTC
10^{-2}	TNTC
10^{-3}	149.10^3
10^{-4}	32.10^4
10^{-5}	4.10^5
10^{-6}	1.10^6
Plates A₂	Colony Counts (Cfu/ml)
10^{-1}	TNTC
10^{-2}	TNTC
10^{-3}	166.10^3
10^{-4}	21.10^4
10^{-5}	5.10^5
10^{-6}	0

Table E.3: Colony counts of Day 9 plates (Samples A₁ and A₂)

Plates A₁	Colony Counts (Cfu/ml)
10^{-2}	TNTC
10^{-3}	$155. 10^3$
10^{-4}	$33. 10^4$
10^{-5}	$4. 10^5$
10^{-6}	0
Plates A₂	Colony Counts (Cfu/ml)
10^{-2}	TNTC
10^{-3}	187.10^4
10^{-4}	34.10^5
10^{-5}	5.10^6
10^{-6}	0

Table E.4: Colony counts of Day 11 plates (Plates A₁, and A₂)

Plates A₁	Colony Counts (Cfu/ml)
10^{-3}	166.10^3
10^{-4}	24.10^4
10^{-5}	6.10^5

Plates A₂	
10 ⁻³	176.10 ³
10 ⁻⁴	31.10 ⁴
10 ⁻⁵	5.10 ⁵

Table E.5: Colony counts of Day 13 plates (Samples A₁, and A₂)

Plates A₁	Colony Counts (Cfu/ml)
10 ⁻³	180.10 ³
10 ⁻⁴	34.10 ⁴
10 ⁻⁵	7.10 ⁵
Plates A₂	
10 ⁻³	176.10 ³
10 ⁻⁴	31.10 ⁴
10 ⁻⁵	5.10 ⁵

Table E.6: Colony counts of Day 15 plates (Samples A₁, and A₂)

Plates A₁	Colony Counts (Cfu/ml)
10 ⁻³	189.10 ³
10 ⁻⁴	36.10 ⁴
10 ⁻⁵	7.10 ⁵
Plates A₂	
10 ⁻³	188.10 ³
10 ⁻⁴	38.10 ⁴
10 ⁻⁵	6.10 ⁵

Table E.7: Colony counts of Day 17 plates (Samples A₁, and A₂)

Plates A₁	Colony Counts (Cfu/ml)
10 ⁻³	189.10 ³
10 ⁻⁴	39.10 ⁴
10 ⁻⁵	8.10 ⁵
Plates A₂	
10 ⁻³	190.10 ³
10 ⁻⁴	38.10 ⁴
10 ⁻⁵	7.10 ⁵

Table E.8: Colony counts of Day 19 plates (Samples A₁, and A₂)

Plates A₁	Colony Counts (Cfu/ml)
-----------------------------	-------------------------------

10^{-3}	202.10^3
10^{-4}	45.10^4
10^{-5}	8.10^5
Plates A₂	
10^{-3}	197.10^3
10^{-4}	44.10^4
10^{-5}	7.10^5

Table E.9: Colony counts of Day 21 plates (Samples A₁, and A₂)

Plates A₁	Colony Counts (Cfu/ml)
10^{-3}	219.10^3
10^{-4}	49.10^4
10^{-5}	7.10^5
Plates A₂	
10^{-3}	199.10^3
10^{-4}	45.10^4
10^{-5}	7.10^5

Table E.10: Colony counts of Day 5 plates (Samples B₁, and B₂)

Plates B₁	Colony Counts (Cfu/ml)
10^{-1}	TNTC
10^{-2}	TNTC
10^{-3}	155.10^3
10^{-4}	25.10^4
10^{-5}	5.10^5
10^{-6}	0
Plates B₂	Colony Counts (Cfu/ml)
10^{-1}	TNTC
10^{-2}	TNTC
10^{-3}	202.10^3
10^{-4}	20.10^4
10^{-5}	5.10^5
10^{-6}	0

Table E.11: Colony counts of Day 7 plates (Samples B₁ and B₂)

Plates B₁	Colony Counts (Cfu/ml)
10^{-1}	TNTC
10^{-2}	TNTC
10^{-3}	150.10^3

10^{-4}	25.10^4
10^{-5}	6.10^5
10^{-6}	0
Plates B₂	Colony Counts (Cfu/ml)
10^{-1}	TNTC
10^{-2}	TNTC
10^{-3}	215.10^3
10^{-4}	14.10^4
10^{-5}	6.10^5
10^{-6}	0

Table E.12: Colony counts of Day 9 plates (Samples A₁ and A₂)

Plates B₁	Colony Counts (Cfu/ml)
10^{-1}	TNTC
10^{-2}	TNTC
10^{-3}	192.10^3
10^{-4}	12.10^4
10^{-5}	7.10^5
10^{-6}	0
Plates B₂	Colony Counts (Cfu/ml)
10^{-1}	TNTC
10^{-2}	TNTC
10^{-3}	200.10^3
10^{-4}	14.10^4
10^{-5}	6.10^5
10^{-6}	0

Table E.13: Colony counts of Day 11 plates (Samples B₁ and B₂)

Plates B₁	Colony Counts (Cfu/ml)
10^{-1}	TNTC
10^{-2}	TNTC
10^{-3}	214.10^3
10^{-4}	18.10^4
10^{-5}	8.10^5
10^{-6}	0
Plates B₂	Colony Counts (Cfu/ml)
10^{-1}	TNTC
10^{-2}	TNTC
10^{-3}	222.10^3
10^{-4}	15.10^4
10^{-5}	7.10^5
10^{-6}	0

Table E.14: Colony counts of Day 13 plates (Samples B₁ and B₂)

Plates B₁	Colony Counts (Cfu/ml)
10 ⁻¹	TNTC
10 ⁻²	TNTC
10 ⁻³	218.10 ³
10 ⁻⁴	25.10 ⁴
10 ⁻⁵	10.10 ⁵
10 ⁻⁶	0
Plates B₂	Colony Counts (Cfu/ml)
10 ⁻¹	TNTC
10 ⁻²	TNTC
10 ⁻³	225.10 ³
10 ⁻⁴	20.10 ⁴
10 ⁻⁵	10.10 ⁵
10 ⁻⁶	0

Table E.15: Colony counts of Day 15 plates (Samples B₁ and B₂)

Plates B₁	Colony Counts (Cfu/ml)
10 ⁻¹	TNTC
10 ⁻²	TNTC
10 ⁻³	205.10 ³
10 ⁻⁴	24.10 ⁴
10 ⁻⁵	10.10 ⁵
10 ⁻⁶	0
Plates B₂	Colony Counts (Cfu/ml)
10 ⁻¹	TNTC
10 ⁻²	TNTC
10 ⁻³	220.10 ³
10 ⁻⁴	21.10 ⁴
10 ⁻⁵	10.10 ⁵
10 ⁻⁶	0

- **The Number of bacteria can be calculated as: $(220 \times 10^3) / 0.1 = 22 \times 10^5$ CFU/ml**
- $AOC (\mu\text{g/L as acetate C}) = \frac{N_{\text{max}}}{Y} \times 100$, where:
Y = yield factor (Y) for acetate = 4.1×10^6 CFU/ $\mu\text{g acetate-C}$.
- $AOC = \frac{(22 \times 10^5) \times 100}{4.1 \times 10^6} = 53.6 \mu\text{g/L as acetate C}$

Table E.16: HPC results of plates A₁ and B₁ after adsorption process with 4, 8, 12 and 16 mg of functionalized MWCNTs.

MWCNTs Concentration	Colony Counts (Cfu/ml) in sample A
4 mg	-
8 mg	-
12 mg	122 x 10 ⁴
16 mg	-
MWCNTs Concentration	Colony Counts (Cfu/ml) in sample B
4 mg	-
8 mg	-
12 mg	130 x 10 ⁴
16 mg	-

Table E.17: HPC results obtained of plates A₁ and B₁ after MSP

Transmembrane	Colony Counts (Cfu/ml) in sample A
	44 x 10 ⁴
	-
	-
	-
	Colony Counts (Cfu/ml) in sample B
	48 x 10 ⁴
	-
	-
	-

Appendix F: Adsorption isotherm models

F.1 Concept of the Langmuir isotherm model:

The Langmuir isotherm model was used to represent the adsorption of AOC onto CTAB-functionalized MWCNTs. The graph of $1/A_e$ versus $1/C_e$ is a graphical representation employed in the Langmuir isotherm model to depict the adsorption of AOC onto CTAB-functionalized MWCNTs. This plot helps to visualize the relationship between the equilibrium adsorption capacity (A_e) and the equilibrium concentration (C_e) of AOC in the solution. By plotting these values, patterns and trends can be observed, allowing for the interpretation of the Langmuir isotherm model. This model provides insight into the adsorption mechanism and helps determine the significance of the observed plot. Ultimately, this plot is crucial in understanding the adsorption behavior of AOC onto CTAB-functionalized MWCNTs and its application in various fields.

F.2 Concept of the Freundlich isotherm model:

The representation of AOC adsorption onto CTAB-functionalized MWCNTs using the Freundlich isotherm model can be depicted through the Freundlich isotherm plot, which shows the relationship between $\ln q_e$ (amount of AOC adsorbed) and $\ln C_e$ (concentration of AOC). The Freundlich isotherm model equation, $\ln q_e = \ln K_F + 1/n \ln C_e$, describes this relationship, where K_F denotes the Freundlich constant, and n is the Freundlich exponent. By analyzing the Freundlich isotherm plot, valuable insights can be gained regarding the adsorption behavior and properties of the AOC-MWCNT system. Additionally, the determination of the amount of AOC adsorbed at a specific time (A_t) involves utilizing the mass balance relationship equation, $A_t = C_0 - C_t \times V/(m)$, where C_0 is the initial concentration of AOC, C_t is the concentration of AOC at time t , V is the initial volume of the solution, and m is the mass of MWCNTs. The Freundlich equation could be employed to determine the actual amount of AOC adsorbed onto the MWCNT surface at different time points during the adsorption process.

Table F1: Effect hybrid adsorption-membrane filtration on AOC removal (sample A)

Initial AOC (C_0),	Final AOC (C_t)	AOC removal
48.8	23	25.8
48.8	21	27.8
48.8	10.72	38.08 (79.5%)
48.8	24	24.8

Table F2: Effect of hybrid adsorption-membrane filtration on AOC removal (sample B)

Initial AOC (C_0),	Final AOC (C_t)	AOC removal
53.6	33	20.6
53.6	31	22.6
53.6	11.71	41.89
53.6	28	25.6

APPENDIX G:

G.1 Methods for Analytical Testing.

Temperature, pH, Total Dissolved Solid (TDS), and Conductivity: The samples were taken using a portable pH meter (Hi 9811-5) at the time.

Dissolved Oxygen (DO): A DO meter (Orion Star A213) was used.

Alkalinity, Free chlorine, and Nitrogen species (Ammonium ions NH₄⁺, Nitrate): The DPD method in accordance with accepted procedures was used, along with a spectroquant Pharo 300 M (Clesceri et al. the year 1998) are described:

➤ **Total alkalinity (acid capacity to pH 4.3)**

Range of measurement: 0.40 to 8.00 mmol/l

20-400 mg/l cacO₃.

➤ **Ammonium**

Range of measurement: 2.0-75.0 mg/l NH₄-N

➤ **Chlorine (Determination of free chlorine)**

Range of measurement: 0.03-6.00 mg/l Cl₂

➤ **Nitrate**

Measuring range: 0.2-10.0 mg/l NO₃-N

APPENDIX H: Error bars in graphs

Table H1: Error bar of the graph on impact of adsorbent concentration on percentage removal of AOC from P17-ultrapure water (With agitation speed = 180 rpm and contact time = 4 hours)

Adsor	A1	A2	Mean	Stdev.
4	52	51,5	51,8	0,4
8	57,6	55	56,3	1,8
12	69	58	63,5	7,8
16	49	48,7	48,9	0,2

Table H2: Error bar in graph on impact of agitation speed on the percentage removal of AOC (initial concentrations of 48.8 and 53.6 g C/L, 12 mg of adsorbent, 4 hours of contact time, pH of 4).

Ag. Speed	A1	A2	Mean	Stdev
45	56	56,3	56,2	0,2
90	57	57,5	57,3	0,4
180	57,4	57	57,2	0,3
220	56	56,3	56,2	0,2
Ag. Speed	B1	B2	Mean	Stdev
45	52,2	52,3	52,25	0,0
90	52	52,2	52,1	0,1
180	52,5	52,2	52,35	0,1
220	52	52,3	52,15	0,1

Table H3: Error graph in graph on impact of contact time on the removal of AOC (initial concentration = 48.8 and 53.6 µg C/L (for A1 and B1 respectively), Agitation speed = 180 rpm, adsorbent concentration = 12 mg)

CT	A1	A2	Mean	Stdev
1	56	56,3	56,15	0,21213
2	56,5	56	56,25	0,35355
3	56	55,5	55,75	0,35355
4	57	56,4	56,7	0,42426
5	56	56,5	56,25	0,35355
CT	B1	B2	Mean	Stdev
1	50	50,5	50,25	0,35355
2	50	50,3	50,15	0,21213
3	50	50,7	50,35	0,49497
4	52	52,7	52,35	0,49497
5	52	50,6	51,3	0,98995

Table H4: Error bar in the graph on variation of DOC concentrations during adsorption process using functionalised MWCNTs as adsorbent (Initial DOC concentrations = 4, 26 and 4, 46 mg/L for B1 and B2 respectively, agitation speed = 180 rpm, and adsorbent concentrations = 4, 8, 12, and 16 mg)

Ads. Conc.	Sample B1	Sample B2	Mean	Stdev
0	4,26	4,46	4,4	0,1
4	4,06	4,26	4,2	0,1
8	3,85	4,04	3,9	0,1
12	4,09	4,25	4,2	0,1
16	4,26	4,8	4,5	0,4

Table H5: Error bar in the graph on variation of BDOC concentration during adsorption process using CTBA- functionalized MWCNTs as adsorbent (Initial BDOC concentrations = 1.08 and 1.39 mg/L for B₁ and B₂ respectively, agitation speed = 180 rpm, and adsorbent concentration = 4, 8, 12, and 16 mg)

Ads. Conc.	Sample B1	Sample B2	Mean	Stdev.
0	1,39	1,08	1,235	0,2192
4	0,2	0,2	0,2	0
8	0,41	0,42	0,415	0,00707
12	0,17	0,21	0,19	0,02828
16	0	0,34	0,17	0,24042

Table H6: The change in flux over the course of filtration at 4.5 bar of constant pressure. The water flux collected after adsorption with 12 mg CTAB-functionalized MWCNTs was utilized for membrane permeation test.

Filt. Time	A1	A2	Mean	Stdev.	B1	B2	Mean2	Stdev.3
15	0,0096	0,0086	0,0091	0,00071	0,0088	0,0086	0,0087	0,0001
30	0,0066	0,0056	0,0061	0,00071	0,007	0,0067	0,0069	0,0002
60	0,0071	0,0068	0,00695	0,00021	0,0081	0,008	0,0081	0,0001
90	0,0071	0,0007	0,0039	0,00453	0,0091	0,0088	0,0090	0,0002
120	0,0057	0,005	0,00535	0,00049	0,0071	0,006	0,0066	0,0008

Table H7: Colony count changes and growth curves of strain P17 over several days

Day	A1	A2	Mean	Stdev
5	140	136	138,0	2,8
7	149	166	157,5	12,0
9	155	167	161,0	8,5

11	166	176	171,0	7,1
13	180	187	183,5	4,9
15	189	188	188,5	0,7
17	189	190	189,5	0,7
19	202	197	199,5	3,5
21	200	197	198,5	2,1

Table H8: The number of colonies and growth curve of the P17 strain change over several days

Day	B1	B2	Mean	Stdev
5	155	202	179	33
7	150	215	183	46
9	192	220	206	20
11	214	222	218	6
13	218	225	222	5
15	215	220	218	4